Improving the efficacy of oncolytic vaccinia virus-mediated breast cancer immunotherapy

by

Brittany Anne Umer

A thesis submitted in partial fulfillment of the requirements for the degree of

Doctor of Philosophy

in

Virology

Department of Medical Microbiology and Immunology

University of Alberta

Abstract

Vaccinia virus (VACV) has shown promise as an oncolytic agent for treating a variety of tumour types, with preliminary results suggesting that this strategy holds promise for treating breast cancer. Our lab has previously modified VACV by deleting virally-encoded enzymes responsible for dNTP production. Specifically, the F4L gene (ΔF4L), responsible for *de novo* dNTP synthesis, and the J2R gene (ΔJ2R), responsible for dTTP salvage, have been deleted from the VACV genome (ΔF4LΔJ2R VACV). These mutations increase viral specificity for replication in cancer cells, presumably due to elevated levels of these enzymes in tumours caused by rapid growth. While this modified VACV was effective in treating orthotopic bladder cancer in rats and mice, only limited therapeutic benefits were observed in mouse models of breast cancer. This project investigated methods to improve the efficacy of vaccinia virus mediated breast cancer immunotherapy.

In the first set of studies, I established improved virus production and quality control protocols for use in pre-clinical testing. Using purified virus, we established the maximum tolerable dose in our intratumoural murine breast cancer models to be used in subsequent studies.

I then tested two strategies for improving the efficacy of VACV treatment of breast cancer. In the first method, VACV was combined with image-guided radiation therapy (IG-RT), a commonly used clinical treatment for breast cancer. While IG-RT causes DNA damage resulting in cell death, it is also known to stimulate the immune system to induce anti-tumour immunity. We hypothesized that VACV and IG-RT would work synergistically to improve therapeutic responses. *In vitro*, radiation synergized with VACV to result in improved cell killing. However, *in vivo*, the combination was antagonistic, and decreased survival compared to radiation alone. This discrepancy between *in vitro* and *in vivo* drug interactions suggested that the cause of this antagonism might be due to effects on the tumour microenvironment. To investigate mechanisms that might be causing antagonism, I performed experiments to investigate how IG-RT+VACV might alter the tumour immune-cell microenvironment (TiME). We observed that treating irradiated tumours with VACV increased CD8+ T cells in tumours and spleens, along with regulatory T cells (Tregs). Despite these increased Tregs, the ratio of CD8+ T cells to Tregs remained constant. Interestingly, virus treatment caused a significant increase in PD-1 expression, leading us to speculate that immune-exhaustion may contribute to antagonism. However, adding an anti-PD-1 antibody to the treatment regimen did not reverse the

antagonistic effect caused by VACV oncotherapy. Although the mechanism remains to be elucidated, our results suggest caution should be taken when assessing treatment combinations in the clinic.

In the second method to improve efficacy, I attempted to improve the immunogenicity of VACV by deleting immunomodulatory genes from the virus genome. Stimulation of the immune system is an important aspect of virotherapy, and the 200 kb VACV genome encodes an arsenal of proteins responsible for inhibiting the immune system of its host. I sought to increase anti-tumour immune responses of VACV therapy by removing immunomodulatory genes from the VACV genome and to decipher how these deletions impact anti-cancer immune responses. I performed a head-to-head comparison of six mutant oncolytic VACVs, each harbouring deletions in genes that modulate different cellular pathways such as nucleotide metabolism, apoptosis, inflammation, and chemokine and interferon signalling. I found that even minor changes to the VACV genome can impact the immune cell compartment in the tumor microenvironment. Viral genome modifications had the capacity to alter lymphocytic and myeloid cell compositions in tumors and spleens, and also impacted PD-1 expression and percentages of virus and tumor-targeted CD8+ T cells. I also observed that the most promising candidate genes for deletion were those which interfere with interferon signalling, mainly, through deletion of the viral B8R and B18R genes, which resulted in improved median survival and complete responses. Collectively, this research helps focus attention on the more critically important pathways that modulate the immune response in the context of VACV oncolytic virotherapy

Preface

The research projects, of which this thesis is a part, received research ethics approval from The University of Alberta Research Ethics Board, Project Name "Analysis of modified vaccinia virus as a cancer therapeutic", ID: AUP00000251 and "Combination radiation and oncolytic virus treatment for cancer", ID: AUP00001914. Animal studies were carried out at the Cross Cancer Institute (CCI) and the University of Alberta, Edmonton Alberta, and conducted in accordance with the Canadian Council on Animal Care Guidelines and Policies with approval from the Cross Cancer Institute's Animal Care Committee and the Animal Care and Use Committee: Health Sciences for the University of Alberta.

A portion of Chapters 2 & 3 of this thesis have been submitted for publication as "Umer BA**,** Noyce RS, Shenouda MM, Favis NA, Desaulniers M, Irwin C, and Evans DH (2020). Production and quality assessment of infectious vaccinia virus stocks of pre-clinical grade purity for oncolytic immunotherapy studies [submitted]".

A portion of Chapters 2, 4 & 5 of this thesis have been submitted for publication as "Umer BA, Noyce RS, Kieser Q, Rans K, Middelton J, Favis NA, Hitt M, and Evans DH (2020). Oncolytic vaccinia virus immunotherapy combined with radiation antagonizes breast tumour clearance despite favorable immune stimulation [submitted]".

A portion of Chapters 2, 6 & 7 of this thesis have been published as "Umer BA**,** Noyce RS, Franczak BC, Shenouda MM, Kelly RG, Favis NA, Desaulniers M, Baldwin TA, Hitt M, and Evans DH. Deciphering the immunomodulatory capacity of oncolytic vaccinia virus to enhance the immune response in breast tumours, *Cancer Immunology Research,* (8)618-31.

Acknowledgments

First and foremost, I would like to thank my supervisor, Dr. David Evans. You have fueled a passion for viruses and all their neat tricks and features. You allowed me to try and test new things, and always supported my curiosity to allow me to grow as a scientist. You were supportive both inside and outside the lab, and I could not have asked for a better supervisor & mentor throughout my graduate studies and beyond.

Thank you to my wonderful committee, Dr. Mary Hitt, Dr. Maya Shmulevitz, and Dr. David Eisenstat. I was so fortunate to have such brilliant minds supporting me during my research. You always pushed me to explore new ideas and provided helpful guidance and direction when I was feeling stuck.

To all the members of the Evans lab throughout the years who have been my colleagues, friends, and mentors (all at the same time): it has been a truly unforgettable experience. This research would not have been possible without your help and support. Thank you to Chad for helping me get my start in the lab and providing the ΔF4LΔJ2R and ΔJ2R viruses. Thank you to Ryan, Les, Nicole, Megan, Mira, Quinten, Sid, and James- you all managed to make those 18 hour days fun by blasting 90's tunes and singing along, all with some hilarious sarcasm peppered in along the way. There were always jokes on the joke board and spare cookies on hand for when I was having a bad day. You all never hesitated to help me, even if it was at 6 am, and I thank you for your kindness, generosity, and support. I loved the escape rooms, the crossword puzzles, the board game nights, and our lab-decorating adventures with the craft box. I am forever grateful for these memories, and you all have such a special place in my heart!

Thank you also to all the wonderful staff and students in the Department of Medical Microbiology and Immunology who have made this journey more enjoyable. To Debbie, Tabitha, Michelle and Melissa in the MMI office, thank you for putting up with my endless lists of questions. You were always so helpful and supportive. The office was always a place of refuge I could go to if I need a bite of candy or a friendly chat with smiling faces to decompress. MMI is lucky to have you all supporting us! To all my fellow graduate students- your friendship & support has been indispensable. Thank you for making the good times better and for getting me through some of the rough spots. I know that the coffee chats, the wine and whines, and TGIFs will continue long after this thesis.

Thank you for all the help I received from collaborators who made this work possible. Thanks to Dr. Baldwin and Rees Kelly for immunology assistance, Kim Rans, Jackie Middleton, Amir Burkhari, and Dan McGuinn for SARRP treatment planning and animal study support, Dr. Anne Galloway and Ray at the Cross Cancer Institute for radiation assistance, Dr. Aja Reiger and Sabina Baghirov of the Faculty of Medicine and Dentistry Flow Cytometry core for assistance and training in flow cytometry, Dr. Brian Franczak of MacEwan University for guidance in statistics, the Hobman and Smiley labs for sharing resources and equipment, the HSLAS team, and the animals involved in this project. I acknowledge the NIH tetramer facility at Emory for providing tetramers in these studies, and Biorender for the generation of figures in this thesis. I gratefully acknowledge the support of my funding agencies: the Canadian

Institutes of Health Research, Alberta Innovates, the Alberta Cancer Foundation, the Canadian Breast Cancer Foundation, the Li Ka Shing Institute of Virology & infrastructure support by the Canadian Foundation for Innovation.

Lastly, thank you to all my friends and family who have provided unconditional love and encouragement. The last year has thrown some unexpected wrenches in the way, but with your support I made it through (despite this crazy pandemic). Thank you, Mom & Dad, Rayna & Arty, and Taylor for all your continued support & Splatoon battles throughout my never-ending studies. I love you all so much! Thank you to my surrogate family, Carol & Duncan, Marcos & Monica and Jessica & Aaron for being my home-away-from-home in Alberta. And last but certainly not least, my partner Josh who always picked me up when I was down and reinvigorated my passion for science when I was feeling drained. I could not have done this without your daily love, support and laughs. You inspire me to be better every single day & I can't wait to see what comes next!

Thank you all for the journey!

Table of Contents

Chapter 1: General introduction 1

1.1 Poxviruses 2
1.1.1 VACV biology 2
1.1.2 VACV immune modulation 2

1.2 Oncolytic viruses 6
1.2.1 History of oncolytic viruses 6
1.2.2 Premise of OV therapy 7
1.2.3 Design of tumour selective OVs 7
1.2.4 Oncolytic poxviruses 8

1.3 Cancer immunotherapy 12
1.3.1 Tumour-immune cell microenvironment 12
1.3.2 Immune checkpoints 15
1.3.3 Clinical development of cancer immunotherapies 16
1.3.4 Current successes of immunotherapy 16
1.3.5 Challenges & opportunities in cancer immunotherapy 17

1.4 Breast cancer & standards of care 17
1.4.1 Breast cancer subtypes and additional treatment regimens 18
1.4.2 Animal models of breast cancer 18
1.4.3 Breast cancer immunology & immunotherapy 20
1.4.4 Radiation therapy and immune responses in breast cancer 21

1.5 Rationale of the project 23
1.5.1 Data chapter overviews 23

Chapter 2: Materials and Methods 25

2.1 *In vitro* methods 26
2.1.1 Cell lines and culture conditions 26
2.1.2 *In vitro* irradiation 26
2.1.3 Growth curves 26
2.1.4 Cytotoxicity assays 26
2.1.5 Protein isolation 27
2.1.6 Western blotting 27
2.1.7 ATP and HMGB-1 quantification 27

2.2 Virus construction and purification 27
2.2.1 Virus construction 27
2.2.2 Virus culture 28
2.2.3 Virus purification 28
2.2.4 Working virus stock 29
2.2.5 Virus titration 30

2.3 *In vivo* assays and animal models 31
2.3.1 Tumour establishment 32
2.3.2 Tumour treatment 32
2.3.3 Tumour monitoring 33
2.3.4 Tissue processing 33
2.3.5 Flow Cytometry staining 34
2.3.6 Cytokine analysis 36

2.4 Analysis software 36
2.4.1 Synergy analysis 36
2.4.2 Statistical analysis 37
Chapter 3: Production and quality assessment of vaccinia virus stocks of pre-clinical grade purity and high infectivity for oncolytic immunotherapy studies 38
3.1 Introduction 40
3.2 Results 41
3.2.1 Selection of a method and surface for culturing VACV. 41
3.2.2 FBS alternatives 43
3.2.3 Sonication 43
3.2.4 Virus characterization and stock management 45
3.2.5 Virus stocks are stable for up to three years at -80°C 46
3.2.6 Flow cytometry can be used as a quality control measure for virus preparations 48
3.2.7 Dose limiting toxicities of oncolytic VACV differ based on route of administration 49
3.3 Discussion 53
Chapter 4: Oncolytic vaccinia virus immunotherapy antagonizes image guided radiation therapy in mammary tumour models 55
4.1 Introduction 57
4.2 Results: 58
4.2.1 Cellular ribonucleotide reductase subunits are present after treatment with 8 Gy of radiation 58
4.2.2 Irradiation of breast cancer cells does not impact oncolytic VACV replication 58
4.2.3 Radiation combined with oncolytic viruses work synergistically to kill cancer cells *in vitro*. 61
4.2.4 IG-RT using the SARRP to test ΔF4LΔJ2R VACV combined with radiation *in vivo* 64
4.2.5 VACV therapy antagonizes IG-RT *in vivo* in TuBo tumours 66
4.2.6 Antagonism is dependent on the timing of virus administration 66
4.2.7 Virus administered 48 hours after 10 Gy radiation is antagonistic *in vivo* In the 4T1 tumour model 69
4.3 Discussion: 69
Chapter 5: Assessing immune responses after combination therapy 72
5.1 Introduction 74
5.2 Results 74
5.2.1 Radiation decreases viral titers in the tumour 74
5.2.2 Combination therapy changes the composition of immune cells in the spleens and tumours of mice 77
5.2.3 T-cells with specificity to viral and tumour epitopes are generated after treatment 86
5.2.4 Combination therapy increases T cell activation and immune checkpoint expression 87
5.2.5 Anti-PD-1 checkpoint inhibition fails to reverse the antagonism of combination therapy. 92
5.3 Discussion 92
Chapter 6: Anti-cancer efficacy of immunomodulatory gene deleted oncolytic VACVs in breast cancer models 94
6.1 Introduction 96
6.2 Results 97
6.2.1 Construction of gene deleted VACVs 97
6.2.2 Immunogenic gene deletions do not impact *in vitro* characteristics, but ΔF4LΔJ2R is attenuated 98
6.2.3 All VACVs were safe, and virus replication was restricted to the tumour 100

6.2.4 Mutant VACVs alter therapeutic outcomes in two breast tumour models 103
6.3 Discussion 107
Chapter 7: Tumor immune-cell microenvironment alterations of immunomodulatory gene-deleted oncolytic VACVs in breast cancer models 109
7.1 Introduction 111
7.2 Results 111
7.2.1 Mutant VACVs alter immune responses in TuBo and 4T1 tumours 111
7.2.2 Mutant VACVs alter lymphocyte activation and immune checkpoints 115
7.2.3 Mutant VACVs alter ratios of T cells directed at viral and tumour epitopes 119
7.2.4 Mutant VACVs alter circulating serum cytokines 119
7.3 Discussion 121
Chapter 8: General discussion and future directions 123
8.1 General summary and key findings 124
8.2 Experimental approach to testing oncolytic VACV therapy in breast cancer models 126
8.2.1 *In vitro* assays for virotherapy studies 126
8.2.2 *In vivo* breast cancer models 127
8.3 VACV and combination therapy 128
8.4 Designing the next generation of VACV oncolytics 129
8.4.1 Viral gene deletion 129
8.4.2 VACV-encoded transgenes 131
8.5 VACV and breast cancer 131
8.6 Conclusions 132
Literature Cited 134

List of Tables

Chapter 1: Introduction

Table 1.1. Overview of VACV genes that inhibit immune-related pathways in the host. 4

Chapter 2: Materials and Methods

Table 2.1. PCR primers for assessing virus purity....30
Table 2.3. Flow cytometry antibodies....36
Table 2.2. Interpretation of CI values from CompuSyn Analysis....37

Chapter 3: Production and quality assessment of pre-clinical grade oncolytic VACV

Table 3.1. Growing VACV on flat culture plates 42

Chapter 6: Anti-cancer efficacy of immunomodulatory gene deleted VACVs

Table 6.1. Target genes deleted to generate immunostimulatory oncolytic VACVs....97

List of Figures

Chapter 1: Introduction

Figure 1.1. Premise of VACV-mediated OV therapy. 8
Figure 1.2 The tumour microenvironment and immune cell functions 15
Figure 1.3 Animal models and molecular subtypes of breast cancer 19

Chapter 2: Materials and Methods

Figure 2.1. Schematic for maintaining virus banks. 30
Figure 2.2. Representative flow cytometry gating strategy 35

Chapter 3: Production and quality assessment of pre-clinical grade oncolytic VACV

Figure 3.1: FBS substitutes do not alter the growth of WT (A) or mutant (B) VACV on BSC40 cells....44
Figure 3.2. Sonication produces more homogenous VACV suspensions and increases virus titers. 45
Figure 3.3.Virus stocks are stable when stored at -80°C. 47
Figure 3.4. The dynamic range of viral particle detection....50
Figure 3.5. Flow cytometry and DNA stains can be used to determine the specific infectivity of VACV preparations..51
Figure 3.6 Oncolytic VACV can be used safely in mouse models of breast cancer 52

Chapter 4: Combining IG-RT with oncolytic VACV antagonizes breast tumour clearance despite *in vitro* synergy

Figure 4.1. Cellular RR subunits R2 and P53R2 after radiation 59
Figure 4.2. Irradiation of breast cancer cells does not impact oncolytic vaccinia virus replication. 60
Figure 4.3. Radiation combined with oncolytic viruses work synergistically to kill cancer cells *in vitro*. 61
Figure 4.4. *In vivo* experimental timeline and image-guided radiation therapy using the SARRP 63
Figure 4.5. Combination therapy antagonizes radiation therapy in the TuBo tumour model. 65
Figure 4.6. Delayed virus administration does not cause antagonism but does not improve therapeutic responses ..67
Figure 4.7. Combination therapy antagonizes radiation therapy in the 4T1 tumour model 68

Chapter 5: Combining IG-RT with oncolytic VACV changes the tumour immune cell microenvironment

Figure 5.1.Virus titers are decreased in irradiated tumours 75
Figure 5.2. Combination therapy changes the composition of immune cells in the spleens in the TuBo model 76
Figure 5.3. Combination therapy changes the composition of immune cells in the spleens of in the 4T1 tumour. 78
Figure 5.4. Ratios of immune cells in the spleens of mice with (A)TuBo or (B)4T1 tumours. 79
Figure 5.5. Combination therapy treatment reprograms the TuBo TiME 80
Figure 5.6. Cell counts normalized to gram of tumour tissue from TuBo tumours....82
Figure 5.7. Combination therapy treatment reprograms the 4T1 TiME....83
Figure 5.8. Cell counts normalized to gram of tumour tissue from 4T1 tumours. 85

Figure 5.9. VACV therapy generates T-cells with specificity to viral and tumour epitopes 86
Figure 5.10. Treatment of TuBo tumours with ΔF4LΔJ2R VACV therapy activates CD8+ T cells. 88
Figure 5.11. Combination therapy increases immune checkpoint expression in the tumour microenvironment. 89
Figure 5.12. Anti-PD-1 checkpoint inhibition does not reverse the antagonism 91

Chapter 6:Anti-cancer efficacy of immunomodulatory gene-deleted oncolytic VACVs

Figure 6.1. Genomic maps of mutant VACV constructs 98
Figure 6.2. *In vitro* growth and cytotoxicity in murine mammary carcinoma cell lines. 99
Figure 6.3. Immunogenic VACV cause release of markers of ICD 100
Figure 6.4. All immunomodulatory VACVs were safe *in vivo*, and virus replication was restricted to tumors. 102
Figure 6.5 .Mutant VACVs alter therapeutic outcomes in the immunogenic HER2/neu+ TuBo tumour model 105
Figure 6.6.Mutant VACVs alter therapeutic outcomes in the non-immunogenic and metastatic 4T1 tumour model 106

Chapter 7: TiME alterations of immunomodulatory gene-deleted oncolytic VACVs

Figure 7.1.Mutant VACVs altered immune responses in TuBo tumors. 113
Figure 7.2. Mutant VACVs altered immune responses in 4T1 tumors.....114
Figure 7.3 Modifications to the VACV genome altered expression of CD69 116
Figure 7.4 Modifications to the VACV genome altered immune checkpoint expression 117
Figure 7.5. Modifications to the VACV genome altered antigen-specific T cell responses 118
Figure 7.6. Immunogenic gene deletions altered the levels of cytokines in the serum.....120

Chapter 8: General discussion and future directions

Figure 8.1. Summary of investigations into combining ΔF4LΔJ2R VACV with IG-RT in breast cancer models.....125
Figure 8.2. Summary of investigations into removal of immunomodulatory genes to improve VACV virotherapy 126

List of abbreviations

ACT-Adoptive cell therapy

AdV-Adenovirus

AR-Adverse reaction

APC-Antigen presenting cell

ATP- adenosine triphosphate

Bp-base pairs

BTB-broad-complex, Tramtrack and Bric

CAR-T-Chimeric antigen receptor T cell

CCI- Cross Cancer Institute

CD-cluster of differentiation

cGAMP-Cyclic guanosine monophosphate-adenosine monophosphate

cGas-CyclicGMP-AMP synthase

CI-Combination Index

CR-Complete responses

CT- Computed tomography

CTL-Cytotoxic T lymphocyte

CTLA-4- cytotoxic T lymphocyte antigen 4

DMEM- Dulbecco's modified essential medium

DAMP- Danger-associated molecular pattern

DC-Dendritic cell

DICOM-Digital Imaging and Communications in Medicine

dsDNA-double stranded DNA

dNTPs-deoxynucleotide triphosphates

dTTPs- deoxythymidine triphosphate

DVH-Dose volume histogram

EEV- extracellular enveloped virus

EGF-Epidermal growth factor

ELISA- Enzyme linked immunosorbent assay

ER-Estrogen receptor

ERBB2-Receptor tyrosine-protein kinase

ERK2-Extracellular regulated kinase 2

FBS-Fetal bovine serum

FDA-Food and drug administration

FMO- Fluorescence minus one

FSC-A Forward-scattered light-area

FSC-H Forward-scattered light-height

GAGs-Glycosaminoglycans

G-CSF- Granulocyte colony-stimulating factor

GM-CSF- granulocyte macrophage colony stimulating factor

GPT-guanine phosphoribosyltransferase

gusA- β-glucuronidase gene

HER2- human epidermal growth factor receptor 2

HI-FBS- Heat-inactivated FBS

ICD- Immunogenic cell death

IDO-Indolamine 2,3-dioxygenase

IFN- interferon

IFITS- interferon-induced proteins

IG-RT- Image-guided radiation therapy

IKKα/β-Inhibitor of nuclear factor kappa-B kinase

IL-interleukin [1α, 1β, 2- 9, 10, 12, 13, 15, 17, 18]

IMV- intracellular mature virus

IR-ionizing radiation

IRAK-Interleukin-1 Receptor-Associated Kinase-2

ISGs-IFN-stimulated genes

ITR-Inverted terminal repeat

IRF (3/7)-IFN regulatory factor

JX-695- Jennerex 594

Kbp-Kilobase pair

KC- Keratinocyte derived chemokine (CXCL-1)

KDa-Kilodalton

HBSS- Hank's balanced saline solution

HMGB-1- high mobility group box protein 1

HSV-Herpes Simplex Virus

lacZ- β-galactosidase gene

LAG-3-Lymphocyte-activation gene 3 (CD223)

LIF-leukemia inhibitory factor

LIX- CXCL-5

loxP- target loxP DNA sequence

MAL-MyD88 Adaptor-like

mCh, mCherry fluorescent protein

MCP-1- Monocyte chemoattractant protein 1 (CCL2)

M-CSF- Macrophage colony-stimulating factor

MDSC-myeloid derived suppressor cell; (M)-Monocytic/ (PMN)-Polymorphonuclear/ (G)-Granulocytic

MEM-Modified essential medium

MFP-Mammary fat pad

MHCI/II- Major histocompatibility complex

MIG- Monokine induced by IFN γ (CXCL-9)

MOI- multiplicity of infection

MyD88-Myeloid differentiation primary response 88

ND-not detected

NDV-Newcastle Disease Virus

Neo- neomycin gene

NF-κB- Nuclear factor kappa-light-chain enhancer of activated B cells

NK cell- Natural Killer cell

nm- no marker

NSCLC-Non small cell lung carcinoma

OV-oncolytic virus

PAMP-Pattern-associated Molecular pattern

PBS-Phosphate buffered saline

PCR-polymerase chain reaction

PD-1- programmed cell death 1

PD-L1/2-programmed cell death ligand 1/2

PFU-Plaque forming units

PK-protein kinase

PKR-protein kinase R

PR-Partial response

PRR-Pattern Recognition Receptor

RANTES-Regulated on activation, Normal T cell Expressed and Secreted (CCL5)

RIPA- radioimmunoprecipitation assay

RR-ribonucleotide reductase

RPMI- Roswell-Park Memorial Institute

RT-Radiation therapy

SARRP- Small Animal Radiation Research Platform

SDS- sodium dodecyl sulfate

STAT1/2-Signal transducer & activator of transcription kinases

STING-Stimulator of interferon genes

TBK-1- TANK-binding kinase 1

TC-Tissue Culture

TiME-Tumour immune cell microenvironment

TIM-3-T-cell immunoglobin and mucin domain-3

TIGIT-T cell immunoreceptor with Ig and ITIM domains

TK-thymidine kinase

TLR-Toll-like receptor

TME-Tumour microenvironment

TNBC-Triple negative breast caner

TNFα- tumor necrosis factor α

TRAM-TRIF-related adaptor molecule

TRAF-TNF receptor associated factor

Treg- Regulatory T cell

TRIF- TIR-domain-containing adapter-inducing IFN β

T-VEC- Talimogene laherparepvec

WR- Western Reserve

WT-wild type

VACV- Vaccinia virus

VCP- Virus complement control binding protein

VEGF-Vascular endothelial growth factor

VGF-Vaccinia growth factor

VISTA-V-domain Ig suppressor of T cell activation

VSV- Vesicular stomatitis virus

YFP- yellow fluorescent protein

Chapter 1: General introduction

1.1 Poxviruses

Poxviruses are a group of double stranded (ds) DNA viruses, notable for their cytoplasmic replication in infected cells, large size, and broad host range. The family *Poxviridae* comprises 83 species across 22 different genera[1]. The most infamous member of the poxvirus family, variola virus, is known for causing mass devastation and deaths as the causative agent of smallpox. Other members of this family, such as vaccinia virus (VACV), are better known for their therapeutic uses, primarily as vectors for vaccination against infectious diseases. In fact, VACV was the virus used in the worldwide vaccination campaign which lead to the eradication of smallpox in 1980[2], and has been regarded as the most effective vaccine in history[3]. VACV-vectored rabies vaccines for livestock have also been integral in the eradication of wildlife rabies in Belgium, France and Luxembourg, and for the control of racoon rabies in Canada[4–7]. In addition to its use as a vaccine, VACV has been investigated as a gene-therapy vector, used to deliver therapeutic payloads to treat various conditions[8,9]. Most recently, VACV has been gaining traction as an oncolytic agent used for the treatment of cancer[10–12], which is the primary topic of this thesis.

1.1.1 VACV biology

Poxviruses were the first viruses to be visualized by microscopy due to their large size[13]. The virion itself is brick-shaped, and measures approximately 300 x 200 x 100 nm in dimension. Inside the virion is a dumb-bell shaped virus core containing a single linear strand of covalently closed ds DNA of approximately 200 kbp. The core is wrapped in one or two lipid membranes, giving rise to intracellular mature virus (IMV), or extracellular enveloped virus (EEV), respectively. Upon binding to host cells, viral particles enter the cell via membrane fusion or endocytosis for IMV[14], or in the case of EEV, by first binding glycosaminoglycans (GAGs) to initiate shedding of the outer envelope prior to entry by membrane fusion in the same manner as IMV[15]. Once the virion core has entered the cytoplasm, virus factories, which are the site of viral replication, are established near the nucleus. Transcription is initiated in a temporal manner, beginning with “early” genes that are required for nucleotide biogenesis, DNA replication, and innate immune inhibition, “intermediate” genes which encode enzymes required as late transcription factors, and “late” genes which encode structural proteins and proteins packaged into the virion, as well as additional immune-modulating genes[16]. DNA replication and virus assembly occur in viral factories, which lead to the formation of IMV. While most IMV remain in the cytoplasm to be released when the cell lyses, a small fraction of IMV are wrapped intracellularly with an additional two membranes. These intracellular enveloped viruses (IEV) can migrate out of the cell where they lose one of these membranes and are released outside of the cell as EEV, or can remain attached to the cell membrane as cell-associated virus (CEV)[17]. At this late point in infection, cell death occurs and virus particles are released to spread to adjacent cells.

1.1.2 VACV immune modulation

The innate immune system counteracts virus infection and relies on complex cellular signalling pathways that converge to produce an anti-viral state in the host. Virus infection is first detected by the recognition of Pathogen-

Associated Molecular Patterns (PAMPs) that are detected by cellular pattern recognition receptors (PRRs) such as toll-like receptors (TLRs) or DNA sensors such as cGAS. Once a PAMP is detected by any number of PRRs in the cell a complex signalling cascade comprised of various adaptor proteins (MyD88, MAL, TRIF, TRAM, IRAK2, TRAF6), signalling molecules (Ikkα/β) and protein kinases (PKR and TBK1) activate NF-κB, IRF3 or IRF7. These molecules initiate the transcription of interferon (IFN), IFN-stimulated genes (ISGs), and other proinflammatory cytokines such as TNFα and interleukins (ILs) that both produce an anti-viral state in the cell, and also bridge the innate and adaptive arms of the immune system to recruit immune effector molecules such as T and B cells to the site of infection.

Viruses have evolved complex countermeasures to subvert this host innate immune response to inhibit activation. It is estimated that VACV devotes up to 50% of its 200 kbp genome to modifying and manipulating the immune response of its host[18]. Despite VACV being studied extensively over the past century, scientists are still working to uncover the roles of all of the VACV proteins and their functions, and new functions are continually being described. VACV proteins have been found to interrupt or highjack many immune-related pathways in the host, primarily at the level of innate cellular immune signalling, which in turn, impacts the adaptive immune response to infection as well. VACV proteins inhibit numerous pathways including, but not limited to: NF-κB signalling, IFN signalling, antigen presentation, lymphocyte activation, complement pathways, and cytokine signalling[18,19]. Oftentimes, virus-encoded proteins serve redundant roles, highlighting the importance of certain anti-viral pathways in the host. For instance, a mutant virus lacking all known NF-κB inhibitors revealed NF-κB signalling was still inhibited, suggesting that unknown NF-κB inhibitors were still present in the genome[20]. Even in the absence of immune modulatory proteins, the different enveloped forms of VACV (IMV, CEV, EEV) also serve as a form as immune evasion, whereby having multiple forms of the virus serve to evade recognition by the immune system. Although not covered in this report, a review of these "alternative" forms of immune evasion can be found in Bidgood and Mercer, 2015[21]. VACV-encoded immunomodulatory genes and their functions can be found in Table 1.1, classified according to the mechanism of inhibition. Of note, many VACV proteins serve multiple functions, and appear in multiple categories[18]. Although additional putative immunomodulators have been predicted based on structure, only proteins with confirmed functions are described[18,22].

Table 1.1. Overview of VACV genes that inhibit immune-related pathways in the host. This table was adapted from Smith et al., 2013[18]

VACV Gene[23]	Locus in WR genome	Protein Function	Additional details
Complement inhibitors: The complement system is composed of plasma proteins which serves as an immediate and innate defense against pathogens. The complement system neutralizes and opsonizes pathogens, and induces an inflammatory response to fight infection[24].			
C21L	VACWR025	Secreted complement binding protein	-Virus complement control binding protein (VCP). -Prevents antibody-dependent complement enhanced neutralization[25]. -A VCP deficient virus had increased T cell accumulation and increased neutralizing antibody responses[26].
A56R	VACWR181	Hemagglutinin protein	-deletion in GLV-1h68 (Slazay lab)-Genelux corp. -functions in evasion of complement by attaching to VCP at the cell surface[27]
B5R	VACWR187	EEV membrane glycoprotein[28]	-Gene encoded is related to the regulators of complement activation gene family in mammals, but no actual role in protecting against complement described[29]. -Impacts plaque size[29].
Innate detection resistance through inhibition of recognition by PRRs			
E3L	VACWR059	Double stranded RNA-binding protein.	-Carboxy-terminal domain resists IFN response by sequestering dsRNA PAMPS to inhibit dsRNA-dependent protein kinase (PKR)[30,31]. -Inhibits the IFN-induced 2-5A synthetase to inhibit apoptosis[32,33] -Inhibits IRF3 and IRF7[34] -antagonizes PKR-dependent and independent cytokine induction to inhibit production of a diverse range of cytokines[35]
A46R	VACWR172	Binds to innate-signalling adaptor proteins	-Binds multiple signalling adaptors (MyD88, MAL, TRIF, TRAM) to block TLR signalling and NF-κB and IRF3 activation [36–38]. -Deletion reduces virulence[38], and enhances immunogenicity of vaccine vectors by increasing TNF, IL-2 and IL-8 secretion by macrophages and enhances B and T cell responses[39].
B2R	VACWR184	Poxin nuclease	-degrades cGAMP to avoid cGAS-STING innate signalling[40]
IFN resistance through inhibition of innate signal transduction pathways (NF-κB, IRF3)			
A49R	VACWR175	NF-κB inhibitor	-Binds to and stabilizes IkBα, binds to and inhibits beta-TrCP to prevent NF-κB activation[41–43]
A55R	VACWR180	NF-κB inhibitor	- NF-κB inhibitor acting downstream of IκBα degradation[44] -deletion caused increased VACV-specific $CD8^+$ T-cell proliferation, activation, and cytotoxicity[44]
A52R	VACWR178	NF-κB inhibitor	-Inhibits IL-1 and TLR activation of NF-κB by binding to TRAF6 and IRAK2[36,45,46]
B14R	VACWR196	NF-κB inhibitor	-Binds to IKK β and prevents phosphorylation. -IL-1 and IL-6 decoy receptor[47]
C4L	VACWR024	NF-κB inhibitor	-inhibits NF-κB activation at or downstream of the IKK complex[48] -knockout had reduced virulence[48]

C7L	VACWR	Host-range, IFN inhibitor	-antagonizes IFN production and signalling, and enhances immune response to challenge in lungs[49,50] -contributes to IFN-resistance to permit virus replication[51]
K1L	VACWR032	Ankyrin-like protein	-inhibits NF-κB activation by inhibiting PKR signal transduction[52–54]
K7R	VACWR039	NF-κB inhibitor	-Binds TLR proteins (IRAK2, TRAF6) to inhibit NF-κB & IRF3 activation[55] -modulates heterochromatin regulation[56] -binds deadbox RNA helicase 3 to inhibit IRF3 activation and therefore IFNβ induction[57,58] -Increased NK infiltration and CD8 T cells, enhanced MHCII presentation, enhanced cytolysis by NK cells and VACV specific CD8 T cells[59]
M2L	VACWR031	NF-κB inhibitor Co-stimulation inhibitor	-Reduces ERK2 phosphorylation and prevents p65 nuclear localization to inhibit NF-κB[60]. - By binding CD80 and CD86, the M2 protein blocks interactions with both CD28 and CTLA4 and potentiates CD80 binding to PD-L1[22,61]
N1L	VACWR028	NF-κB inhibitor apoptosis inhibitor	-Inhibits NF-κB and IRF3 signaling[62] -inhibits apoptosis signaling[63] (disputed)[64] -deletion enhanced CD8 T- cell effector and memory response, increased T-cell cytotoxicity[65]
C6L	VACWR022	IRF3 and IRF7 inhibitor IFN inhibitor	-inhibits IRF3 and IFN signaling[66] through degradation of histone deacetylase 4[67] -deletion enhanced VACV specific T-cells with increased cytotoxicity[68], enhanced antibodies and protection against challenge as a vaccine vector[69,70]
C16L/ B22R	VACWR010	Inhibits IRF3 signalling	-DNA-PK is a cytoplasmic PRR that initiates an innate immune signalling cascade. C16L binds to DNA-PK and inhibits IRF3 signalling[71] -Deletion of C16L induces higher levels of chemokines and cytokines *in vivo*[71]
N2L	VACWR029	IRF3 inhibitor	-inhibits IFR3 after translocation to the nucleus[72,73]
H1L	VACWR099	Protein phosphatase	- dephosphorylates STAT1 and STAT2 to block transcription of IFN-stimulated genes[74,75]
K3L	VACWR034	Interferon resistance	-EIF2a mimic that acts as a non-phosphorylatable pseudosubstrate for PKR to inhibit signaling[76–78]
C9L	VACWR023	IFN resistance protein	-counteracts the IFN-induced antiviral state by an unknown mechanism[79]
F17R	VACVWR056	ISG inhibitor	-subverts cGAS-STING intracellular signalling and preventing interferon stimulated gene expression[80]
Decoy chemokine/ cytokine receptors to prevent receptor engagement with ligands			
B18R	VACWR199	IFN signalling inhibitor	- Binds type I IFN (Soluble and on the cell surface) and is more effective against IFNα than β[81,82] -deletion reduces virulence in intranasal mouse models[82]
B8R	VACWR190	IFN signalling inhibitor	- Soluble, binds secreted interferon γ [83] -deletion had no enhanced immunogenicity on its own[84], however enhanced immunogenicity observed when deleted in addition to B18R[85]
B15R	VACWR197	IL-1β decoy receptor	-Prevents IL1β binding to its natural receptor[86,87].

A53R	VACWR179	TNFα receptor	-binds and sequesters TNFα while lacking signaling domain; not present in all VACV strains[88–91]
A41L	VACWR166	Chemokine receptor	- Secreted protein. Proposed to disrupt chemokine concentration gradients[22,92] - deletion increased VACV CD8+ T-cell responses, enhanced protection against challenge[93]. Mutant cleared more readily due to increased infiltration of leukocytes[94].
C12L	VACWR205	IL18 binding protein	- soluble IL18 binding protein to sequester IL18 and prevent it from reaching target cells[95,96]. - binding affinity is higher for murine IL18 than human[95]. -Deletion lead to increased CD8 T cell responses and IFN γ production[97]
Apoptosis inhibitors			
F1L	VACWR040	Inhibitor of apoptosis and inflammasome	Inhibits apoptosis and inflammasome activation. Decreases caspase-1 and IL-1β secretion to increase inflammation in lungs of infected mice[98,99].
M1L	VACWR030	Inhibits apoptosis	Blocks procaspase-9 processing, targeting apoptosome to inhibit apoptosis[100]
B13R	VACWR195	Serine protease inhibitor (SPI-2) -inhibits apoptosis -inhibits IFNβ	-binds caspase1 and blocks IL-1β cleavage to prevent caspase-1 induced apoptosis[101,102] -inhibits IFNβ by disrupting IRF3 signaling complexes[103] -deletion had no enhanced immunogenicity in the context of use as a vaccine vector
Other inhibitors			
A35R	VACWR158	MHC II antigen presentation inhibitor	-inhibits MHC II antigen presentation, T cell priming, and subsequent chemokine and cytokine expression[104] -enhanced immunogenicity when deleted from MVA by increasing VACV specific IFN γ secreting splenocytes, enhanced IgG production and class switching of IgG isotypes[105]
A39R	VACWR164	Phagocytosis inhibitor	- Binds plexin C1 and inhibits phagocytosis by neutrophils and dendritic cells[106] -inhibits DC cross-priming *ex vivo*[106]
C9L	VACWR019	Ankyrin-repeat/F-box proteins	- Counteracts IFN-induced state in cell by promoting degradation of interferon-induced proteins (IFITS)[79,107]
F3L	VACWR042	BTB/kelch protein	-BTB/kelch protein, inhibitor of innate immune responses[108] -deletion caused mild virus attenuation and increased NK infiltration to infection site and a decrease in γΔT cells[108].

1.2 Oncolytic viruses

1.2.1 History of oncolytic viruses

Oncolytic viruses (OVs) are viruses that infect and kill cancerous cells. While interest in oncolytic virus research has surged in recent years, the first observations of naturally occurring oncolytic virus infection can be dated back to the 1800's. During this time, case reports described remission of cancer, often hematological malignancies, when patients were simultaneously afflicted with a viral infection such as influenza[109] or chicken pox[110]. Reportedly, the first studies examining oncolysis in an experimental setting were performed in 1922 with VACV in mouse and rat models, which showed that inoculation with the smallpox vaccine could inhibit tumour growth. In the 1950's, durable remission

of melanoma was noted in a patient after receiving a rabies vaccine, prompting the physician to immunize 12 other patients, two of which underwent remission. At this time, however, it was not understood how or why remission was occurring in these case reports. Our understanding of cancer development over the past century has helped further our understanding of how viruses can be used as therapeutics to treat cancer[111–113]. These developments have allowed OVs to enter the clinic as approved therapeutics in various malignancies. In 2006 a modified adenovirus (AdV)-based OV was approved to treat head and neck cancers in China[114]. A decade later talimogene laherparepvec (T-VEC), a modified herpes simplex virus (HSV), was approved by the FDA to treat melanoma[115,116].

1.2.2 Premise of OV therapy

It has been realized that many of the hallmarks of cancer development, mainly sustained proliferative signalling, evading growth suppressors, dysregulated immune-signalling pathways, and resisting cell death are also the hallmarks of virus infection. In other words, these are favourable states in a cell that permit increased virus infection, and thus a cancer cell provides a hospitable environment to promote virus growth when compared to a normal cell. This preferential replication in cancer cells allows the virus to lyse these cells while sparing normal tissue. The OV progeny can then go on to infect and kill additional tumour cells while simultaneously releasing danger-associated molecular patterns (DAMPs) that recruit immune cells to the tumour site, promoting tumour cell killing and generating an immune response against both the tumour and virus (Figure 1.1). Currently, numerous different viruses have been explored as OVs including, but not limited to VACV, AdV, HSV, measles virus, reovirus, vesicular stomatitis virus (VSV), Maraba Virus, coxsackie virus, Newcastle disease virus (NDV) and poliovirus.

1.2.3 Design of tumour selective OVs

While many viruses are “naturally” oncolytic, that is, wild-type (WT) forms of the virus can be used as anti-cancer agents, most need modifications to impart cancer selective replication as a safety measure. Some viruses, however, preferentially infect and kill cancer cells without any alterations. Examples of naturally oncolytic viruses include reovirus and Newcastle disease virus (NDV). In the case of reovirus, the virus is able to replicate in cancer cells with activated RAS signalling pathways[111]. For NDV, an avian virus, the virus is able to replicate in cancer cells with deficient IFN signalling, and unable to replicate in normal human cells[117,118]. Even WT VACV was shown to be naturally oncolytic in early studies. Nowadays, oncolytic virus development is more intentional, and viruses are designed with the objective of promoting replication in and lysis of tumour cells, while avoiding infection of normal cell tissue. Even oncolytic viruses that do not require genetic modification to preferentially infect and kill cancer cells are being modified and selected to improve its oncolytic potency and to induce improved immune stimulation, which will be discussed in further detail below.

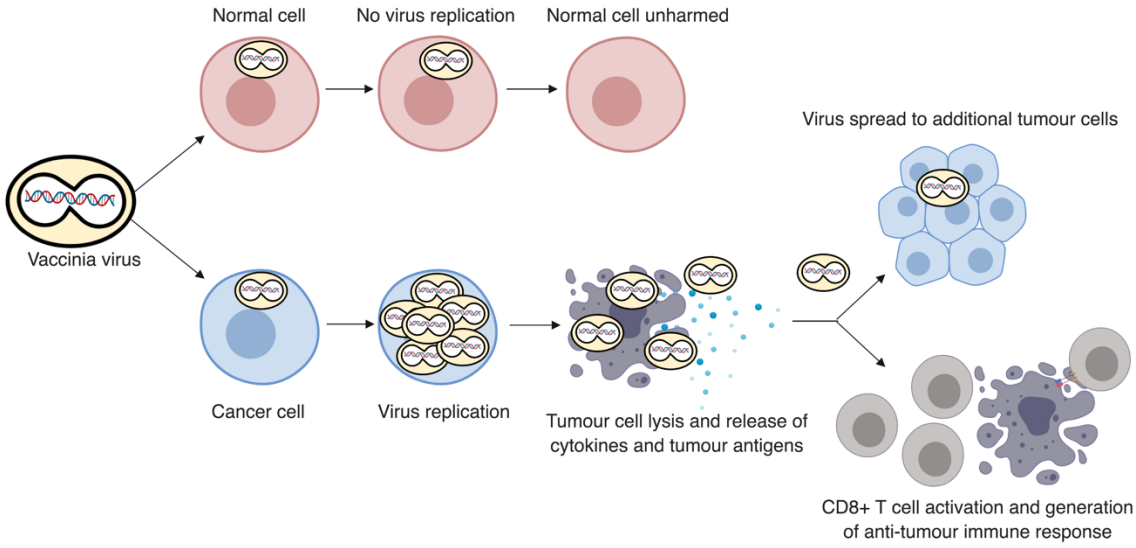

Figure 1.1. Premise of VACV-mediated OV therapy. Adapted from Potts et al., 2018[119]

1.2.4 Oncolytic poxviruses

The origin of oncolytic poxviruses dates back to 1922, when Levaditi and Nicolau demonstrated that the WT VACV of the smallpox vaccine inhibited epithelial tumour growth in mouse and rats[120]. However, the anti-cancer effects of WT-VACV were not universally observed, with mixed results obtained in mouse and human studies[121,122]. In the late 1950's attempts were made to improve the oncolytic efficacy of poxviruses by serial passage of the virus in tumour bearing mice, and while tumour killing was improved, the passaged virus was found to be more toxic to mice and shortened survival[123]. Significant advancements in oncolytic poxvirus research were not reached until recombinant DNA techniques became available, which allowed for targeted and intentional manipulation of the VACV genome[124].

1.2.4.1 Benefits of VACV as an oncolytic agent

After reviewing the literature of OV research available in the 1960's, Dr. Chester Southam stated: "There is no tumour that is uniformly susceptible to oncolysis by all viruses. There is no virus that is uniformly capable of oncolysis against all tumours"[125]. This statement still remains true, and while it is likely that different OVs will be utilized for different purposes and tumour types, where all else is equal, VACV possesses many attributes that make it an attractive candidate for oncolytic virotherapy relative to other candidates:

Rapid cytoplasmic replication cycle: VACV replicates and produces between 4000-5000 new progeny virions per cell as early as 24 hours after infection[126] resulting in cell death within the first 48 hours[16]. The unique cytoplasmic replication feature of VACV, particularly its lack of integration within the host cell genome is an attractive safety prospect. VACV genomic DNA is compartmentally separated from the host cellular DNA, and the two do not mix[127,128]. For comparison,

In the case of oncolytic HSV, viral genomic DNA is maintained as extrachromosomal DNA within the cell which can then integrate into the host genome[129].

Large coding capacity for foreign transgene insertion: The VACV genome is large and malleable. It is amenable to large-scale genomic alterations and deletions. Importantly, VACV can accommodate up to 25 000 bp genomic insertions, and expresses transgenes to high levels[130]. This permits the use of VACV as a vector that can be used to express tumour antigens, cytokines, and other immunostimulatory molecules that are too large to be inserted into smaller and more genomically-restricted candidates.

Stability as lyophilized particle: T-VEC, the oncolytic HSV approved for use by the FDA, was manufactured such that the virus must be shipped on dry ice and received within 96 hours, followed by storage at -80°C, requiring the use of specialized freezers and handling components[131]. Preparations of VACV for smallpox vaccines were freeze-dried as early as the 1950s, resulting in stable doses for up to 20 years or more[132,133]. This lyophilization greatly facilitated the distribution of the vaccine, as a continuous cold-chain was not required to be maintained[134]. VACV's historic past as a lyophilized preparation lends well to its use as an oncolytic, minimizing supply chain and stability issues.

Historic clinical use & known safety profile: Having been used extensively over the past century for vaccination, the safety profile of WT-VACV strains is well documented[134]. Minor side effects include fever, muscle aches, fatigue and pox lesions or rash at the injection site[134], while major adverse events occur at rates of 1 per million vaccinees for death, or generalized vaccinia at a rate of 241 per million vaccinees[134]. Doses for vaccination with WT-VACV can vary between 10^6-10^8 pock forming units, administered once via a percutaneous route[135–137] compared to oncolytics which are administered intratumourally or intravenously in multiple injections up to $3x10^9$ PFU[138–140]. While the safety profile of WT-VACV is known, improvements are still necessary to ensure patient safety.

1.2.4.2 Further improving VACV safety through viral attenuation

While the clinical and safety profile of WT-VACV is known based on vaccination use, one drawback of VACV as an oncolytic agent are safety concerns among immunocompromised individuals. It is important to note, however, that vaccination with VACV occurred with non-modified WT-VACV. While WT-VACV can be considered a naturally oncolytic virus, current VACV-based OVs are genetically modified to permit cancer-selective replication while limiting infection in normal tissues. These modifications attenuate the virus and further decrease its pathogenicity[119,141,142]. Traditionally, oncolytic VACV is created by removal of the thymidine kinase (TK) gene, which minorly attenuates virus replication in normal cells compared to cancer cells. In clinical trials oncolytic VACVs have been shown to be well-tolerated with fever, malaise and nausea being the predominant symptoms[143]. Nevertheless, improvements to the safety profile of oncolytic VACV have been made by further attenuating virus replication. Notably, by deletion of the small subunit of ribonucleotide reductase, encoded by the F4L gene in the virus genome, the safety of VACV was

improved in rat and mouse models of bladder cancer, without decreasing efficacy[119,144]. To increase the safety of oncolytic VACV for use in cancer patients who oftentimes can be immunosuppressed, VACV has been modified to attenuate its growth. These deletions seek to impede virus replication in normal cell tissue, while retaining high growth and cytotoxic properties in normal tissues. The most common attenuating mutations to increase safety in oncolytic VACVs are discussed below.

Thymidine kinase deletion (encoded by J2R gene): A thymidine kinase (TK) deleted VACV was manufactured by deletion of the J2R gene[124] and shown to be less virulent in mice[145]. Thymidine kinase (TK) , also known as the viral J2 protein, is involved in the salvage pathway for deoxythymidine triphosphate (dTTP) synthesis. It was shown that this deletion afforded the virus higher replication in tumour cells when compared to normal tissue[141]. In initial studies, the primary intent of using TK-deleted VACV (which can also be referred to as a ΔJ2R VACV), was as a gene-therapy delivery vector to deliver cytokines to the tumour site[141]. Nowadays, ΔJ2R VACV forms the basis of nearly all oncolytic VACVs designed. The oncolytic VACV that has progressed furthest in the clinic is JX-594, a ΔJ2R VACV encoding the immunostimulatory cytokine GM-CSF. Marketed by Jennerex, JX-594 was granted orphan drug status by the FDA, and, at the time of writing, has 18 clinical trials registered with the NIH. (https://clinicaltrials.gov/ct2/results?cond=&term=JX-594&cntry=&state=&city=&dist=).

VGF deletion (encoded by C11L gene): The C11L gene, which encodes for the vaccinia growth factor (VGF) is another gene that can be targeted for deletion to reduce virulence[146]. VGF has amino acid sequence similarity to epidermal growth factor (EGF), and competes with EGF for binding to its receptor[147]. As a mitogen, this protein induces the cell to proliferate, promoting virus growth. When deleted from the VACV genome, virulence is attenuated as the virus' ability to induce a favourable replication state in the cell is diminished. In cancer cells with continuous proliferation, the VGF function is redundant and VACV replication is sustained despite the absence of VGF, making a VGF-deleted virus (ΔC11L) a viable mutant for safety in oncolytic applications of VACV[148]. Dose escalation studies for VACV containing deletions of both the VGF and TK genes were unable to establish a maximum tolerable dose since the treatment was well tolerated[138]. While safety is improved through removal of J2R, it was documented to cause vaccinia necrosum lesions in some patients, which eventually clears and is indicative of virus replication[139].

Ribonucleotide reductase deletions (encoded by F4L and I4L genes): Ribonucleotide reductase (RR) enzymes catalyze the de novo synthesis of deoxyribonucleotide triphosphates (dNTPs) to use for DNA synthesis and is critical for cell proliferation. VACV encodes the viral homologs of cellular RR proteins, F4 and I4, encoded by the F4L and I4L genes, respectively. These proteins function to provide dNTPs for virus replication. Previous work in the Evans' laboratory demonstrated that deletion of the F4L gene from the VACV genome was found to further attenuate VACV growth relative to a ΔJ2R mutant alone in normal cells, while retaining high replication in cancer cells[149]. This virus was safer in immune-deficient mouse models of bladder cancer compared to ΔJ2R VACV, while retaining similar treatment

efficacy[119]. This is particularly relevant, as a widespread concern of using replicative poxviruses as cancer therapies is the perceived safety risk in immunocompromised cancer patients. Although research in the Evans' lab demonstrated that it was the F4 subunit as opposed to the I4 subunit that was critical for attenuation[149], research groups have also introduced deletions in the I4L gene to provide an additional level of safety[150,151].

1.2.4.3 Methods to improve the efficacy of OV therapy

While safety considerations have largely been addressed through the virus-attenuating modifications described above, efficacy is the primary hurdle which now needs to be improved prior to large-scale adoption in the clinic. Methods to improve the potency of VACV therapy generally focus on 3 different strategies: encoding therapeutic payloads, deletion of virally-encoded immunomodulatory genes, and combination with additional therapies[12]. Other VACV modifications being employed for various purposes in cancer research include theranostic and imaging applications, which are reviewed in Rojas and Thorne, 2012[152].

Encoding therapeutic payloads : In the early 2000's VACV was originally intended to be used as a gene therapy vector to deliver therapeutic cytokines to the tumour site[148]. This has continued to be a prevalent strategy to increase the anti-cancer effects of oncolytic VACV, and various transgenes have been inserted into the virus for expression at the tumour site. This has included pro-drugs[153], immune-stimulating cytokines[148,154], tumour antigens[155,156], and most recently, therapeutic antibodies[157–159]. This strategy has a dual impact on the tumour cell, where the virus promotes oncolysis and immune stimulation, and the inserted transgene can exert additional enhancing effects often with the intent of synergizing with the OV. A recent review highlighting different therapeutic payloads which have been inserted into VACV can be found in Pelin et al., 2020[10].

Deletion of genes to improve immunogenicity : As discussed above, immune modulation is a key feature of VACV, and VACV devotes a large portion of its coding capacity to produce proteins that inhibit host immune responses. A frequently employed strategy to improve immune stimulation in response to OV therapy is to remove or delete one or multiple of these immune-modulating genes[12,160]. For example, GLV-1h68, an experimental OV developed by Genelux corporation, has removed the VACV hemagglutinin protein, A56R, to aid in evasion of complement, or deleting B18R to promote IFN signalling, among others[160–162]. This strategy has also shown promise for enhancing immune responses to vaccinia-vectored vaccine candidates[39,45,163]. However, one potential *caveat* of this strategy is striking an appropriate balance between immune-stimulation and viral clearance[10]. If too many immune suppressing genes are removed, the virus may be targeted for clearance more readily before appropriate anti-tumour immunity is established. This possibility was explored in vaccine studies where Geoffrey Smith's group demonstrated that deletion of four immune-stimulating genes simultaneously resulted in decreased efficacy with vaccines delivering HIV-antigens due to increased viral clearance[164]. Nevertheless, this strategy is being investigated to improve the oncolytic potential of VACV backbones in OV research[10,12].

Combination with additional therapies: To increase efficacy, oncolytic VACV has been combined with numerous other forms of cancer treatment in pre-clinical models such as surgery[165], radiation[166,167], chemotherapies[168] and other immunotherapies[169]. In some cases, such as when combined with surgery, the principal objective is to remove or debulk the primary tumour mass, and the addition of VACV is used to stimulate an immune response. When combined with chemotherapies or immunotherapies, the selection of drug combination is strategic by targeting complimentary mechanisms of action[170]. For instance, when combined with immunotherapies such as checkpoint blockade, the rationale is that pre-treatment of a tumour with VACV would recruit immune cells to the tumour, followed by treatment with immunotherapies that further enhance or stimulate the immune cells which have been recruited by the virus. It is becoming increasing recognized that OVs will likely be used most often in combination therapy approaches as opposed to single agent treatment[11,170,171].

1.2.4.4 Mechanism of action of VACV oncolytics

Oncolytic VACV works to kill cancer cells through a variety of mechanisms. The most well understood mechanism of action is through the direct lysis of tumour cells caused by virus infection resulting in cell death. Progeny virions are then released to continue the cycle in remaining tumour cells. VACV can also mediate tumour destruction through targeting of tumour vasculature to impede blood supply[144,172,173], and infecting and killing cancer stem-like cells that contribute to tumour growth[144]. Although these mechanisms contribute to tumour death, initiation of an anti-tumour immune response is largely regarded as the most relevant mechanism of action for OVs[174]. VACV initiates a strong and robust immune response leading to an "in situ" cancer vaccine effect where the presence of the virus stimulates and recruits immune cells to the tumour site, leading to anti-tumour immunity and cancer cell destruction[175]. This anti-tumour immunity is durable and systemic, oftentimes leading to eradication of secondary tumour lesions at non-injected tumour sites. This attribute of immune-mediated tumour clearance classifies oncolytic VACVs as an emerging form of cancer therapy known as immunotherapy.

1.3 Cancer immunotherapy

Cancer immunotherapy is a form of cancer treatment whereby a patient's own immune system is stimulated to target and eliminate cancer cells. Underlying the basic principles of cancer immunotherapy is the tumour immune-cell microenvironment (TiME) and tumour immunology, which will be discussed below.

1.3.1 Tumour-immune cell microenvironment

Immune cells within the TME play an important role in tumor development and progression. The concept of cancer immunoediting suggests 3 phases of cancer development in relation to the immune system: Elimination (sometimes referred to as immunosurveillance), equilibrium and escape[176]. Each state is a reflection of the interplay between anti-tumour actions of the immune system, and the tumorigenesis and growth of the cancer cells. In the

elimination phase, the immune system is capable of monitoring and sufficiently eliminating tumour cells. In the equilibrium phase, anti-tumour immune cells are keeping tumour growth at bay and suggests on ongoing battle between the immune system and cancer. In the final phase, "escape", the tumour cells, with assistance from the suppressive TME, are able to evade and outgrow the immune response through generating resistance, with the tumour declaring victory. It is the cells in the TiME that mediate these stages, with some of the major contributors described below and shown in Figure 1.2.

CD8+ T cells: CD8+ cytotoxic T lymphocytes (CTLs) are considered to be the major effector population of cells directly targeting and eliminating tumour cells[177]. CD8+ T-cells recognize cognate antigen when presented by MHC-I molecules. T-cell receptor (TCR) engagement of CD8+ T cells with antigen is the first signal for activation and proliferation, but a secondary co-stimulatory signal by antigen-presenting cells (APCs) is also required whereby CD80/86 on APCs engages CD28 on CD8+T cells[178]. When activated, CD8+ T cells release granzyme B and perforin which induce apoptosis in target cells[179] and can also produce IFN-γ and tumor necrosis factor α (TNFα). Upon T cell activation, various cell surface markers are upregulated at different stages in the activation process which can be used to identify activated T-cells within the TME. The earliest activation marker is CD69, which is an inducible cell surface glycoprotein and plays a role in the proliferation and survival of activated T cells[180]. Furthermore, upon T cell activation, cells express various checkpoint molecules such as PD-1 or CTLA-4 that limit or restrict their responsiveness, which is discussed in further detail in section 1.3.2.

CD4+ T cells: CD4+ T cells, also known as T helper cells, recognize cognate antigen presented in the context of MHCII molecules. T helper cells are critical for supporting and directing the actions of other immune cell subtypes through the production of cytokines and inflammatory mediators. In the context of tumour immunology, IL-2, I IFN-γ and other cytokines secreted by CD4+ T cells are important mediators of CTL priming and proliferation. CD4+ T helper cells are capable of directing and assisting in the activation of CD8+ T cells via cross presentation by DCs. CD4+ T cells also provide co-stimulatory signals to B cells for activation.

T-regulatory cells: A subset of CD4+ T cells that express CD25 and intracellular FoxP3 are known as T regulatory cells (Tregs) and exert potent immune-suppressive functions to maintain self-tolerance. These cells antagonize the antitumour activities of tumour-clearing immune cells, primarily CD8+ T cells, by expressing high levels of co-inhibitory molecules such as cytotoxic T lymphocyte antigen 4 (CTLA-4), depriving the TME of IL-2 which is important for CTL proliferation[181], producing immunosuppressive cytokines, and can directly trigger apoptosis of T-cells[89,182–184].

Dendritic cells (DCs): DCs function as antigen presenting cells (APCs) that cross-present antigens to CD8+ T cells and provide critical co-stimulatory signals for activation such as CD80/CD86 (also known as B7-1 and B7-2, respectively)[178].

Cytokine expression by DCs allows activated CTLs and other immune cells to migrate into proliferate within the tumour[177].

B-lymphocytes: B lymphocytes/ B cells are adaptive immune cells that recognize circulating antigen and produce antibodies in response[185]. B cells can produce cytokines to direct the activity of CTLs and function as APCs. While they have been identified in infiltrating tumours, B cells play debated roles in tumour clearance and their specific subtypes and effector functions have yet to be elucidated[177].

*Natural Killer (NK) cells***:** NK cells are part of the innate immune response and recognize cells based on molecular patterns as opposed to targeted and antigen specific recognition by CTLs. NK cells induce apoptosis in target tumour cells via production of perforin and granzyme B. NK cells have largely been implicated in the "immunosurveillance" stage of tumour progression, and work to identify and eliminate newly transformed cells, however, their killing-function is rapidly inhibited within established tumours[186].

Myeloid-derived suppressor cells (MDSCs): Although only recently characterized, MDSCs have been implicated as a major immunosuppressive cell population in cancer. These cells are of myeloid origin and exist as either monocytic (M-MDSCs) or polymorphonuclear (PMN-MDSCs), also known as granulocytic (G) MDSCs. Both types exert broad immunosuppressive action and limit the functional activity of CD8+ T cells in the TiME. This suppression occurs through the production reactive oxygen species and nitric oxide, high levels of arginase-1, and immunosuppressive cytokines[187]. In an experimental setting in mice, MDSCs can be identified by cell surface expression of $CD11b^{+}$ $Ly6C^{+}Ly6G^{-}$ for M-MDSCs and $CD11b^{+}Ly6C^{mid}Ly6G^{+}$ for PMN-MDSCs[188].

While the cell types listed above may be considered primary targets of immunotherapy research based on their contributions to immunosurveillance, many other cell types and features contribute to the TME which were not included for review. These additional factors include other cell populations such as tumour associated macrophages (TAMs) and neutrophils, tumours vasculature and endothelial cells in the TME, and secreted cytokines, signalling and metabolic factors surrounding the tumour. These features are reviewed by Lei et al.,2020, [177] and Labani-Motlagh *et al*.,2020[189].

Further details about how these cell types within the TME contribute to prognosis and treatment of breast cancer is discussed in section 1.4.3.

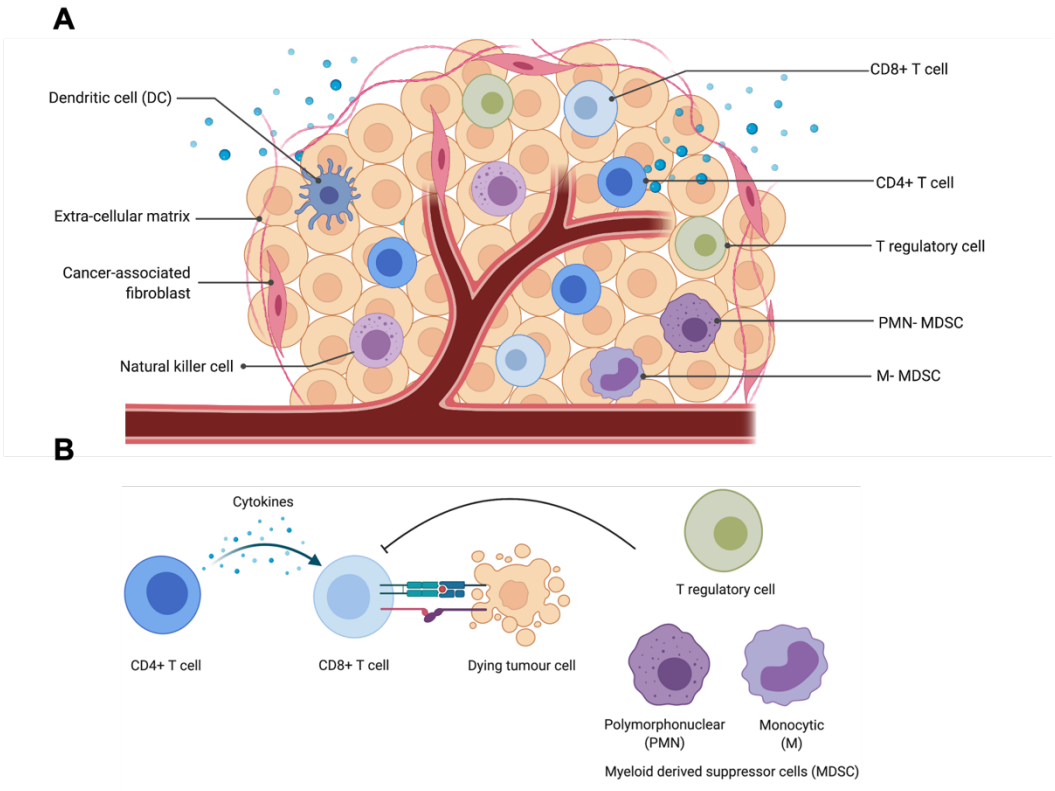

Figure 1.2. The tumour microenvironment (A) and immune cell subtypes and their functions studied in this thesis (B).

1.3.2 Immune checkpoints

An important consideration in cancer immunotherapy and the TiME is immune checkpoints, particularly with respect to CTL inhibition. Checkpoints are a critical negative regulator of T cell activation that limit autoimmune reactions by shutting down the functional activity of T-cells and other immune cells. However, these checkpoints contribute to immunosuppression within the TiME allowing for resistance to immune-mediated clearance[190]. Two of the most extensively studied immune checkpoints are CTLA-4 and programmed cell death 1 (PD-1)[178]. In the case of CTLA-4, when presented on CD8+ T cells, interferes with the binding of CD28 to CD80/86 on APCs, and prevents activation and proliferation[178,191,192]. PD-1 signalling involves the interaction of PD-1, expressed on activated T-cells[193], with its ligand programmed death ligand 1 (PD-L1), also known as B7-H1, expressed on tumour cells or other immune cells[190]. When PD-1 on T-cells engages with PD-L1 it induces a state of exhaustion exhibited by T-cell dysfunction. This exhausted state is characterized by decreased cytokine production, proliferation, and survival and overall functions to antagonize the action of CTLs against tumour antigens[194,195]. Tumours can upregulate PD-L1 on the cell surface causing T-cell apoptosis[196]. While CTLA-4 and PD-1 are the most well recognized immune checkpoints, additional negative regulators are continually discovered with more recent checkpoint molecules of therapeutic focus being LAG-3, TIGIT, TIM-3, IDO and VISTA, among others[190].

1.3.3 Clinical development of cancer immunotherapies

Cancer Immunotherapy utilizes the existing knowledge about the tumour microenvironment to stimulate immune cells, primarily CD8+ T cells, to attack and kill cancerous cells. This involves strategies to both activate and retarget T-cells to tumours and overcoming the effects of the suppressive TiME/ immune checkpoints. The history of cancer immunotherapy dates back to the late 19th century with the experimental use of Coley's toxin to treat tumours, however, the success of radiotherapy and chemotherapy at the time resulted in these two strategies becoming the primary pillars of cancer treatment alongside surgery[197]. Recent advances in cancer immunotherapy research, mainly the use of immune checkpoint inhibitors, have shown unparalleled success in previously untreatable cancers such as malignant melanoma. Immunotherapy is now considered the fourth pillar of cancer immunotherapy[198].

While oncolytic viruses are an up-and-coming form of immunotherapy, the predominant form of cancer immunotherapy used in the clinic is currently immune checkpoint blockade/ immune checkpoint inhibitors. Immune checkpoint blockade therapy re-stimulates T-cell function by blocking or inactivating regulatory receptors that inhibit anti-tumour activities. Typically, this involves the use of monoclonal antibodies that bind to immune checkpoints to prevent interaction with target ligands, such as CTLA-4[199], PD-1 or PD-L1[198]. The first immune checkpoint blockade therapy approved by the FDA was ipilimumab, a monoclonal antibody that binds to CTLA-4 and prevents it's inhibitory binding to CD80/86 allowing the CTL to regain its tumour-killing action[199]. Blocking antibodies for the PD-1 signaling axis either using monoclonal antibodies directed at PD-1 or PD-L1 were soon to follow and demonstrated success in treating multiple tumour types[200,201]. Pembrolizumab, a monoclonal antibody targeting PD-1 was approved by the FDA in September 2014 in the treatment of metastatic melanoma, quickly followed by the approval of in nivolumab, another anti-PD-1 antibody marketed by Bristol-Myers Squibb in December 2014[202].

While checkpoint inhibitors are the most clinically utilized drugs, other immunotherapeutic strategies exist that have also achieved unparalleled success in different malignancies. Adoptive cell therapy (ACT) involves the *ex vivo* manipulation of a patient's own immune cells which are then infused back into the blood[198]. Chimeric antigen receptor T-cells (CAR-T) involves genetically modifying patient T-cells isolated from the blood and inserting a receptor to target a specific antigen of interest. Kymriah and Yescarta, the first two CAR-T therapies approved by the FDA, both have CARs targeting CD19, expressed on B-cells. This allows CD19-targetting CAR-T therapies to eliminate B-cell malignancies with unprecedented specificity[198]. Other types of immunotherapy include bi-specific T-cell engagers[203], NK-cell engagers[204], cancer vaccines, and of course, oncolytic viruses.

1.3.4 Current successes of immunotherapy

Checkpoint inhibitors have yielded the biggest therapeutic advances in metastatic melanoma. Prior to the introduction of immunotherapies, the median survival of patients with advanced melanoma was 9 months in 2010[205]. The introduction of ipilimumab now allowed a small fraction of patients to undergo long term remission[206,207]. Anti-

PD-1 therapy then provided a secondary option for CTLA-4 refractory metastatic melanoma and showed improved safety and efficacy relative to CTLA-4 blockade. Checkpoint inhibitors against both pathways can be used in tandem to achieved further enhancements. In 2019, the median survival for metastatic melanoma is now over 3.5 years[205]. This therapeutic success has been translated to other malignancies where PD-1 axis blockade has achieved success in treating non-small cell lung cancer (NSCLC), bladder cancer, head and neck cancer, ovarian cancer, among many others[208–212]. With respect to CAR-T therapies, successes have been observed in hematological malignancies such as leukemia, lymphomas, and myelomas, particularly in the paediatric population[212–215].

1.3.5 Challenges & opportunities in cancer immunotherapy

Despite the success of current immunotherapeutic interventions, there are opportunities for improvement. Safety is still an issue with immunotherapies, and efforts are underway to circumvent the negative and sometimes serious adverse events observed[212,216]. Primarily these efforts are focused on using combination immunotherapies with the intent of synergizing anticancer effects while strategically limiting adverse reactions (ARs)[177,205,212]. As not all patients respond to immunotherapies, efforts are underway to both understand why this occurs and to develop novel immunotherapeutics with alternative mechanisms, oftentimes with the intent of activating or promoting different elements of the immune response to synergize together. For instance, it is proposed that virotherapy will be used to stimulate and convert non-immunogenic tumours to immunogenic forms that will then be rendered susceptible to other immunotherapies like checkpoint blockade[212]. Increased research and efforts are being directed at the development of predictive biomarkers for responses to immunotherapy to better direct treatment strategies[178,202,212]. As immunotherapy targets the immune system as opposed to a distinct tumour type, this strategy is thought to be applicable to most cancer types. Despite this, response rates of immunotherapy between tumour types are broad and variable. For instance, in analyzing the benefit of immune checkpoint blockade for different tumour types, the biggest cancer-specific benefit was observed in NSCLC, with a 4.67% increase if >50% of the tumour was PD-L1+. This is in comparison to other tumour types like Merkel cell carcinoma and cervical cancer with cancer-specific benefits of 0.05% and 0.1%, respectively[217]. Other solid tumours have been challenging to treat with immunotherapies, such as brain, colorectal, prostate and breast cancer and are an ongoing focus of research[218].

1.4 Breast cancer & standards of care

Approximately 1/8 women are expected to develop breast cancer in their lifetime, with 1/33 dying due to disease[219]. Treatment options and prognosis vary depending on the type, size and location of the tumour[219], but oftentimes surgery and radiation are used as a first line treatment[219]. Surgery can consist of breast-conserving surgery, mastectomy, and lymph node removal[220]. Radiation therapy (RT) often follows surgery, for instance, in early stage cancer lumpectomy is followed by whole breast RT[221]. Further details describing radiation therapy can be found in section 1.4.4.

1.4.1 Breast cancer subtypes and additional treatment regimens

Depending on the sub-type of breast cancer, following surgery and/or radiation, adjuvant or additional treatments are used. There are currently 4 different subtypes generally recognized: Luminal subtype A, luminal subtype B, human epidermal growth factor receptor 2 (HER2) overexpression, and basal-like[222–224]. A previous molecular subtype known as "normal-like" has since been removed from subtyping categories and is not included in this review[225].

Luminal A&B: Luminal breast cancers are estrogen receptor (ER) positive, and further classified into subtypes A and B based on expression of progesterone receptor (PR), HER2, and the proliferative marker Ki67. Luminal A cancers are ER+, +/- PR, HER-, Ki-67^{lo}, while luminal B are ER+, PR+ HER2+ and Ki67^{hi} [223,226,227]. As these tumours are hormone-receptor positive, first-line treatment is hormone therapy, with luminal A benefitting from combined endocrine therapy and luminal B typically treated with concurrent chemotherapy[223,228]

HER2 Overexpression: The HER2 overexpression subtype represents 10-15% of breast cancer cases and is characterized by overexpression of human ERBB2/HER2, which is known to promote tumour proliferation and inhibit apoptosis[223,229] Tumours overexpressing HER2 typically have a poorer prognosis compared to the luminal subtypes and are often sensitive to anthracycline and taxane neoadjuvant chemotherapy. Trastuzumab (Herceptin®), a therapeutic antibody that binds to HER2 on cancer cells slows tumour progression when combined with standard chemotherapy compared to chemotherapy alone in metastatic HER2 overexpressed tumours, and is approved by the FDA[223,230].

Basal-like: Basal-like breast cancer is ER-, PR- HER2-, with high expression of basal cell markers, high proliferative gene expression[222] and mutated p53 status[224].Lack of ER, PR and HER2- classifies these tumours as triple negative breast cancer (TNBC), known for aggressive growth, and are difficult to treat[231]. Typically TNBC is treated with cytotoxic chemotherapy, but because of the lack of targeted therapeutic treatments for TNBC this is a common target for breast cancer research[223].

1.4.2 Animal models of breast cancer

Various model systems exist to study breast cancer in a laboratory setting to conduct pre-clinical testing of novel therapies. Murine models for breast cancer can be generally categorized as xenograft or syngeneic models. In xenografts, passaged or patient-derived human cancer cells are injected into immune-deficient mice. While commonly used to assess chemotherapeutics, these xenograft models are of limited utility for immunotherapeutic studies, as the immune system in these models is impaired to prevent tumour rejection. Syngeneic models are cancers of mouse origin (either chemically/ virally or radiation induced or genetically modified) in an immune-competent mouse, enabling for immune analysis. In the studies performed throughout this thesis immune competent mammary fat pad (i.e., orthotopic) breast cancer models were used to allow for contributions of the immune system to be assessed. Two

different models known at TuBo and 4T1 tumours were used in these studies which resemble human HER2 overexpression and TNBC, respectively (Figure 1.3).

TuBo model: TuBo tumors are derived from a mammary carcinoma of HER2/*neu* transgenic mice, and therefore over-express rat HER2/*neu*[232] to resemble HER2/*neu* overexpressing tumours in humans. In BALB/c mice, rat HER2/*neu* is a foreign antigen permitting CD8+ T cell targeting to the tumour with specificity to the HER2/*neu* epitope. Experimentally, anti-HER2/*neu* targeting T cells can be quantified and studied in this model by various assays, such as tetramer staining to detect CD8+ T cells with TCR targeting HER2/*neu* epitopes, or functional studies by HER2/*neu* peptide stimulation[232,233]. The presence of increased lymphocyte infiltration and T-cells that target a cancer epitope classify TuBo tumours as an immunogenically "hot" mammary tumor model[234]. TuBo tumours are also characterized by relatively slow growth with no ability to form metastasis[235].

4T1 model: The 4T1 tumor model is derived from a spontaneously arising BALB/c mammary tumor. It is considered to be is poorly immunogenic with low inflammation, and therefore immunogenically "cold"[236]. We can find no reports of 4T1-specific neo-antigens that can be used to detect tumor-specific T-cell responses in this model. 4T1 tumours do not express ER, PR, or HER2/*neu* and are representative of TNBC in patients. 4T1 tumours spontaneously metastasize to the lungs and liver, which is analogous to human metastatic disease spread[236,237]. Experimentally, the resistance of 4T1 cells to 6-thioguanine allow for quantitative assessments of metastasis to the lungs, allowing this parameter to be studied easily in murine models[237].

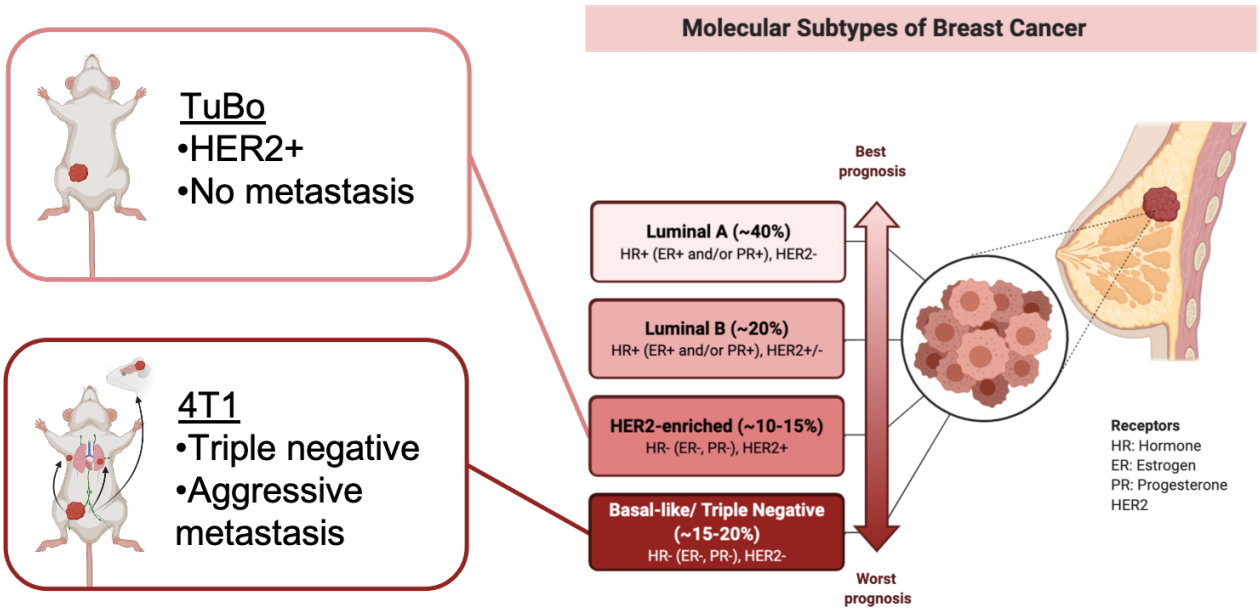

Figure 1.3 Animal models and molecular subtypes of breast cancer used in the current study. Figure adapted from template available on BioRender.com

1.4.3 Breast cancer immunology & immunotherapy

Breast cancers are generally regarded as immunogenically "cold" tumours, meaning they have less immune cell infiltration and do not respond as strongly to immunotherapy compared to "hot" tumours with high numbers of tumour infiltrating lymphocytes (TILs). The TME varies between breast cancer subtypes due to hormonal contributions, somatic mutation rates, and immune cell recruitment. As such, data regarding the prognostic value of immune cells in breast cancer is conflicting. Pre-existing TILs, primarily CD8+ T cells, are considered good prognostic indicators for immunotherapy for TNBC and HER2+ breast cancer[238,239]. The data are less clear when considering CD4+ T cells, likely due to the complex composition of CD4+ cells, which can consist of Th1, Th2 and Th17 subtypes with differing functions and cytokine production[240]. For instance, estrogen exerts immunosuppressive effects on the TME by polarizing CD4+ T cells to a Th2 rather than Th1 effector phenotype which directs humoral versus cell mediated immunity[241]. As part of the innate immune system, NK cells are another powerful ally in the fight against breast cancer. While particularly important for combating tumours in the early stages of development in the immune surveillance phase, NK cells have also shown efficacy in reducing tumour growth and metastasis[242]. NK cells were correlated with improved responses in breast cancer patients receiving neoadjuvant chemotherapy[242], however studies have suggested that the cytotoxicity of NK cells is reduced in progressive disease, limiting their anti-cancer abilities in advanced breast cancer[243].

While CD8+, CD4+ and NK cells are favourable in the TME of breast cancer, a high amount of immunosuppressive cell types are known to become enriched in breast cancer. Tregs, MDSCs and other immune-inhibitory molecules and metabolic factors dampen the positive effects of CD8+ and CD4+ T cells[223]. Studies have demonstrated that breast cancer cells themselves can recruit Tregs, MDSCs, and suppressive macrophages to yield a tumour-promoting habitat[244,245]. High levels of Tregs, which use a variety mechanisms to dampen CD8+ mediated immune responses, were significantly associated with decreased patient survival[246], although differences were found to exist between the molecular subtypes[247]. Nevertheless, breast cancers with a higher ratio of CD8+ T cells to Tregs were found to be associated with improved survival in a meta-analysis that included 5183 breast cancer patients[248]. In TNBC high levels of Tregs, MDSCs, and PD-1/PD-L1 are a significant barrier to overcome for the successful use of immunotherapy[249]. In addition to the immunosuppressive functions of MDSCs described in section 1.3.1 the presence of MDSCs facilitates the progression of metastasis[250]. It was demonstrated that patients with lower levels of circulating MDSCs had a higher probability of favourable treatment outcomes in a clinical trial assessing adjuvant chemotherapies in HER2+ breast cancers[251].

Further contributing to the complexities of the TME, breast cancers are typically recognized as being less immunogenic in terms of neoantigen development compared to melanoma or NSCLC, which have high somatic mutation rates which allow CD8+ T cells to target and become activated against specific cancer epitopes[252,253]. While the overall mutational burden is lower in breast cancer compared to other tumours, in practice, it is difficult to make

generalized conclusions, as the breast cancer subtypes each have different average somatic mutations rates[254]. For instance, hormone receptor + (luminal) breast cancers have the lowest mutational burden, with HER2 and basal-like having a higher mutation rate[253,255,256]. There are also various mechanisms of escape that allow breast cancer to evade the immune system. Common mechanisms of resistance and escape by breast cancers include resistance to cell-mediated cytotoxicity, loss of tumour antigens through MHC I downregulation, and loss of antigen processing machinery[223].

It is for these reasons that immunotherapy for breast cancer treatment has not achieved the same level of success for patients when compared to other solid tumour types such as melanoma and NSCLC. That being said, in 2019 the FDA approved the first checkpoint inhibitor for breast cancer when combined with nab-paxitaxel in metastatic TNBC patients[253]. While progress has been made, immunotherapy in breast cancer has yet to reach its full potential[253].

1.4.4 Radiation therapy and immune responses in breast cancer

Radiation therapy (RT) is one of the most commonly used treatment options in cancer and can be delivered by a variety of mechanisms. For breast cancer treatment in Canada, RT is delivered using an external beam to direct radiation to the tumour site[220]. The Ionizing radiation (IR), delivered via either gamma or X-rays, causes DNA damage either directly or indirectly through the production of free radicals to cause dsDNA breaks[257]. Apoptosis is the primary outcome of radiation-induced DNA damage, however the cell can also die through mitotic catastrophe and genomic instability[258]. In some instances, irradiated cells can progress to stress-induced cellular senescence, which is the a permanent arrest of cell division[259]. These senescent cells can contribute to remodelling of the TME through the production of proinflammatory cytokines, and can contribute to radio-resistance in neighbouring cells[259].

While the mechanism of action of RT has traditionally been attributed to the DNA-damage response, in recent years, evidence has emerged that the immune response is also a critical component for the efficacy of RT. In some instances, RT leads to abscopal effects in patients, where targeted radiation of once tumour site leads to regression in distant nodules. Indeed, it has since been shown that radiation can impact both innate and adaptive immune responses to contribute to anti-tumour immune responses[260]. Innate immune responses to radiation have been examined in recent years and are known to induce downstream CD8+ T cell responses (reviewed in Storozynsky and Hitt, 2020[260]). Type I IFN, in particular, was shown to be indispensable for anti-tumour immune responses generated in response to radiation therapy [261]. Further aiding in the adaptive immune response, the drastic damage to cells caused by radiation results in the release of tumour antigens for uptake and cross-presentation by DCs to CD8+ T cells, allowing RT to function as an *in situ* cancer vaccine[262].

While anti-tumour immunity induced by radiation alone has been documented, the occurrence of abscopal effects in patients is considered rare, and more typically observed in immunogenic tumours such as renal and hepatocellular carcinoma, and melanoma[263]. Improved responses rates have been observed in the clinic when radiation is combined with other immunotherapies, and efforts are underway to improve anti-tumour immune effects by combining radiation with other forms of immunotherapy for breast cancer[263–265]. In clinical trials, breast cancer has been combined with numerous immune check point inhibitors with promising results[263]. Previous studies have reported benefits to OV therapy when combined with radiation[166,167,266–268]. Future studies are needed to inform better combinations of immunotherapies with radiation to improve abscopal effects, and to determine optimal radiation treatment schedules (i.e. fractionated or non-fractioned treatment, dose intensity, etc.) which can enhance strategic drug combinations[263].

1.4.4.1 Future directions for breast cancer immunotherapy

The approval of a checkpoint inhibitor therapy to treat breast cancer in 2019 suggests that immunotherapy holds potential in treating breast tumours, particularly HER2+ and basal-like cancers with higher somatic mutation rates and where new treatment options are needed. Two primary areas of interest for breast cancer immunotherapy research are finding ways to make "cold tumours" (i.e. those with low levels of infiltrating T cells) "hot" by recruiting T cells to increase the immune response, and also as combination therapy with existing standard of care agents just as chemotherapy or radiation[202,223]. Oncolytic viruses are known for robust immune-stimulation and recruiting T cells to the tumour site, and likely hold promise for treating breast tumours. However, further research into the use of oncolytic VACV in breast cancer treatment is necessary.

VACV has been tested in various stages of clinical development for breast cancer with promising results. In pre-clinical studies, where treatments are tested in animal models, various modified VACVs (with different gene deletions, transgenes inserted, and combination studies) have demonstrated appreciable levels of success[269–279]. In human testing, at the time of writing, VACV has been tested in 10 phase I studies designed to test the safety of an investigational new drug, and to establish dosing[280]. Where results are posted, the virus treatment was shown to be safe at all doses, and in some instances clinical responses were observed[281,282]. Phase II studies, which recruit larger numbers of participants, test for efficacy and side effects. VACV has been trialled in 7 studies, with one currently recruiting testing a combination of VACV with pembrolizumab (anti-PD-1 antibody) in solid tumours[283]. Phase III studies are used to determine a drug's therapeutic effect in a large cohort of patients, while simultaneously testing safety. There are currently no registered Phase III trials testing VACV in breast cancer patients. While the promising pre-clinical results are encouraging, this lack of late-stage trials emphasizes the need for further research in this area to develop novel VACVs better suited to treat breast cancer.

1.5 Rationale of the project

VACV has shown promise as an oncolytic agent for treating a variety of tumour types, with preliminary results suggesting that this strategy holds promise for treating breast cancer. Our lab has previously modified VACV by deleting virally-encoded enzymes responsible for dNTP production[149]. Specifically, the F4L gene (ΔF4L), responsible for *de novo* dNTP synthesis, and the J2R gene (ΔJ2R), responsible for dTTP salvage, have been deleted from the VACV genome (ΔF4LΔJ2R VACV)[119]. These mutations increase viral specificity for replication in cancer cells, presumably due to elevated levels of these enzymes in tumours caused by rapid growth[119,149]. While this modified VACV was effective in treating orthotopic bladder cancer in rats and mice, only limited therapeutic benefits were observed in mouse models of breast cancer[144]. This project further investigated the use of VACV as a breast cancer immunotherapy. Specifically, after determining optimal VACV production protocols and establishing maximum dosing in breast cancer models (Chapter 3), I sought to improve the efficacy of VACV therapy by two separate methods. In the first method VACV was combined with image-guided radiation therapy (IG-RT) (Chapter 4 & 5). In chapter 4, I found that despite synergistic interactions *in vitro*, the combination was shown to be antagonistic *in vivo*. I then attempted to investigate the cause of this antagonism by investigating TME changes in response to combination therapy (Chapter 5). In the second method tested (Chapter 6 & 7) I created next generation oncolytic VACVs by removing genes from the VACV genome that inhibit the immune response of the host, with the objective of improving treatment efficacy. I compared multiple different VACVs for their treatment efficacy (Chapter 6) and their capacity to modulate the TiME (Chapter 7).

1.5.1 Data chapter overviews

Chapter 3-Production and quality assessment of vaccinia virus stocks of pre-clinical grade purity and high infectivity for oncolytic immunotherapy studies

- In this chapter production methods of VACV stocks were assessed and maximum dosing limits were established in our murine breast tumour models.

Chapter 4- Combining image-guided radiation therapy (IG-RT) with oncolytic VACV antagonizes breast tumour clearance despite *in vitro* synergy

- I investigated the impact of combining IG-RT with ΔF4LΔJ2R VACV *in vitro* and *in vivo* models.
- *In vitro*, the two therapies synergized to result in improved cell killing.
- *In vivo*, antagonism occurred and survival of combination-therapy treated mice was shorter than after radiation treatment alone.

Chapter 5- Combining IG-RT with oncolytic VACV changes the tumour immune cell microenvironment

- In an attempt to deciper the mechanisms behind the antagonism between radiation and IG-RT, in this chapter I performed an immune analysis of mice treated with the different therapies.
- I found that combination treatment increased both immune stimulation and immune exhaustion in the TiME.
- Immune checkpoint blockade was introduced to circumvent immune exhaustion, however this did not abrograte antagonism.

Chapter 6-Anti-cancer efficacy of immunomodulatory gene-deleted oncolytic VACVs in breast cancer models

- As a strategy to enhance the therapeutic effectiveness of VACV, I created a panel of immunomodulatory VACVs with targeted genomic deletions encoding VACV proteins that modulate host immune responses.
- I performed *in vitro* assessments of the cytotoxic effects of these viruses and tested their efficacy in syngeneic immune competent breast cancer models to determine if any particular deletion pathway resulted in improved therapeutic outcomes.

Chapter 7-Tumor immune-cell microenvironment alterations of immunomodulatory gene-deleted oncolytic VACVs in breast cancer models

- In Chapter 7 I determined how the viruses produced in Chapter 6 impacted host immune responses in murine breast cancer models.
- I investigated splenic and tumour-infiltrating immune cell populations to determine if and how each immunogenic gene-deleted VACV impacted anti-tumour immunity.

Collectively, this project adds to the body of literature dissecting the immune-mediated responses by modified VACV for breast cancer treatment. It helps refine stratgies for improving oncolytic immunotherapy in breast cancer by providing information about immune-related pathways that improve efficacy. Importantly, it also provides evidence to suggest that not all combinations of drugs might be beneficial in the clinic, and that caution should be taken when trialling dual-therapy strategies, even when *in vitro* results are initially promising.

Chapter 2: Materials and Methods

2.1 *In vitro* methods

2.1.1 Cell lines and culture conditions

TuBo mouse mammary carcinoma cells, provided by Dr. Landuzzi in 2016 (Istituto Ortopedico Rizzoli)[232], were cultured in Dulbecco's modified Eagle's medium (DMEM) containing 2mM L-glutamine, 100U/mL anti-mycotic/antibiotic, 1X non-essential amino acids and 1mM sodium pyruvate supplemented with 20% fetal bovine serum (FBS). Cells were passed through a syringe prior to plating to separate cell clumps. TuBo cells were authenticated upon receipt, showing them to be of mouse origin and free from adventitious agents (Charles River Mouse Essential Clear Panel and Contamination Panel). 4T1 cells (ATCC RRID:CVCL_0125) received in 2008 from ATCC, MDA-MB-231 cells, and MCF7 cells, were cultured in DMEM supplemented as above, containing 10% FBS. ZR75.1 and T47D cells were cultured in RPMI supplemented as above with 10% FBS. BSC40 cells, received in 2005 from ATCC, were grown in minimal essential medium supplemented as above using 5% FetalGro bovine growth serum (RMBIO). All cells were passaged fewer than 20 weeks, and routinely tested for mycoplasma.

2.1.2 *In vitro* irradiation

Cells were transported to the Cross Cancer Institute (CCI) in an insulated container 24 hours post-seeding. The cells were irradiated using a GammaCell cesium-source irradiator at the CCI and then returned to the Katz facility where they were incubated at 37°C until further use.

2.1.3 Growth curves

For multistep growth curves, cells at 70% confluency were infected with VACV at a MOI of 0.03 for one hour. The virus inoculum was then removed and replaced with fresh medium. At various time points post infection, cells and medium were harvested by collection with a cell scraper and freeze-thawed three times at -80° C to lyse cells. Once lysed, the samples were diluted, plated in triplicate on BSC-40 cells and incubated for 48 hours in media containing 1% carboxymethylcellulose. Cells were fixed and stained with crystal violet and plaques counted to determine viral titers.

2.1.4 Cytotoxicity assays

For cell viability assays, cells were seeded in 96-well plates and infected at indicated MOIs in triplicate wells. After three days, the medium was replaced with fresh cell culture medium containing 44 µM resazurin agent (Sigma-Aldrich). Plates were incubated for four hours at 37°C, and fluorescence was measured using a microplate reader with 560-nm excitation and 590-nm emission filters. Cell survival was determined as a percent value based on the fluorescence of non-treated mock infected cells (100% survival), after subtracting the background fluorescence determined as 0% cell survival after killing with 10% Triton X-100.

2.1.5 Protein isolation

Cells were cultured and treated as described in above sections. At indicated time points, cells were harvested using a cell scraper into cold PBS and concentrated by centrifugation at 1000× G for 5 minutes. Cells were lysed on ice in radioimmunoprecipitation assay (RIPA) buffer containing 1× protease inhibitor cocktail (Roche Diagnostics, Mannheim, Germany) in 150mM NaCl, 1mM EDTA, 1% NP-40, 0.25% Na-deoxycholate in 50 mM Tris-HCl pH 7.4 buffer. The concentration of protein in the sample was determined using a commercial Bradford Assay Kit according to manufacturer's instructions (BioRad, Mississauga). Samples were denatured at 100°C for 10 minutes in sodium dodecyl sulfate (SDS) buffer containing 3.7% SDS, 0.6M β-mercaptoethanol,1.5mM bromophenol blue, and 40% glycerol in 50 mM Tris-HCl pH 6.8 buffer and stored at -4°C until further use.

2.1.6 Western blotting

Protein samples were size-separated using 12-15% SDS-polyacrylamide gel electrophoresis and transferred to a nitrocellulose membrane using the semi-dry Turboblot transfer system using the mixed molecular weight setting (BioRad, Mississauga). The membrane was blocked with Odyssey Blocking Buffer (PBS) (Li-Cor, Lincoln NE, USA) either overnight at 4°C or for 30 min at room temperature and rinsed twice with PBS. Proteins were then incubated with appropriate primary antibodies (1:1000 dilution) either at room temperature for 30 minutes or overnight at 4°C, followed by rinsing three times with 1% tween 20 in PBS followed by three rinses in plain PBS. For detected housekeeping proteins (tubulin or β-actin) antibody dilutions were 1:20 000. The membranes were then incubated with appropriate infrared-dye conjugated secondary antibodies at 1:20 000 dilutions for 30 minutes or overnight at 4°C, followed by rinsing three times with 1% tween 20 in PBS followed three more in plain PBS. Membranes were imaged using a Li-Cor Odyssey scanner, and gel images were processed using Li-Cor Image Studio Lite Software (Li-Cor, Lincoln NE, USA). Antibodies: goat anti-RRM1(Santa Cruz sc-1733), anti-p53R2 (Abcam ab8105).

2.1.7 ATP and HMGB-1 quantification

To determine ATP and HMGB-1 release cells were seeded in 6 well plates and infected with the indicated viruses at an MOI of 3. One-hour post infection, the inoculum was replaced with fresh culture medium. Medium was collected from cells 24 hours post infection to measure ATP using the ATP bioluminescence kit (Sigma Aldrich), and 72 hours post infection to measure HMGB-1 concentrations using the HMGB-1 ELISA kit (IBL International) as per manufacturer instructions.

2.2 Virus construction and purification

2.2.1 Virus construction

All viruses were derived from a clonal isolate of VACV strain Western Reserve (WR) using traditional homologous recombination techniques[119,149,284]. The parental ΔJ2R virus was constructed using a modified pSC66 plasmid to insert a yellow fluorescent protein (YFP)/ guanine phosphoribosyltransferase (GPT) cassette flanked by loxP

sites into the J2R gene locus. The selectable marker was then removed by growing the virus on BSC40 cells in the presence of cre-recombinase as described in by Rintoul et al., 2011, yielding a virus with the J2R gene disrupted by a loxP site. To create the remaining viruses, we used the pDGloxPKO^{DEL} plasmid bearing a copy of a GPT marker fused to either mCherry fluorescent protein (ΔF4L, previously described [119], ΔF1L, ΔC6L, ΔA41L, ΔB8R) or YFP (ΔK7R, ΔN1L, ΔB18R), flanked by regions of homology to the target gene to allow site-specific recombination. BSC40 cells were infected with ΔJ2R VACV at an MOI of 2 and transfected two hours later with 2 μg of linearized plasmids using Lipofectamine 2000 (Invitrogen). The progeny virus was harvested 24 hours later and purified using two rounds of drug selection under mycophenolic acid (MPA) and three rounds of plaque picking under agar. PCR (Table 2.1) and whole-genome sequencing were used to confirm the identity and purity of the recombinant virus.

2.2.2 Virus culture

BSC40 cells were grown to 80-90% confluency and infected at MOI=0.03 PFU/cell by adding inoculum to fresh cell culture media (20 mL per 150 mm TC plate and 70 mL per roller bottle). Cells were incubated at 37˚C for 2-3 days until a cytopathic effect was observed, as assessed by rounding of cells. The ΔJ2R strain was cultured for 48 hr and the ΔJ2RΔF4L virus for 72 hr. For tissue culture plates, the cells were detached using a cell scraper, and the medium was collected into centrifuge bottles. The cells were centrifuged at 2000×G for 10 minutes and the supernatant discarded. This step was repeated using more of the cell-containing medium until all the cells had been collected. The cell pellets were resuspended in 20 mL of ice-cold PBS and pooled, then centrifuged again at 2000×G for 10 minutes and the supernatant discarded. The cell pellets were then frozen at -80˚C until further purification.

2.2.3 Virus purification

To purify virus, the cell pellets were thawed by continuous swirling in in a 37°C water bath and then resuspended using 5.5 mL of ice-cold extraction buffer (10 mM Tris·HCl pH 9.0, 2 mM $MgCl_2$). The suspension was transferred to a 7 mL Dounce and homogenized using 20 strokes of a tight pestle (0.05 mm clearance, Wheaton cat#06-435A, New Jersey). The mixture was transferred to a conical tube, centrifuged at 2000×G for 10 min at 4°C, and the supernatant transferred to a new tube on ice. The pellet was resuspended in another 5.5 mL of extraction buffer, and the homogenization and centrifugation repeated. The supernatants were then pooled, Benzonase (Millipore, Germany) was added to a final concentration of 50 U/mL, and the mixture incubated at 37˚C to degrade nucleic acid contaminants. The lysate was centrifuged at 2000×G for 10 min and the pellet discarded.

The volume of the supernatant was adjusted to 19 mL with extraction buffer. The virus lysate was then layered over a 19 mL sucrose cushion (36% w/v sucrose, 10 mM Tris-HCl pH 9.0) in a 38 mL Oakridge centrifuge tube. The tubes were centrifuged in a swinging bucket rotor at 26,500×G for 90 minutes and then the supernatant was aspirated off and the pellets resuspended in 10 mM Tris·HCl pH 8.0. Adding 0.1 mL of 10 mM Tris·HCl pH 8.0 per 150 mm plate typically yields virus titers >$2.0x10^9$ PFU/mL. The virus can be stored frozen (-80˚C) at this point if desired.

2.2.4 Working virus stock

The purified and concentrated virus in 10 mM Tris·HCl pH 8.0 was sonicated for 1.5 min in an ice water slurry using a cup-horn sonicator. The treatment was delivered using three 30 sec pulses with a 30 sec break between each pulse. The virus suspension was then filtered through a 70 µm cell strainer wetted with sterile PBS to remove any residual debris. Virus aliquots (0.5 - 1mL) were prepared as shown in Figure 2.1, plus some smaller 25 µL aliquots for use in titering. These virus preparations (a "pre-diluted virus stock") were snap-frozen and stored at -80°C. To determine the titer of the pre-diluted virus stock, one of the 25 µL aliquots was quick thawed and titered as described below. One aliquot of the larger volume pre-diluted virus stock was then thawed, sonicated, and diluted to a final concentration of ~$2x10^9$ PFU/mL based on the titer from the 25 µL sample. A number of 100 µL "working virus stocks" were then aliquoted from this material plus three more 25 µL aliquots. All of the virus stocks were then snap frozen and stored at -80˚C. In advance of starting a new experiment, one of the new 25 µL aliquots was thawed, sonicated, and titered. This was repeated with the other two 25 µL samples, and the average of the three titers was used to determine the exact concentration of the working virus stock. A sample schematic showing the maintenance of virus banks is shown in Figure 2.1. PCR was used to confirm the purity of the virus stock using the same primers found in Table 2.1.

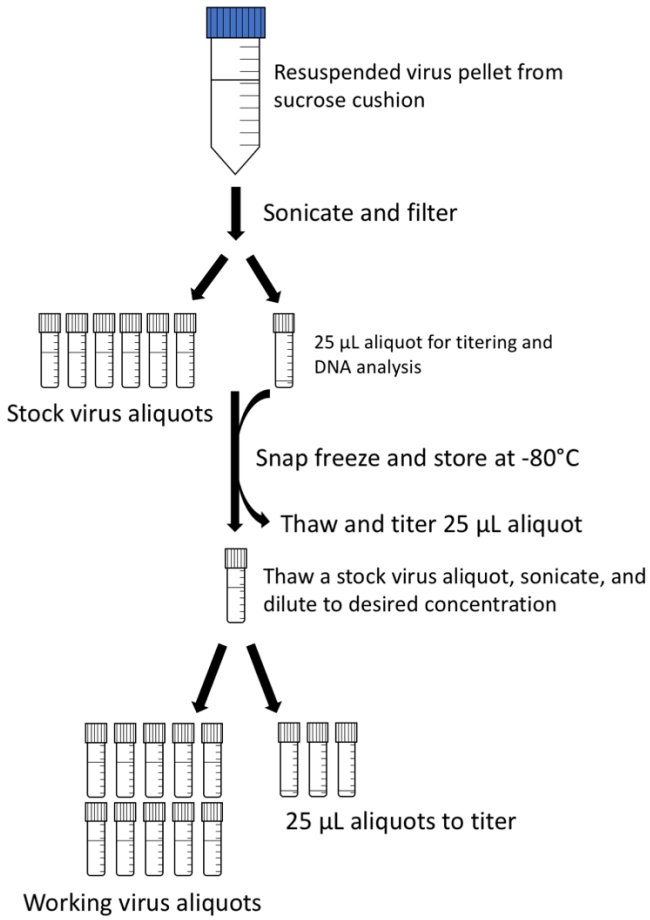

Figure 2.1. Schematic for maintaining virus banks. Method for aliquoting, storing, and maintaining virus banks for use in preclinical studies.

2.2.5 Virus titration

The purified and concentrated virus in 10 mM Tris·HCl pH 8.0 was sonicated as described above. Ten-fold serial dilutions were prepared in serum-free MEM in polypropylene tubes and then 0.3 mL aliquots of diluted virus were applied in triplicate onto 70% confluent monolayers of BSC40 cells on a 12-well plate. Alternatively, 0.5 mL volumes were plated on 6-well plates. The plates were incubated for 1 hr at 37˚C, with rocking at 10 min intervals so the cells do not dry out. The inoculum was aspirated after an hour and replaced with 1 mL or 2 mL of fully supplemented MEM containing 1% carboxymethylcellulose for 12- and 6-well plates, respectively. The cells were then returned to the incubator. Two days later a crystal violet staining solution (0.1% w/v crystal violet, 5% v/v ethanol, and 11.1% v/v formaldehyde) was added to each well. The stain was decanted after an hour, and the plates rinsed with water and set aside to dry. Plaque counts were subjected to statistical analyses using GraphPad Prism version 8 for Mac OS 10.15 (GraphPad, San Diego, California USA, www.graphpad.com).

Table 2.1. PCR primers for assessing virus purity

Target	Primer set	WT amplicon size	Mutant amplicon size
J2R	5' TATTCAGTTGATAATCGGCCCCATGTTT 5' GAGTCGATGTAACACTTTCTACACACCG	~500 bp	~700 bp
F4L	5' TCAGCACCCATGGTCGAT 5' TGACGTAAATGTGTGCGAAAGT	~4000 bp	~1000 bp
F1L	5' CAAGGGTTTGGATCAACAGGAC 5' GATATAGGGGTCTTCATAACGC	785 bp	1476 bp
K7R	5'ACGGCTACTGTCTTTTGTGAG 5'GCGTTATGAAGACCCCTATATC	500 bp	1426 bp
N1L	5' AGATCTCAATGTACATACATCGCC 5' TGGCGATTGACCATTATG	~600 bp	~1500 bp
C6L	5'AATGCTTACAGGATCTATACC 5' GAATATCAACGGCGTTAATAG	545 bp	1479 bp
A41L	5' TAAGAATGCCACGAAGAATGG 5' AGTCTTGTAATCAACGATGGC	764 bp	1476 bp
B8R	5' ATCACTTCAGTGACAGTAGTC 5' AGGACTATAATCAGGGACCTC	966 bp	1425 bp
B18R	5' CCACCTACCAAAGTATAGTTG 5' CGGTGAGATACAAATACCTAG	1250 bp	1643 bp

2.3 *In vivo* assays and animal models

Animal studies were carried out at the Cross Cancer Institute (CCI) and the University of Alberta, Edmonton Alberta, and conducted in accordance with the Canadian Council on Animal Care Guidelines and Policies with approval from the Cross Cancer Institute's Animal Care Committee and the Animal Care and Use Committee: Health Sciences for the University of Alberta.

Female BALB/c mice between 6-8 weeks of age were ordered from Charles River (Saint Constant, Canada). For irradiation experiments, animals were housed at the CCI biosafety level 1 animal facility in negatively ventilated cages in groups of four and five and given at least 7 days to acclimate to the housing facility, and following radiation, the University of Alberta biosafety level 2 animal facility and given 24 hours to acclimate. For animal experiments that did not require radiation treatment, animals were housed solely at the University of Alberta level 2 animal facility and given at least 7 days to acclimate to housing following their arrival at the facility. Environmental conditions were a temperature of 21°C ±2°, humidity of 55% ±10%, lighting of 350 lux and a 12**:**12 light: dark cycle with lights on at 0600 and off at 1800 at the CCI, or 0700 and off at 1900 at the University of Alberta. Animals were housed in 595×380×200 mm cages (Animal Care Systems, Colorado USA at the CCI or Ehret, Germany at the University of Alberta) and given

access to mouse maintenance food (LabDiet, St.Louis, MO) and water *ad libitum*. Environmental enrichment included bedding (Warrensburg, NY), one red tinted mouse tunnel (Bio-Serv, Flemington NJ), one 50mm × 50mm Nestlet (Ancare Bellmore, NY) and one 4-8g portion-controlled nesting material (Anderson Lab Bedding Maumee, Ohio).

2.3.1 Tumour establishment

To establish orthotopic tumors in the mammary fat pad, the cells were trypsinized, washed twice with cold PBS, and concentrated by centrifugation at 500×G for 5 minutes in PBS to yield the final cell count desired for injection in 25 µL of PBS. Cells were kept on ice during processing. Immediately prior to injection, 25 µL of Matrigel was mixed with 25 µL of cells to yield a final dose of 1×10^6 TuBo cells or 1×10^4 4T1 cells in a total of a 50 µL volume per mouse. Animals were anaesthetized with isoflurane, and the cells were injected into the inguinal mammary fat pad of mice below the fourth nipple. Palpable tumors were detected after approximately eight days in both the TuBo and 4T1 tumor models. For secondary tumour re-challenge experiments, the same procedure was followed, however cells were injected into the opposite mammary fat pad of where the initial primary tumour had been established.

2.3.2 Tumour treatment

2.3.2.1 Oncolytic virus administration

Mice were randomized into treatment groups using a random number generator (https://www.google.com/search?q=random+number). Viruses were sonicated in a cup horn sonicator for 1.5 minutes to dissociate aggregated virus particles and diluted to a final concentration of 2×10^8 PFU/mL with sterile PBS, or serially diluted for dose-escalation studies. Mice were anaesthetized with isoflurane and injected intratumorally with 50 µL of virus yielding a dose of 1×10^7 PFU/tumor. Animals received two additional doses administered at 48-hour intervals. For intravenous virus administration, mice were restrained without anaesthetic and virus was injected via tail vein injection.

2.3.2.2 *In vivo* radiation treatment with the SARRP

Once palpable tumours were established, mice were treated with IG-RT. Mice were anaesthetized with isoflurane and transferred to the treatment stage of the small animal radiation research platform (SARRP) (XStrahl Inc, Sunwanee, GA) (Figure 4.4). Computed tomography (CT) imaging was performed from 360° angles (Figure 4.4C). The CT images were uploaded onto the XStrahl MuriPlan treatment planning software (XStrahl Inc. Sunwanee, GA). During treatment planning, a heat lamp was placed near the mouse to maintain temperature, and an operator continually monitored the mouse while anaesthetized on the stage. Once CT images were uploaded, tissue segmentation was performed to allow the software to differentiate between different tissues, and correctly attenuate and adjust radiation doses as it passes through various tissues. Tissue segmentation was manually adjusted to ensure various tissues were properly identified. The tumour was manually contoured through DICOM slices to allow the software to register the exact size and location of the tumour mass. The isocenter of the tumour was selected and is the point at

which all radiation treatment beams converge (Figure 4.4E). The angles and weighting dose of each beam were manually adjusted with each mouse to avoid or limit radiation exposure to any non-tumour tissue. The total dose delivered to each isocenter was 10 Gy, split between multiple beams, with each beam delivering between 20-50% of the total dose, adjusted on a per case basis. Tissue doses to off-target tissue was evaluated based on isodoses calculated by the MuriPlan software (Figure 4.4), and the dose to the tumour was calculated as a dose-volume histogram (DVH), showing the fractional volume of tumour receiving the corresponding radiation dose (Figure 4.4). Treatment plans were customized for each individual mouse, where a minimum of 80% of the tumour volume receives 90% of the target dose of 10 Gy, while minimizing doses delivered to sensitive tissue, primarily in the bone. If a treatment plan did not meet these requirements, the beam angles and weights were adjusted to increase the fractional volume receiving the target dose, or to minimize off-target radiation exposure. Once the treatment plan was verified, the radiation beams were executed on the SARRP to deliver radiation to the mouse. Mice were placed back in cages, and 24 hours later were transported to the BSL-2 vivarium at the University of Alberta for virus treatment after being given an additional 24 hours to acclimatize to their new housing.

2.3.2.3 Anti-PD-1 antibody administration

Mice were anaesthetized with inhaled isoflurane and 200 μg of anti-PD-1 antibody (Clone RMP1-14, Bio X Cell, New Hampshire USA) or isotype control were administered intraperitoneally twice per week for three weeks.

2.3.3 Tumour monitoring

Animals were anaesthetized with inhaled isoflurane, weighed, and tumor growth was measured twice per week with calipers. Tumor volume was calculated using the equation: $V = (1/24) \times \pi \times L \times (W+H)^2$. Mice were euthanized by CO2 inhalation at tumor burden endpoint (1500 mm^3), or at first indication of illness or discomfort (hunched posture, ruffled fur, or weight loss exceeding 10% of body weight).

2.3.4 Tissue processing

Tumours: Tumors were collected into HBSS and cut into pieces. Tumor pieces were added to a GentleMACS C-tube containing 5 mL Roswell-Park Memorial Institute (RPMI) medium containing 0.5 mg/mL collagenase type 1A (Sigma-Aldrich), 10 μg/mL of DNAse I (Roche) and 10% HI-FBS. Tumors were dissociated using the m_impTumor01.01 protocol on a GentleMACs dissociator (Miltenyi Biotec). The digested tumor samples in enzymatic cocktail were incubated while shaking for 30 minutes at 37°C, filtered through a 70 μm cell strainer into PBS containing 2% HI-FBS and centrifuged at 500 × G for 5 minutes. Cells were resuspended in 40% Percoll (GE Healthcare) in HBSS and overlaid onto 80% Percoll. After centrifugation at 325 × G for 30 minutes, leukocytes at the interface between the 40% and 80% fraction were collected and washed twice in PBS, while tumor cells at the top of the 40% fraction were collected for virus titering.

Spleens: Spleens were mashed through a 70 µm cell strainer into isolation buffer (PBS + 2% heat-inactivated FBS (HI-FBS) + 0.5 mM EDTA) using the rubber end of a 3 mL syringe, centrifuged at 300 x g for 5 minutes and resuspended in 3 mL of 1X red blood cell lysis buffer (eBioscience) for 5 minutes. RBC lysis was stopped by the addition of 10 mL isolation buffer followed by centrifugation at 300 x g for 5 minutes and then washed twice with isolation buffer.

Lungs: Lung processing for quantification of metastases was previously described[237]. Briefly, lungs were collected and rinsed twice in Hank's buffered salt solution (HBSS). The lungs were minced for three minutes using a scalpel blade and incubated in HBSS containing 2mg/mL collagenase at 4°C for 75 minutes. The cells were then passed through a 70 µm cell strainer and washed twice with HBSS. After dilution, cells were plated in fully supplemented 10% FBS DMEM containing 60 µM of 6-thioguaninine. and cultured, undisturbed, at 37°C . After two weeks the colonies were fixed in 100% methanol, stained with methylene blue, and counted for quantification of metastases.

Brain, kidney, heart, liver, lymph nodes: Tissue was manually cut into smaller pieces using a surgical scalpel and transferred to a 70µm cell strainer pre-wet with sterile PBS. Using the rubber end of a 3mL syringe, the tissue was forced through the strainer to yield a single cell suspension. After rinsing the strainer with PBS, the cells were spun at 500×G for 5 minutes, resuspended in 1 mL of PBS and frozen at -80°C. Cells were freeze thawed three times to lyse cells, and virus titers were determined as described previously by plaque assay on BSC40 cells.

2.3.5 Flow Cytometry staining

Two million splenocytes were aliquoted into individual wells of 96 well plates, and the remaining splenocytes were pooled into a single sample for use in fluorescence minus one (FMO) gating controls, where all but one antibody is added to the pooled samples to use for setting appropriate gates during analysis. For tumor samples, the entirety of the cells isolated from tumors were split between 2 wells (for TuBO experiments) or 1 well (for 4T1 experiments) of a 96 well plate with 5% of each sample volume removed for control wells. The cells were rinsed in PBS in the absence of any serum, and stained with fixable viability dye eflour506 (Invitrogen, Cat. 65-086614). This, and all subsequent staining steps, were performed in the dark for 30 minutes at 4°C. Fc receptors were blocked using anti-CD16/CD32 antibody (BioLegend). The cells were stained with antibodies described in Table 2.2. After staining, cells were fixed and permeabilized according to manufacturer's instructions using the BD Cytofix/Cytoperm Kit (San Jose, CA, USA). Samples were run on the BD Fortessa X20 Flow Cytometer and analyzed with FlowJo v8 or v10 software. To determine absolute cell counts, the entirety of the tumour sample was run, and total cell counts were calculated. A representative example of the gating strategy can be found in Figure 2.2.

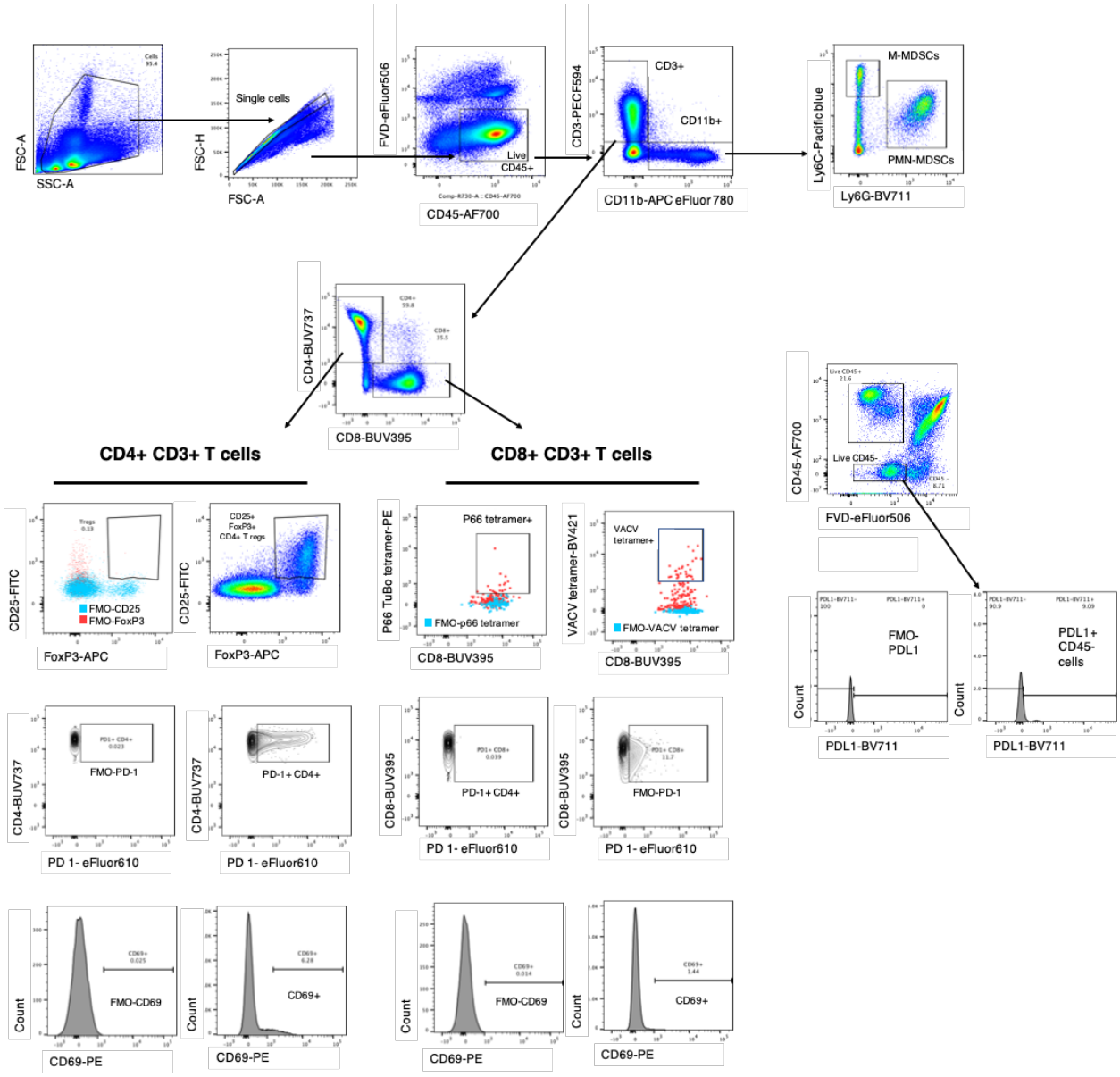

Figure 2.2. Representative flow cytometry gating strategy to identify immune cell subsets and marker expression on splenic and tumour cells. FMO- fluorescence minus one gating control.

Table 2.2. Flow cytometry antibodies used in the current study

Antibody	Clone	Company
CD45-AF700	30-F11	Invitrogen
CD3-PE or FITC or PE-CF594	145-2C11	Invitrogen or BD Bioscience
CD4-BUV737	RM4-5	BD Bioscience
CD8-BUV395	53-6.7	BD Bioscience
CD25-FITC	P4A10	Invitrogen
FoxP3-AF647	FJK-16S	Invitrogen
CD69-APCefluor780 or PE	H1.2F3	Invitrogen
CD11b-APCefluor780	M1/70	Invitrogen
Ly6C-efluor450	HK1.4	Invitrogen
Ly6G-biotin	IA8	Biolegend
PD1-efluor610	J43	Invitrogen
PDL1-biotin	10F.9G2	Biolegend
Streptavidin-BV711	Not applicable	BD Bioscience
H-2K^{d} VACV A52$_{75-83}$ KYGRLFNEI-BV421 Tetramer	Not applicable	NIH Tetramer Facility
H-2K^{d} HER2/*neu* p66 TYVPANASL- PE Tetramer	Not applicable	NIH Tetramer Facility

2.3.6 Cytokine analysis

Blood was collected from mice at endpoint by cardiac puncture by inserting a needle into the chest cavity of mice under anaesthesia and drawing blood from the heart. The animals were then immediately euthanized, and blood was allowed to clot for 30 minutes at room temperature. Blood was centrifuged at 1000 x G for 10 minutes at 4°C and serum was collected and frozen at -20°C. Serum cytokines were then sent for analysis by Eve Technologies (Calgary, AB Canada) using the Mouse Cytokine 31-plex discovery assay to measure the following analytes: Eotaxin, G-CSF, GM-CSF, IFNγ, IL-1α, IL-1β, IL-2, IL-3, IL-4, IL-5, IL-6, IL-7, IL-9, IL-10, IL-12 (p40), IL-12 (p70), IL-13, IL-15, IL-17, IP-10, KC, LIF, LIX (not validated), MCP-1, M-CSF, MIG, MIP-1α, MIP-1β, MIP-2, RANTES, TNFα, and VEGF.

2.4 Analysis software

2.4.1 Synergy analysis

CombuSyn drug synergy analysis software (http://www.combosyn.com/) was used to determine combination index (CI) values for dual treatment *in vitro* using data obtained from resazurin viability assays[285,286]. The average values of effect sizes (determined as the fraction of cells non-viable after treatment) from three experimental replicates was

analysed using the CombuSyn software. Interactions were assessed using the 'non-constant' drug ratio setting. CI values were reported, and heatmaps were generated based on the scale shown in Table 2.3 For visual clarity, and as no computed CI values were higher than 1.88, the CI heatmap scale was clipped at a CI value of 3, representative of "antagonism"

Table 2.3. Interpretation of CI values from CombuSyn Analysis

CI value	Interpretation
<0.1	Very strong synergism
0.1-0.3	Strong synergism
0.3-0.7	Synergism
0.7-0.85	Moderate synergism
0.85-0.9	Slight synergism
0.9-1.1	Nearly additive
1.1-1.20	Slight antagonism
1.20-1.45	Moderate antagonism
1.45-3.3	Antagonism
3.3-10	Strong antagonism
>10	Very strong antagonism

2.4.2 Statistical analysis

Data were analyzed using GraphPad Prism 7 or 8. If data were determined to be normally distributed by the Shapiro-Wilk normality and the Kolmogorov-Smirnov test, parametric one-way ANOVA testing was performed with Tukey's multiple comparisons testing for radiation experiments or Dunnett's testing for immunogenic virus studies. If data was not parametric, Kruskal-Wallis testing was performed with Dunn's multiple comparisons testing. Significance was determined if $p \leq 0.05$. Tumor growth curves were analyzed using a two-way ANOVA to compare tumor volumes at multiple time points. Survival data were analyzed by both the log-rank (Mantel-Cox) and Gehan Brexlow Wilcoxon testing for immunogenic virus studies. In immunogenic virus studies, the significance threshold was adjusted for multiple comparisons, where the significance threshold was set as $p=0.05/K$ where K is the number of comparisons being made.

Chapter 3: Production and quality assessment of vaccinia virus stocks of pre-clinical grade purity and high infectivity for oncolytic immunotherapy studies

Preface

Portions of this chapter have been submitted as:

Umer BA, Noyce RS, Shenouda MM, Favis NA, Desaulniers M, Irwin C, and Evans DH (2020). Production and quality assessment of infectious vaccinia virus stocks of pre-clinical grade purity for oncolytic immunotherapy studies [submitted].

Contributions

BU - development of methodology, performed experiments, editorial revisions, manuscript preparation

RN -study supervision, development of methodology, technical and experimental assistance, editorial revisions, manuscript preparation

MD - development of methodology, technical & experimental assistance

CI - development of methodology, editorial revisions

NF & MS - Technical & experimental assistance and animal support

DE - Study supervision, editorial revisions, manuscript preparation

*Experiments performed by other authors have been identified in figure legends.

3.1 Introduction

Oncolytic viruses are viruses that used for the treatment of cancer. These viruses work by a combination of direct lysis of cancer cells and/or modulation of the patient's immune system[287]. The field of oncolytic viruses has advanced immensely in the past few decades and one of the viruses in various stages of nonclinical and clinical research is the Orthopoxvirus vaccinia virus (VACV)[10–12].

VACV is a large ds DNA virus that was once widely used as a smallpox vaccine. This virus has been adopted for use as an oncolytic virus for several reasons. This includes an ability to infect and preferentially replicate in various cancer cell types and a favorable safety profile which is supported by its longstanding use as a vaccine. Furthermore, compared to other viruses, the genome of VACV is easily modified and has the capacity to encode a large number of transgenes. In addition to its potential use as an oncolytic virus, VACV continues to be studied as a vaccine vector for expressing recombinant antigens[288].

VACV preparations used in clinical trials are often made at large scales and purified by complex processes (e.g. tangential flow filtration)[143]. These processes are often not feasible or necessary for laboratory research, especially when evaluating multiple virus candidates. However, pre-clinical studies (particularly animal studies) still require virus stocks that are of a high enough titer to accommodate the small injection volumes permitted by animal use protocols. The materials need also be of suitable purity so that contaminating biological debris can't cause deleterious side effects and should reproducibly exhibit a high infectivity (i.e., plaque forming units [PFU] to particle ratio) to permit the proper interpretation of dose/response data in animals.

A number papers have been published that describe how to produce laboratory scale poxvirus preparations that are suitable for animal studies[289,290]. However, in our experience there remain several critical steps in these procedures that can affect the outcomes of such studies and deserve special attention. In particular VACV needs to be purified carefully, and the resulting stocks needs to be assessed for both quality and titer before use. As research in this field continues to increase and new research groups initiate studies with different oncolytic VACV candidates, we sought to share our practices pertaining to the production of VACV stocks for *in vivo* cancer therapeutic studies. The methods used in this study are based on many years of accumulated experience growing and purifying these viruses and most of the technologies should be accessible to any well-equipped academic laboratory. In particular the work emphasizes the importance of managing problems associated with storing and titering high concentration stocks of a virus that is prone to aggregation. We also include accompanying data that compares the yields of virus using different production methods and recommendations for identifying where dose-limiting toxicities begin to compromise the safety of intravenous versus intratumoural administration of oncolytic VACV in mammary tumour models. Finally, we show how recent advances in flow virometry can provide a new tool for documenting the infectivity of these virus

stocks, a biological parameter that has historically been difficult to evaluate but is of potential importance when conducting dose-response trials.

3.2 Results

VACV can be propagated using many different conditions (e.g., chicken eggs, cells grown in suspension or as monolayers) and will grow on most commonly available cell types (e.g., Vero, HeLa, BGMK, CV-1, and BSC-1 or its derivative BSC-40). HeLa cells are often used for convenience although we have found that yields vary considerably among different subclones, CCL-2 may be one of the better choices. However, in our experience BSC-40 cells are probably the best choice of cell line for most routine experimental purposes. They grow fast in media containing serum supplements (see below), can be used to propagate attenuated viruses (e.g. ΔF4LΔJ2R strains[149]), are highly infectable, plaque well [289], and provide excellent yields of virus[291]. For these reasons our laboratory routinely uses monolayers of BSC40 cells to construct and propagate VACV.

3.2.1 Selection of a method and surface for culturing VACV.

A few 150 cm^2 tissue culture (TC) plates can yield enough VACV to perform many cell-based assays. However, animal studies often require a lot more virus at relatively high concentrations. Suspension culture technologies offer one possible way of doing this, but we have tested different implementations of these methods over the years, including suspended microcarriers, and unfortunately never obtained enough improvement in yield to justify the additional complexity of these methods.

Roller bottles are more frequently used to scale up production of large amounts of VACV and we have previously used this technology to produce VACV for our own tumour treatment studies[119]. However, in reviewing the yields of virus obtained using this method we had observed that not much more virus was recovered from these proportionately larger units when viruses were grown in roller bottles compared to when these stocks were cultivated on flat adherent-cell TC dishes. Therefore, we sought to more accurately assess the yields of virus using each approach to better inform our production processes.

A standard Corning ridged roller bottle encloses a surface area of 1700 cm^2, while a commonly used TC dish has a surface area of 150 cm^2. Despite this >10-fold difference in surface area, we determined that each method actually produced comparable amounts of virus per device, yielding 2.5 – 6x10^8 PFU per roller bottle versus 2 - 4x10^8 PFU per dish (Table 3.1) This observation was consistent between multiple handlers (data shown from average of three virus yield experiments, each performed by a different handler). Even though these methods produced similar yields of virus, ridged roller bottles require considerably more media than a standard TC plate; 75 mL versus 20 mL, respectively. This larger media requirement thus increases the cost as does the requirement for specialized roller-

bottle incubators or adaptors. Moreover, cell scrapers can be used to harvest infected cells from a flat TC plate while trypsin and a trypsin inhibition step are required to harvest infected cells from ridged roller bottles. This further complicates the processing and increases handling time. Perhaps most importantly, because the yield of virus per cell is reduced ~10-fold, relatively more cellular contaminants must be removed by the purification step from viruses prepared using roller bottles compared to TC plates. In accordance with this observation, we sometimes observed that when large amounts of a more attenuated VACV ΔF4LΔJ2R virus were produced using roller bottles, the final preparation of purified virus was very viscous, likely due to increased amounts of cell DNA being released when large numbers of cells were lysed. This was not observed when the same virus was grown on flat TC plates, nor was it seen with a higher yielding strain ΔJ2R VACV. Nevertheless, since these methods resulted in variable levels of contamination with cellular DNA, we introduced a Benzonase™ digestion step into the purification process to eliminate contaminant cellular nucleic acids from our virus preparations[292].

Based on these observations and the greater ease of use of TC plates, our laboratory stopped growing virus using roller bottles and now produces preclinical VACV using only TC plates. A standard dose of oncolytic VACV used in mice is ~$1x10^7$ PFU, so one can produce ~500 doses of virus using 45 TC plates with a total surface area of 6300 cm^2. This is about the same surface area as one CF10 culture flask (6360 cm^2). At three doses per mouse, this scale of production produces enough virus to treat >150 animals and is well suited for academic studies using murine models. Our research using a rat model for bladder cancer required significantly larger quantities of virus for treating orthotopic tumours (3 doses of $3x10^8$ pfu/animal[119]), but the demands of experiments like these could still be accommodated within this production framework.

Table 3.1. Growing VACV on flat culture plates produces a higher yield of virus per cell than growing virus on ridged roller bottles

	Tissue Culture plate	Ridged Roller Bottle
Total cells	~$1x10^7$ cells	~$1x10^8$ cells
Virus yield	2-4 $x10^8$ PFU	$2.5x10^8$ – $6x10^8$ PFU
Surface Area	150 mm^3	1700 mm^3
Medium (MEM)	20 mL	70 mL
Trypsin	-	10 mL
HEPES	-	1 mL

*RN & MD contributed experimental replicates to this data to reproduce cross-technician handling

3.2.2 FBS alternatives

We have also examined whether we could improve virus yields by using cells grown in media containing FBS substitutes or additional supplements. This is particularly relevant given the increasing desire to reduce the amounts of fetal bovine components in cell culture media for ethical, cost, and safety reasons[293]. We tested both a wild type (WT) strain of VACV Western Reserve (WR), which has no growth-attenuating genome modifications, and a ΔF4LΔJ2R strain. Deleting the F4L and J2R genes renders virus growth highly dependent on cellular levels of dNTPs, and dNTP levels are affected by cell growth rates[119,149]. We compared MEM media supplemented with one of three supplements: traditional fetal bovine serum (FBS), FetalGro® (RMBIO, Missoula MT) a calf serum supplemented with other additives and bovine cholesterol concentrate, or FB Essence (Avantor, Pennsylvania), an FBS-derived product supplemented with bovine calf and equine serum, and additional proprietary supplements. We saw no differences in the yields of either virus over three days when comparing the yield of virus on FBS or either of the two alternatives supplements (Figure 3.1). We also noted that increasing the concentration of each FBS alternative did not affect virus yields either (Figure 3.1A&B). This suggests that FetalGro, and FB Essence, could be used as alternatives to traditional FBS supplements.

3.2.3 Sonication

Once the BSC-40 cells have been infected and cultured for three days they are scraped into the culture medium, recovered by centrifugation, resuspended in a hypotonic medium and broken with a Dounce homogenizer as described in the Materials and Methods. After treatment with Benzonase the cell debris is removed and then the concentrated virus suspension is further purified by sedimentation through a 36% sucrose gradient. At this stage these purification methods can produce very high titer stocks of VACV. However, we noticed that when preparing virus with titers >10^9 PFU/mL, a white precipitate was often seen (Figure 3.2A). This precipitate persisted after filtering the suspension through a 70 μm filter and collected at the bottom of the tube following centrifugation (Figure 3.2A). We hypothesized that VACV was aggregating at this high virus concentration and precipitating out of solution. The precipitate could be broken up and disbursed to form a homogenous solution by sonicating the virus in an ice water bath for 3 minutes (with 1-minute cooling intervals) using a cup sonicator. Such suspensions of virus were relatively stable and no longer sedimented to the bottom of the tube during centrifugation (Figure 3.2B). Furthermore, we observed a small but consistent increase in virus titer after sonicating virus stocks spanning a wide range of initial concentrations (5x10^8 PFU/mL to 5x10^9 PFU/mL). The percentage increase in virus titer was independent of the starting concentration, and sonication increased the titers by amounts ranging from 100 to 180% (Figure 3.2B). In a separate experiment we took a single stock of virus, divided it into three aliquots, and froze them at -80°C. After rethawing, each aliquot was titered before and after sonication. We observed that, on average, virus titers increased by ~150% after sonication (Figure 3.2C). Collectively, these observations suggest that sonication of viral stocks can reduce particle aggregation and increase the accuracy of virus titration.

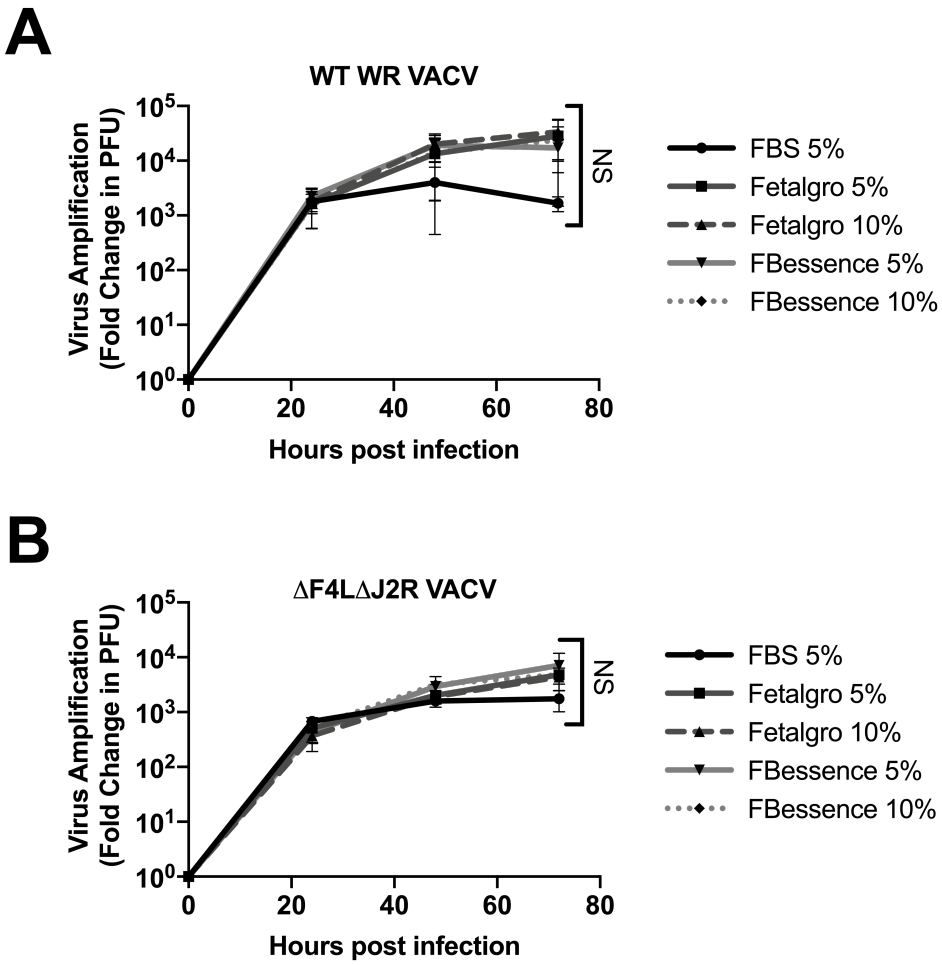

Figure 3.1: FBS substitutes do not alter the growth of WT (A) or mutant (B) VACV on BSC40 cells VACV was grown on BSC40 cells in media supplemented with 5% FBS or with 5 or 10% of two FBS alternatives: FBEssence or FetalGro. The cells were infected at MOI=0.03, the virus harvested at the indicated times post-infection, and titered by plaque assay on BSC40 cells. Error bars denote +/- standard deviation from three experimental replicates and were analyzed using 2-way ANOVA.

*Data provided by MD

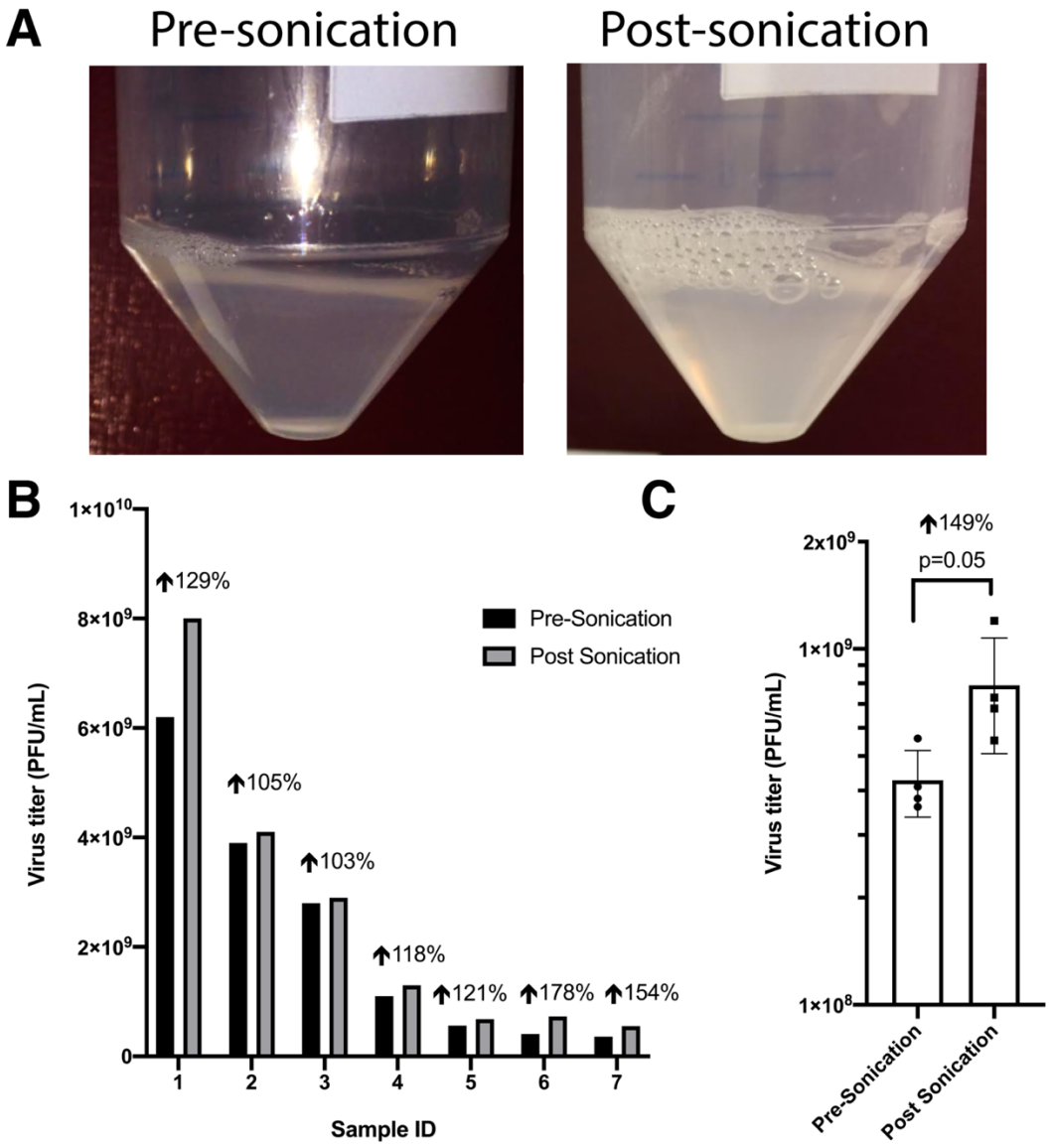

Figure 3.2. Sonication produces more homogenous VACV suspensions and increases virus titers. A) A preparation of virus was centrifuged at 2000×G for 5 min and then photographed immediately before (left) and after (right) sonication. The virus that had collected on the bottom of the tube after centrifugation was visibly transferred into suspension. B) Effect of sonication on virus titer before and after sonication of different virus preparations. C) Effect of sonication on virus titer before and after sonication using a single virus stock aliquoted into multiple aliquots. All of the virus stocks were titered by plaque assay in triplicate on BSC40 cells. Error bars denote +/- standard deviation from four experimental replicates analyzed using an unpaired T-test.

3.2.4 Virus characterization and stock management

Our virus stocks are stored in a designated area and sequenced in their entirety to confirm the identity of the virus and the accuracy of any genetic manipulations. This sequence data can obviate the need to reconstruct a

"revertant" virus, an important control that is used to show that an unknown mutation, acquired during the construction of the virus, isn't responsible for any observed phenotype(s). Although we routinely test for the presence of undesirable agents like mycoplasma in our cell lines, genome sequencing also produces sufficient read depths to provide independent insights into this concern. If sequencing is not possible, at a minimum PCR and Sanger sequencing should be used to confirm gene-deletions or transgene insertion, and to ensure there is no contamination by wild-type virus. Once these steps have been accomplished, we routinely prepare working virus stocks from a single virus seed to limit access to the primary virus bank. These working stocks are aliquoted along with several smaller but otherwise identical virus aliquots. These additional samples are used to determine the titer of the working stock in advance of any experiments, to ensure the doses are accurately known for *in vivo* studies. A sample scheme for preparing working banks can be found in Figure 2.1. Although the titer of VACV does not seem to change significantly after two freeze-thaw cycles (see below), we nevertheless still aliquot the virus into single use vials, so that a stock is not repeatedly re-frozen, thawed, and re-used.

3.2.5 Virus stocks are stable for up to three years at -80°C

To assess the stability of the virus we performed multiple freeze-thaw cycles. The virus stocks were snap-frozen in liquid nitrogen or a dry-ice ethanol mix and stored at -80˚C. A sample of virus was then removed from the freezer, warmed with continuous swirling in a 37°C water bath until the ice had just thawed, and then titered to determine the concentration of infectious material. Using this method, we observed no loss of titer after the two freeze-thaws (Figure 3.3A). To assess virus stability over time, a virus stock was aliquoted into multiple vials, snap-frozen, and stored at -80°C. Over the next three years aliquots of virus were retrieved and titered. We observed no loss of titer, showing that these virus preparations are stable over at least that time at -80°C (Figure 3.3B).

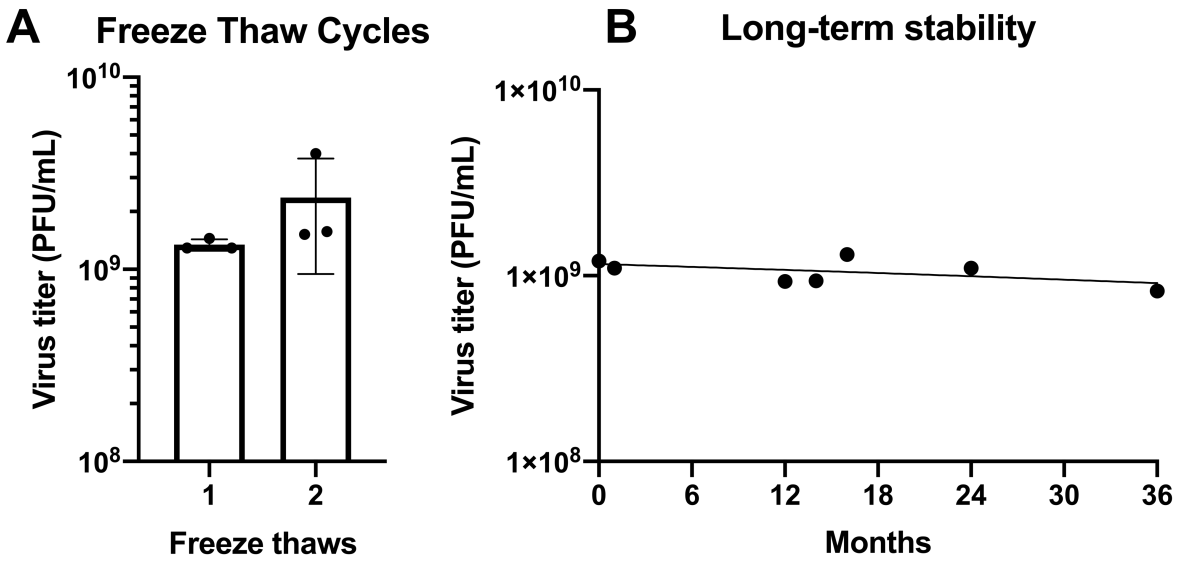

Figure 3.3.Virus stocks are stable when stored at -80°C. A) Virus stocks were frozen and thawed twice with no loss of infectious titers as measured by plaque assay. Error bars denote +/- standard deviation from three experimental replicates and the difference is not significant when analyzed using an unpaired T-test. B) Virus stocks are stable for up to three years with no loss of infectious titer. Individual data points are plotted, with line of best fit from simple linear regression shown as solid line. Slope was not significantly different than zero. Virus titers were measured by plaque assay on BSC40 cells.

3.2.6 Flow cytometry can be used as a quality control measure for virus preparations

The virus is exposed to stresses that may reduce the infectivity of the particles during the propagation and purification processes. This effect is expected to produce changes in the ratio of particle numbers to plaque forming units (PFU). The particle/PFU ratio is potentially an important parameter, but one that is not commonly monitored as it can be difficult to evaluate. It's important because several studies have shown that non-replicating or inactivated poxviruses can still induce anti-tumour effects[294,295], and this effect would complicate the interpretation of any study where dosing is based solely on estimates of PFU. To assess how the purification process affects the infectivity, we developed a flow-cytometry based method that can determine the numbers of virus-sized DNA-containing particles. To do this, virus preparations were fixed, optionally stained with SYBR Gold, and then analyzed by a Beckman CytoFLEX flow cytometer. This instrument can size particles as small as 80 nm, which is well suited for characterizing particles with the dimensions of poxviruses (100 x 200 x 300 nm). When these numbers are combined with data obtained through plaque assays, they provide a measure of the particle to PFU ratio in a virus sample. The method can also test whether a virus preparation is of uniform composition and monodisperse.

We first tested the instrument using a VACV strain encoding the A5 core protein fused to yellow fluorescent protein (YFP)[296] (SYBR Gold stain was not used in this pilot study due to spectral overlap with YFP). Our virus stocks were seen to contain particles of an appropriate size range and the presence of a bright fluorescent tag detectible in the FITC channel confirmed that these particles were virus particles (Figure 3.5A). A size assessment based on comparing the violet side-scatter height (violet SSC-H) parameter showed that the apparent virus particle size was appropriate for VACV and could be distinguished from 110 nm diameter GFP-tagged silica beads and non-fluorescent 180-300 nm Apogee silica beads. The slight discrepancy between the known size of the internal standards and the measured size of VACV are reportedly due to the different refractive indices of silica versus biologics, which has been previously observed[297]. During these studies we also used a stock of untagged virus to examine the dynamic range of this instrument (Figure 3.4A-C). An undiluted sample at $5x10^9$ PFU/mL showed evidence of "swarming", which is undesirable as it leads to an undercounting of particles (Figure 3.4A). Conversely it was found that high dilutions ($<10^5$ PFU/mL) led to problems with background counts. It was found that particle counts were directly proportional to dilution using samples diluted between 1/100 and 1/1000 (Figure 3.4C). A sample of virus at ~$5x10^7$ PFU/mL provided good counting accuracy with minimal background interference.

After establishing that VACV particles are well resolved on this instrument, we next examined whether a virus that did not incorporate a fluorescently tagged core protein could also be detected and quantified. Using a method previously used to quantify virus particles in environmental water samples[298], we stained the virus DNA with SYBR Gold. This should produce a count of any VACV sized particle that is potentially transcriptionally active, whether or not fully infectious. We found that particles stained in this manner were bright enough to clearly distinguish between unstained and DNA-stained particles (Figure 3.5B). We couldn't obtain sufficient brightness using other DNA stains in

alternative channels, such as the red fluorescent "SYTO" family dyes (data not shown). Using this combination of size determination and SYBR Gold DNA-staining, we assessed the quality of preparations of both the ΔJ2R and ΔF4LΔJ2R VACV strains (Figure 3.5C&D). We found that particle counts were slightly higher than PFU (Figure 3.5E), leading to an estimate of the particle to PFU ratios of ~1.6 for the ΔJ2R and ~1.3 for the ΔF4LΔJ2R stocks Figure 3.5F). The virus preparations also appeared to be monodispersed judging by the minimal numbers of larger aggregated particles. These particle to PFU ratios lies near a theoretical ratio of one and show that Orthopoxviruses can assemble infectious DNA-containing progeny with remarkable precision.

3.2.7 Dose limiting toxicities of oncolytic VACV differ based on route of administration

To assess the maximum tolerable dose for oncolytic VACV, we performed dose escalation experiments using both intravenous (IV) and intratumoral (IT) administration routes. An orthotopic mouse TuBo tumour model was used. We tested three doses of $1x10^6$, $1x10^7$ and $1x10^8$ PFU (Figure 3.6A) and found that all of these doses were well tolerated when administered through tail-vein IV injection. Nor was any weight loss observed over time thus showing the fitness of these VACV preparations for this purpose (Figure 3.6B). When the virus was delivered via an IT administration route, 2/5 mice did not recover after injecting the first of the three highest doses of virus ($1x10^8$ PFU) and had to be euthanized. This effect had been observed before at this dose (data not shown) and is characterised by an inability to recover after removal of anaesthesia with no response to stimuli, gasping, and inactivity. In an effort to determine cause of death, a veterinary pathologist examined these mice, but no gross post-mortem abnormalities were observed. Regardless of the reason(s), the inability of a portion of mice to recover at doses of $1x10^8$ PFU suggests that the maximum safe dose administered IT is $1x10^7$ PFU. There were no adverse events or weight loss seen at this or lower doses (Figure 3.6C).

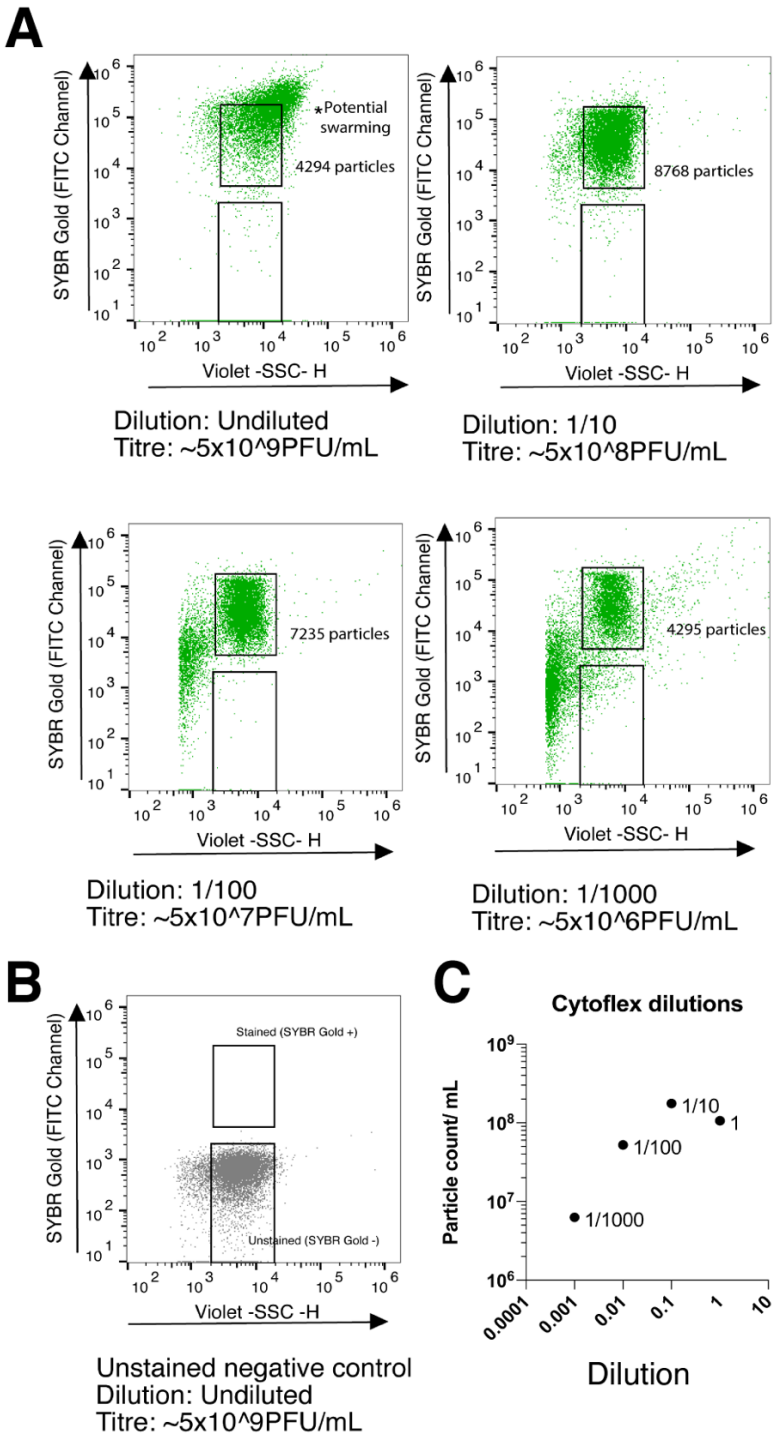

Figure 3.4. The dynamic range of viral particle detection for ΔF4LΔJ2R VACV is between $1x10^7$- $1x10^8$ particles/mL. A. Flow cytometry dot plots showing ten-fold dilutions from an original stock concentration of $5x10^9$ infectious PFU/mL. * denotes potential swarming. B. Flow cytometry dot plot of the unstained original virus stock solution containing $5x10^9$ infectious PFU/mL C. Scatter plot showing particle counts per mL in a dilution series of the original virus stock preparation.

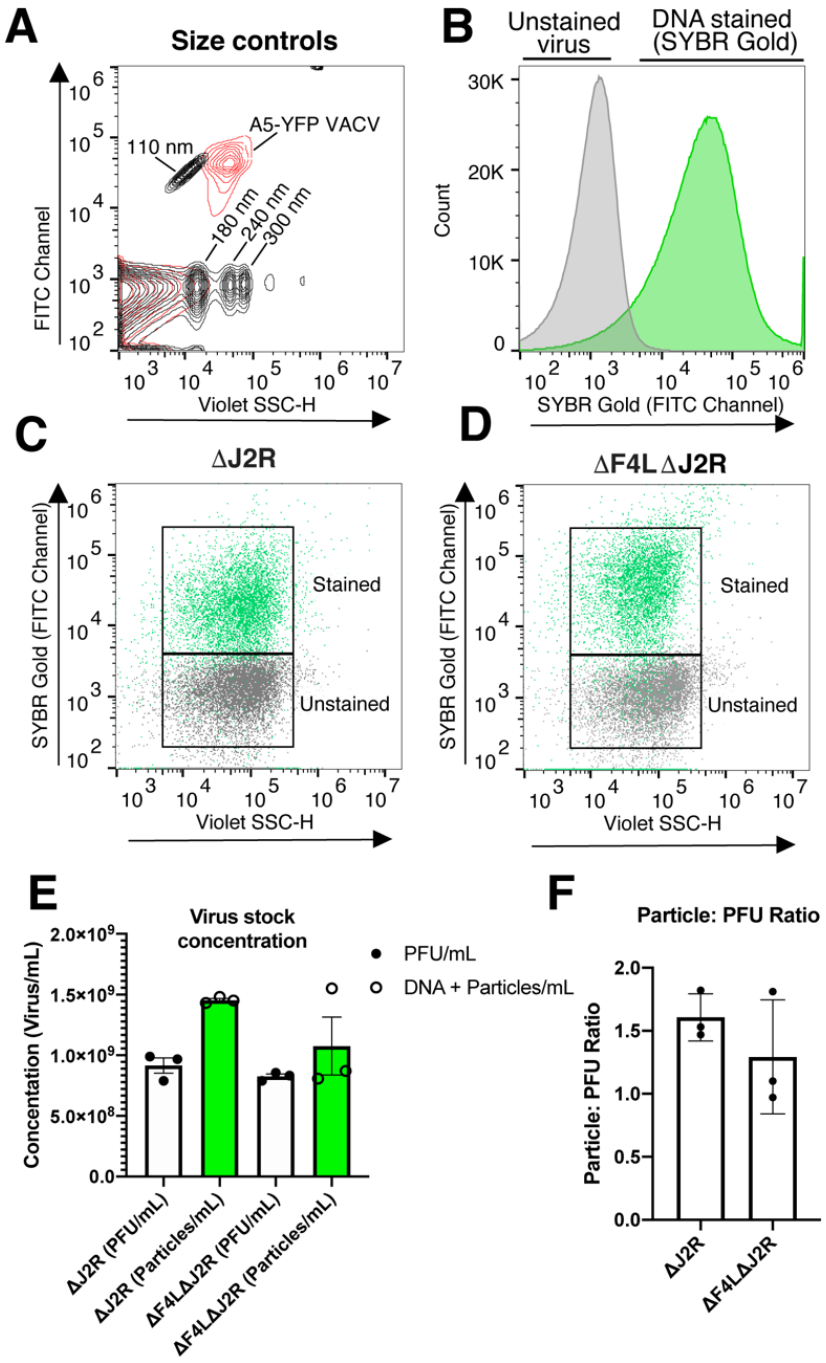

Figure 3.5. Flow cytometry and DNA stains can be used to determine the specific infectivity of VACV preparations A) Contour plots showing size calibration beads (100-500 nm in diameter, indicated), overlaid with the distribution of A5-YFP VACV particles. X-axis: Size measured as Violet SSC-H, Y-axis: Fluorescence intensity in the FITC channel. B) Histogram showing the shift in the distribution of the fluorescent signal between unstained (grey) and SYBR Gold stained (green) viruses. C&D) Superimposed dot plots showing the distribution of the ΔJ2R (C) or ΔF4LΔJ2R (D) virus particles either unstained (grey) or stained with SYBR Gold stained (green). E) Quantification of virus using either plaque assays (PFU/mL) or from a count of DNA-positive particles by flow virometry (particles/mL). F) Virus infectivity as represented by particle-to-PFU ratios (from data shown in panel E). Error bars denote +/- standard deviation from the mean value of three experimental replicates.

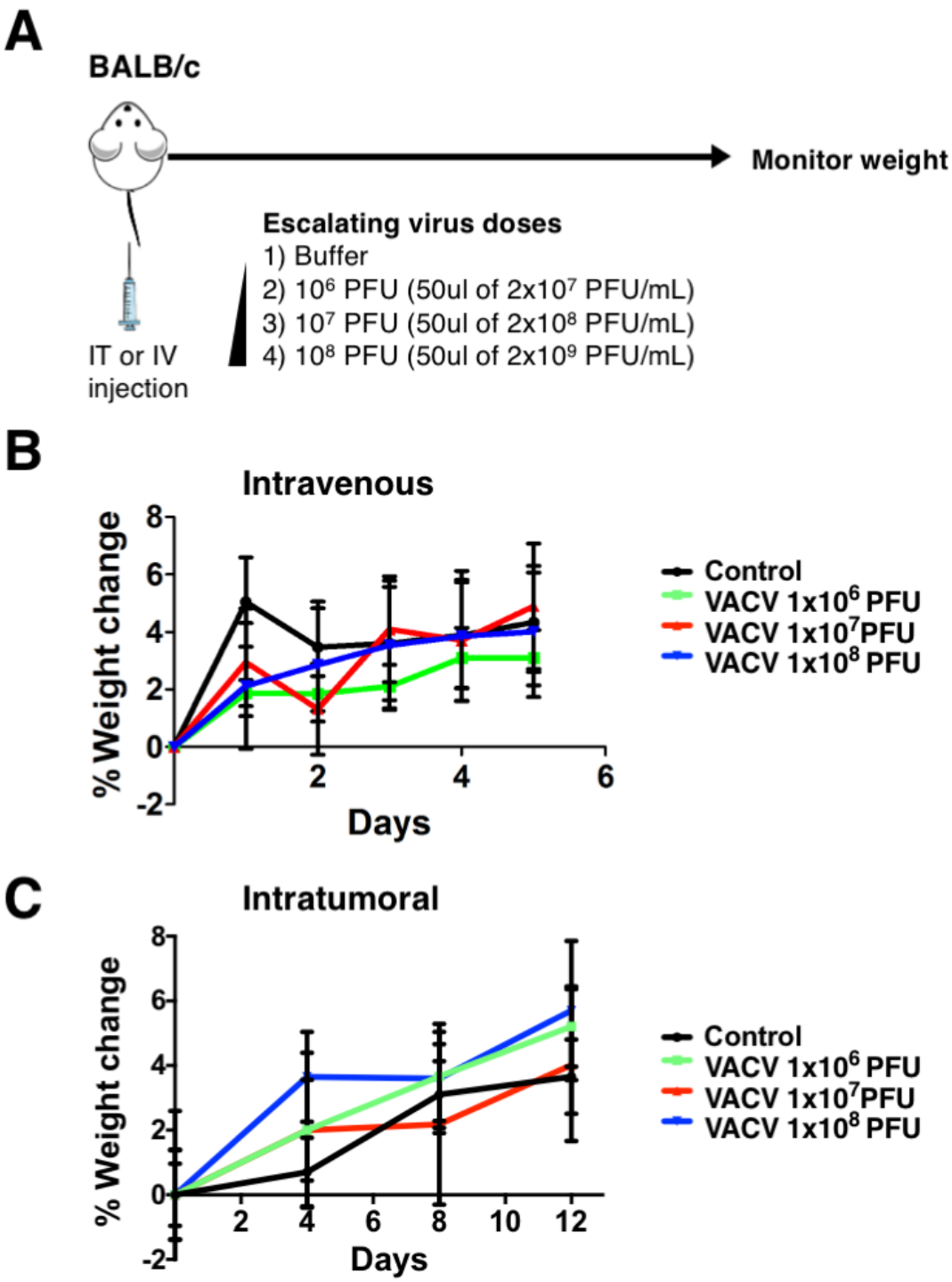

Figure 3.6 Oncolytic VACV can be used safely in mouse models of breast cancer although the route of administration determines the maximum tolerable dose. A) Schematic showing how different doses of preclinical grade oncolytic VACV were tested in mouse mammary models of breast cancer. B) Percent weight change in cohorts of TuBo tumour-bearing mice treated intravenously via tail vein injection with increasing doses of ΔF4LΔJ2R VACV (C) Percent weight change in tumour-bearing mice treated with increasing doses of oncolytic VACV via intratumoral injection into mammary fat pad tumours. In the cohort of mice treated with 10^8 PFU of intratumoral VACV, 2/5 animals died at injection #1, therefore, N=3 in 1 x10^8 PFU (blue) group, and N=5 for all other groups (black, green and red)* NF & MS contributed to these experiments.

3.3 Discussion

As oncolytic virus research progresses, it is becoming increasingly important to standardize the quality of virus preparations to ensure reproducibility between preclinical studies. It is also important to consider national guidelines on animal use and care, such as those issued by the Canadian Council on Animal Care, where there is a commonly held requirement to reduce the numbers of animals used in research and minimize the harm caused to these animals during treatment. These requirements can be promoted in preclinical research by following procedures designed to consistently ensure the purity, titer, safety, and identity of the virus stocks produced for *in vivo* studies.

These studies show that growing VACV on adherent cell culture plates produced higher yields of virus per cell and was more cost-effective and less labour intensive than growing the virus in roller bottles. Further savings can be implemented by replacing FBS with FBS-alternatives with no loss of yields. The relatively greater virus yields on plates also meant that less cellular contaminants needed to be removed through purification. We don't know why VACV would grow better on flat plate surfaces, but others have reported that the virus likewise grows better on adherent HeLa cells compared to suspension cultures[289]. Nor have we ever achieved better yields of virus per cell after testing several other kinds of cell suspension technologies (unpublished data). This situation may be unavoidable and caused by the sheer forces that are created as media flows past suspended cells.

Most, although not all authors have observed that VACV tends to aggregate and that sonication promotes the dispersal of virus particles without inactivating the virus[289,292,299–301]. This problem is observed when the virus is concentrated to titers exceeding ~$1x10^9$ PFU/mL and is likely exacerbated when virus suspensions are concentrated in a slowly frozen mixture. (This is a reason for using a "snap freezing" protocol.) In our experience a sonication step produced an increase in viral titer of ~50% and shows how sonication is needed to ensure accurate titers and thus reproducible dosing. When these VACV stocks were snap frozen, stored at -80˚, rapidly thawed, and sonicated, our long-term testing could detect no loss of titer for up to three years. Vaccinia is known to be a very stable virus and stockpiles of lyophilized smallpox vaccine have been stored now for several decades with little loss of titer.

In assessing the quality of virus preparations, the particle to PFU ratio is frequently cited as a critical measure of infectivity. It shows how much culturable virus is produced relative to the total number of virus-like particles[302]. The reported particle to PFU ratios for poxviruses vary greatly in the literature, ranging from 2 to 500 particles per PFU[302]. This likely reflects differences in the methods used to produce and purify the virus including the use of different cell lines and infection protocols[299]. There are also major differences in how the particle numbers are calculated and this could be a source of significant error. Optical density, electron microscopy, and particle counters have all been used to assess particle numbers, and using different cell lines for plaque assays gives rise to different estimates of the virus titer[302]. We used an advanced particle counter, a strict definition of what's considered a VACV particle (defined by size

and DNA content), and a highly permissive BSC40 cell host. Using this approach our purification methods yielded VACV stocks exhibiting particle to PFU ratios close to one (~1.6 for the ΔJ2R and ~1.3 for the ΔF4LΔJ2R stocks). This is perhaps not as surprising as it would seem since the high infectivity of some Orthopoxvirus preparations has long been known[302].

Fergusson et al. have recently offered recommendations for reporting on preclinical OV therapeutic studies[303]. In this article they stressed the importance of providing a complete and accurate description of the methods used to conduct the trials and analyze the data. However, they did not address methods relating to oncolytic virus production[303]. We propose that it would also be helpful to standardize how these OV are grown and purified, or at least one should offer a sufficiently detailed description of these steps to aid an interpretation of the author's conclusions. For instance, VACV grown on different cell lines or stored and titered improperly may exhibit different particle to PFU ratios[299]. Depending on how the virus was purified it may also contain varying quantities of contaminants like DNA. Such experimental variables could affect the immune response to viral therapy and could be addressed by reporting a parameter like the particle to PFU ratio. These parameters are carefully controlled when preparing clinical grade OV[304] and preclinical studies would benefit from similar considerations. This will ensure that the development of oncolytic viruses is supported by the best possible preclinical animal trials.

Chapter 4: Oncolytic vaccinia virus immunotherapy antagonizes image guided radiation therapy in mammary tumour models

Preface

A portion of this chapter has been submitted as a manuscript to Cancers as: Umer BA, Noyce RS, Kieser Q, Rans K, Middelton J, Favis NA, Hitt M, and Evans DH (2020). Oncolytic vaccinia virus immunotherapy combined with radiation antagonizes breast tumour clearance despite favorable immune stimulation [submitted].

Author contributions:

BU - development of methodology, performed experiments, editorial revisions, manuscript preparation

RN -study supervision, development of methodology, technical and experimental assistance, editorial revisions, manuscript preparation

QK-technical & experimental assistance

KS & JM - development of methodology, technical & experimental assistance

NF & MS - Technical & experimental assistance and animal support

MH- Study supervision, editorial revisions, development of methodology, technical and experimental assistance

DE - Study supervision, editorial revisions, manuscript preparation

4.1 Introduction

The field of immunotherapy, which mobilizes a patient's own immune system to target and kill cancerous cells, has been advancing rapidly in recent years. Much success has been achieved using immunotherapy to treat hematological malignancies and some solid tumours, although immunotherapy has not achieved the same level of success treating breast cancers[305]. As research in the field progresses, there has been a growing interest in combining immunotherapies with other treatments to achieve a therapeutic effect superior to single-agent treatments alone[305].

Oncolytic viruses promote a form of immunotherapy in which a virus is used to infect and kill tumour cells, while also stimulating anti-tumour immunity[306]. To date, only one oncolytic virus, a herpesvirus, has been approved for use in the clinic by the FDA, and it is currently indicated for use in advanced melanoma[116]. No oncolytic virus has been approved for use to treat breast cancer. Similar to other forms of immunotherapy, the greatest therapeutic benefit of OVs will likely require combinations with additional therapies.

Our laboratory studies oncolytic vaccinia virus (VACV), a large DNA virus that was once used widely to vaccinate against smallpox[16]. By deleting viral genes encoding components of the nucleotide metabolism machinery, F4L (the small subunit of ribonucleotide reductase) and J2R (thymidine kinase), a ΔF4LΔJ2R VACV strain is rendered dependent on the host cell to produce dNTPs for virus replication[149]. These dual deletions in F4L and J2R restrict virus replication to tumours and improve safety, while maintaining therapeutic efficacy and promoting anti-tumour immunity in bladder cancer models[119]. Despite the success in treating orthotopic mouse and rat models of bladder cancer, ΔF4LΔJ2R VACV was not therapeutically beneficial in mouse breast tumour models[175].

Previous pre-clinical studies have shown that different oncolytic viruses can sometimes synergize with ionizing radiation (IR) therapy to result in improved therapeutic responses[170]. With oncolytic herpes simplex virus (HSV), increased viral titers and oncolysis occurs through upregulation of ribonucleotide reductase following radiation therapy[268]. Some recombinant VACVs also improve outcomes when combined with various forms of radiation in other tumour models[166,167,266,267,307]. This evidence led us to speculate that improved therapeutic outcomes could be achieved by combining ΔF4LΔJ2R VACV with IR in breast cancer models.

One factor that complicates the interpretation of some earlier studies is that the way the radiation was delivered rarely replicated the way solid tumours are nowadays treated in humans. Current methods use image-guided radiation to ensure that the majority of the dose is distributed in a region defined by the tumour boundaries[308]. In the current study, we assessed therapeutic outcomes when VACV was combined with highly targeted image-guided radiation therapy (IG-RT) using a high-resolution research device designed for treating mouse tumour models. IG-RT combines advanced tumour imaging with radiation delivery, allowing the operator to irradiate the tumour with high accuracy and precision, while avoiding damage to off-target tissue. We speculated that using IG-RT prior to viral

infection would reduce the bulk of the tumour mass, and that ΔF4LΔJ2R VACV would infect and kill any tumour cells that might remain alive on the tumour periphery.

4.2 Results:

4.2.1 Cellular ribonucleotide reductase subunits R2 and P53R2 are present after treatment with 8 Gy of radiation

Previous work in our lab has shown that replication of ΔF4LΔJ2R VACV is dependent on cellular levels of the small subunit of ribonucleotide reductase (RR), R2, which is the cellular homolog of the VACV F4 protein[119,149]. To determine when RR subunits were highest following treatment with IR, human breast cancer cell lines of varying p53 status (MDA-MB 231 and ZR 75.1 having mutated P53, and MCF 7 having functional P53[309]) were treated with 8 Gy of IR or mock irradiated. At various time points following radiation treatment, cells were harvested and western blotting was performed to detect both R2 and its p53-inducible subunit, p53R2. We found that both R2 and P53R2 were present and detectable following treatment with IR (Figure 4.1). While levels of R2 tapered off after approximately 24 hours in MDA-MB-231 and MCF7 cell lines, it remained high up to a week post IR in ZR75.1 cells. P53R2, on the other hand, remained detectable in all cell lines up to one week post-IR. This suggested that virus replication would be sustained following IR treatment, and that virus treatment should be administered soon after radiation therapy, ideally within the first 24 hours. We also observed no correlation between P53 status and expression of R2 and P53R2.

4.2.2 Irradiation of breast cancer cells does not impact oncolytic VACV replication

After determining that RR subunits were present after radiation in human breast cancer cell lines, we sought to assess if radiation had an impact on virus yields over time in both mouse and human breast cancer cell lines. In selecting cell lines for our panel, we opted to include both human and mouse breast cancer cell lines. We selected both a P53 positive (MCF 7) and a P53 negative/mutated (MDA-MB 231) human cancer cell line, and three murine breast cancer cell lines: 4T1 (P53 deficient[310]), TuBo (P53 positive[311]) and MTHJ (unknown P53 status). Cells were irradiated with either 4 or 8 Gys of radiation using a cesium source gamma irradiator or remained non-irradiated. Twenty-four hours post radiation, cells were infected with a MOI of 0.03 and, at various time points, cells were harvested, and virus amplification was assessed by plaque assay on BSC40 cells. In the murine mammary cancer cells lines, TuBo, 4T1, and MTHJ, the per cell yield of ΔF4L, ΔJ2R, and ΔF4LΔJ2R was not impacted by radiation at any dose tested (Figure 4.2A-C). Similarly, in the human breast cancer cell lines MDA MB 231 and MCF 7, virus amplification was not significantly impacted by radiation at any dose tested for any virus tested and P53 status did not seem to impact these results (Figure 4.2D,E).

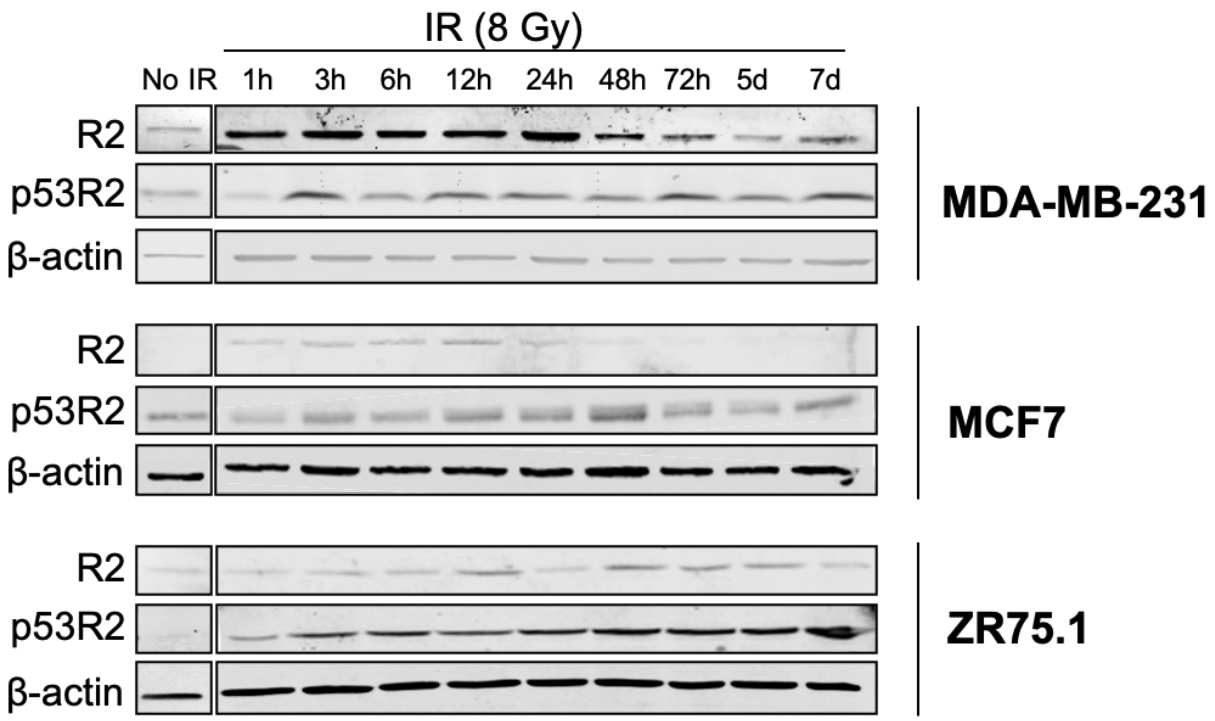

Figure 4.1. Cellular RR subunits R2 and P53R2 are present after treatment with 8 Gy of ionizing radiation (IR). Western blots of cellular R2 and P53R2 isolated from human breast cancer cell lines up to one week following 8 Gy of IR treatment.

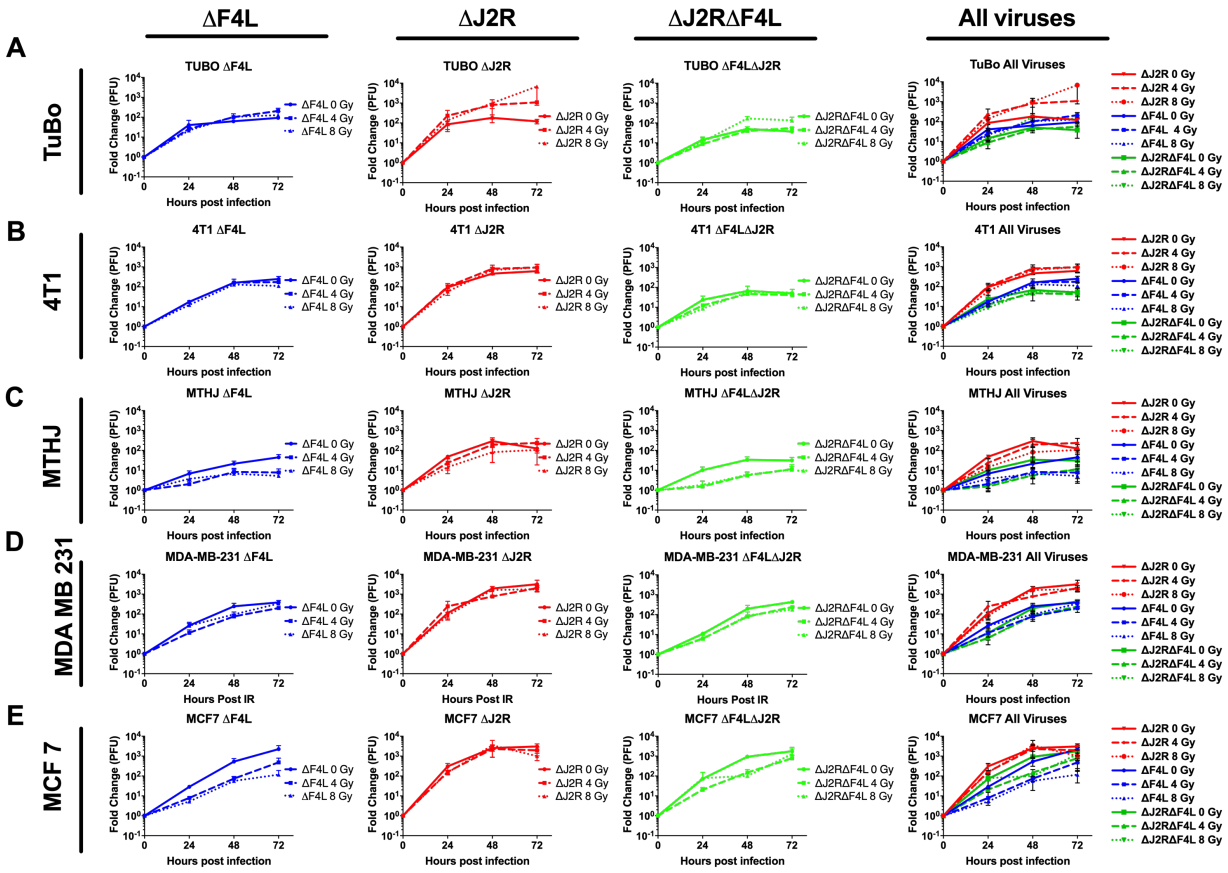

Figure 4.2. Irradiation of breast cancer cells does not impact oncolytic vaccinia virus replication. Viral growth kinetics *in vitro* in A)TuBo, B) 4T1 and C)MTHJ mouse mammary carcinoma cells and D) MDA MB 231 and E) MCF 7 human breast cancer cell lines infected with ΔF4L (blue), ΔJ2R (red) and ΔF4LΔJ2R (green) oncolytic VACVs. Cell lines were irradiated with 4 or 8 Gys (dashed and dotted lines, respectively) with a cesium source gamma irradiator, or mock irradiated (solid line) and infected 24 hours later with the indicated viruses at an MOI of 0.03 PFU. Cells were harvested at the indicated time point, freeze thawed three times and titered by plaque assay on BSC-40 cells. Virus growth is shown as fold change in PFU based on the input virus. Error bars indicate ± SEM of three experimental replicates. Two-way ANOVA showed no significant differences ($p>0.05$) between virus amplification over time between radiation treatments.

*QK contributed to this figure

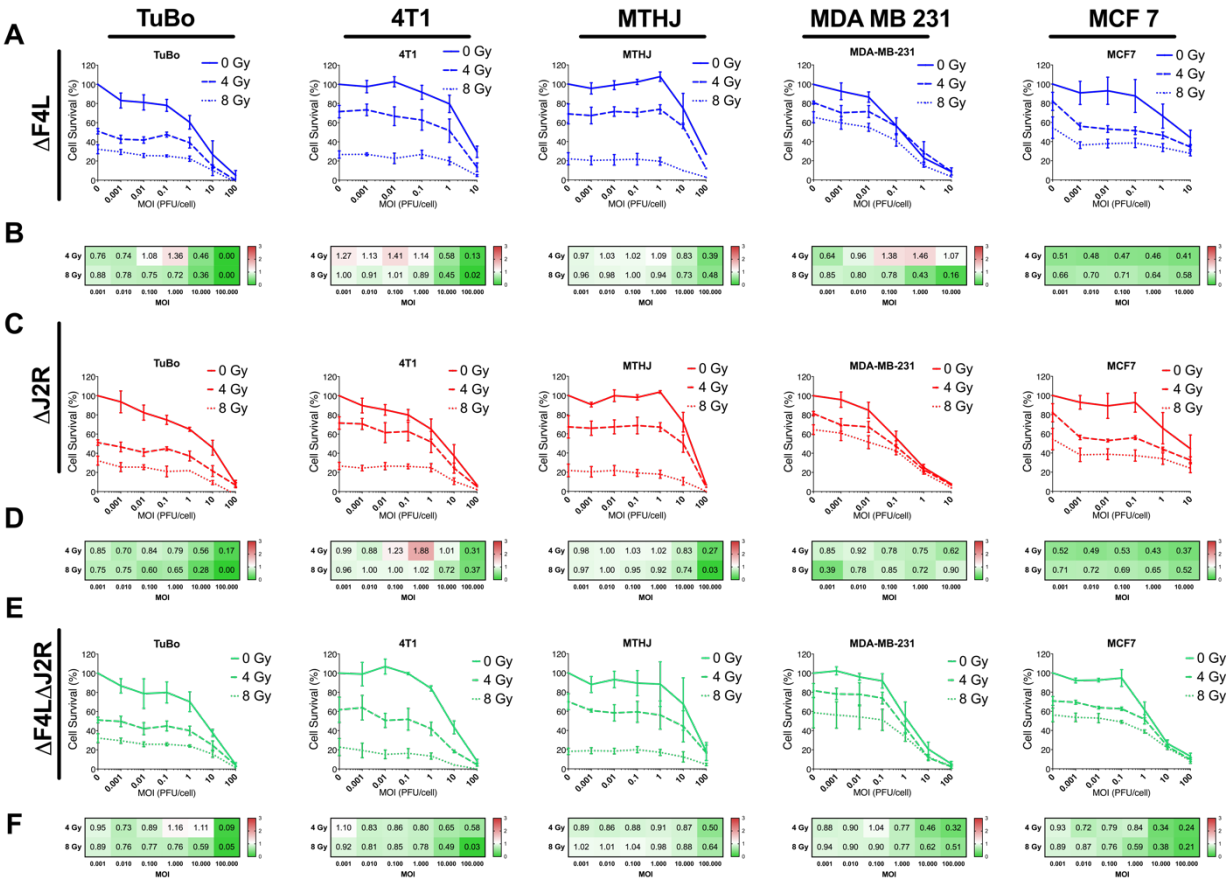

Figure 4.3. Radiation combined with oncolytic viruses work synergistically to kill cancer cells *in vitro*. A,C,E) Resazurin assay measuring cell viability 72 hours post infection with A)ΔF4L VACV, B) ΔJ2R VACV and C) ΔF4LΔJ2R VACV of irradiated murine mammary tumour cell lines (TuBo, 4T1, MTHJ) and human breast cancer cell lines (MDA MB 231, MCF 7). Cells were irradiated 24 hours prior to infection with indicated MOIs. Mean value is plotted, with error bars denoting +/- SEM from three experimental replicates. B, D, F) Heat-maps showing CompuSyn drug synergy analysis combination index (CI) values, where green indicates synergy (CI<1.1), white is additive (CI=1.1), and red is antagonistic (CI>1.1), computed using average viability values from A,C,E.

*QK contributed to this figure.

4.2.3 Radiation combined with oncolytic viruses work synergistically to kill cancer cells *in vitro*.

After demonstrating that VACV replicated in irradiated cells, we assessed the cytotoxicity caused by combining radiation plus oncolytic VACV therapy using the same panel of breast cancer cell lines. Cells were irradiated with 4 or 8 Gy, or mock irradiated, and infected 24 hours later with various MOIs of our three oncolytic VACVs, ΔF4L (Figure 4.3A), ΔJ2R (Figure 4.3C), and ΔF4LΔJ2R (Figure 4.3E). All oncolytic viruses combined with radiation increased cell death in all cell lines (Figure 4.3A,C,E), and in no instance did we observe reduced cell death in the presence of

virus infection compared to radiation alone, (i.e., at MOI = 0). This showed that VACV does not prevent or impair the ability of radiation to cause cell death *in vitro.*

To quantify the drug-like interactions between the two treatments, we employed CompuSyn Drug Synergy analysis software. This analysis takes data from viability assays when two drugs are combined and computes a combination index (CI) value to determine how drugs are cooperating. A detailed description of the interpretation of CI values from CompuSyn Analysis can be found in the materials and methods section in Table 2.3. Briefly, a CI value of <1 is considered synergistic, CI=1-1.1 is considered additive, and CI >1.1 is antagonistic. For visual clarity, and as no computed CI values were higher than 1.88, the CI heatmap scale was clipped at a CI value of 3, representative of "antagonism". Generated CI values indicated that primarily synergistic interactions were observed between radiation and oncolytic vaccinia virus therapy (Figure 4.3B,D,F), with slight differences observed with different viruses and doses of radiation. Treatment with ΔF4LΔJ2R VACV produced almost exclusively synergistic interactions, with the strongest synergy observed at the highest doses of virus (MOI 100) and highest dose of radiation (8 Gy) (Figure 4.3F). Of 60 CIs evaluated for this virus across the 5 different cell lines, only two dose combinations demonstrated slight antagonism in TuBo cell line at 4 Gy doses at MOIs of 10 and 1. Aside from these, all other values indicated synergistic or additive effects. Treatment with ΔF4L and ΔJ2R viruses each yielded mostly synergistic co-operation (Figure 4.3B,D), again with the most favourable benefits at higher doses of virus and radiation. However, in the 4T1 cell line, treatment with 4 Gy of radiation and infection at an MOI of 1 and 0.1 with ΔJ2R virus, or MOIs of 0.001-1 for ΔF4L was determined to be antagonistic. Additionally, infection of TuBo cells with ΔF4L VACV at an MOI of 1, or MDA MB 231 cells at an MOI of 1 or 0.1 were also shown to be antagonistic.

Overall, the increased cytotoxicity to cells when combining radiation and virus, and the calculation that this reflects some synergy between the two treatments, suggests that combining virus and radiation therapy were more beneficial than either treatment on their own *in vitro*. Practically speaking it suggests that infecting irradiated cells with VACV does not interfere with the ability of radiation to kill cells. These promising results led us to evaluate the effects of combining these therapies *in vivo.* Previous work in our lab suggested that, in bladder cancer models, the ΔF4LΔJ2R VACV was the safest OV compared to ΔF4L or ΔJ2R VACV, while maintaining therapeutic efficacy[119]. We also observed the most synergistic interactions in cytotoxicity assays between radiation and ΔF4LΔJ2R VACV *in vitro* (Figure 4.3E,F). Therefore, were selected the ΔF4LΔJ2R VACV to investigate *in vivo.*

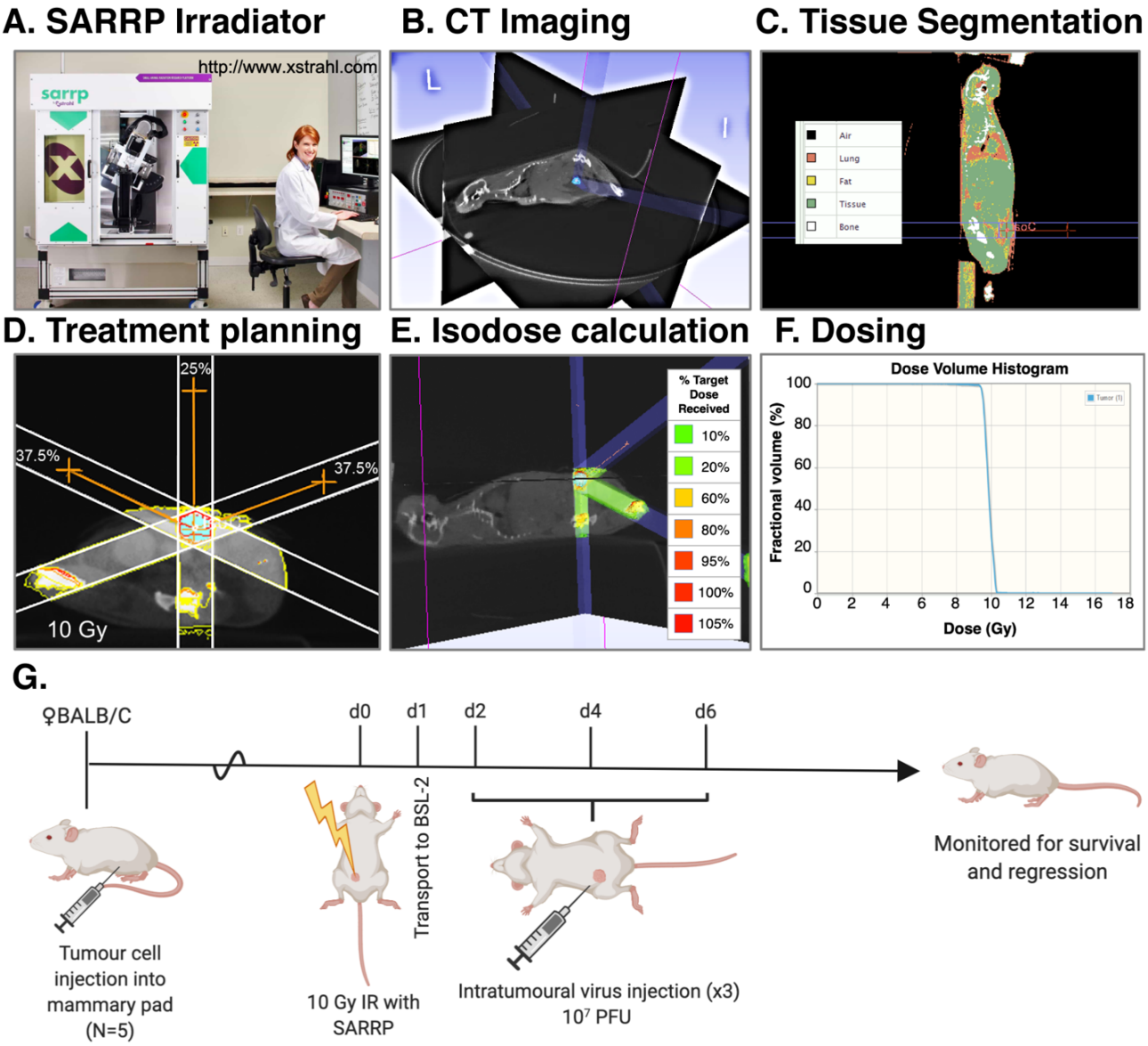

Figure 4.4. *In vivo* experimental timeline and image-guided radiation therapy using the SARRP and MuriPlan treatment planning software by XStrahl. A. Picture of the SARRP image-guided radiation therapy platform for targeted radiation delivery to small animals, capable of CT imaging and targeted radiation dose delivery with 0.5mm precision (courtesy of xstrahl.com). B. 360° CT imaging from SARRP viewed using MuriPlan treatment planning software showing tumour location (blue). C. MuriPlan manual tissue segmentation allowing for dose attenuation through various tissues, where black=air, pink=lung, yellow=fat, green=tissue, white=bone. D. Treatment planning using the MuriPlan program showing three beams converging on tumour isocenter to deliver a total of 10 Gy with dose distributed over 3 beams (37.5% for two beams and 25% for remaining beam). E. MuriPlan isodose calculations showing doses as a percent of targeted dose delivered to non-tumour tissue. F. Dose volume histogram of tumour target showing the fractional tumour volume receiving the tumour dose. G. Experimental treatment timeline to test combination therapy with radiation and ΔF4LΔJ2R VACV. Image created using BioRender.com. SARRP=Small animal radiation research platform, IR= irradiation, BSL-2= biosafety level 2 containment suite, CT=computed tomography, IsoC=isocenter of tumour.

4.2.4 IG-RT using the SARRP to test ΔF4LΔJ2R VACV combined with radiation *in vivo*

In order to assess the therapeutic efficacy of combining radiation with ΔF4LΔJ2R VACV *in vivo*, we made use of the XStrahl Small Animal Radiation Research Platform (SARRP) to deliver targeted image-guided radiation therapy (IGRT)(Figure 4.4A). This machine is capable of 360° CT imagining (Figure 4.4B), and the XStrahl MuriPlan treatment planning software allows for radiation delivery to small animal models that mimics patient treatment in the clinic. Using the SARRP, a CT scan is taken of the mice and uploaded onto the MuriPlan Software (Figure 4.4B). Once uploaded, tissue segmentation is used to differentiate between air, lung, fat, tissue, and bone (Figure 4.4.C), which allows for the treatment planning software to correctly attenuate and adjust radiation doses as it passes through various tissue. Advanced treatment planning allows the user to identify the tumour isocenter where the radiation beams converge (Figure 4.4D), and the angles and doses of the beam can be adjusted to avoid or limit radiation exposure to non-tumour tissue, which is reported in isodose calculations, showing the percent of target dose delivered to off-target tissues (Figure 4.4E). Lastly, the software is able to determine the dose delivered to the tumour target, reported as a dose volume histogram (DVH), showing the fractional volume of tumour receiving the corresponding radiation dose (Figure 4.4F). Treatment plans were customized for each individual mouse, where a target dose of 80% of the tumour volume receives 90% of the target dose of 10 Gy, while minimizing doses delivered to sensitive tissue, primarily in the bone. If a treatment plan did not meet these requirements, the beam angles and weights were adjusted to increase the fractional volume receiving the target dose, or to minimize off-target radiation exposure.

To test a combination therapy regimen *in vivo*, we first injected female 6-8-week-old BALB/C mice with tumour cells in the mammary fat pad (Figure 4.4G). Once tumours were palpable (~8 days post injection), the mice were anaesthetized and a SARRP was used to deliver 10 Gy of IG-RT to the tumour isocenter. The next day the mice were transported to the BSL-2 vivarium for virus treatment, where they were allowed to acclimatize overnight. At 2 days post-IG-RT, the mice were treated with 3 intratumoural doses of 10^7 PFU of ΔF4LΔJ2R VACV, administered at 48-hour intervals, or PBS as an injection control. Tumour volumes and weights were monitored twice per week until mice reached endpoint. Five mice were used per group per experimental repeat, and the experiment was performed three times for a total of 15 mice per group.

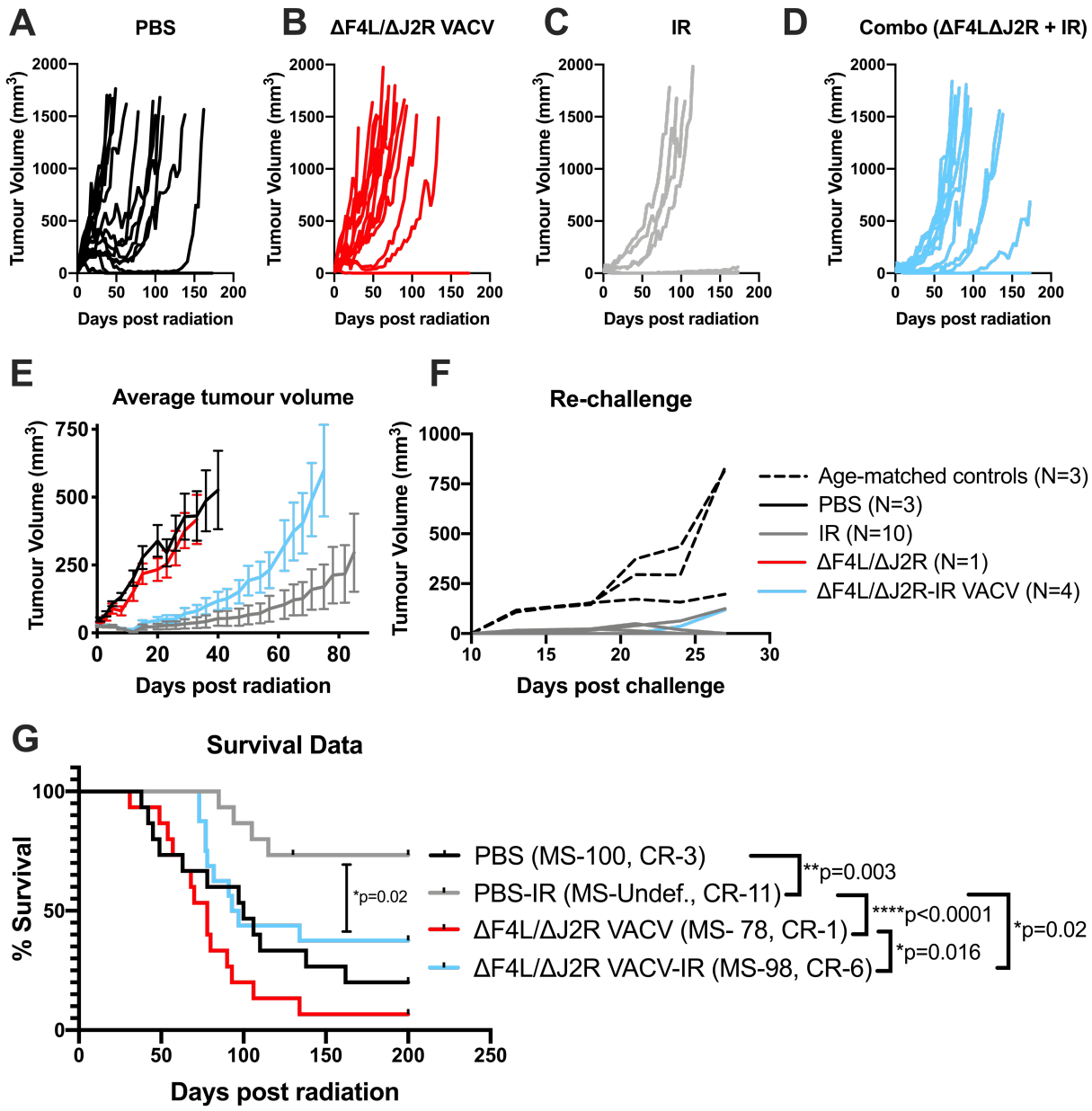

Figure 4.5. Virus administered 48 hours after 10 Gy radiation does not improve tumour regression and worsens survival in the orthotopic TUBO tumour model. (A-D) Tumour growth of each individual mouse measured twice per week after treatment with (A) PBS, (B)ΔF4LΔJ2R alone, (C)10 Gy of IR, or (D)combination therapy with ΔF4LΔJ2R and 10 Gy IR. (E) Average tumour volume of treatment groups shown in A-D, until first mouse reached endpoint in each group, with error bars denoting +/- SEM (F) Tumour re-challenge experiment from mice with complete responses to determine if anti-tumour immunity is established. Mice were re-challenged with fresh TuBo cells in the opposite mammary fat pad from the primary tumour and tumour growth was measured. (G) Kaplan-Meier survival curves of data shown in A with p values calculated using a Mantel-Cox log-rank test. MS- Median survival, CR-complete responses, undef-undefined MS. N=15 mice per group total, (5 mice per experimental repeat, performed three times). Tumour re-challenge experiments performed with mice with complete responses from the second and third experimental repeat.

4.2.5 VACV therapy antagonizes IG-RT *in vivo* in TuBo tumours

Despite the positive synergistic/additive effects *in vitro*, we observed that the two therapies were antagonistic *in vivo* in the orthotopic syngeneic TuBo mammary tumour model (Figure 4.5). When assessing tumour growth (Figure 4.5A-E), PBS-treated tumours had the fastest growth rate (Figure 4.5. A,E), similar to that of ΔF4LΔJ2R treated tumours (Figure 4.5B,E). While IR alone could slow tumour growth (Figure 4.5C,E), the addition of virus appeared to decrease the effectiveness of IG-RT, as tumours grew more rapidly when virus was added (Figure 4.5D,E). Survival was also decreased in the combination therapy treatment group relative to IR only ($p=0.02$). We observed 11/15 complete responses in IR-treated animals and median survival time was >200 days compared to the combination therapy group where only 6/15 mice exhibited complete responses and cleared the tumour, with a median survival of 98 days (Figure 4.5G). Independent of treatment, all mice that had cleared the primary tumour developed functional anti-tumour immunity, as assessed in tumour challenge experiments in the opposite mammary fat pad. Tumours either did not establish, or grew slightly initially, but all eventually cleared and we undetectable (Figure 4.5F).

After establishing that antagonism was occurring in the TuBo tumour model, we wanted to see if this effect was dependent on the timing of virus administration. When given 48 hours post-radiation, it appeared that virus combined with IG-RT controlled TuBo tumour growth until about 3 weeks after virus treatment, after which tumour growth resumed and overtook the rate of growth of tumours treated only with radiation (Figure 4.5E). Therefore, we wanted to assess if delaying virus treatment until 21 days after radiation would still result in antagonism (Figure 4.6A).

4.2.6 Antagonism is dependent on the timing of virus administration

When virus treatment was delayed until 21 days post virus therapy, it was found that this effect was, indeed, dependent on the timing of virus administration. Antagonism was not seen in the delayed virus-treatment group (Figure 4.6B-G). However, this still did not improve the overall outcome as a combination of IG-RT and virus therapy did not alter tumour growth and survival relative to the radiation alone treatment group (Figure 4.6B-G).

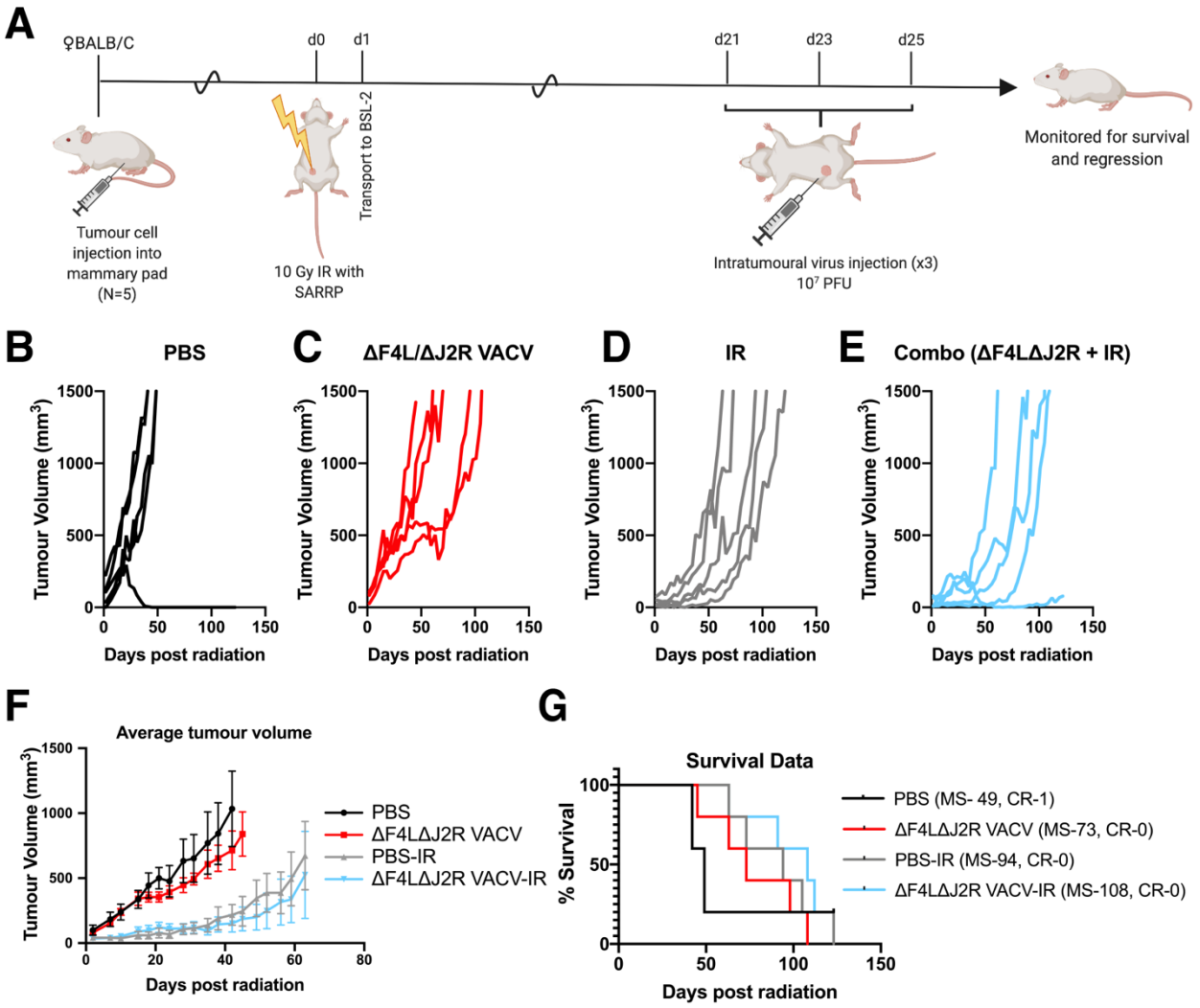

Figure 4.6. Delayed virus administration does not cause antagonism but does not improve therapeutic responses. A. Experimental timeline testing delayed virus administration combined with radiation therapy. B-E. Individual mouse tumour volumes F. Average tumour volume of treatment groups shown in B-E, until first mouse reached endpoint in each group, with error bars denoting +/- SEM. G. Kaplan-Meir survival curve of mice from A-E. No significant differences were found between any of the treatment groups.

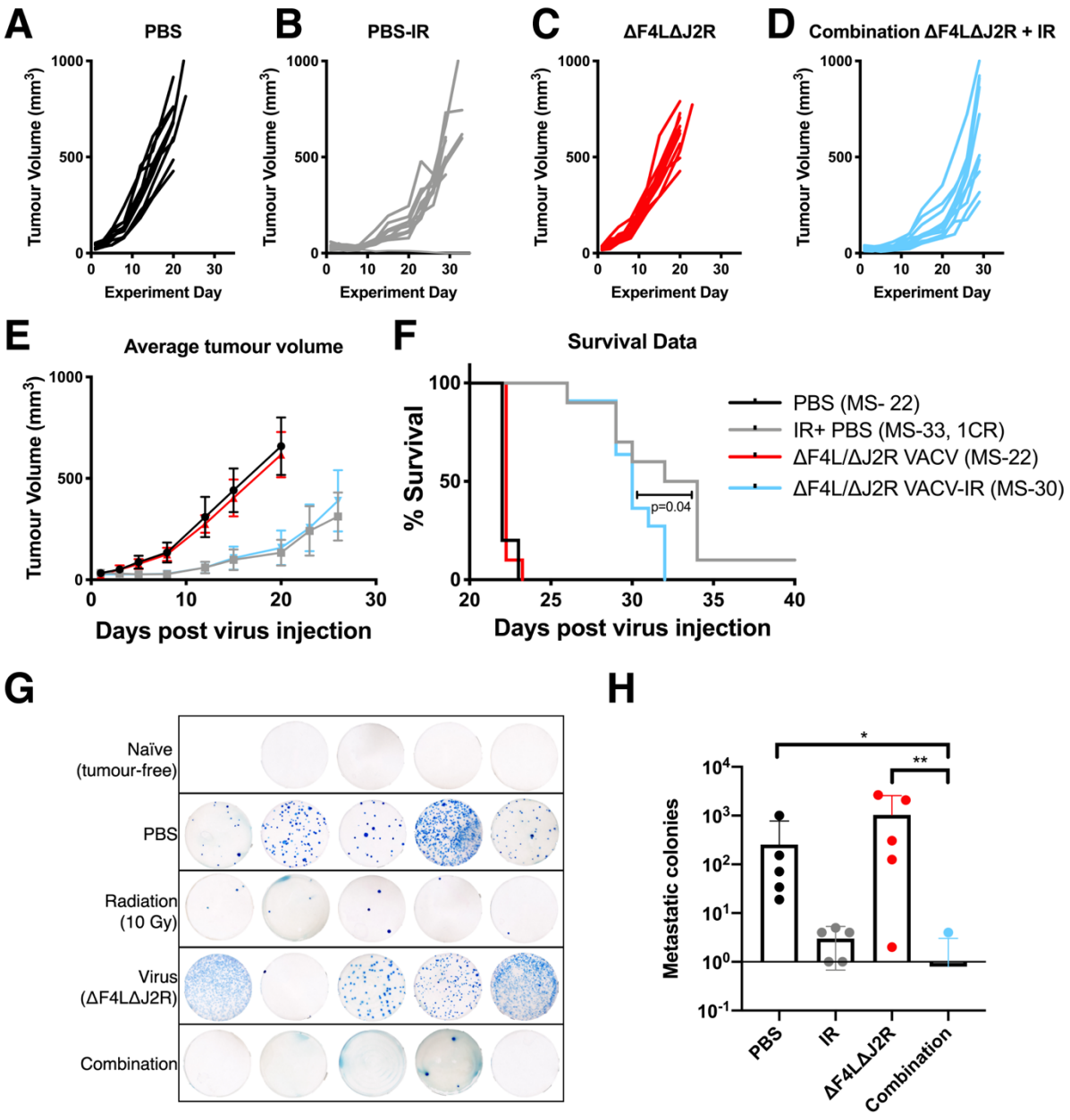

Figure 4.7. Virus administered 48 hours after 10 Gy radiation does not improve tumour regression, and worsens survival in the orthotopic 4T1 tumour model, despite a reduction in metastasis to the lungs (A-D) Mammary tumour growth of each individual mice measured twice per week with calipers (E) Average tumour volume of treatment groups until first mouse reached endpoint with error bars denoting +/- SEM (F) Kaplan-Meier survival curves of data shown in A with p values calculated using a Mantel-Cox log-rank test. N=10 mice per group (5 mice per experimental repeat performed twice). (G). Metastatic cells harvested from lungs of mice bearing 4T1 tumours 1 week post administration of the final virus treatment, as assessed using a colony formation assay under 6-thioguanine. (H) Cell colonies counts of data shown in G. Error bars denoting +/- SEM, N=5. *P<0.05, **P<0.01 determined using Kruskal-Wallis testing with Dunn's multiple comparisons test.

4.2.7 Virus administered 48 hours after 10 Gy radiation is antagonistic *in vivo* In the 4T1 tumour model

To determine if the antagonism observed when combining ΔF4LΔJ2R with radiation was limited to the TuBo model, or if this effect was consistent across multiple models, the combination was trialled in the aggressive 4T1 tumour model in BALB/C mice. 4T1 tumours exhibit accelerated growth properties, regularly metastasizes to the lungs, and are equivalent to a human triple-negative breast tumour based on hormone receptor status[237]. We used the same experimental timeline as described in Figure 4.4G, where tumours were established in the mammary fat pad, irradiated with 10 Gy using the SARRP, and transported and injected with virus 48 hours later. Due to the aggressive nature of this tumour model, mice are euthanized at first indicators of illness or distress, primarily weight loss, ceased grooming, social isolation, or hunched posture.

Although to a lesser extent, this antagonism was still observed in the 4T1 tumour model (Figure 4.7A-F). Tumour growth properties of virus treatment alone was nearly identical to that of PBS-treated tumours, while radiation-treated tumours grew at a comparable rate to combination therapy-treated tumours (Figure 4.7A-E). We did observe a minor decrease in median survival with the combination compared to mice treated with radiation alone (30 vs. 33 days) (Figure 4.7G), and while this was statistically significant (P=0.04), this difference in survival was modest. One mouse treated with radiation only had no evidence of a remaining primary tumour by day 30, which was the only occurrence of 4T1 tumour clearance observed in these studies (Figure 4.7). A subsequent tumour re-challenge experiment was performed on this mouse, where fresh 4T1 tumour cells were injected into the opposite mammary fat pad of where the primary tumour was established. Despite primary tumour clearance, the secondary challenge tumour was quickly established, demonstrating no lasting anti-tumour immunity occurred in this model (data not shown). To assess the effects of the different therapies on metastasis to the lungs, lungs were harvested and processed 1 week following the last virus treatment and plated under the drug 6-thioguanine (6-TG). As 4T1 cells are resistant to 6TG, this allows for quantification of metastasis to the lungs using a colony formation assay (Figure 4.7G). This analysis demonstrated that there were no differences in metastatic colonies on the lungs between radiation alone and combination therapy-treated mice (Figure 4.7H). However, the combination of ΔF4LΔJ2R and IR was able to statistically reduce the number of metastatic cells in the lungs compared to untreated (PBS) or virus-treated (ΔF4LΔJ2R) mice (Figure 4.7H).

4.3 Discussion:

In this study we have shown that combining radiation with oncolytic ΔF4LΔJ2R VACV is synergistic *in vitro*, but antagonistic *in vivo*. This antagonism was dependent on the timing of virus administration, but later dosing still did not improve therapeutic outcomes.

Previous studies have shown that timing is important when combining oncolytic VACV with other immunotherapies[312], and also when combining radiation with other immunotherapies[313]. Therefore, it was not

surprising that changing the timing of treatment affected the outcome of combination therapy and reduced the antagonistic effect. Although delaying virus administration had no added therapeutic benefit, it suggests that there may still be some treatment window that could deliver different therapeutic outcomes. Ideally, we would have liked to have tested whether administering the virus prior to radiation would have produced a different effect, but due to biosafety constraints we were unable to treat virus-infected animals with the SARRP irradiator. It is also known that single-dose irradiation, as used in this study, is less immunogenic than fractionated doses of radiation[313,314]. In an effort to try to find an optimal combination of virus and IG-RT, fractionated radiation dosing could also be tested.

It is difficult to compare our results with earlier work as few investigators have used a combination of an oncolytic virus, IG-RT, and orthotopic immune-competent tumour models. Xenografts have been used to explore these kinds of questions but are especially problematic as it is well established that while xenografted tumours often respond exceedingly well to oncolytic virotherapy, the same efficacy is never seen in more biologically relevant immune-competent hosts. However, there are some studies assessing other forms of radiation combined with VACV that have shown synergistic effects *in vivo*. For example, in a rat model of sarcoma, VACV GLV-1h68, containing deletions in the J2R, F14.5L and A56R viral genes, and delivered via isolated limb perfusion, improved survival when followed with 13 Gy of fractionated radiation given over two doses[266]. In another immune-competent model, a VACV strain engineered to express a sodium iodide symporter (GLV-1h153[307]) was more effective in an immune competent model for prostate cancer when the virus was combined with ^{131}I co-therapy than was virus alone. Unfortunately, one cannot draw any generalizations about VACV oncolytic virotherapy from these few studies using different tumour models, viruses, and forms of radiation.

Similar discrepancies in the literature exist with respect to combining other non-VACV based oncolytic viruses with radiation. In testing oncolytic mutant adenoviruses in combination with radiation, despite promising synergistic results *in vitro* and in subcutaneous xenograft models of glioma[315], when tested using orthotopic intracranial models, the combination was no better than single agent therapy[316]. Similarly, despite literature supporting the use of recombinant oncolytic HSV in combination with radiation, Jorgensen *et al*., found that there was no improvement in therapeutic responses when combined to treat human and mouse prostate cancer models[317]. Although in neither case was antagonism observed, the authors of the aforementioned study suggested that differences in dosing and timing of administration of the therapies might result in the variability in treatment outcomes.

In clinical trials with immunotherapies an unexplained phenomenon known as hyperprogression in solid tumours has become evident[318]. In this scenario, which is estimated to occur in 4-29% of patients, acceleration of tumour growth and a decrease in survival occurs after checkpoint blockade[318]. The antagonism we observed in these studies might be occurring by a similar phenomenon, however mechanisms are unknown emphasizing the need to more fully understand the complex interactions occurring with immunotherapies. This topic will be investigated in the

next chapter where I performed an analysis of the TiME to uncover potential insights into the interactions between radiation and ΔF4LΔJ2R VACV.

In conclusion, the results of our study show that more is not necessarily better when it comes to combining therapies in cancer treatment. While many reports show that IR can synergize with viruses to enhance killing of cancer cells, our observations show that *in vitro* assays may not represent reality in an *in vivo* context. Considering the potential risk this poses for patients, more studies are needed to fully understand how these two therapies interact *in vivo* to produce the effects we've seen. Such studies would also be expected to produce important insights into how one might improve the effectiveness of both IR and oncolytic viruses.

Chapter 5: Assessing immune responses after combination therapy

Preface

A portion of this chapter has been submitted for publication as: Umer BA, Noyce RS, Kieser Q, Rans K, Middelton J, Favis NA, Hitt M, and Evans DH (2020). Oncolytic vaccinia virus immunotherapy combined with radiation antagonizes breast tumour clearance despite favorable immune stimulation [submitted].

Author contributions:

BU - development of methodology, performed experiments, editorial revisions, manuscript preparation

RN -study supervision, development of methodology, technical and experimental assistance, editorial revisions, manuscript preparation

QK-technical & experimental assistance

KS & JM - development of methodology, technical & experimental assistance

NF & MS - Technical & experimental assistance and animal support

MH- Study supervision, editorial revisions, development of methodology, technical and experimental assistance

DE - Study supervision, editorial revisions, manuscript preparation

*Contributions by other authors have been identified in figure legends.

5.1 Introduction

Oncolytic viruses are known to stimulate the immune system, and a large portion of the therapeutic efficacy observed from OV therapy is mediated through adaptive immune responses[319–321]. Ionizing radiation, on the other hand, is largely regarded as a physical agent that causes dsDNA breaks, causing cell death[257]. However, recent evidence is emerging that the efficacy of radiation therapy is also mediated through systemic immune-mediated effects, and is an integral component of therapy[322–324]. In fact, there has been a surge of studies exploring radiation in combination with other immunotherapies to compliment therapeutic effects[265,324–326].

The observation in Chapter 4 that IG-RT and ΔF4LΔJ2R were co-operative *in vitro* but antagonistic *in vivo* led us to speculate that VACV therapy might be having an effect on the irradiated tumour microenvironment that was impairing tumour clearance. Based on the immune-mediated effects of both VACV and radiotherapy, we hypothesized that this might be immune-mediated. Therefore, we performed an immune analysis after combination therapy to determine how these two therapies were impacting the tumour bearing host.

5.2 Results

To evaluate virus distribution and immune responses in response to combination therapy, we performed a fixed endpoint experiment where mice were euthanized one week following the final administration of virus (Figure 5.1A). Tumours and spleens were collected for immune cell analysis and virus titering.

5.2.1 Radiation decreases viral titers in the tumour

We noted that virus yields were decreased in irradiated TuBo tumours compared to non-irradiated tumours (Figure 5.1B). Although the trend was similar for 4T1 tumours and less virus was isolated from the combination-therapy treated tumours, this difference was not statistically significant (p=0.056)(Figure 5.1C). Since approximately equal titers were observed *in vitro* in the presence and absence of radiation (Figure 4.2A,B), these differences in virus titers in different tumour models are more likely due to differences in the immune response as opposed to differences in viral replication. No virus was isolated from the spleens in either treatment group, nor was any virus recovered from the draining lymph nodes, heart, or liver.

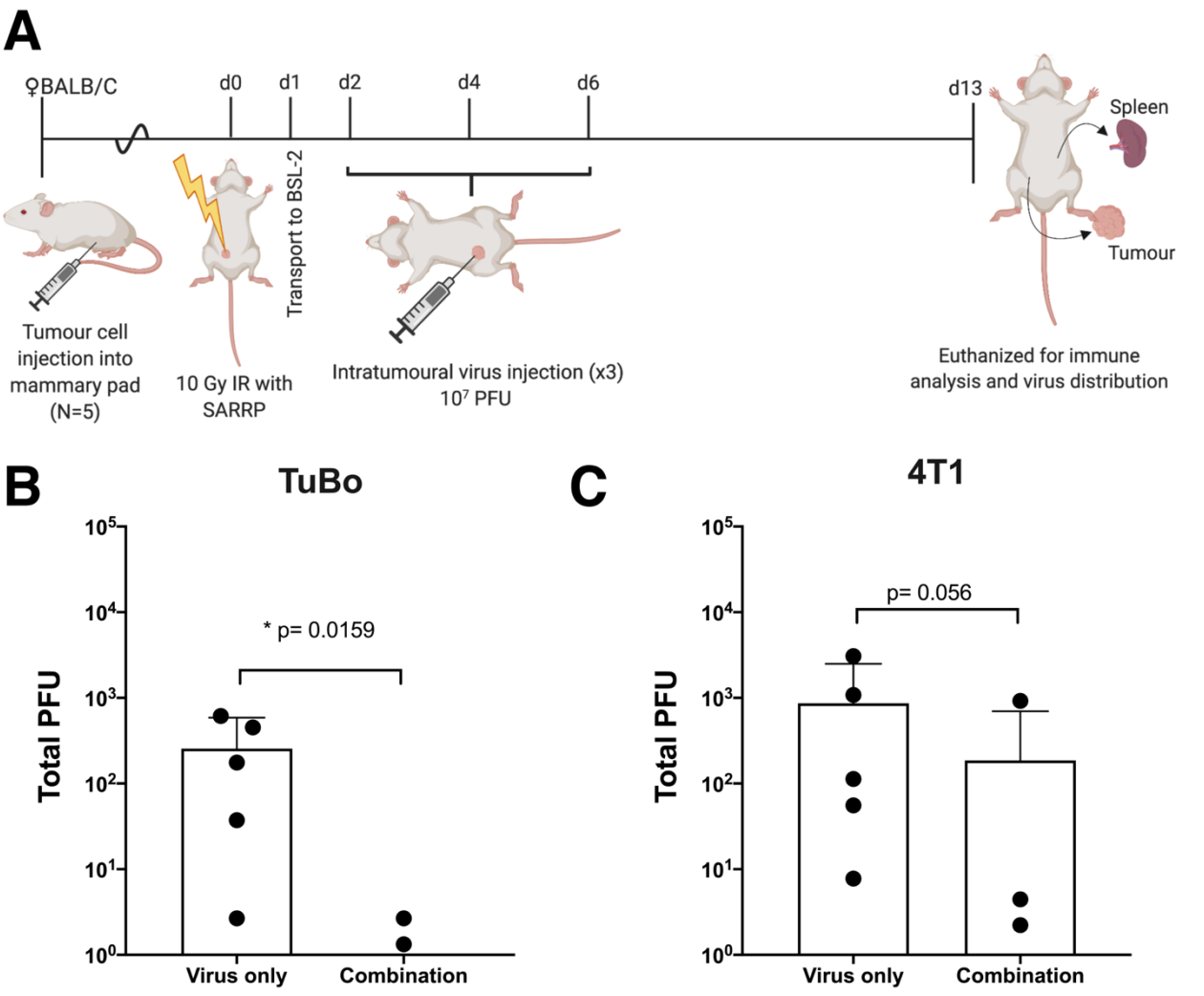

Figure 5.1.Virus titers are decreased in irradiated tumours relative to non-irradiated tumours one week after virus therapy. A. Experimental outline to assess the impact of irradiation on the tumour microenvironment and virus distribution. Tumours were established, irradiated, treated with ΔF4LΔJ2R virus therapy, and euthanized one week following the last virus treatment and organs were collected for immune analysis and virus titering. B,C. Virus titers isolated from B. TuBo and C. 4T1 tumours. Tumours were dissociated by enzymatic digestion and tumour cells were separated from immune cells on a percol gradient. Tumour cells were freeze-thawed three times and viral titers were determined by plaque assay on BSC40 cells. Bars show mean value with error bar representing 95% CI from mean. N=5 per group. P values reported from Mann-Whitney testing.

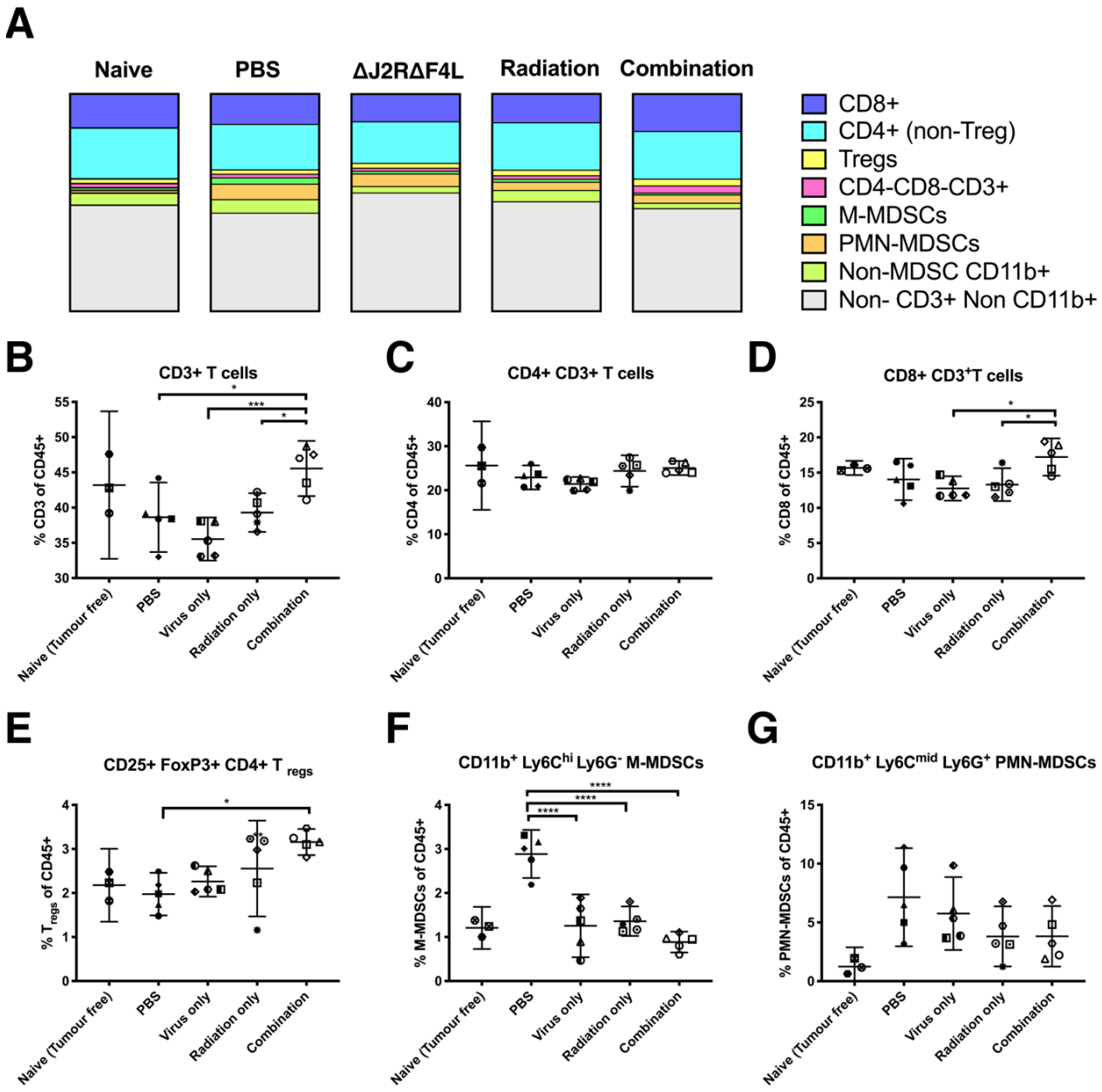

Figure 5.2. Combination therapy changes the composition of immune cells in the spleens of mice in the TuBo model

A. Overall average composition of immune cells in the spleens of mice harbouring TuBo tumours as a percentage of CD45+ cells in the spleens. Naïve tumour free-mice shown for comparisson. Values determined by the average value from 5 mice per group, with 3 mice in the naïve group. B-G. Percentage of immune cell subsets in the spleen , showing T cells (B), T helper cells (C), Cytotoxic T cells (D), T regs (E), M-MDSCs (F) and PMN-MDSCs (G) cell populations expressed as a percentage of CD45+. Each data point representative of individual mice, consistent across graphs, with error bars showing +/- 95% confidence intervals (CI) where *p<0.05, **p<0.01 ***p<0.005 and ****p<0.005 assessed using ANOVA if data determined to be parametric and Kruskal-Wallis testing if data shown to be non-parametric.

5.2.2 Combination therapy changes the composition of immune cells in the spleens and tumours of mice one week after virus treatment

We then performed an immune analysis of the composition of spleens from treated mice with TuBo tumours as described in Figure 4.4A. Spleens were processed into a single cell suspension, and multi-parameter flow cytometry was used to characterize immune cell subsets as a percent of $CD45^+$ cells. In assessing the overall composition of the spleens, it was shown that combination therapy increased the percentage of CD3+ T cells in spleens (Figure 5.2A,B) and this was primarily caused by an increased in the proportion of CD8+ T cells, as there were no significant differences between treatment groups in the proportion of CD4+ T cells (Figure 5.2A,B,C). The shift in immune cell percentages showing an increase in CD8+ cells is generally considered a favourable immune cell scenario. However, when looking at unfavourable suppressor cell populations, Tregs percentages increased in the combination therapy treated group relative to PBS. Despite the increase in Tregs after combination therapy treatment, the ratios of CD8+ T cells to Tregs remained consistent (Figure 5.4).Monocytic-myeloid derived suppressor cell (M-MDSCs) populations decreased in all treatment groups relative to PBS (Figure 5.2A,E&F). Although not statistically significant, similar to the reduction in M-MDSCs populations, there was a small decrease in PMN-MDSCs populations in treated groups relative to PBS (Figure 5.2A,G).

As we had observed antagonism in the 4T1 tumour model, albeit to a lesser extent than in the TuBo tumour model, we performed the same experiment with 4T1-tumour bearing mice. Interestingly, we observed more drastic changes between treatments when assessing the splenocyte composition in the 4T1 tumour model (Figure 5.3A). Here, we saw that the immune-cell composition of PBS-treated tumours were more similar to ΔF4LΔJ2R-treated tumours than irradiated tumours and were primarily composed of $CD11^+Ly6C^{mid}Ly6G^+$ PMN-MDSCs and non-MDSC $CD11b^+$ cells (Figure 5.3A). In irradiated tumours, independent ΔF4LΔJ2R treatment, spleens were more normalized and more closely resembled naïve tumour-free mice, where spleens were predominantly composed of non-CD3+ non-CD11b+ immune cells (Figure 5.3A).

In assessing the overall composition of the spleens, it was shown that both radiation alone and combination therapy increased the percentage of CD3+ T cells in spleens relative to virus only and PBS-treated mice (Figure 5.3B) and this was primarily caused by an increased proportion of CD8+ T cells and a reduction of CD4+ T cells (Figure 5.3B,C). Treatment-induced changes in suppressor cell populations in 4T1-tumours were also consistent compared to the changes that occurred in the TuBo model. Treg percentages increased in the combination therapy treated group relative to PBS, however, Tregs also increased with radiation-treated tumours relative to PBS, which was not observed in the TuBo model. M-MDSCs decreased relative to PBS in the radiation only and combination treated groups but increased after virus treatment alone (Figure 5.3E&F). A similar trend was observed in the TuBo model with PMN-MDSCs was also observed in 4T1 tumour models, which exhibited a decrease in PMN-MDSCs populations in combination and radiation-alone treated groups relative to PBS and virus-only treated (Figure 5.3G).

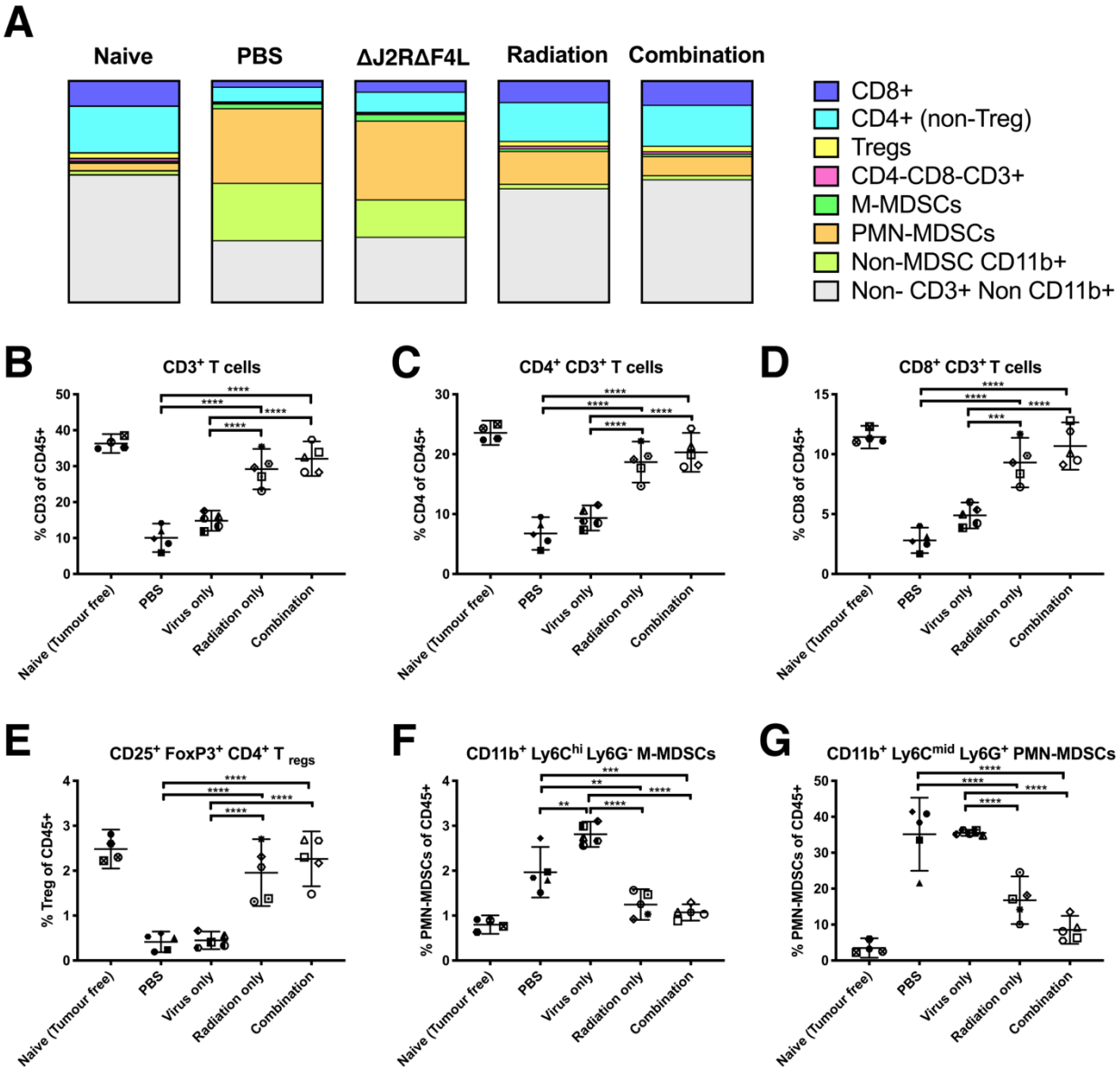

Figure 5.3. Combination therapy changes the composition of immune cells in the spleens of mice in the 4T1 tumour model one week after virus treatment. A. Overall average composition of immune cells in the spleens of mice harbouring 4T1 tumours as a percentage of CD45+ cells in the spleens. Naïve tumour free-mice shown for comparisson. Values determined by the average value from 5 mice per group, with 3 mice in the naïve group. B-G. Percentage of immune cell subsets in the spleen , showing T cells (B), T helper cells (C), Cytotoxic T cells (D), T regulatory cells (E), M-MDSCs (F) and PMN-MDSCs (G) cell populations expressed as a percentage of CD45+. Each data point representative of individual mice, consistent across graphs, with error bars showing +/- 95% confidence intervals (CI) where *p<0.05, **p<0.01 ***p<0.005 and ****p<0.005 assessed using ANOVA if data determined to be parametric and Kruskal-Wallis testing if data shown to be non-parametric.

Collectively, the splenocyte analysis of TuBo and 4T1 tumour models after combination-therapy treatment with radiation and ΔF4LΔJ2R VACV demonstrated promising immunological changes to the spleens, causing increases in favourable CD8+ T cells and decreases in un-favourable MDSCs. However, even though the increase in CD8+ T cells was favourable, there were also increases in unfavourable Treg percentages. Despite the increase in Tregs, there was still an overall positive ratio of CD8 T cells to Tregs in all groups (Figure 5.4).

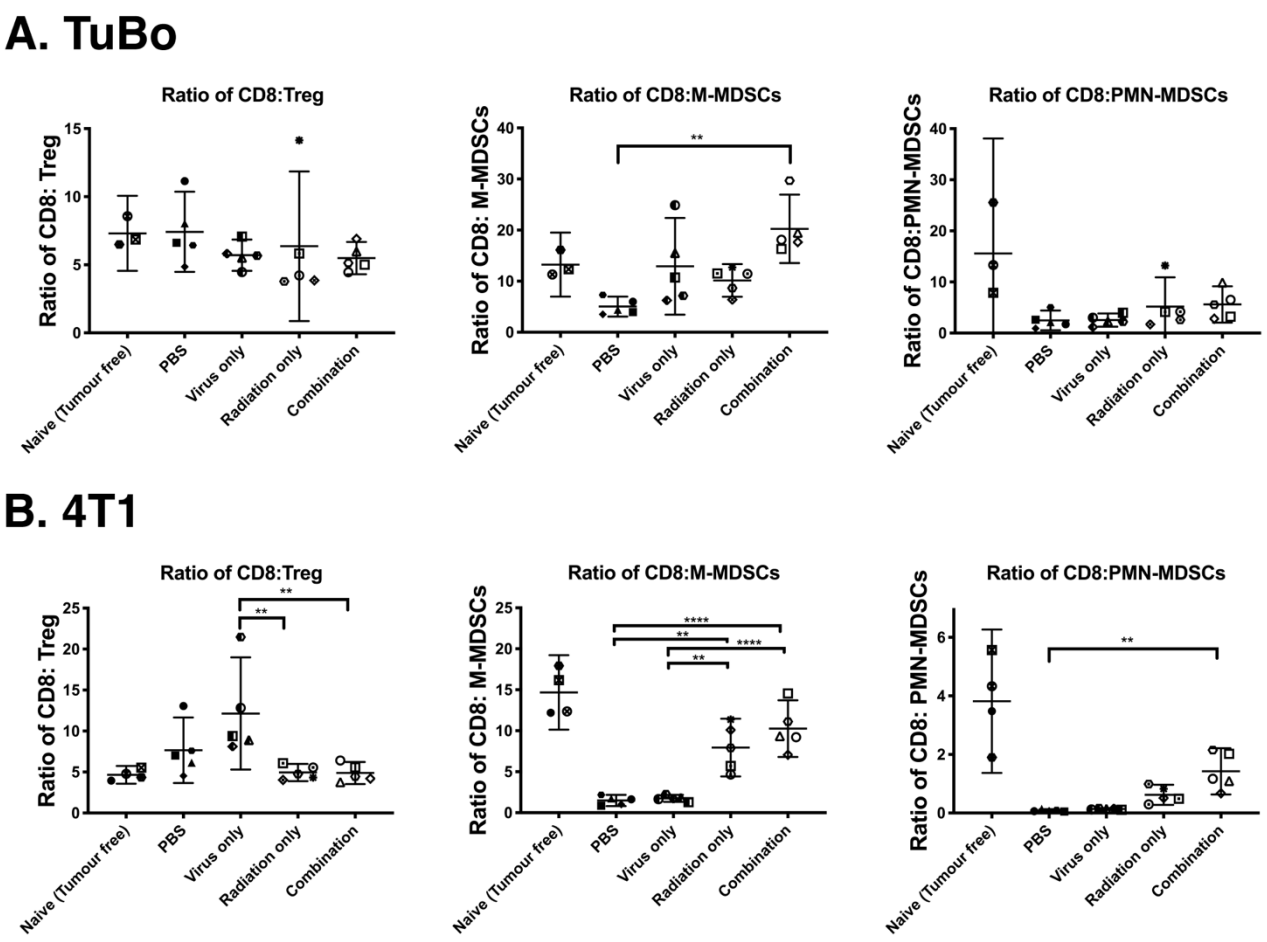

Figure 5.4. Ratios of immune cells in the spleens of mice with (A)TuBo or (B)4T1 tumours. Each data point representative of individual mice, consistent across graphs, with error bars showing +/- 95% confidence intervals (CI) where *p<0.05, **p<0.01 ***p<0.005 and ****p<0.005 assessed using ANOVA if data determined to be parametric and Kruskal-Wallis testing if data shown to be non-parametric.

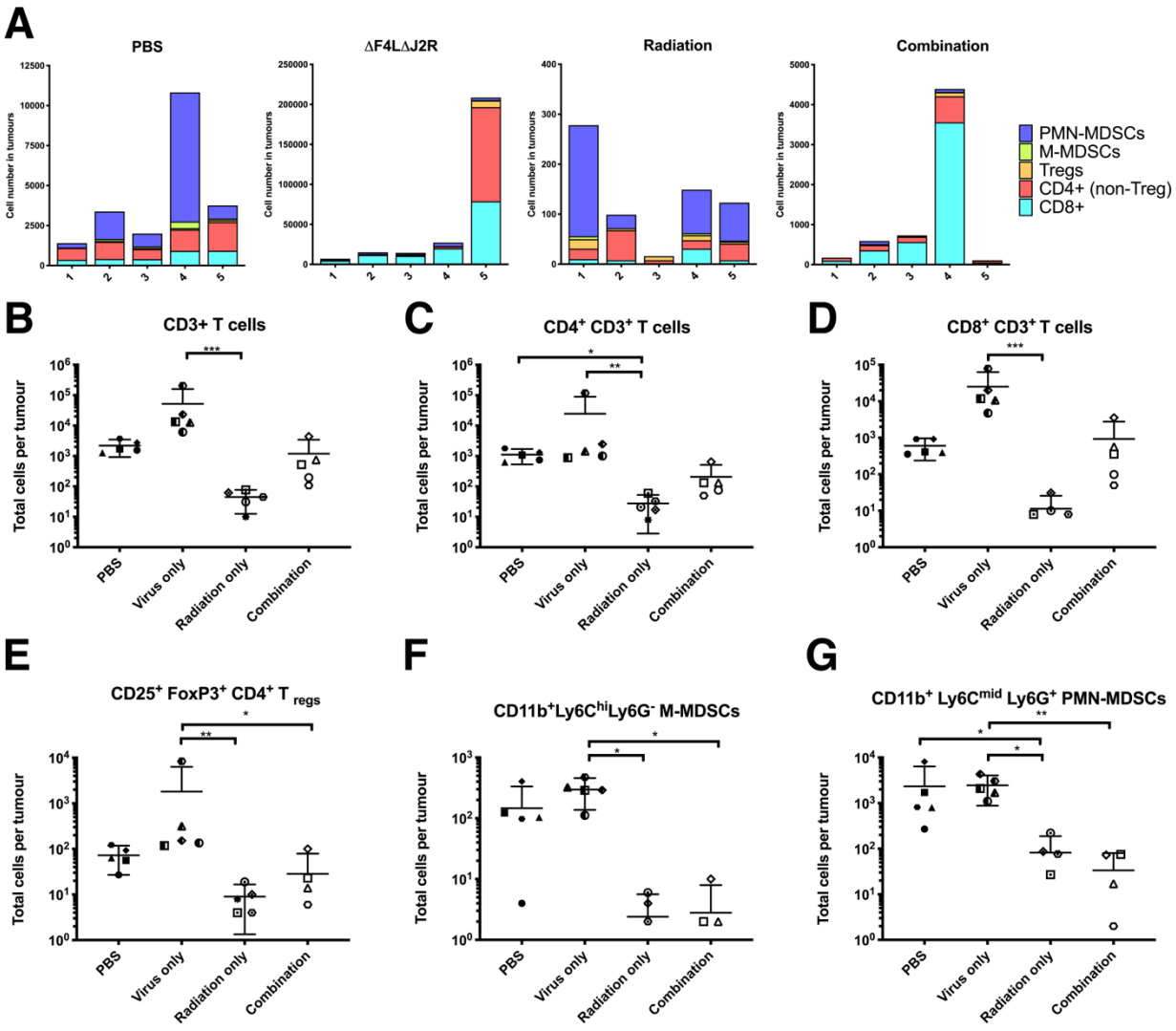

Figure 5.5. Combination therapy treatment reprograms the TuBo TiME one week after virus therapy. A. Numbers of immune cells isolated from tumours where each bar shows results from individual mice in each treatment group. X axis numbering refers to mice 1-5 in each group. B-G. Total numbers of $CD3^+$ T cells (B), $CD4^+$ T helper cells (C), $CD8^+$ cytotoxic T cells (D), $FoxP3^+CD25^+$ Tregs (E), $CD11b^+$ $Ly6C^{hi}Ly6G^-$ M-MDSCs (F), and $CD11b^+Ly6C^{mid}Ly6G^{hi}$ PMN-MDSCs detected in tumours. Data points are representative of individual mice where each mouse is represented by a different symbol, consistent across all graphs. Error bars depict + 95% confidence intervals from the mean, where *p<0.05, **p<0.01 ***p<0.005 and ****p<0.005 assessed using ANOVA if data determined to be parametric and Kruskal-Wallis testing if data shown to be non-parametric.

Although splenocyte analysis gives an indication of what is going on with immune cells systemically, we still needed to assess the site of treatment and perform an immune cell analysis of the TME. Tumours were processed into a single-cell suspension, and immune cells were separated from tumour cells using a Percoll gradient. Immune cells within the tumour were then phenotyped using multiparameter flow cytometry.

As we observed in the splenocyte analysis, there were also notable changes in the composition of tumour-infiltrating immune cells. ΔF4LΔJ2R virus treatment caused substantial increases in the total immune cell numbers in tumours, increasing profiled immune-cell numbers to up to $2x10^5$ cells in mouse #5. (Figure 5.5A). The average total immune cell count of profiled cell types from PBS tumours was approximately 5000 cells per tumour, which increased tenfold to ~55000 in ΔF4LΔJ2R-treated tumours, with less than 300 cells for radiation treatment alone. Combination therapy treated mice showed an increase compared to radiation only, however infiltration was still minor with an average of ~1100 profiled immune cells recovered (Figure 5.5A). Interestingly, within TuBo tumours, virus treatment appeared to be the dominant factor for reprogramming of the immune cell profile and caused a noticeable difference in the overall composition of these cells thereby changing the immune cell landscape (Figure 5.5A). While PBS and radiation-only tumours were primarily dominated by PMN-MDSCS, shown in purple, tumours that were infected with virus, whether irradiated of not, displayed reduced PMN-MDSCs and were primarily dominated by increased $CD8^+$ T cells, shown in aqua (Figure 5.5A).

In assessing the individual cell types, there were statistically significant differences in TIL infiltration between treatment groups. Overall numbers of T cells were decreased when comparing radiation-only treated tumours to virus-only treatment, which was reflected in reductions in $CD8^+$, $CD4^+$, and Tregs cells (Figure 5.5B-E). However, the addition of virus-treatment to irradiated tumours in the combination therapy group partially recovered T cell numbers, causing slight increases in all T cell populations relative to radiation-alone treatment, with Tregs in combination-treated tumours still significantly reduced compared to virus treatment. With respect to MDSCs, radiation and combination therapy groups both had reduced M-MDSCs and PMN-MDSCs relative to virus-only treated tumours. These patterns in TIL changes were consistent even after normalizing relative to tumour volume (Figure 5.6).

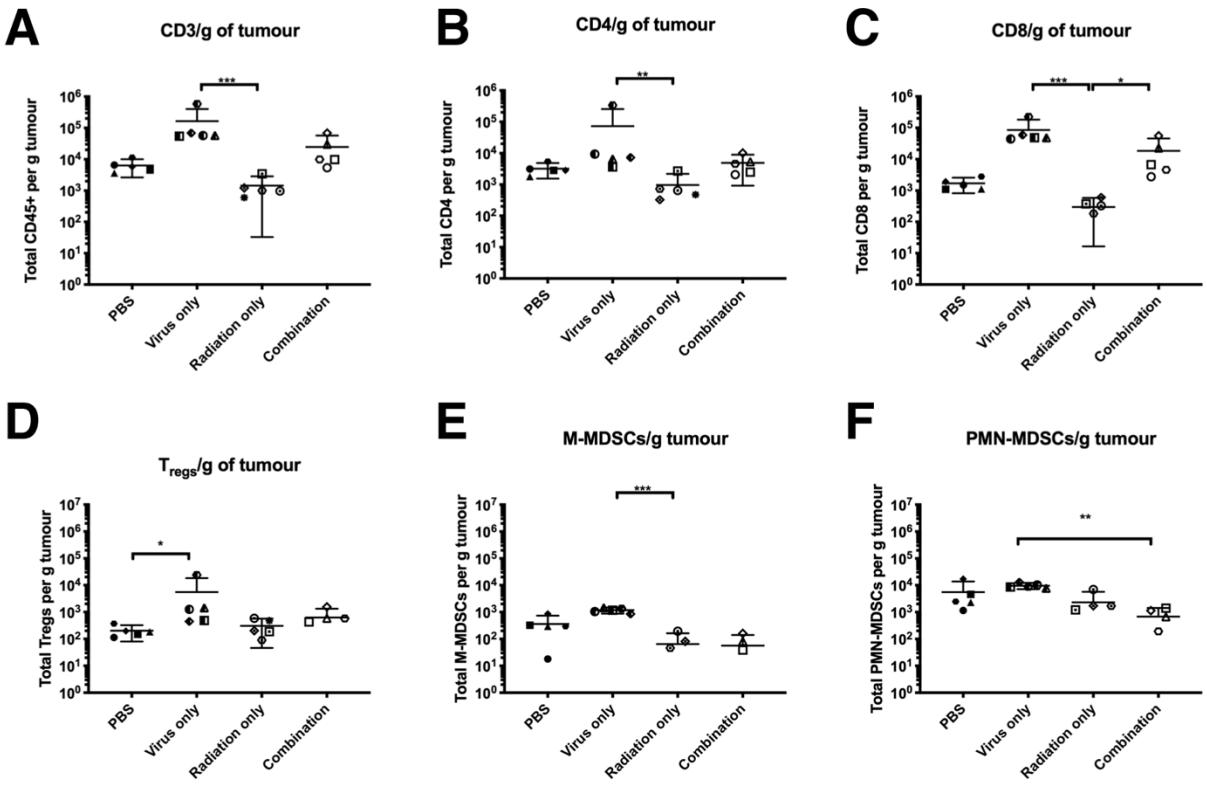

Figure 5.6. Cell counts normalized to gram of tumour tissue from TuBo tumours. (A)$CD3^+$ T cells (B), $CD4^+$ T helper cells (C), $CD8^+$ cytotoxic T cells (D), $FoxP3^+CD25^+$ Tregs cells (E), $CD11b^+$ $Ly6C^{hi}Ly6G^-$ M-MDSCs (F), and $CD11b^+Ly6C^{mid}Ly6G^{hi}$ PMN-MDSCs detected in tumours. Data points are representative of individual mice where each mouse is represented by a different symbol, consistent across all graphs. Error bars depict + 95% CIs from the mean, where *p<0.05, **p<0.01 ***p<0.005 and ****p<0.005 assessed using ANOVA if data determined to be parametric and Kruskal-Wallis testing if data shown to be non-parametric

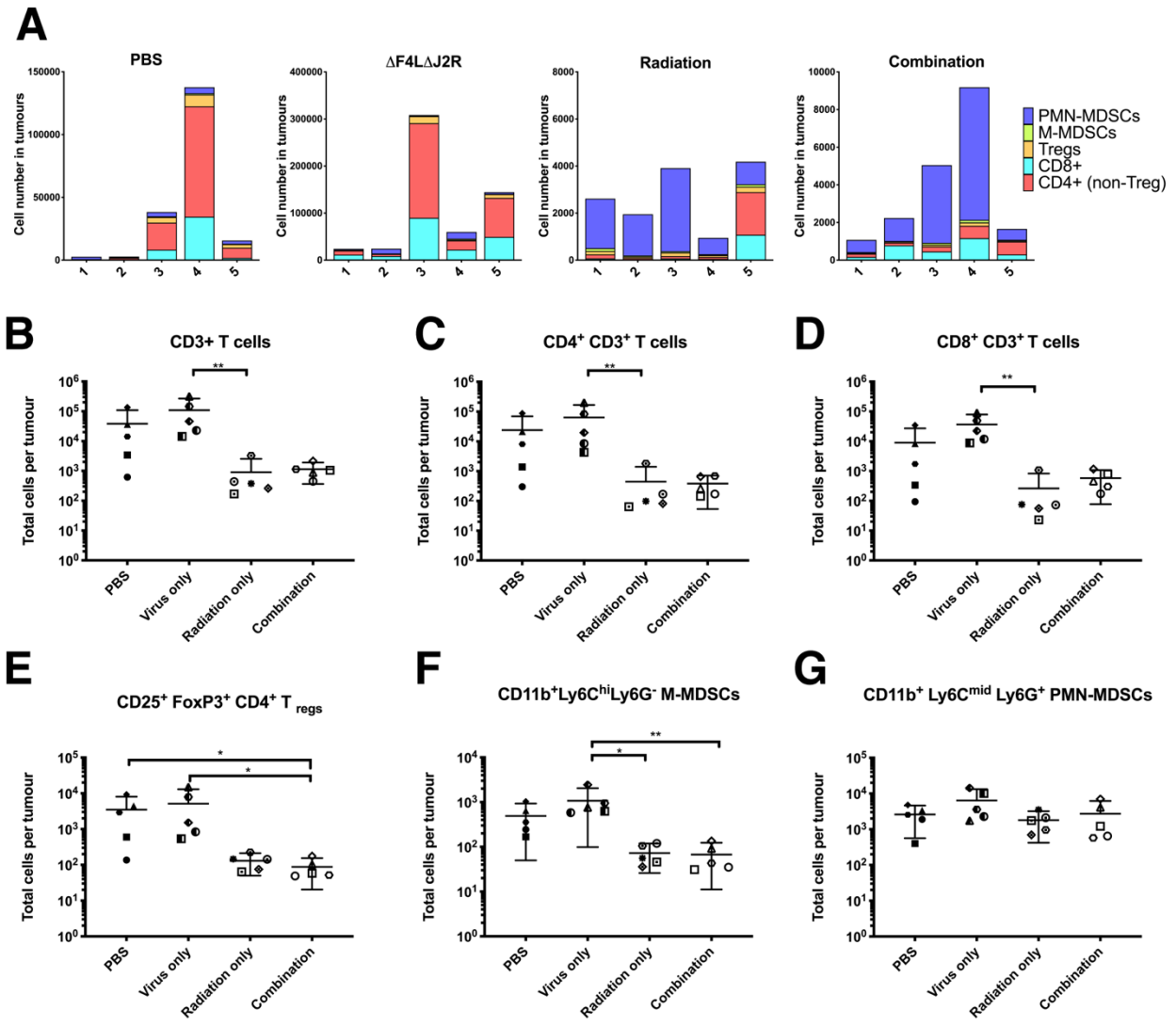

Figure 5.7. Combination therapy treatment reprograms the 4T1 TiME one week after virus therapy. A. Numbers of immune-cells isolated from tumours where each bar shows results from individual mice in each treatment group. X axis numbering refers to mice 1-5 in each group. B-G. Total numbers of $CD3^+$ T cells (B), $CD4^+$ T helper cells (C), $CD8^+$ cytotoxic T cells (D), $FoxP3^+CD25^+$ $T_{regulatory}$ cells (E), $CD11b^+$ $Ly6C^{hi}Ly6G^-$ M-MDSCs (F), and $CD11b^+Ly6C^{mid}Ly6G^{hi}$ PMN-MDSCs detected in tumours. Data points are representative of individual mice where each mouse is represented by a different symbol, consistent across all graphs. Error bars depict + 95% CIs from the mean, where *p<0.05, **p<0.01 ***p<0.005 and ****p<0.005 assessed using ANOVA if data determined to be parametric and Kruskal-Wallis testing if data shown to be non-parametric.

In assessing the TIL populations in 4T1 tumours after treatment, the immune cell profile was different than what was observed in TuBo tumours. In this instance, the immune cell composition of PBS-treated tumours was more similar to ΔF4LΔJ2R virus treatment alone, and both irradiated tumour groups were more similar to each other than to non-irradiated tumours (Figure 5.7A). Similar to the TuBo model, the highest numbers of profiled immune cells found within tumours was the ΔF4LΔJ2R treatment group, which had an average of over 100 000 immune cells in tumours, with PBS having ~40 000, combination therapy with ~4000 and radiation alone with ~3000 cells average found infiltrating tumours. Both PBS and virus treated tumours seemed to be dominated by CD4+ T cells and CD8+ T cells, and in the irradiated groups, PMN-MDSCs were the dominant immune cell type compared to the other cells (Figure 5.7A).

In individually assessing numbers of each cell type found in tumours, again, virus treated tumours had the highest numbers all T cell populations and MDSC populations (Figure 5.7B-G). These cell types were all statistically less in the radiation-only treated groups with the exception of PMN-MDSCs where there was no statistical difference between treatment groups based on total cell numbers in tumours. In the combination therapy group, Tregs and M-MDSCs were reduced relative to virus or PBS treatment, and there were no statistical differences between radiation only and combination therapy treatment. However, similar to the TuBo tumour model, there was a slight increase in CD8+ T cell numbers when comparing radiation only to combination treated tumours, which increased from an average of 260 $CD8^+$ T cells recovered from radiation-treated tumours, which doubled to approximately 580 CD8+ T cells in the combination therapy group (Figure 5.7D). The patterns observed in immune cell changes were consistent after normalization to the weight of the tumours, albeit with less statistical significance (Figure 5.8)

Collectively, the TiME appeared to show positive immune cell population changes, increasing CD8+ T cell numbers, and a general decrease in suppressive cell populations, with these presumably favourable changes being more pronounced in the TuBo tumour model. Typically, as CD8+ T cells act against the tumour and Tregs and MDSCs suppress CD8+ immune responses, an increase in CD8+ cells and a decrease in MDSCs should be indicative of a favourable and therapeutically beneficial immune cell repertoire. However, we know from our regression and survival experiments that this is not the case, and therefore something else must be contributing the lack of therapeutic efficacy. However, simply assessing T-cell numbers is not the only parameter to consider when looking at immune stimulation. With recent advances in cancer immunotherapy analysis demonstrating that CD8+ T cell characteristics such as activation and checkpoint expression status are imperative for a functional anti-tumour immune response, we decided to further examine the properties of the CD8+ T cells recovered from the spleens and tumours of treated mice.

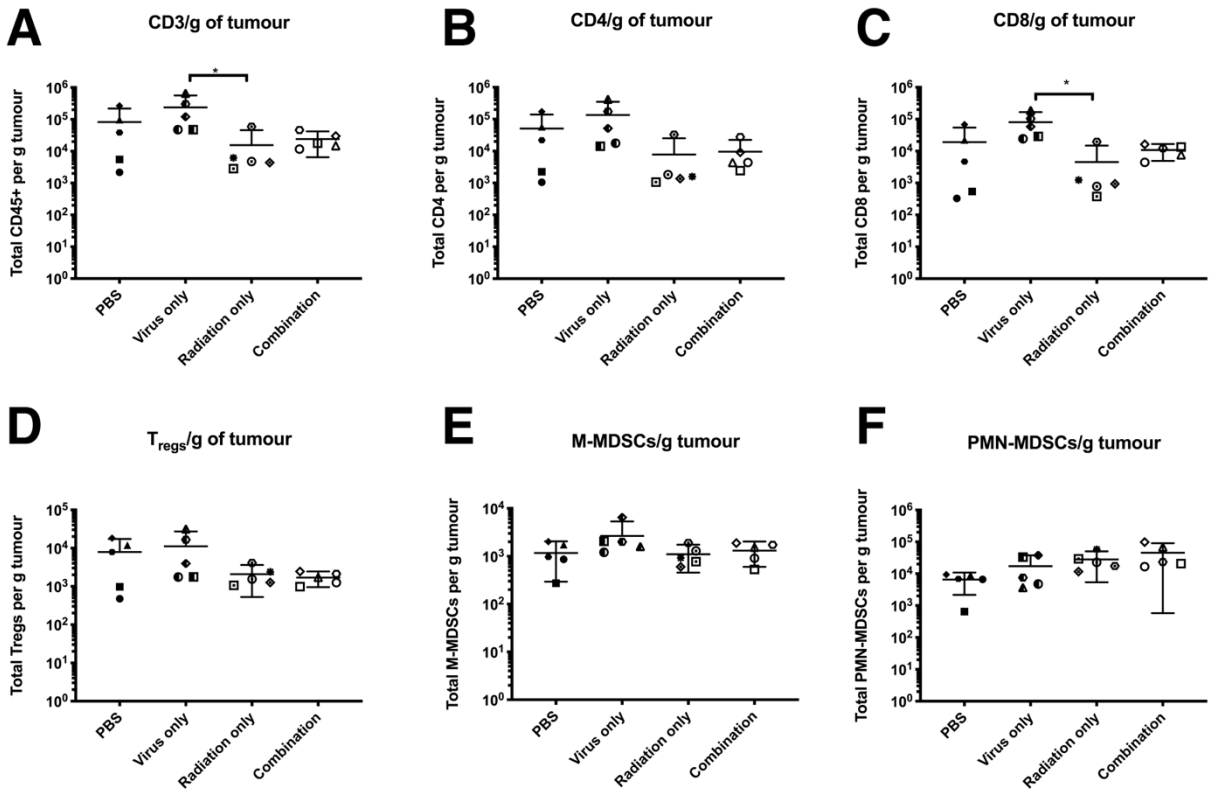

Figure 5.8. Cell counts normalized to gram of tumour tissue from 4T1 tumours. (A)$CD3^+$ T cells (B), $CD4^+$ T helper cells (C), $CD8^+$ cytotoxic T cells (D), $FoxP3^+CD25^+$ Tregs cells (E), $CD11b^+$ $Ly6C^{hi}Ly6G^-$ M-MDSCs (F), and $CD11b^+Ly6C^{mid}Ly6G^{hi}$ PMN-MDSCs detected in tumours. Data points are representative of individual mice where each mouse is represented by a different symbol, consistent across all graphs. Error bars depict + 95% CIs from the mean, where *p<0.05, **p<0.01 ***p<0.005 and ****p<0.005 assessed using ANOVA if data determined to be parametric and Kruskal-Wallis testing if data shown to be non-parametric

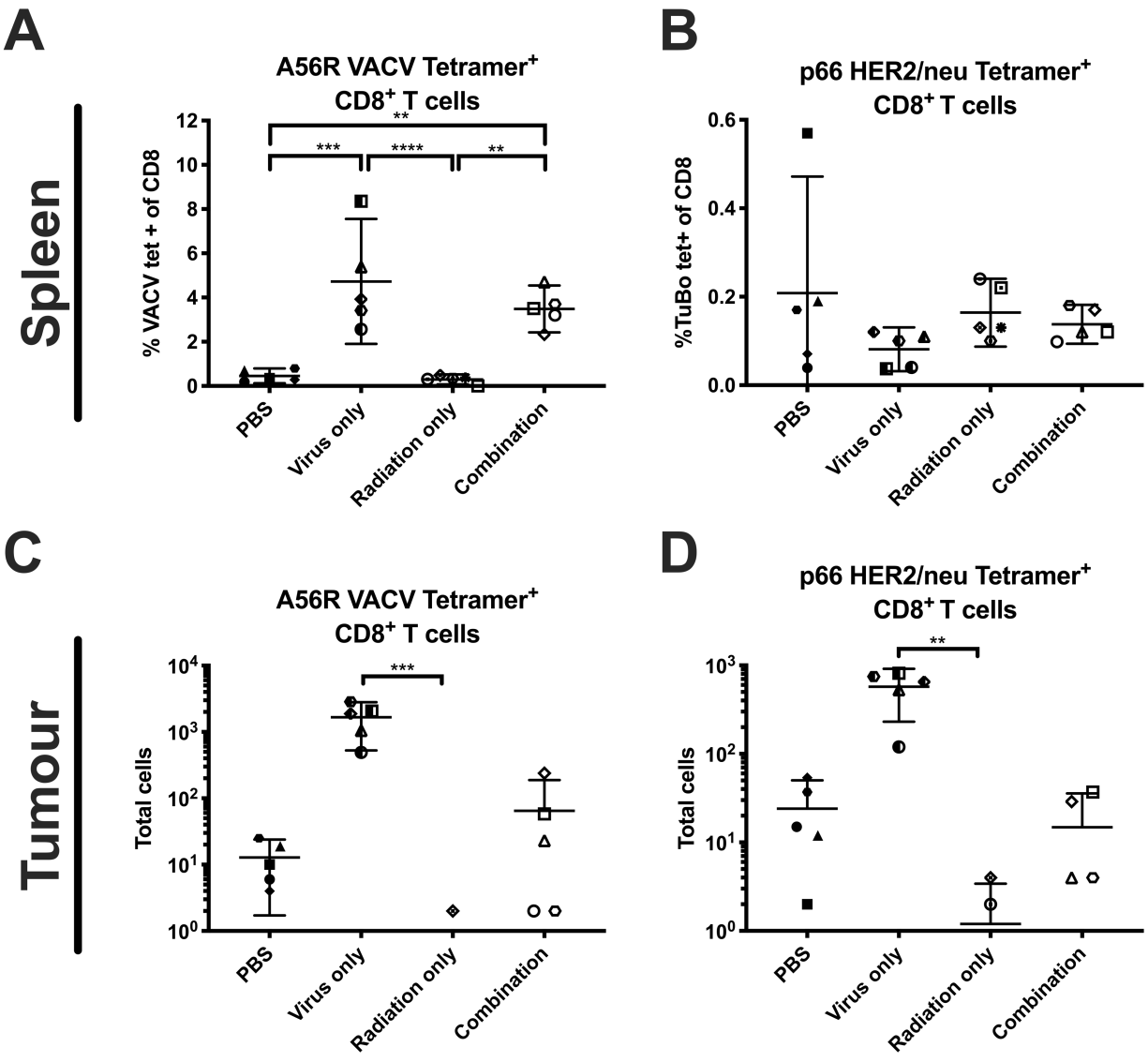

Figure 5.9. Treatment of TuBo tumours with radiation and/or ΔF4LΔJ2R VACV therapy generates T-cells with specificity to viral and tumour epitopes. A&B. Percent of A56R VACV tetramer+ (A) or p66 HER2/neu tetramer+ (B) CD8+ T cells isolated from spleens of treated mice one week following the final virus treatment. C&D. Numbers of tumour infiltrating A56R VACV tetramer+ (C) or p66 HER2/neu tetramer+ (D) CD8+ T cells isolated from TuBo tumours one week following the final virus treatment. Data points are representative of individual mice where each mouse is represented by a different symbol, consistent across all graphs. Error bars depict +/- 95% CIs from the mean, where *p<0.05, **p<0.01 ***p<0.005 and ****p<0.005 assessed using Kruskal-Wallis testing.

5.2.3 Treatment of TuBo tumours with radiation and/or ΔF4LΔJ2R VACV therapy generates T-cells with specificity to viral and tumour epitopes

After observing increased numbers of CD8+ T cells in spleens and tumours, we further characterized these T cells to determine how combination therapy was impacting immune responses of these treatment(s). We first employed $H2k^d$-restricted tetramers to detect T-cell receptors (TCRs) targeting virus or tumour peptide antigens. TuBo cells express HER2/*neu*$^+$, and therefore tetramer staining of TCRs binding the immunodominant HER2/*neu* p66 peptide epitope were used to detect T cells targeting TuBo tumour epitopes[327]. Likewise, tetramers were used to detect the TCRs that recognize VACV A56 protein epitopes, the immunodominant VACV epitope for our VACV strain in BALB/C mice[328], as a surrogate for assessing T-cell responses to VACV infection. We noted that while VACV-targeted T cells were increased one week after tumour treatment in spleens, we did not see any differences between the control and treatment groups with respect to HER2/*neu*-directed T cell responses (Figure 5.9A). This might be due to the differences in the rate at which T-cell responses are mounted and amplified against infectious pathogens, typically within one week after exposure, versus responses generated against cancer antigens, which tend to take two weeks or longer. When we typed the T cells isolated from the tumour site, we detected both anti-viral and anti-tumour CD8+ T cells (Figure 5.9B). T cell numbers targeting both tumour and virus were highest in ΔF4LΔJ2R treated mice and were lowest in radiation treatment. Although not statistically significant, we noted an increase in TuBo tetramer+ CD8+ T cells in combination therapy treated tumours relative to tumours treated with radiation alone, suggesting that there are T-cells being generated against the tumour antigens in the combination therapy group. Thus, the lack of therapeutic efficacy is unlikely to be due to the inability of T-cells to target tumour epitopes in mice treated with combination therapy. This agrees with data shown in the previous chapter, which demonstrated secondary tumour rejection in combination therapy treated mice after challenge, showing functional anti-tumour immunity is generated in mice which have cleared their primary tumour.

5.2.4 Combination therapy increases T cell activation and immune checkpoint expression

We also evaluated CD69 expression on T cells isolated from spleens and tumours of mice bearing TuBo tumours as a marker of T cell activation[180]. We noted that virus treatment, either alone or in combination with IG-RT, increased CD8+ T cell activation in spleens. In tumours the numbers of activated CD69+ CD8+ T cells was highest in the virus treated group, and lowest in radiation-only treated tumours, with a small increase in the combination therapy group relative to radiation only (Figure 5.10C).

Collectively, these data suggest that CD8+ T cells targeting both viral and tumour antigens are present after combination therapy, and that the T cells at the tumour site are activated. This anti-tumour immunity is functional, and is sufficient to prevent the establishment of secondary tumours.

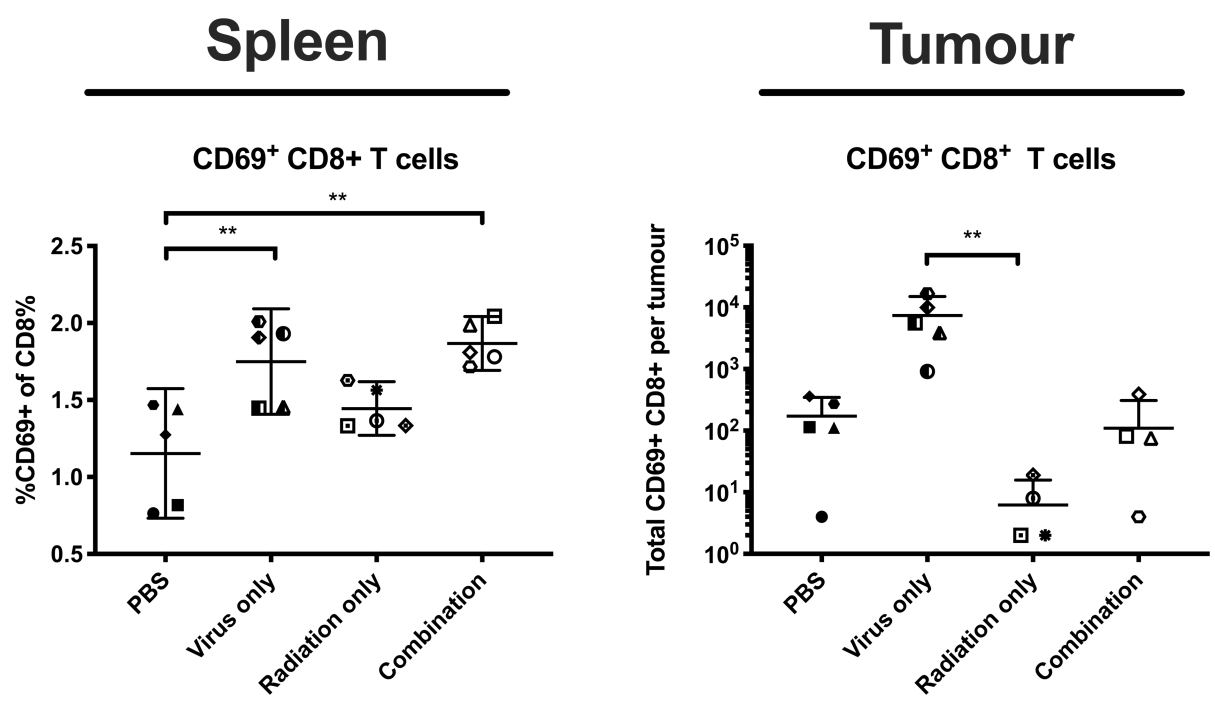

Figure 5.10. Treatment of TuBo tumours with ΔF4LΔJ2R VACV therapy activates CD8+ T cells. A&B. Percent of CD69+ CD8+ T cells isolated from spleens or tumours of mice one week following the final virus treatment. Data points are representative of individual mice where each mouse is represented by a different symbol, consistent across all graphs. Error bars depict +/- 95% CIs from the mean, where *p<0.05, **p<0.01 ***p<0.005 and ****p<0.005 assessed using Kruskal-Wallis testing.

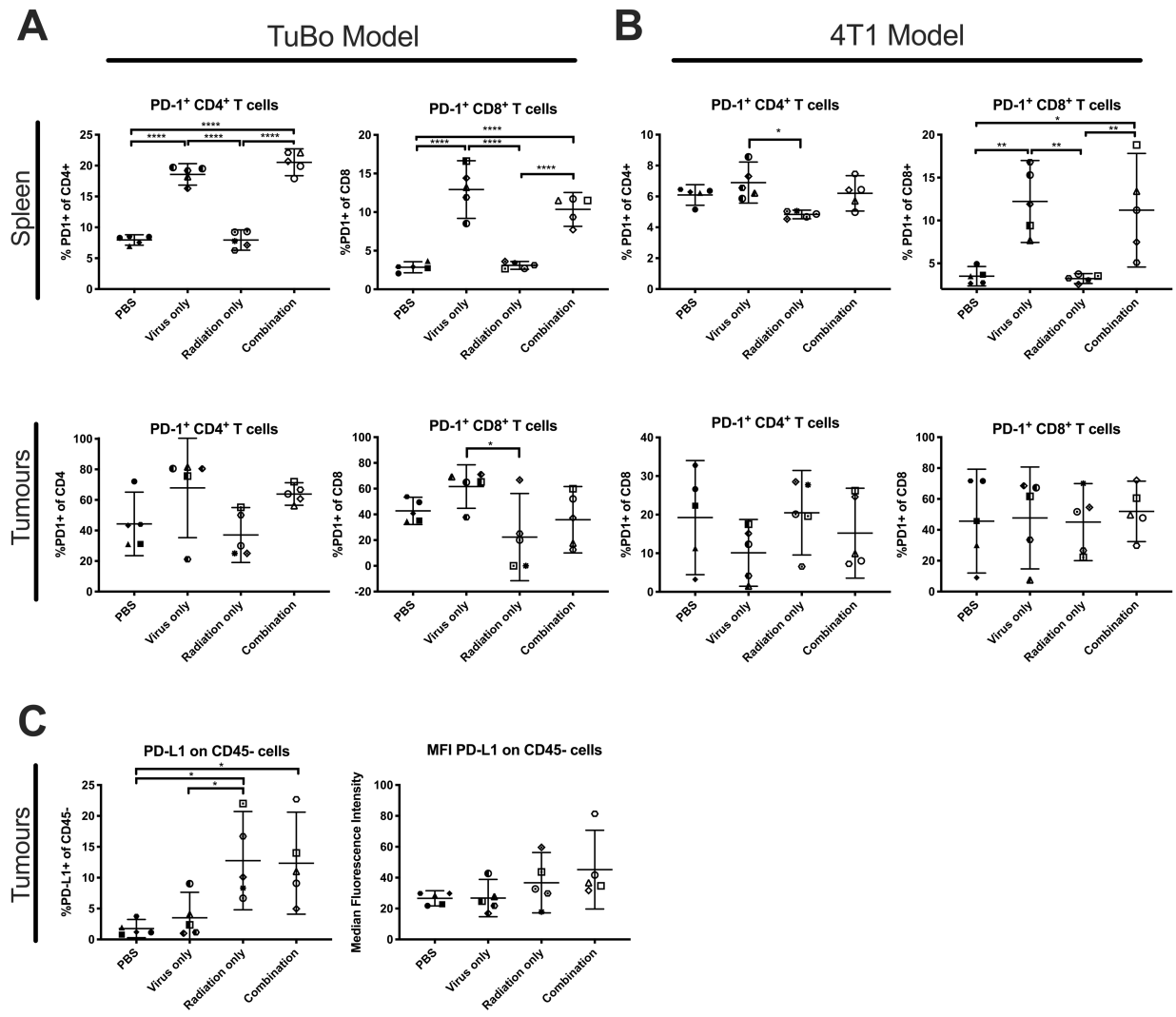

Figure 5.11. Combination therapy increases immune checkpoint expression in the tumour microenvironment. A) Percentage of PD-1$^+$ CD4 or CD8 T cells isolated from spleens and tumours after treatment in the TuBo mammary tumour model (A) or 4T1 tumour model (B) one week after the final virus treatment. (C) PD-L1 expression on CD45- cells isolated from TuBo tumours one week after the final virus treatment represented as percent PD-L1 + cells (left) and median fluorescence intensity (right). Data points are representative of individual mice where each mouse is represented by a different symbol, consistent across all graphs. Error bars depict +/- 95% CIs from the mean, where *p<0.05, **p<0.01 ***p<0.005 and ****p<0.005 assessed using one-way ANOVA where data was shown to be parametric or Kruskal-Wallis testing if data was non-parametric.

We wanted to assess if negative regulators of immune responses were being selectively altered by combination therapy. As a first step, we measured PD-1 expression on T cells isolated from spleens and tumours (Figure 5.11), where overexpression of PD-1 on CD8+ T cells is considered an indicator of immune exhaustion. We observed that PD-1 was upregulated on CD4+ and CD8+ T cells in spleens of both the TuBo and 4T1 tumour model

(Figure 5.11A,B). PBS and radiation-only treated mice had low levels of PD-1 expression: <10% for CD4+ T cells and <5% for CD8+ T cells. Virus or combination therapy treated mice exhibited higher percentages of PD-1 positive T cells, which were >15% in spleens of TuBo treated mice for CD4+ T cells, and >10% for CD8+ T cells. In the 4T1 model, CD4+ T cells were reduced in mice treated with radiation only, where PD-1 expression was found on ~5% of CD4+ T cells, and about 6-7% for virus or combination-therapy treated mice. On CD8+ T cells, virus and combination therapy treated increased the percentage of PD-1+ CD8+ T cells to ~12%.

In tumours, the differences in PD-1 expression between treatments was not as profound as the differences between treatment groups observed in splenocyte samples. However, the total percentage of PD-1+ cells on T cells in tumours was much higher than in spleens. In the TuBo tumour model, PD-1 expression was lowest in the radiation-treatment group, averaging ~40% positive on CD4+ cells and 20% for CD8+ cells. With PBS treatment, ~40% of CD4+ and ~40% of CD8+ T cells were PD-1+. This increased to ~60% on CD4+ cells after treatment with either virus alone or combination therapy, and for CD8+ T cells, ~60% were PD-1+ after virus-only treatment or 40% after combination-therapy treatment. In the 4T1 model, PD-1 expression on CD4+ cells was more similar between groups, at approximately 15-20% after PBS, radiation, and combination therapy treatment and ~10% after virus treatment alone. Similarly, ~40% of CD8+ T cells were PD-1 positive in all groups in 4T1 timours. In tumours, overall, PD-1 expression was more variable than what was observed in tumours. For instance, in the 4T1 tumour model after virus treatment, CD8+ TILS had anywhere from 5% PD-1+ cells up to 70% PD-1+ cells, suggesting intratumoural PD-1 expression on TILs is more variable compared to PD-1 expression in spleens.

PD-1 suppresses T cell responses upon binding to a ligand, PD-L1 or PD-L2, and these ligands are expressed on tumour cells[196,329]. So we also measured the levels of PD-L1 expression on CD45- cells (non-immune cells) isolated from TuBo tumours. We found that radiation therapy, both with and without virus treatment, increased the percentage of PD-L1+ CD45- cells in tumours relative to PBS treated tumours (Figure 5.11). While not statistically significant, the MFI of PD-L1 was highest in mice treated with virus plus IG-RT (Figure 5.10). Collectively, these data show that the combination of radiation and oncolytic VACV increased the immune checkpoint receptor PD-1 and its ligand PD-L1 in the immune-cell microenvironment of mammary tumours.

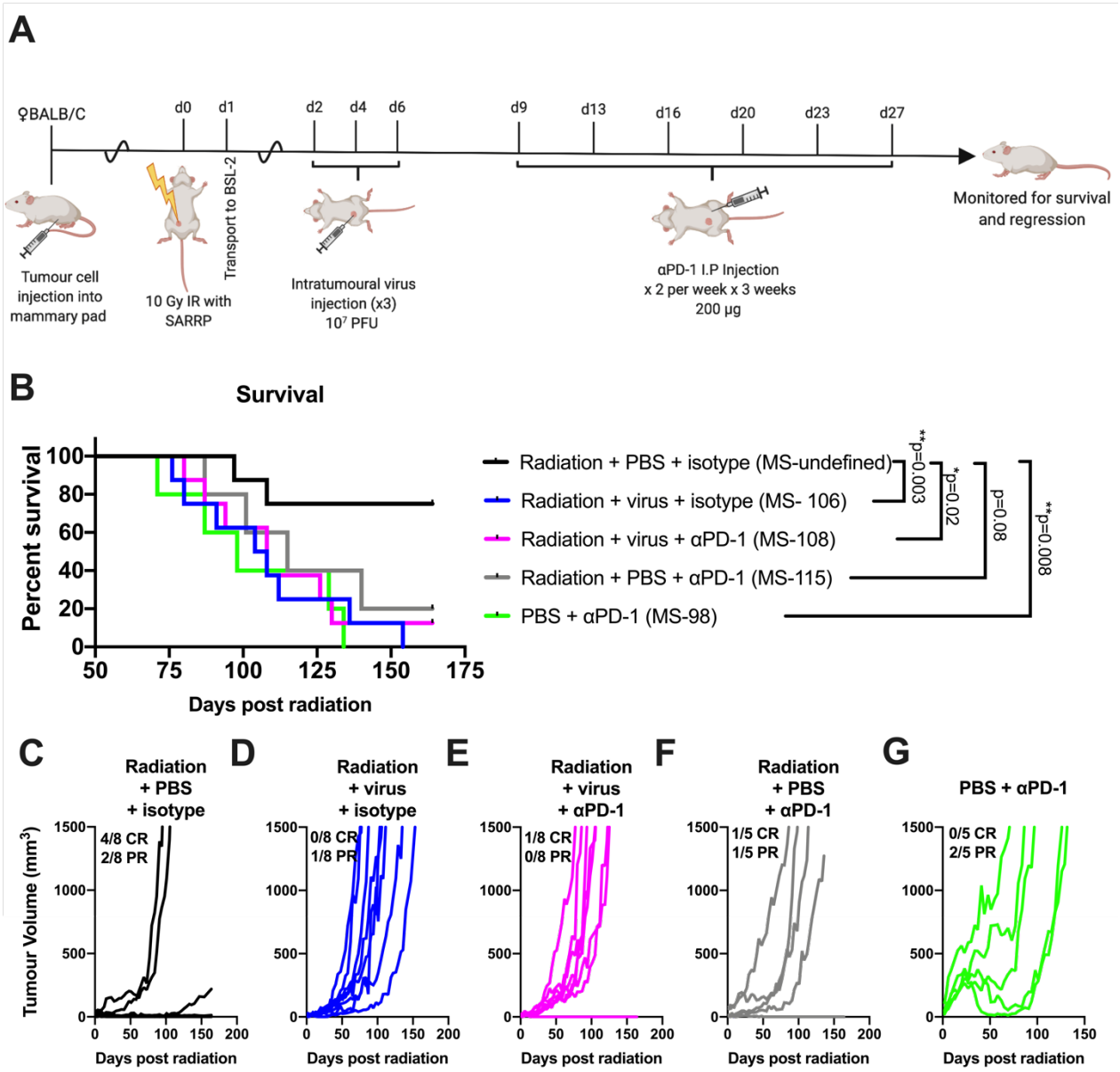

Figure 5.12. Anti-PD-1 checkpoint inhibition does not reverse the antagonism of radiation + ΔF4LΔJ2R combination therapy. A) Experimental outline to assess triple- combination therapy. Orthotopic TuBo tumours in BALB/C mice were irradiated with 10 Gy radiation, transported to the Katz BSL-2 vivarium and treated with three intratumoural doses of 10^7 plaque forming units of ΔF4LΔJ2R VACV. Intraperitoneal (IP) doses of 200 ug of anti-PD-1 antibody were administered twice per week for three weeks. Tumour volume was measured twice per week for the duration of the study. B) Kaplan-Meir curve comparing survival of mice administered each treatment regimen. MS- median survival time. P values determine from Log-rank (Mantel-Cox) testing comparing individual growth curves C-G) Individual tumour growth curves of mice shown in B), with CR- complete responses and PR- partial responses shown on the graph. CRs defined as no detectable tumour mass at day 150, and partial responses defined as a tumour mass that was had no change in tumour size or a reduction in size for a period of 50 days, after which remission occurred. N=5 for PBS + anti-PD1 and radiation + PBS + anti-PD-1 treatment groups, and N=8 for the remaining groups.

5.2.5 Anti-PD-1 checkpoint inhibition does not reverse the antagonism of radiation + ΔF4LΔJ2R combination therapy.

Despite combination therapy eliciting favourable immune cell stimulation as determined by increased CD8+ T cell infiltration, the combination of the two therapies was shown to decrease survival relative to mice treated with radiation only (Figure 4.5). As PD-1 expression was elevated in the combination-therapy treated tumour groups, this led us to postulate that combination therapy was accelerating immune-exhaustion, limiting the cytotoxic effects of these T-cells. To determine if T-cell exhaustion by increased PD-1 expression was contributing to the antagonistic interaction between ΔF4LΔJ2R VACV and irradiation, we decided to test if checkpoint inhibition by anti-PD-1 antibody therapy could reverse the antagonism observed. To test this, we again made use of the TuBo tumour model and followed the same treatment schedule as in prior experiments, where tumours are established, irradiated, and treated with three intra-tumoural doses of ΔF4LΔJ2R. Anti-PD-1 antibody (200 μg per dose) was then given via intraperitoneal injection twice per week for the next 3 weeks (Figure 5.12A).

However, despite the increases in PD-1 and PD-L1, adding an anti-PD-1 checkpoint therapy to the treatment regimen did not reverse the antagonism (Figure 5.12B-E). Checkpoint inhibitor therapy did not improve therapeutic responses, and overall mouse survival was unchanged compared to radiation + virus + isotype control groups. Triple combination therapy was less effective and decreased survival compared to radiation alone (P=0.02) and was no different than when radiation was combined with virus on its own. This suggests that immune cell exhaustion is not contributing to the antagonism observed in tumour clearance, and another mechanism must be contributing towards the negative interplay between radiation and VACV oncolytic virotherapy.

5.3 Discussion

In the previous chapter, it was shown that combining radiation with oncolytic ΔF4LΔJ2R VACV is synergistic *in vitro*, but antagonistic *in vivo*. This antagonism was dependent on the timing of virus administration, but later dosing still did not improve therapeutic outcomes. In the current chapter, the tumour immune cell microenvironment (TiME) was assessed in an attempt to determine possible mechanisms and immune mediated changes that could explain the antagonism observed. However, this antagonism occurred despite favourable changes to the TiME, such as increased CD8+ T cells and increased T-cell activation. Although PD-1 and PD-L1 expression was elevated after treatment, checkpoint inhibition did not reverse the *in vivo* antagonism.

When attempting to dissect possible mechanisms for the reduced efficacy of combination therapy, we focused our efforts on investigating immune responses. This was due to the observation that on a direct cellular level, virus and radiation were synergistic *in vitro*, and only when tested in an immune-competent animal model did the antagonism become apparent. The majority of our analyses suggested that the changes induced in the TiME were generally favourable. Suppressive MDSC populations were decreased, while CD8+ T cells were increased. And despite

elevated regulatory T cells, the ratio of CD8+ T cells to Tregs remained consistent between treatments, suggesting that the increase in Tregs was likely not the cause of the antagonism.

We did see notable differences in the distribution of HER2/neu TCR+ CD8+ T cells. Such cells were not found in the spleen but were detected in tumours. In contrast, VACV TCR+ CD8+ T cells were detected at both sites. This might reflect differences due to increased TCR affinity to viral epitopes compared to cancer epitopes, which may impact the rate at which T-cell responses are mounted and amplified against infectious pathogens versus cancer epitopes [330]. The fact that we can detect such HER2/*neu* CD8+ T cells at the tumour site showed that there are T-cells being generated (or perhaps recruited) to the tumour that recognize tumour antigens in the combination group. However, despite the presence of these cells, and the presence of activated CD69+ CD8+ T cells, the tumours were not cleared. Whatever the reason for this lack of therapeutic efficacy, it is not due to the absence of the T-cells that target tumour epitopes in mice treated with IG-RT plus VACV.

Given that PD-1 and PD-L1 were both upregulated after combination therapy, we were surprised that adding checkpoint blockade therapy to the treatment schedule did not improve responses. The lack of response to anti-PD-1 checkpoint therapy suggests that this antagonism is unrelated to PD-1-mediated exhaustion and arrest of T-cell function. In this study we did not assess the impact of other immune checkpoints, and this remains a possible avenue for future investigation. For example it has been shown that TIM-3 and T regulatory cell infiltration contribute to resistance in murine models of head and neck carcinoma after radiation and PD-L1 blockade[145]. As we only tested anti-PD-1 therapy and not anti-PD-L1, we cannot rule out the possibility that PD-L1 engagement on tumour cells with CD80 contributed to the negative responses and promoting tumour survival[61,331].

Another factor that may need to be considered are the effects of combining radiation and VACV therapy on the tumour cells themselves. The immune response is important for the effectiveness of radiation therapy[218,324,332,333]and a mechanism of escape from radiation includes altered IFN signalling[334]. MHC expression is regulated by many signaling pathways, including NF-KB, and type I/II IFNs[335,336]. Importantly, VACV is known to interfere with the immune response, in particular with IFN signaling[18,261]. In this way, virus-induced changes to the microenvironment could impact responses in non-infected tumour cells by altered cytokine signaling or MHC downregulation. As deleting VACV genes that inhibit IFN signaling can increase the efficacy of oncolytic VACV-immunotherapy[162,175] it is possible that using different oncolytic VACV mutants would work differently when combined with IG-RT.

Chapter 6: Anti-cancer efficacy of immunomodulatory gene deleted oncolytic VACVs in breast cancer models

Preface

A portion of this chapter has been published in the manuscript: Umer BA, Noyce RS, Franczak BC, Shenouda MM, Kelly RG, Favis NA, Desaulniers M, Baldwin TA, Hitt M, and Evans DH. Deciphering the immunomodulatory capacity of oncolytic vaccinia virus to enhance the immune response in breast tumours, *Cancer Immunology Research,* (8)618-31.

Permissions: Cancer Immunology Research of the American Association for Cancer Research (AACR) States: **"**Authors of articles published in AACR journals are permitted to use their article or parts of their article in the following ways without requesting permission from the AACR. All such uses must include appropriate attribution to the original AACR publication. Authors may do the following as applicable:

1. Reproduce parts of their article, including figures and tables, in books, reviews, or subsequent research articles they write;
2. Use parts of their article in presentations, including figures downloaded into PowerPoint, which can be done directly from the journal's website;
3. Post the accepted version of their article (after revisions resulting from peer review, but before editing and formatting) on their institutional website, if this is required by their institution. The version on the institutional repository must contain a link to the final, published version of the article on the AACR journal website so that any subsequent corrections to the published record will continue to be available to the broadest readership. The posted version may be released publicly (made open to anyone) 12 months after its publication in the journal;
4. Submit a copy of the article to a doctoral candidate's university in support of a doctoral thesis or dissertation.

6.1 Introduction

VACV has many attributes which make it a suitable cancer therapeutic, including a large coding capacity for transgenes, easy manipulation, a good safety profile, and the inability to integrate into the host genome[12]. VACVs are in clinical trials[12], and there is continuing research aimed improving the long lasting antitumor immunity by encoding cytokines like GM-CSF or IL-2 into the virus genome[337,338]. VACV encodes many gene products that can suppress host immune responses which undermines the purpose(s) served by the aforementioned transgenes[12,18]. An alternative approach to increase the immunogenicity of oncolytic virotherapy involves deleting virus-encoded immunomodulatory genes, a strategy which has improved immune responses to recombinant vaccine vectors[45,69,93,163,164]. Although reports show that this strategy offers promise as a way of improving oncolytic therapies[162], the "one-off" nature of each report (i.e. often investigating only one candidate gene per study and sometimes simultaneously encoding additional transgenes), makes it difficult to identify which gene targets and immune pathways offer the most promise.

In this chapter, I examined the therapeutic effects of deleting individual VACV immunomodulatory genes. Specifically, I determined whether any one of the several antiviral pathways targeted by VACV affects the efficacy of virotherapy in breast tumor models. I performed a head-to-head comparison of six isogenic mutant oncolytic VACVs, each harbouring gene deletions that modulate different cellular pathways [nucleotide metabolism, apoptosis, inflammation, and chemokine and interferon signalling (Table 1)]. All of these viruses were also mutated in the thymidine kinase locus (J2R), and were compared to a ΔJ2R mutant, as this is a common attenuating mutation[12]. In *in vitro* assays, I assessed if any of the immunogenic deletions would have an impact on virus growth and cytotoxicity in breast cancer cell lines, and also tested whether individual deletions caused the release of ATP and HMGB-1, which are indicators of immunogenic cell death (ICD). I also tested the tumour specificity and safety of these new viruses in animal models. Finally, we determined how these deletions altered the anti-tumour treatment efficacy in two orthotopic and syngeneic mouse breast tumor models.

Curiously, I observed that some gene deletions statistically increased survival in the non-immunogenic 4T1 tumor model, but the therapeutic benefits were less clear in the HER2/*neu*+ TuBo model. Nevertheless, the most promising candidate genes for deletion were those previously identified as interfering with the IFN response, either directly [B8R[83]/B18R[81]], or indirectly by inhibiting components of the signalling pathways [C6L[66,67], N1L[62]]. Collectively, this research helps determine which genetically encoded viral components are suppressing immune responses and should perhaps be removed to improve the oncolytic activity of VACV. It also suggests that although these virus mutations can modulate the TME of immunogenic tumours, the greatest statistical benefits in survival are attained in the context of non-immunogenic tumour models.

6.2 Results

6.2.1 Construction of gene deleted VACVs

Previous studies have identified that deletion of VACV F1L, K7R, N1L, C6L, A41L, and B8R plus B18R genes enhance immune responses to recombinant vaccine vectors *in vivo*[45,59,62,81,83,93,99,163,164,339,340], and these genes were selected for deletion (Table 6.1) Except for B18R alone, most have not been previously investigated in the context of cancer virotherapy[162,341]. For comparison, we also deleted F4L, the small subunit of ribonucleotide reductase, as this mutation renders recombinant viruses highly tumor selective while leaving the virus genes regulating immune signalling pathways intact[119], and compared all viruses to the parental ΔJ2R virus from which the mutant viruses were derived. All of the mutant viruses were derived from a clonal isolate of WR strain VACV using traditional homologous recombination techniques to yield viruses with the target gene being replaced with a GPT marker fused to a fluorescent protein (Figure 6.1)[119,149,284]. PCR (primers found in Table 2.1) and full genome sequencing were used to confirm identity

Table 6.1. Target genes deleted to generate immunostimulatory oncolytic VACVs

Gene	Locus	Protein Product Function	Pathway	*In vivo* immune response in single gene-deleted virus
F4L	VACWR-043	Small subunit of ribonucleotide reductase.	Nucleotide biogenesis	Induced anti-tumor immune responses in bladder cancer models, with superior safety compared to ΔJ2R-only virus[119].
F1L	VACWR-040	Inhibitor of apoptosis and inflammasome.	Apoptosis and inflammasome signaling	Inhibited apoptosis and inflammasome activation, decreased caspase-1 and IL-1b secretion to increase inflammation in lungs of infected mice[98,99].
K7R	VACWR-039	Binds TLR proteins, inhibits NF-κB, IRF3. Inhibits hetero-chromatin methylation.	NF-κB & IRF3 signaling[55], heterochromatin regulation[56]	Increased natural killer (NK) cell infiltration and CD8+ T-cells, and enhanced MHCII presentation, enhanced cytolysis by NK cells and VACV specific CD8+ T-cells[59].
N1L	VACWR-028	Virulence factor. NF-κB inhibitor, possible apoptosis inhibitor.	NF-κB and IRF3 signaling[62], apoptosis signaling[63] (disputed)[64]	Enhanced CD8 T- cell effector and memory responses, and increased T-cell cytotoxicity[65].
C6L	VACWR-022	IRF3 inhibitor, IFN inhibitor through degradation of histone deacetylase 4[67].	IRF3 and IFN signaling[66]	Enhanced VACV specific T-cells with increased cytotoxicity[68], enhanced antibodies and protection against challenge[69].
A41L	VACWR-166	Secreted protein. Proposed to disrupt chemokine concentration gradients[22,92].	Chemokine binding	Increased VACV CD8+ T-cell responses, and enhanced protection against challenge[93]. Mutant was cleared more readily due to increased infiltration of leukocytes[94].
B18R	VACWR-199	Binds type I IFN (Soluble and surface), more effective against IFNα than β[81].	IFN signaling	When combined, enhanced adaptive immune responses to HIV antigens[85]. Increased HIV and VACV-specific T-cell responses compared to TLR-targeting VACVs[69].
B8R	VACVWR-190	Soluble and binds secreted IFNγ[83]		

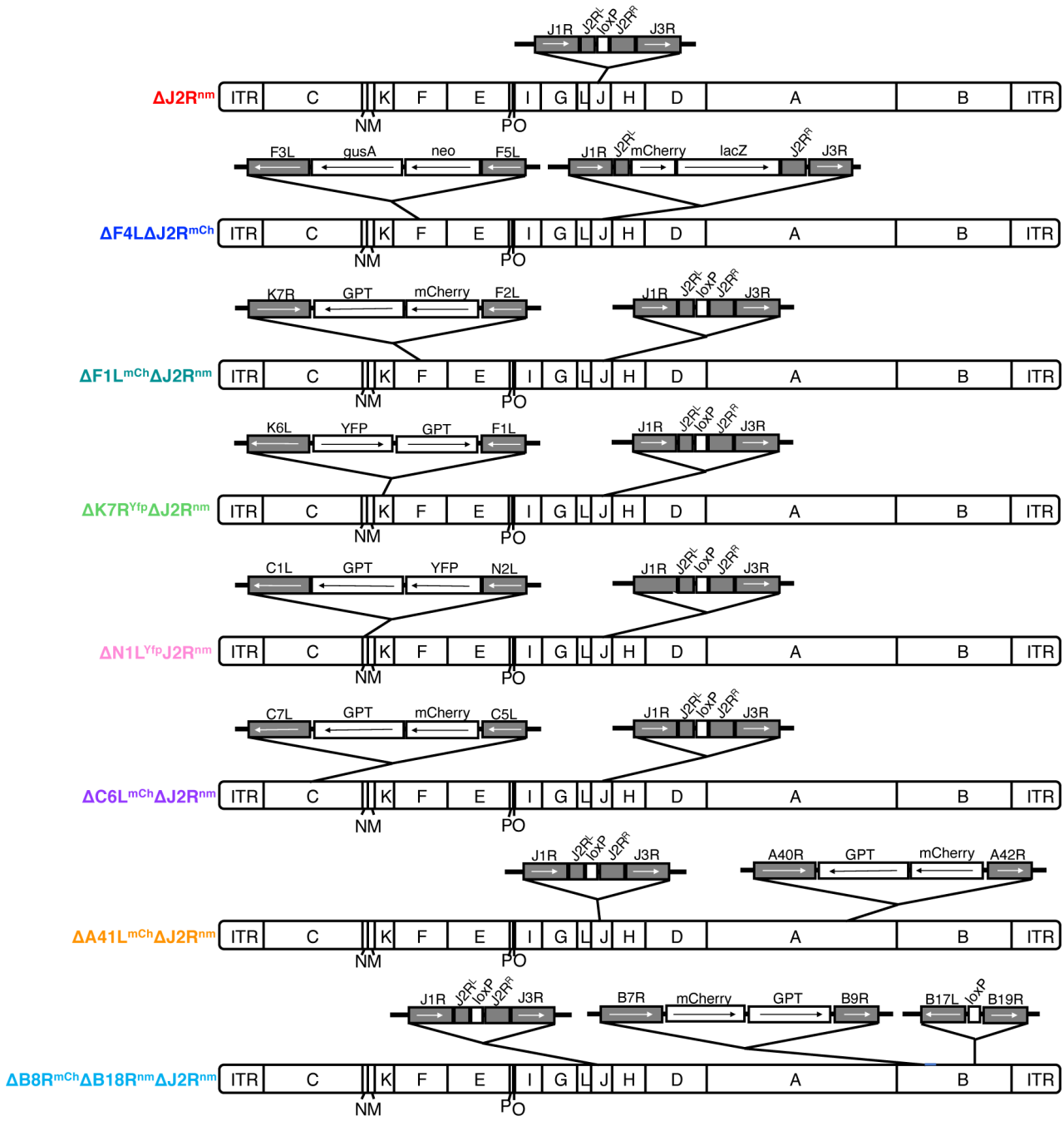

Figure 6.1. Genomic maps of mutant VACV constructs neo, neomycin gene; gusA, β-glucuronidase gene; lacZ, β-galactosidase gene; ITR, inverted terminal repeat; GPT, guanine phosphoribosyltransferase; Yfp, yellow fluorescent protein; loxP, target loxP DNA sequence; mCh, mCherry fluorescent protein; nm, no marker.

6.2.2 Immunogenic gene deletions do not impact *in vitro* characteristics, but ΔF4LΔJ2R is attenuated

When one examines the relationship between virus amplification *in vitro* and cell killing over 72 hr, most of the mutations had little effect on either phenotype when compared to the ΔJ2R virus (Figure 6.2A,B). In particular, the

viruses were equally cytotoxic in both TuBo and 4T1 cells when plated at equal multiplicity of infections (MOIs) (Figure 6.2B). The ΔF4LΔJ2R virus was an exception to this rule, where two different phenotypes were observed depending upon the cell type. In TuBo cells the ΔF4LΔJ2R virus grew more slowly than the ΔJ2R virus and was 30% less cytotoxic than other viruses at comparable MOIs (Figure 6.2B). However, this effect was cell-line dependent as the ΔF4LΔJ2R virus grew quite poorly in 4T1 cells and yet exhibited comparable levels of cell killing as seen with the other viruses. Collectively, the data show that deleting these immunomodulatory genes has little effect on VACV growth and does not affect cytotoxicity *in vitro*, whereas deleting the F4L gene can sometimes inhibit replication and reduce cytotoxicity, at least in certain (TuBo) cells.

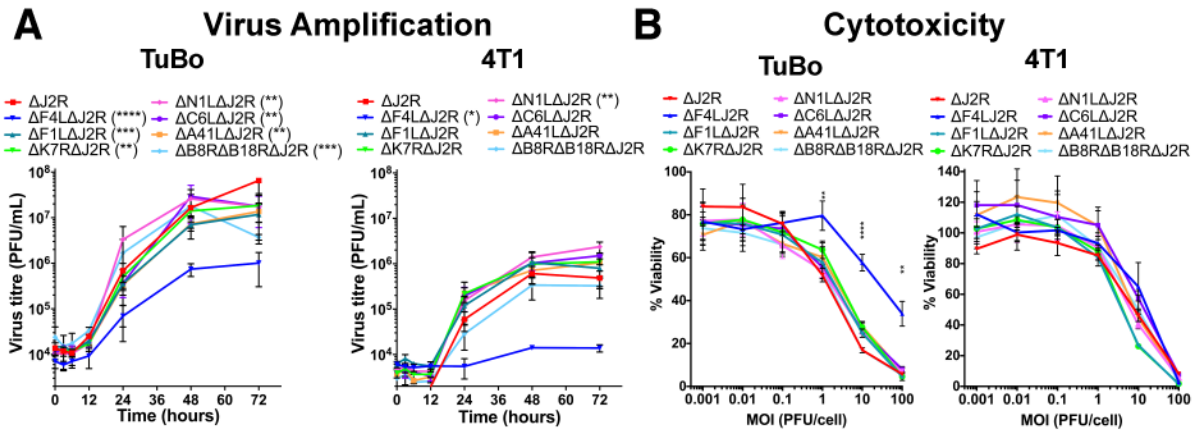

Figure 6.2. *In vitro* growth and cytotoxicity in murine mammary carcinoma cell lines. A) Viral growth kinetics of mutant VACVs on TuBo and 4T1 cells. Significance calculated at the 72-hour time point relative to ΔJ2R VACV using one-way ANOVA shown in the figure legends. B) Resazurin assay of cell viability 72 hours post infection in TuBo and 4T1 cells. Two-way ANOVA comparing cell viability after each virus treatment relative to parental ΔJ2R was used with Dunnett's multiple comparisons correction and is shown on the graph at applicable points. Error bars denote +/- SEM from three experimental replicates. *p<0.05, **p<0.01 ***p<0.001 ****p<0.0001

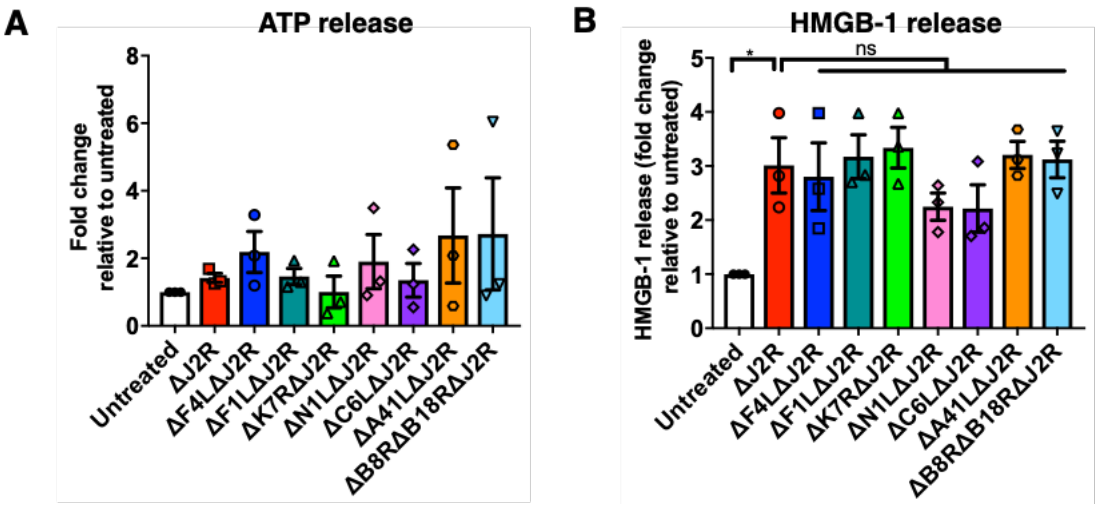

Figure 6.3. Immunogenic VACV cause release of markers of ICD. A Fold change in ATP release relative to untreated (mock-infected cells) as measured using a bioluminescence assay from the media of virus-infected TUBO cell lines 24 hours post infection at an MOI of 3. One-way ANOVA of each virus compared to ΔJ2R shows no significant differences. B. Fold change in HMGB-1 release relative to untreated (mock-infected cells) as measured using ELISA from the media of virus-infected TUBO cells 72 hours post infection. One-way ANOVA of each virus compared to ΔJ2R shows no significant differences. Data shown from 3 independent experiments. Error bars ± SEM.

We wanted to determine if any gene deletions in our newly synthesized VACVs had an impact on the release of DAMPs known to be indicative of immunogenic cell death (ICD)[342]. These assays are typically used to assess treatments *in vitro* which should stimulate an immune response *in vivo*. We evaluated the release of two of the most-well known ICD indicators, ATP and HMGB-1. A bioluminescence-based assay was used to determine ATP levels in media 72 hours following infection with the viruses at an MOI of 3. It was found that none of the viruses tested significantly increased the release of ATP from infected TuBo cells (Figure 6.3A). HMGB-1 in the media was also tested using a commercial ELISA kit. In this assay, virus infection caused a release of HMGB-1 into the medium relative to mock-infected cells, however there was no difference in HMGB-1 release from the newly deleted virus mutants compared to the parental ΔJ2R virus (Figure 6.3B). We attempted to assess a third indictor of ICD, which is translocation of calreticulin to the cell surface. However, we were unable to detect this DAMP at the cell surface using flow cytometry, imaging cytometry, or by fluorescence-microscopy assays with known ICD-inducing agents mitoxantrone and doxorubicin due to autofluorescence caused by treatment.

6.2.3 All VACVs were safe, and virus replication was restricted to the tumour

The safety and biodistribution of the mutant VACVs were tested *in vivo* in two different orthotopic and syngeneic models of breast cancer. After the tumors became palpable (~30 mm^3), three doses of each virus at $1x10^7$ PFU or PBS as an injection control were given by intratumoral injection at 48 hr intervals (Figure 6.4A). No significant

weight loss or adverse events associated with virus treatment were observed in either model, indicating that all of the recombinant viruses were safe (Figure 6.4B, C). Live viruses were isolated from most of the TuBo tumors three weeks after virus treatment, although VACV ΔF4LΔJ2R was not detected in any sample (Figure 6.4D). In 4T1 tumors, which grow more rapidly than TuBo tumors, virus growth and biodistribution were assessed two weeks after virus treatment. In this model, virus was recovered from tumors in all the groups (Figure 6.4E), but not in spleens, ovaries, kidneys or liver, suggesting that these are tumor selective viruses. Collectively, these data suggest that all the recombinant viruses are safe, and that virus replication is restricted to tumors without dissemination to distant organs.

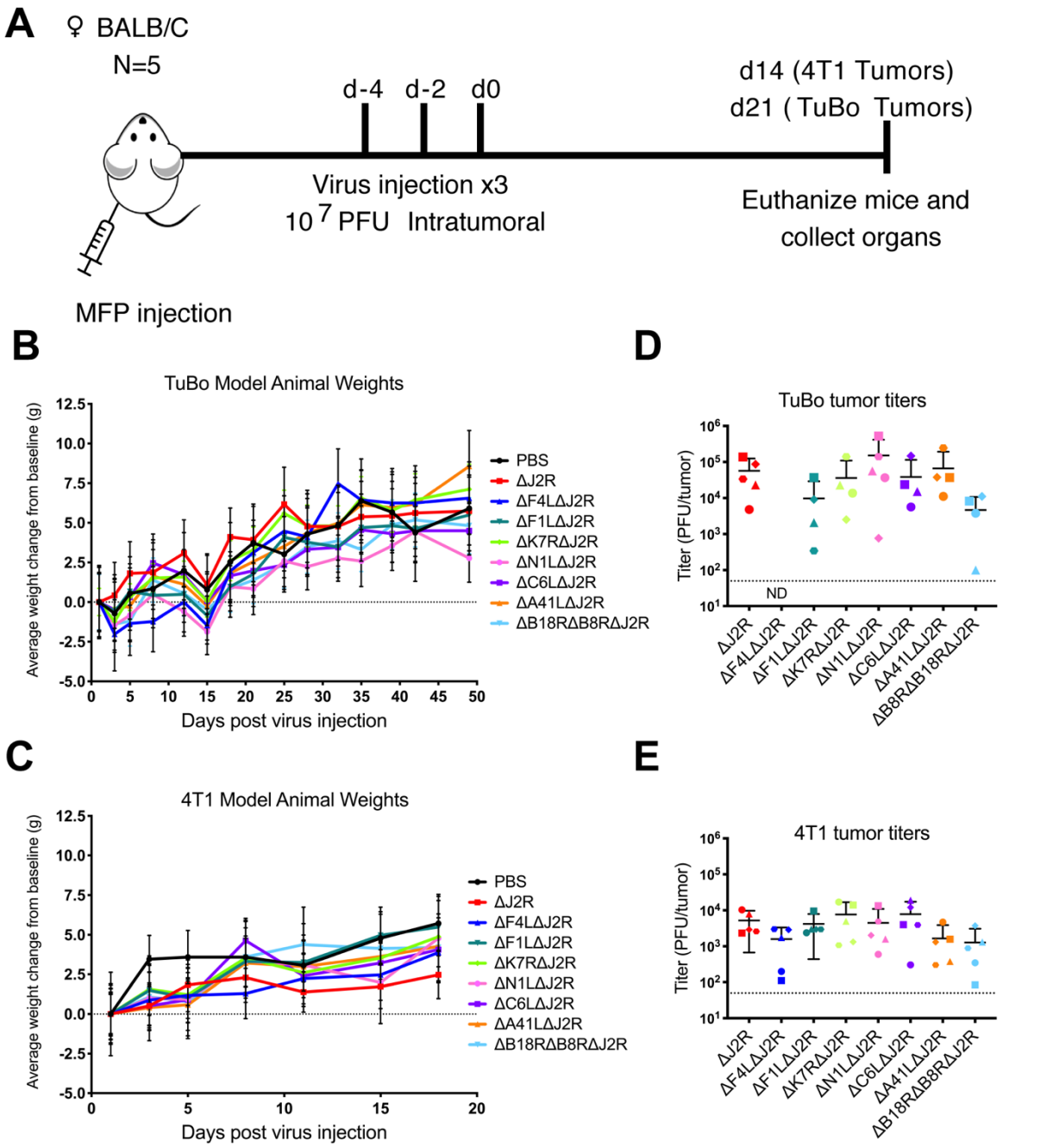

Figure 6.4. All immunomodulatory VACVs were safe *in vivo*, and virus replication was restricted to tumors. A. Experimental design to assess safety, biodistribution, and immune-microenvironment changes after treatment with mutant oncolytic viruses. 8-13-week-old female BALB/C mice were injected with tumor cells into the mammary fat pad. Once palpable, three intratumoral 1x10^7 PFU doses of VACVs were administered. Mice were euthanized after 14 days (4T1), or 21 days (TuBo). Tumors and organs were collected for immune-analysis and viral titering. B&C. Weight change from baseline of mice during treatment with oncolytic VACVs in the TuBo(B) and 4T1(C) tumor model. D&E. Virus titers isolated from tumors where dotted line shows the limit of detection. ND- not detected.

6.2.4 Mutant VACVs alter therapeutic outcomes in two breast tumour models

Next, we monitored tumor regression and mouse survival in the TuBo breast tumor model. TuBo tumors are derived from a mammary carcinoma of HER2/*neu* transgenic mice, and therefore over-express rat HER2/*neu*[232]. It is considered an immunogenic HER2+ mammary tumor model and is also characterized by relatively slow growth with no ability to form metastasis[235].

Tumors were treated as described above (Figure 6.4A) and tumor growth was compared to both untreated controls (PBS) and to VACV ΔJ2R-treated controls (Figure 6.5). The VACV ΔJ2R mutant significantly decreased the rate of tumor growth in the TuBo model compared to the PBS-treated controls (Figure 6.5B). However, none of the recombinant VACV produced any further improvement in the antitumor response compared to ΔJ2R. In fact, ΔF4LΔJ2R and ΔF1LΔJ2R showed significantly higher tumor volumes at day 60 when compared to ΔJ2R-treated tumors (Figure 6.5B). The tumor volumes after treatment with ΔK7RΔJ2R, ΔN1LΔJ2R, ΔC6LΔJ2R, ΔA41LΔJ2R, or ΔB8RΔB18RΔJ2R viruses (at 60 days) were not statistically different compared to ΔJ2R alone. We examined the long-term survival, following the animals out to 300 days post-treatment. Virus treatment initially appeared to significantly increase survival relative to PBS treatment (Figure 6.5C). Gehan-Breslow Wilcoxon significance testing of survival curves yielded $p=0.05$ when comparing survival of PBS treated mice to ΔC6LΔJ2R treated mice, and $p=0.03$ when comparing ΔJ2R treated mice to ΔF4LΔJ2R. However, these values were deemed not significant, as the Bonferroni-corrected multiple comparisons threshold for significance was determined to be $p<0.003$. These results showed that no virus treatment significantly impacted mouse survival relative to untreated mice, and nor did any gene deletion significantly change survival compared to the parental ΔJ2R virus in this model.

Although no significant changes in overall survival were observed, the ΔB8RΔB18RΔJ2R virus treatment produced the highest median survival time of 192.5 days, followed by ΔC6LΔJ2R and ΔN1LΔJ2R viruses at 163 and 159.5 days, respectively, while the median survival of PBS controls was just 87.5 days (Figure 6.5C). The ΔB8RΔB18RΔJ2R and ΔN1LΔJ2R treatments also yielded the highest number of complete responses (CR) with 4/8 CR (50%) per group, determined as no detectable tumor mass at the end of the experiment (Figure 6.5A,C). Treatment with VACV ΔC6LΔJ2R produced 3/8 CR (37.5%) and one partial response (PR). The ΔJ2R, ΔF1LΔJ2R, and ΔK7RΔJ2R mutants each also showed 3/8 (37.5%) CRs, followed by ΔA41LΔJ2R with 2/8 CR (25%) and ΔF4LΔJ2R with 1/8 CR (12.5%) (Figure 6.5A,C). No CRs were seen with PBS-treated tumors although one PR was observed (Figure 6.5A,C). To determine if treated mice had acquired antitumor immunity, mice with stable or undetectable tumors at day 150 were re-challenged with fresh TuBo cells in the opposite mammary fat pad. While tumors appeared within 10 days in all of the naïve age-matched control mice, all but one of the 24 mice that had cleared a TuBo tumor rejected the implanted cells. The one exception was a mouse treated with VACV ΔF1LΔJ2R. It developed a palpable tumor that still eventually cleared (Figure 6.5D).

The 4T1 tumor model is derived from a spontaneously-arising BALB/c mammary tumor, is poorly immunogenic, has rapid growth, and is highly metastatic[236]. We can find no reports of 4T1-specific neo-antigens that can be used to detect tumor-specific T-cell responses in this model. Due to the rapid growth and metastasis of 4T1 tumors to the lungs, it was an animal welfare issue, rather than tumor volume, that was used to determine the endpoint. Mice were euthanized at the first behavioural indicators of distress, mainly the cessation of grooming, weight loss, and squinted eyes or hunched posture.

In the more aggressive, non-immunogenic 4T1 tumor model, all of the virus treatments delayed tumor growth at day 18 relative to the PBS-treated tumors (Figure 6.6A,B). It was also quite striking that in this model, most of the new viruses, except the ΔF4LΔJ2R and ΔF1LΔJ2R strains, improved survival relative to ΔJ2R treated mice (Figure 6.6C). This correlated with TuBo data where we saw that the ΔF4LΔJ2R and ΔF1LΔJ2R VACV were less effective than the ΔJ2R control virus at slowing growth. Although the gained survival benefit was statistically significant, the actual extension of lifespan was minor (Figure 6.6C). The median survival of VACV ΔC6LΔJ2R-treated mice was 26 days compared with 22 days for PBS treated (Figure 6.6C). This difference was probably explained by the fact that the VACV ΔC6LΔJ2R-treated mice had an average of 1000 metastatic cells in the lungs when they reached endpoint, whereas 10- and 100-fold more cells were detected in the ΔJ2R- and PBS-treated animals, respectively (Figure 6.6D).

Collectively, these data showed that additional immunogenic deletions did not significantly improve survival in a TuBo immunogenic tumor model and may only have minor impacts on tumor regression, median survival length and incidences of complete and partial responses compared to ΔJ2R. However, in non-immunogenic 4T1 tumors, immunogenic gene deleted VACVs imparted a survival benefit relative to the parental ΔJ2R virus. Moreover, where benefits could be detected they were associated with mutations in the B18R/B8R, C6L, N1L, and K7R genes, all of which modulated the interferon response[59,62,66,67,81,83]. The F1L and F4L mutations, which promote apoptosis [98,99] and tumor specificity[119], respectively, did not offer advantages in these breast cancer models, and the ΔA41L mutation, which impairs chemokine signaling[22,92], only enhanced survival in the 4T1 model.

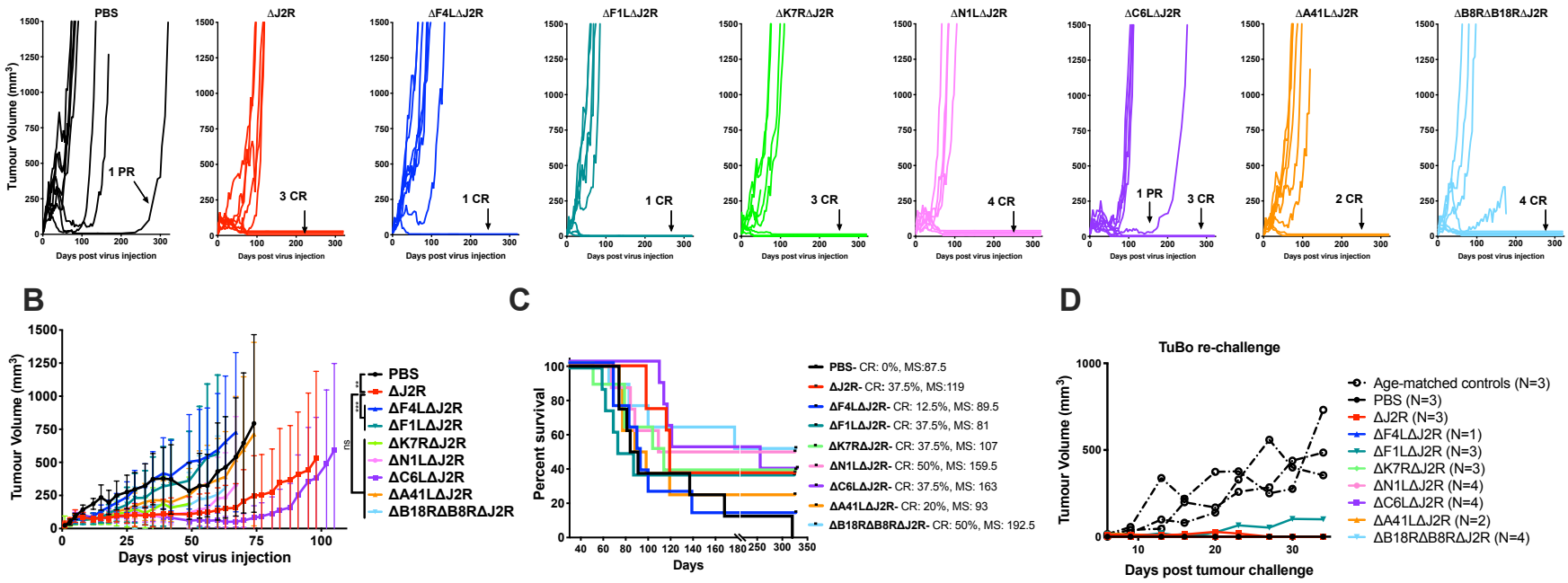

Figure 6.5 .Mutant VACVs alter therapeutic outcomes in the immunogenic HER2/neu+ TuBo tumour model A. Individual tumor growth for each mouse in TuBo tumors treated with immunostimulatory oncolytic VACVs. B. Average tumor volume until first death observed in each group. Error bars show ± 1 SD from mean. Two-way ANOVA was used to evaluate differences in tumor growth over time compared to ΔJ2R treatment until first non-censored death at day 60; *p<0.05, **P<0.001, ****P<0.0001. B. Kaplan-Meir survival plot of data shown in A&B. C. Individual tumor volumes of mice re-challenged with TuBo tumors in the opposite mammary fat pad after stable disease to determine establishment of antitumor immunity. Partial responses (PR) indicate where tumor growth is undetected or stagnant for a prolonged period but eventually recurs, or complete responses (CR), where tumors are undetectable, and a secondary tumor challenge was rejected.

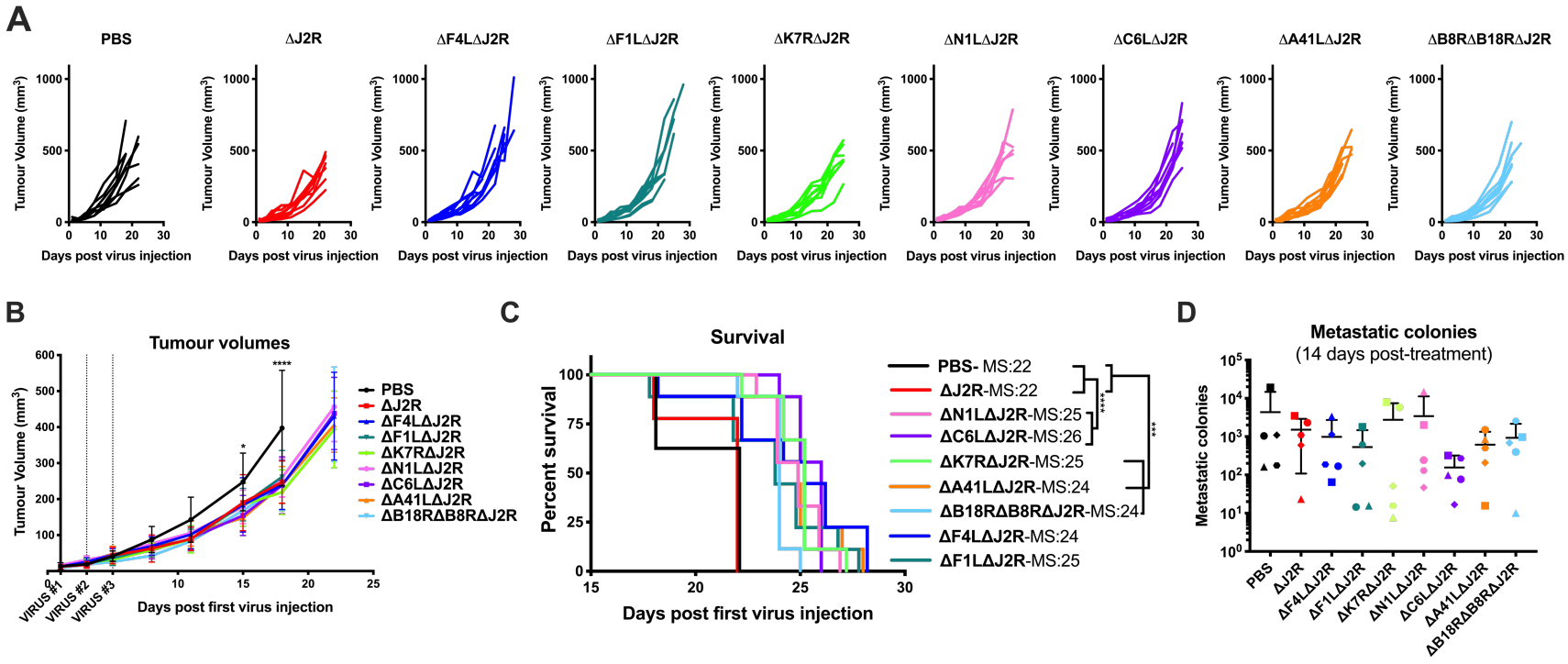

Figure 6.6.Mutant VACVs alter therapeutic outcomes in the non-immunogenic and metastatic 4T1 tumour model A. Individual tumor growth for each mouse in 4T1 tumors treated with immunostimulatory oncolytic VACVs. B. Average tumor volume until first death observed in each group. Error bars show ± 1 SD from mean. Two-way ANOVA was used to evaluate differences in tumor growth over time compared to ΔJ2R treatment until first non-censored death at day 18; *p<0.05, **p<0.01***P<0.001, ****P<0.0001. C. Kaplan-Meir survival plot of data shown in A&B with median survival (MS) indicated next to the legend. D. Lung metastasis analysis as determined by colony formation assays of digested lung tissue plated under 6-thioguanine. N=8-9 mice per group

6.3 Discussion

Numerous oncolytic VACVs have been developed that harbour deletions of various viral genes[12], and many target genes have been suggested for removal from VACV to increase antitumor immunity[12]. To our knowledge, however, there have been no systematic attempts at deciphering which gene deletions have an impact on a tumor bearing host, and what the relative contribution of gene removal has in the overall immune response against the virus in this context. Here we sought to decipher how removal of genes from the VACV genome could impact immune cells in the TME post-oncolytic virus treatment. We removed eight different genes from VACV and compared the effects of these deletions in head-to-head comparisons in immune-competent breast tumor models.

Overall, we observed that gene deleted viruses imparted a more significant survival benefit in our non-immunogenic 4T1 tumor model than they did in our immunogenic TuBo tumor model, despite these viruses causing more drastic changes to the TME in the TuBo model. This suggests that minor tweaks to the virus genome used to manipulate the TME even slightly may be more beneficial in non-immunogenic or more aggressive tumor models, where slight changes in the immune response may impart more therapeutic benefits.

Throughout these studies we determined a few candidate gene deletions that warrant further analysis. In the TuBo tumor model, ΔB8RΔB18RΔJ2R and ΔN1LΔJ2R had more complete responses than ΔJ2R. These two viruses, along with ΔC6LΔJ2R improved median survival. In the 4T1 tumor model these viruses all statistically improved survival relative to ΔJ2R treatment. These promising candidates are all viruses with gene deletions that either directly inhibit interferon responses [ΔB8R[83], ΔB18R[81]], or indirectly interfere with interferon signalling through NF-κB or IRF3 inhibition [ΔC6L[66,67], ΔN1L[62], ΔK7R[59]]. This suggests that removal of VACV genes that inhibit interferon signalling may be a promising strategy for improving oncolytic VACV therapy. This is in agreement with previous studies that show targeting IFN pathways by deletion of B18R enhances therapeutic efficacy of oncolytic VACV in cancer models, however this may be improved with the additional removal of B8R[162,343]. A recent report also showed that a ΔN1LΔTK virus was more effective than ΔJ2R alone in treating flank models of lung cancer[344]. This is not surprising given the mounting body of evidence suggesting that IFN signalling is critical for the success of cancer immunotherapies[345–347].

A few VACV deletions in the models tested did not cause any survival improvement or therapeutic enhancement. VACV ΔF1LΔJ2R did not cause substantial changes to the immune response relative to ΔJ2R and was less effective than ΔJ2R alone in controlling tumor growth in the TuBo tumor model. It also did not impart a survival benefit in the 4T1 tumor model compared to ΔJ2R, whereas the rest of our immunogenic knockout viruses did improve this response. It can be noted, however, that a ΔF1LΔJ2R virus is more effective than ΔJ2R alone in treating subcutaneous colon tumors in mice[348]. Similarly, ΔF4LΔJ2R VACV, which demonstrated superior safety and equal treatment efficacy in bladder tumor models compared to a ΔJ2R VACV[119], was not therapeutically superior in 4T1 or

TuBo breast tumor models. This suggests that certain oncolytic viruses and the immunological changes they induce may be beneficial in one circumstance or tumor type, while being potentially unhelpful in other tumor types.

Chapter 7: Tumor immune-cell microenvironment alterations of immunomodulatory gene-deleted oncolytic VACVs in breast cancer models

Preface

A portion of this chapter has been published in the manuscript:

Umer BA, Noyce RS, Franczak BC, Shenouda MM, Kelly RG, Favis NA, Desaulniers M, Baldwin TA, Hitt M, and Evans DH. Deciphering the immunomodulatory capacity of oncolytic vaccinia virus to enhance the immune response in breast tumours, *Cancer Immunology Research,* (8)618-31.

Permissions: Cancer Immunology Research of the American Association for Cancer Research (AACR) States: "Authors of articles published in AACR journals are permitted to use their article or parts of their article in the following ways without requesting permission from the AACR. All such uses must include appropriate attribution to the original AACR publication. Authors may do the following as applicable:

1. Reproduce parts of their article, including figures and tables, in books, reviews, or subsequent research articles they write;
2. Use parts of their article in presentations, including figures downloaded into PowerPoint, which can be done directly from the journal's website;
3. Post the accepted version of their article (after revisions resulting from peer review, but before editing and formatting) on their institutional website, if this is required by their institution. The version on the institutional repository must contain a link to the final, published version of the article on the AACR journal website so that any subsequent corrections to the published record will continue to be available to the broadest readership. The posted version may be released publicly (made open to anyone) 12 months after its publication in the journal;
4. Submit a copy of the article to a doctoral candidate's university in support of a doctoral thesis or dissertation.

7.1 Introduction

In the previous chapter I investigated how deletion of immunomodulatory genes from VACV could impact treatment outcomes in murine models of breast cancer. As a major component in the efficacy of OV therapy is the immune response to tumour infection, in the current chapter I analyzed the tumour immune cell microenvironment (TiME) after treatment with each of the mutant viruses to determine the impact of these gene deletions on the immune response of the host. The objective of these studies was to determine how each individual gene deletion contributed to sustained changes or "reprogramming" of the TiME and to utilize this knowledge to direct and guide immune responses of the host to futher improve the benefits of treatment.

To assess immune responses I again utilized the TuBo and 4T1 orthotopic syngeneic murine mammary tumour models. I assessed immune responses after treatment with the mutant VACVs previously described in Chapter 6; ΔF4LΔJ2R, ΔF1LΔJ2R, ΔK7RΔJ2R, ΔN1LΔJ2R, ΔC6LΔJ2R, ΔA41LΔJ2R, ΔB8RΔB18RΔJ2R compared to the parental ΔJ2R VACV and PBS as a control. In both models, I performed a general assessment of the immune cell composition in both tumours and spleens, focusing on major cell types such as CD4+ and CD8+ T cells, Tregs, and M/PMN-MDSCs. I then honed in on lymphocyte parameters that provide insight into the activity of these cells, such as markers of activation (CD69), checkpoint expression (PD-1 and PD-L1), and T-cell receptor specificity (tetramer staining). Finally, I performed an analysis of serum cytokines to determine the effects on systemic circulating cytokines after treatment with these viruses.

7.2 Results

I first started these investigations by characterizing the immune cell compartment in tumors and spleens of both the TuBo and 4T1 tumour models. To determine if virus treatments caused lasting alterations to the TME we waited three weeks after the last virus injection in the TuBo model, and two weeks in the 4T1 model to assess immune-cell subtypes in the tumors and spleens.

7.2.1 Mutant VACVs alter immune responses in TuBo and 4T1 tumours

Overall, the immune cell composition within tumors varied greatly between the TuBo and 4T1 tumour models (Figure 7.1, Figure 7.2A), both in number and cell types. When qualitatively comparing the immune cell composition after virus-treatment compared to PBS-treated tumours, the general compositions were similar, but differed in the magnitude of infiltrating cell numbers (Figure 7.1A, Figure 7.2A). VACV ΔF4LΔJ2R treated tumors appeared to have reduced numbers of purported polymorphonuclear myeloid-derived suppressor cells (PMN-MDSCs) infiltrating tumors in the TuBo model (Figure 7.1A), and VACV ΔF1LΔJ2R-treated tumors appeared to have less immune cells overall in the 4T1 tumor model (Figure 7.2A). All of the virus treatments increased the percentage of tumor infiltrating $CD8^+$ T-cells and decreased the numbers of suppressive Tregs (Figure 7.1B,D,Figure 7.2B,D). The magnitude of these changes was larger in the TuBo model compared to the 4T1 model, increasing the percentage of CD8+ T cells by approximately

30% and 15%, respectively, compared to PBS-treated tumors. However, none of the additional VACV gene deletions significantly altered these percentages compared to tumors infected with the VACV ΔJ2R parent strain. This suggests that no single deletion of one of these genes can substantially alter the levels of tumor infiltrating lymphocytes (TILs). The one exception was ΔB18RΔB8RΔJ2R, where we detected a reduction in the percentage of $CD4^+$ T cells in TuBo tumors compared to tumors treated with ΔJ2R (Figure 7.1D). PMN-MDSCs, which are potent suppressors of cytotoxic T cell activity [349], increased in tumors after all virus treatments except for those treated with ΔJ2RΔF4L (Figure 7.2F).

More subtle changes were detected in the immune compartment of the spleen and these differed from what was seen in the tumors. Virus treatment, independent of mutations, altered the overall composition of the spleens compared to PBS-treated mice in TuBo tumors, but not in 4T1 (Figure 7.1G-L, Figure 7.2J-L). In either model, no obvious differences in overall splenocyte composition were found between virus mutants (Figure 7.1G, Figure 7.2G). Rather, differences were apparent between virus treatments when assessing more minute cellular characteristics (Figure 7.1H-L,Figure 7.2H-L). We observed a decrease in the overall myeloid/MDSC populations in the spleens of mice treated with VACV in the TuBo tumor model compared to the 4T1 tumor model (Figure 7.1K,LFigure 7.2K,L). This was not surprising, given that accumulation of these suppressor cells in the spleen is usually directly associated with tumor burden[349]. We detected decreased percentages of $CD8^+$ T cells in the spleens of mice treated with the ΔF4LΔJ2R, ΔK7RΔJ2R, and ΔN1LΔJ2R viruses compared to tumors treated with VACV ΔJ2R (Figure 7.1H). This might have explained why ΔK7RJ2R and ΔN1LΔJ2R-treated tumors had increased percentages of $CD4^+$ T cells. Similar effects were seen in the spleens of 4T1 tumor-bearing mice but with less magnitude (Figure 7.2H).

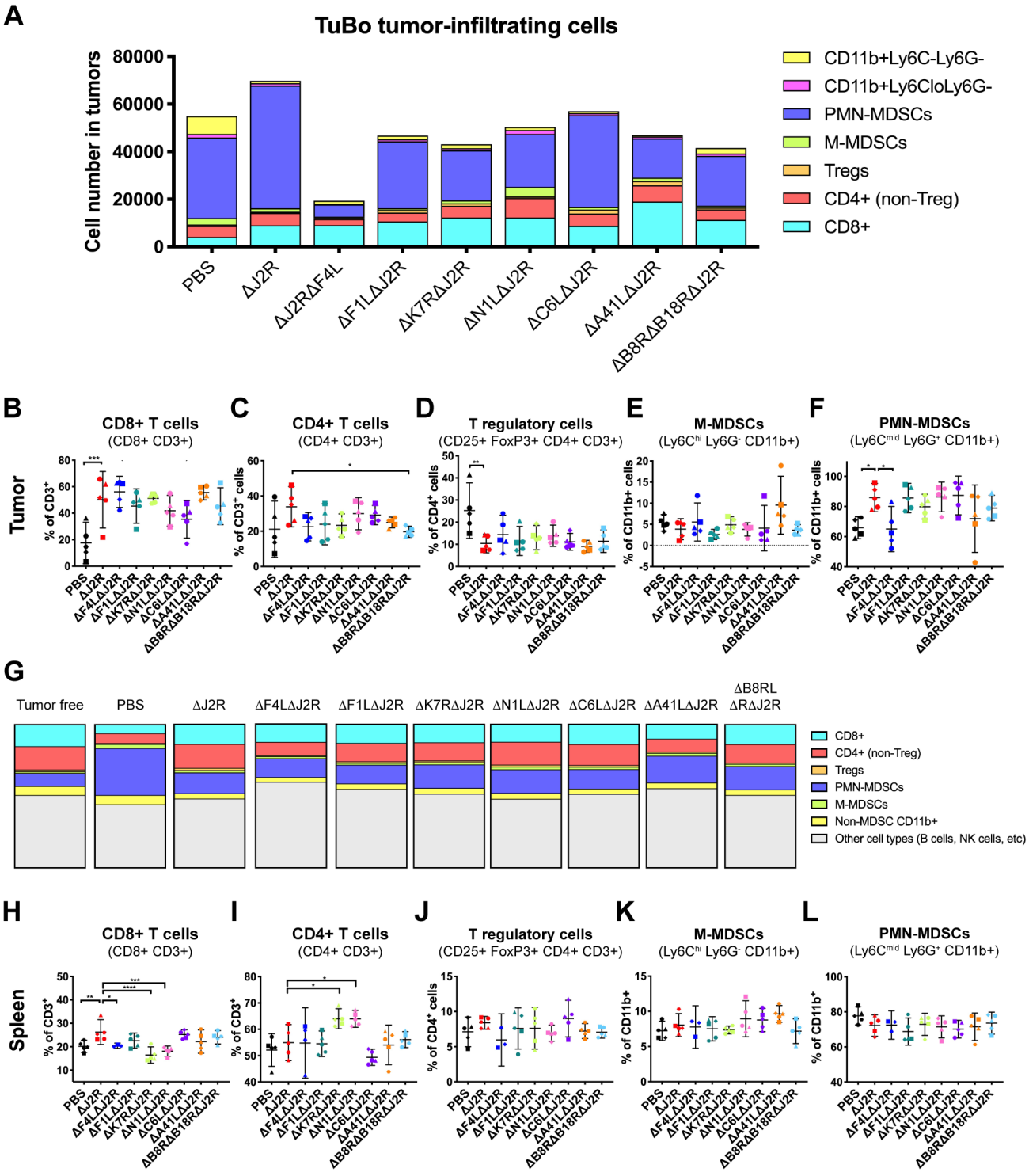

Figure 7.1.Mutant VACVs altered immune responses in TuBo tumors. A. Flow cytometric quantification of average numbers (A) and percentages (B-F) of immune cells in tumors. G. Overall average splenocyte composition as a percent of total cells isolated from spleens. H-L. Immune-cell percentages from spleens of mice after treatment. Organs were harvested three weeks after virus treatment. Statistical analysis was performed using one-way ANOVA where data was shown to be parametric, or Kruskal-Wallis testing when data was non-parametric with Dunnett's or Dunn's multiple comparisons test, respectively; *p<0.05, **p<0.01, ***p<0.001, ****p<0.0001. Data points represent individual mice in B-F and H-L with error bars denoting 95% CIs, and average values for groups in A and G.

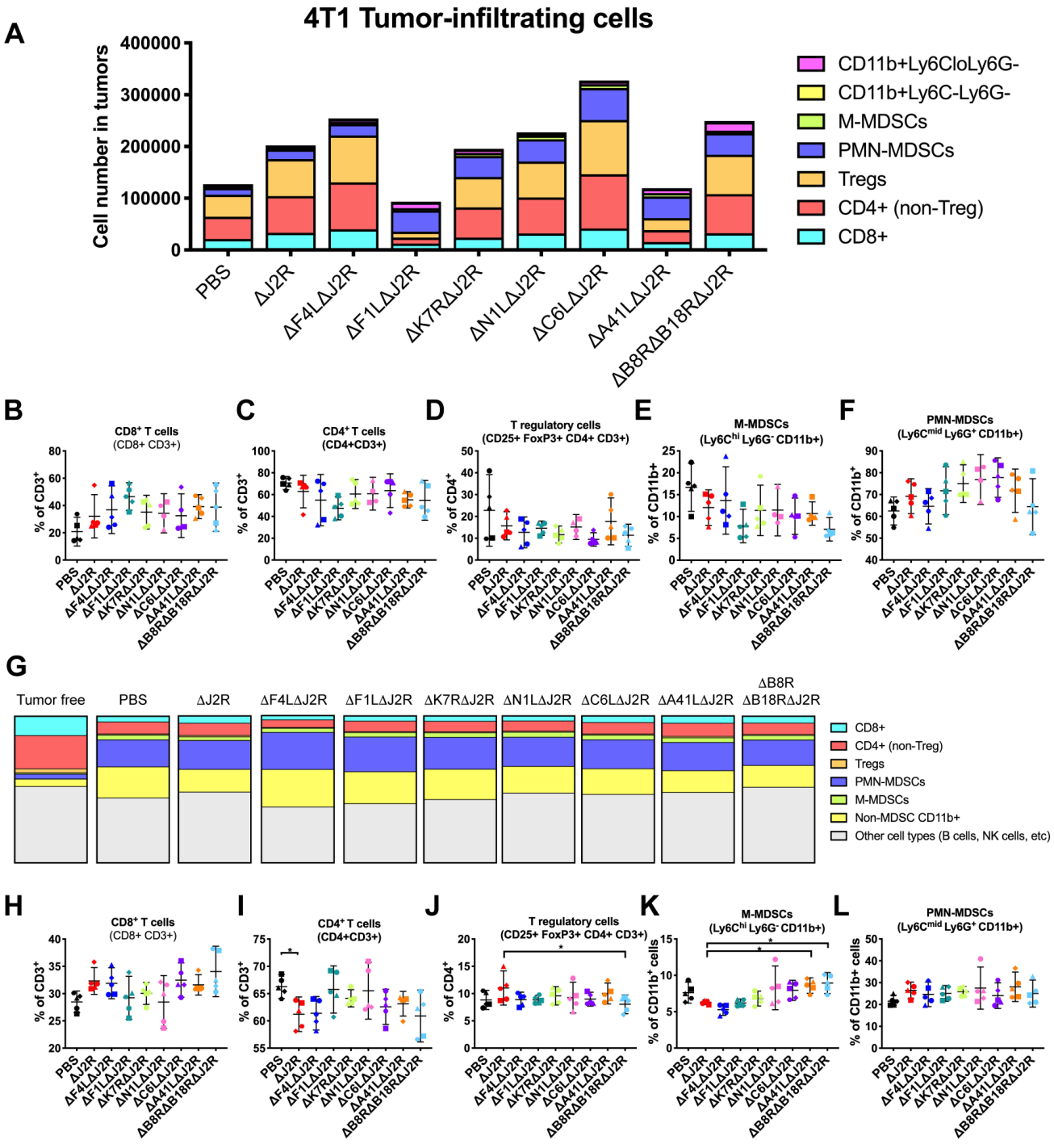

Figure 7.2. Mutant VACVs altered immune responses in 4T1 tumors. A. Flow cytometric quantification of average numbers (A) and percentages (B-F) of immune cells in tumors. G. Overall average splenocyte composition as a percent of total cells isolated from spleens. H-L. Immune-cell percentages from spleens of mice after treatment. Organs were harvested two weeks after virus treatment. Statistical analysis was performed using one-way ANOVA where data was shown to be parametric, or Kruskal-Wallis testing when data was non-parametric with Dunnett's or Dunn's multiple comparisons test, respectively; *p<0.05, **p<0.01, ***p<0.001, ****p<0.0001. Data points represent individual mice in B-F and H-L with error bars denoting 95% CIs, and average values for groups in A and G.

7.2.2 Mutant VACVs alter lymphocyte activation and immune checkpoints

While an overall assessment of the TiME provides an indication of the cell types located within the tumour and spleen, it does not provide information about the functionality of these cells. In particular, the presence of CD8+ T cells is a promising immune-response indicator, but an assessment of cell surface markers on these CD8+ T cells can provide further insights into the activity of the immune response. Considering this information, we further assessed CD4+ and CD8+ T cells in the TuBo tumour model for CD69, a marker of T-cell activation (Figure 7.3). In tumours, while CD69 expression remained unchanged between treatments on CD8+ T cells, expression was elevated after ΔJ2R virus treatment relative to PBS (Figure 7.3A,B). In the spleen, it ΔA41LΔJ2R VACV decreased CD69 expression relative to ΔJ2R VACV treatment in both CD4+ and CD8+ T cell populations, while ΔK7RΔJ2R VACV only decreased CD69 expression on CD4+ T cells (Figure 7.3 C,D).

To further assess lymphocyte characteristics, expression of programmed cell death protein (PD-1) and its ligand, PD-L1, were measured in tumors and spleens of both tumour models (Figure 7.4A-E). VACV ΔJ2R decreased PD-1 expression on Tregs in TuBo spleens and tumors relative to the PBS-treated controls (Figure 7.4B,D), an effect not observed in the non-immunogenic 4T1 tumor model (Figure 7.4C-E). Alternatively, VACV ΔK7RΔJ2R did not cause this PD-1 down regulation on Tregs, which appeared more similar to Tregs isolated from untreated tumors. It was difficult to generalize effects on PD-1 expression, as each virus affected PD-1 expression differently. Compared to tumors treated with VACV ΔJ2R, ΔA41LΔJ2R infections were associated with up-regulated PD-1 expression on both $CD4^+$ and $CD8^+$ T cells in 4T1 mouse spleens, but not in tumors, while a VACV ΔB8RΔB18RΔJ2R infection was associated with an increase in PD-1 on $CD8^+$ cells in the spleen. When analyzing PD-L1 expression on CD11b-CD3- cells isolated from TuBo tumors, we noted that VACV ΔF4LΔJ2R caused a marked upregulation of PD-L1 (Figure 7.4F,G), which may have partially explained the poor antitumor response relative to VACV ΔJ2R treatment. These observations show that different virus mutations have different effects on PD-1 and PD-L1 expression.

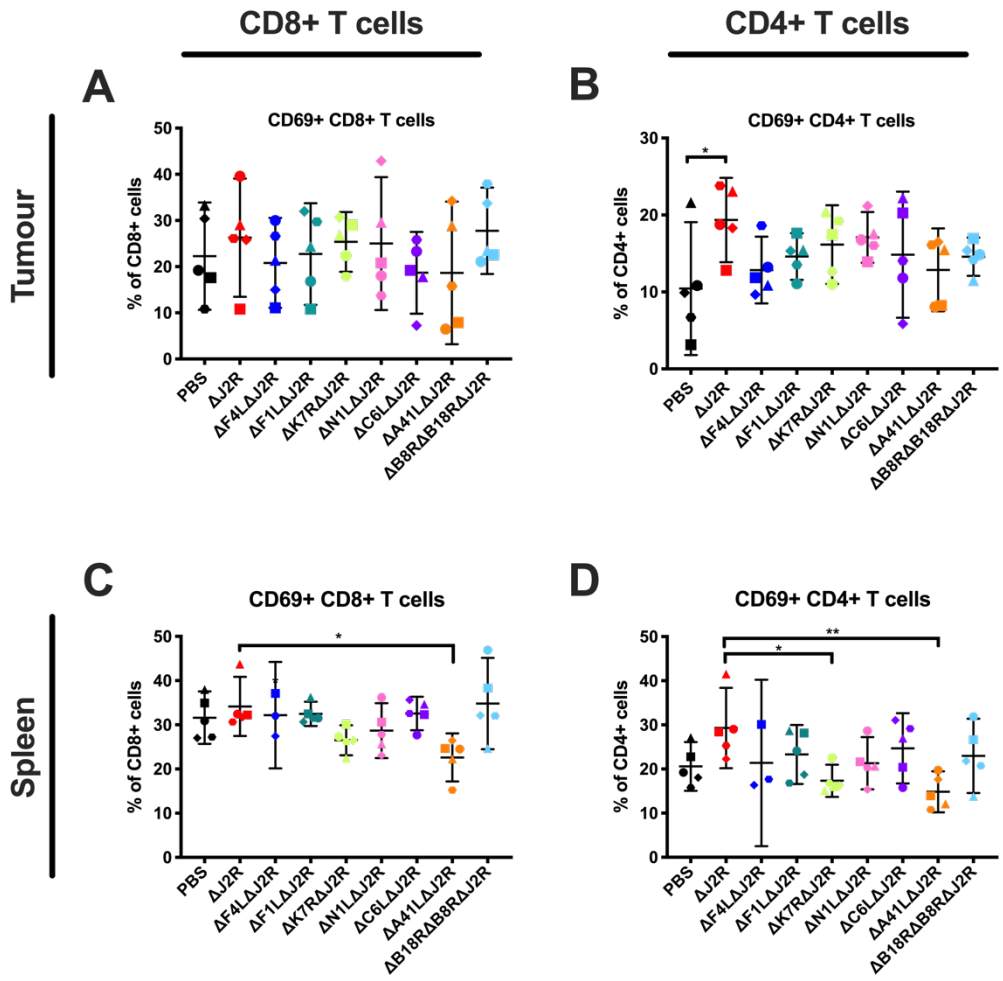

Figure 7.3 Modifications to the VACV genome altered expression of CD69, a marker of lymphocyte activation, on CD4+ and CD8+ T cells in TuBo tumors and spleens. A-D. Percentage of CD69+CD8+ (A&C) and CD69+ CD4+ (B&D) from tumours (A&B) and spleens (C&D). Statistical analysis was performed using one-way ANOVA where data was shown to be parametric, or Kruskal-Wallis testing when data was non-parametric with Dunnett's or Dunn's multiple comparisons test, respectively; *p<0.05, **p<0.01, ***p<0.001, ****p<0.0001. Data points represent individual mice with error bars denoting 95% CIs from the mean.

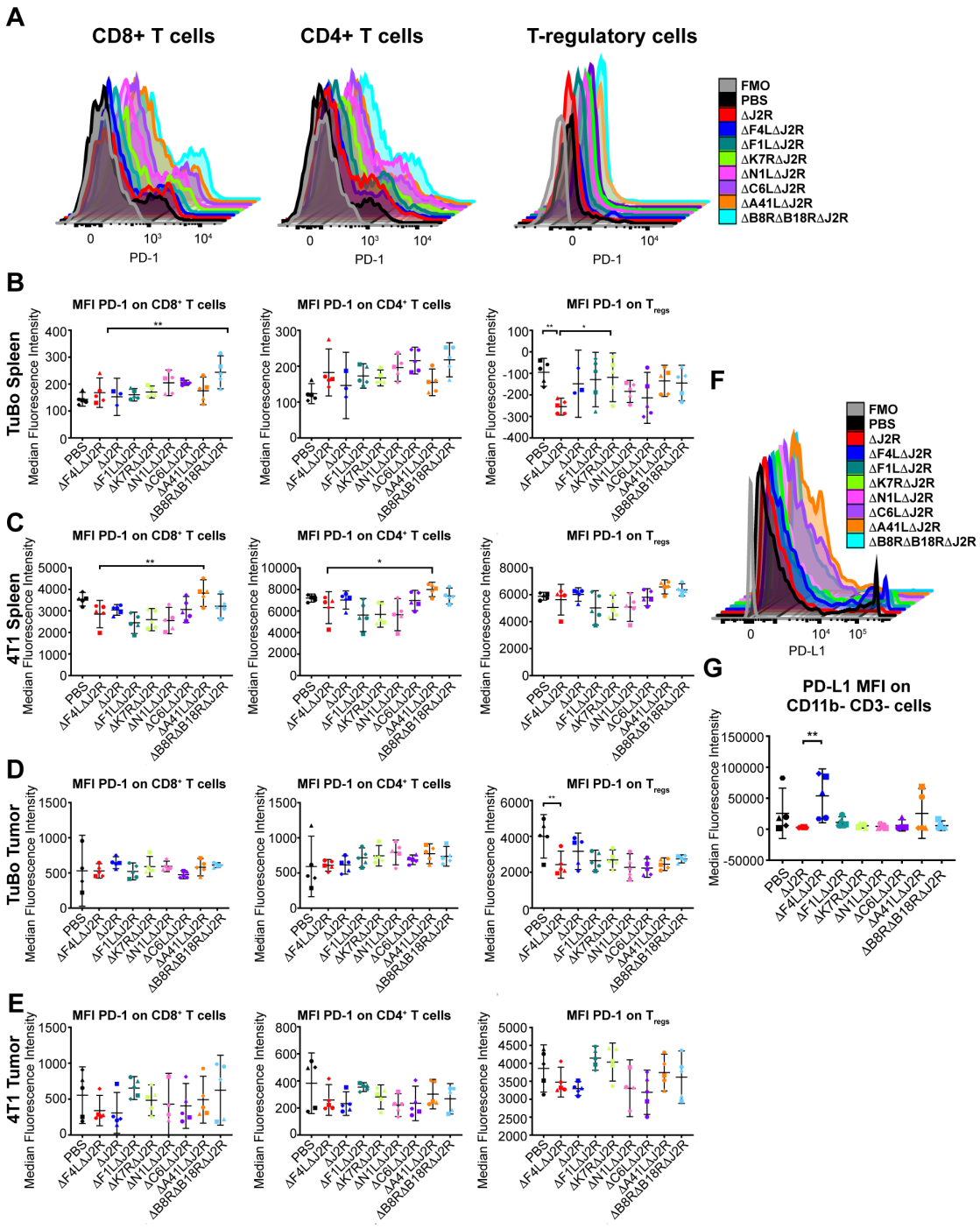

Figure 7.4 Modifications to the VACV genome altered immune checkpoint expression on immune cells in TuBo tumors and spleens. A. Representative histograms of PD-1 expression on CD8⁺ T cells, CD4⁺ T cells, and T_{regs} from spleens. B-E) Median fluorescence intensity (MFI) on lymphocytes from spleens (B, D) or tumors (C, E) of mice with TuBo (B&C) and 4T1 (D&E) tumors. F. Representative histogram of PD-L1 expression from CD3- CD11b- cells in TuBo tumors. G. MFI of PD-L1 on CD11b- CD3- cells from TuBo tumors. Statistical analysis was performed using one-way ANOVA where data was shown to be parametric, or Kruskal-Wallis testing when data was non-parametric with Dunnett's or Dunn's multiple comparisons test, respectively; *p<0.05, **p<0.01, ***p<0.001, ****p<0.0001. Data points represent individual mice in B-E & G with error bars denoting 95% CIs.

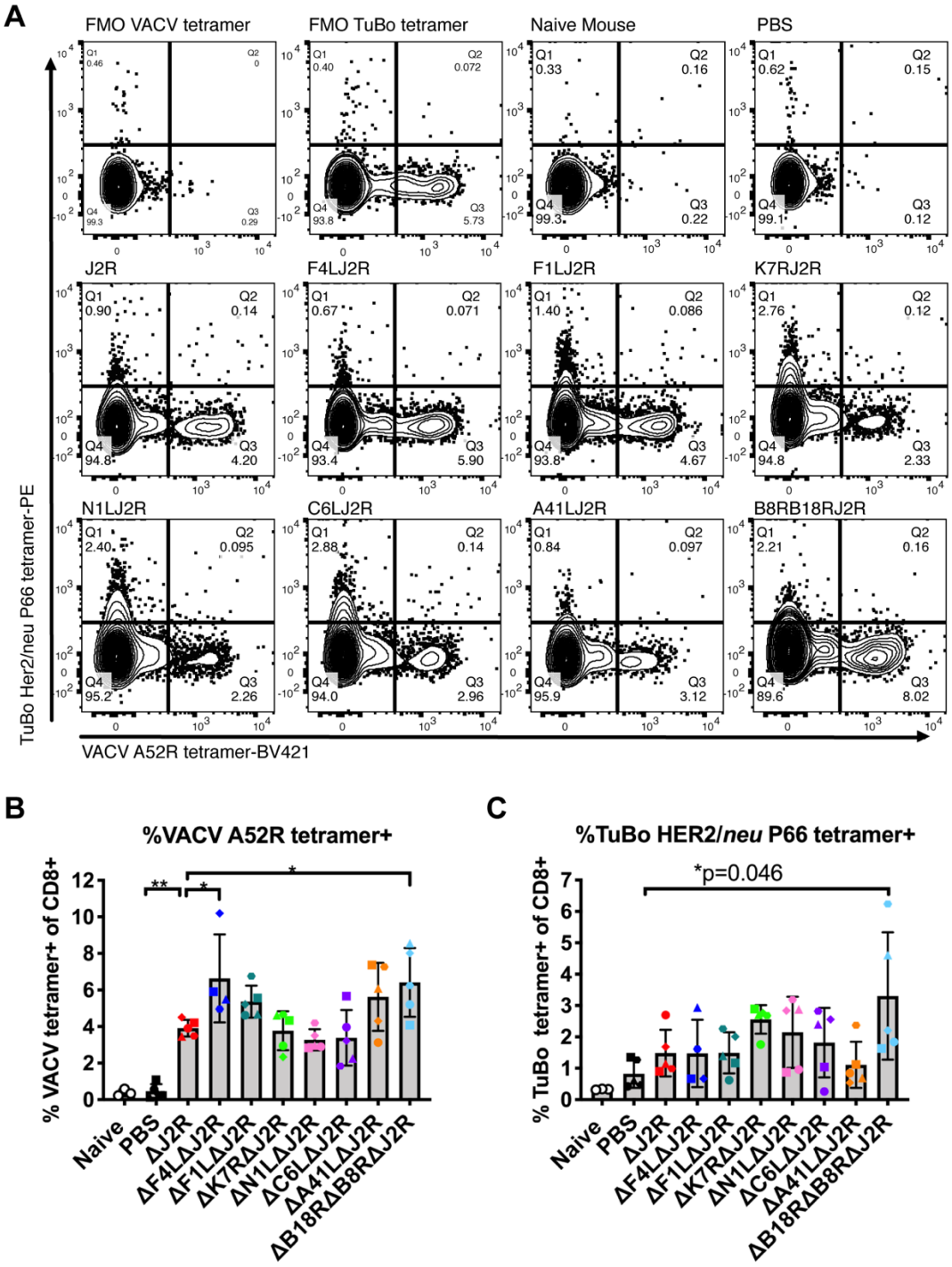

Figure 7.5. Modifications to the VACV genome altered antigen-specific T cell responses against tumor and virus A.

Representative flow plots of splenocytes stained with $H2K^d$ tetramers specific for p66 HER2/*neu* of TuBo tumors (y-axis) and A52R of VACV (x-axis). Representative flow plots selected for sample with median value of p66 staining. B, C. Frequency of tetramer+ $CD8^+$ T cells as described in (A) where each symbol represents one mouse. Error bars denote 95% CIs from mean values. Statistical significance determined using one-way ANOVA with Dunnett's multiple comparisons testing. FMO- fluorescence minus one gating control.

7.2.3 Mutant VACVs alter ratios of T cells directed at viral and tumour epitopes

A primary goal of virotherapy is to increase antitumor immunity while limiting anti-viral immunity. We used H2-K^d-restricted tetramers, specific for CD8+ T cells recognizing immunodominant epitopes of TuBo tumors and vaccinia virus, to determine if these VACV mutations altered the percentages of antitumor versus anti-viral splenic $CD8^+$ T cells (Figure 7.5A). Specifically these experiments were designed to detect $CD8^+$ T-cells recognizing the p66 rat HER2/*neu* or VACV A52R peptides[327,328]. The PBS-treated mice exhibited a small increase in the percentage of p66 HER2/*neu* specific $CD8^+$ T cells compared to mice that had not encountered tumor; 0.83% compared to 0.33% respectively (Figure 7.5B). This basal frequency of tumor-targeting T cells was not unexpected and may have explained why some tumor regression was seen even in PBS treated controls. All of the virus treatments further increased these percentages of tumor-targeting T cells, with averages ranging from 1.1% of CD8+ T cells after ΔA41LΔJ2R treatment to 3.3% after ΔB8RB18RΔJ2R virus treatment. When compared to the parental ΔJ2R virus, the ΔK7RΔJ2R and ΔB8R18RΔJ2R mutants most improved the percentage of p66 HER2/*neu* targeting T cells with the latter treatment invoking a statistically significant 3-fold increase relative to mice treated with VACV ΔJ2R (Figure 7.5B).

All of these virus treatments enhanced $CD8^+$ T cell responses to the VACV A52R tetramer with no background (<0.2%) detected in naïve and PBS-treated animals (Figure 7.5C). Treatment with the ΔB8RΔB18RΔJ2R mutant significantly increased these percentages relative to VACV ΔJ2R treatments. This suggests that this virus was perhaps the most immunogenic of all the mutants tested, as it increased the percentage of T cells targeting both the tumor *and* viral antigens. A significant increase in antiviral $CD8^+$ T cell responses was also seen in animals treated with VACV ΔF4LΔJ2R relative to VACV ΔJ2R treatment (Figure 7.5C) although without inducing a parallel increase in p66 HER2/*neu* specific T cell percentages (Figure 7.5B). The same trend was also seen in animals treated with VACV ΔA41LΔJ2R. The greatest (ΔB8RΔB18RΔJ2R) and least (ΔF4LΔJ2R; ΔA41LΔJ2R) numbers of long-term survivors were seen when comparing these viruses, pointing again to the critical value of balancing antitumor and anti-viral cellular immune response.

7.2.4 Mutant VACVs alter circulating serum cytokines

To assess systemic impacts of tumour-infection with the mutant oncolytic viruses, blood was collected from treated mice three weeks after the final virus injection in TuBo tumours. Serum was collected and cytokines were assessed by Eve technologies (Calgary, Canada) and reported as concentrations per mL of serum. To compare how intratumoral virus treatments caused systemic changes in circulating serum cytokines, I assessed the fold change in serum levels of cytokines compared to PBS-treated mice (Figure 7.6A). Most cytokines were reduced after virus treatment compared to PBS (Figure 7.6A). Importantly, statistical significance between treatment groups was only found in two cytokines, LIX (Figure 7.6B) and G-CSF (Figure 7.6C). Mice treated with VACV ΔK7RΔJ2R exhibited reduced neutrophil-recruiting cytokine LIX (CXCL5) in serum, compared to mice treated with ΔJ2R (Figure 7.6B). The presence

of VACV, independent of deletions, caused a significant reduction in G-CSF (Figure 7.6C). which was associated with a reduction of granulocytes in the spleens of VACV-treated mice, and an overall increase in monocytes (Figure 7.6).

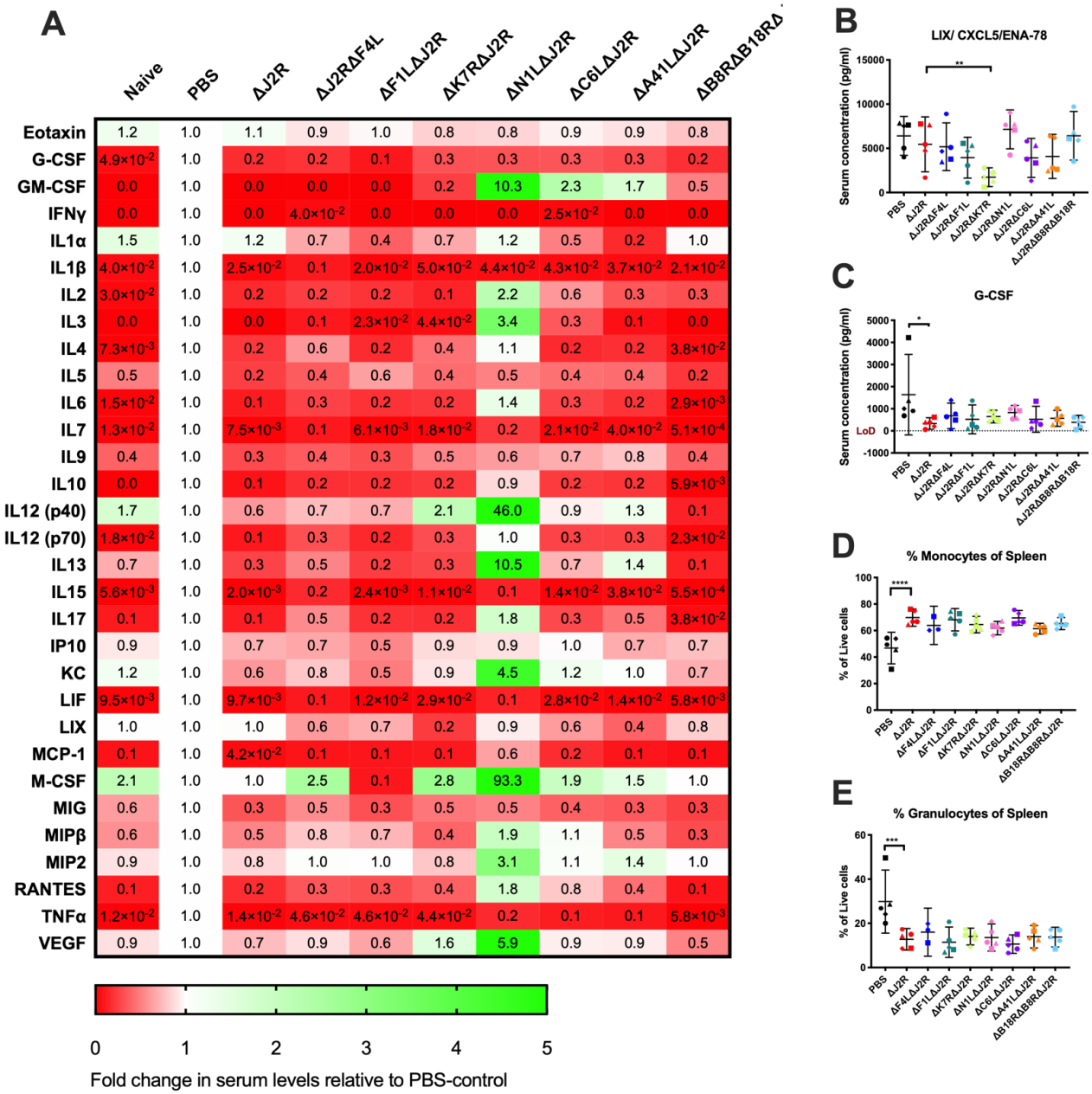

Figure 7.6. Immunogenic gene deletions altered the levels of cytokines in the serum of mice after treatment of TuBo tumours with oncolytic VACVs. A. Average fold change compared to untreated (PBS) TuBo tumours in levels of circulating serum cytokines three weeks post virus treatment. B&C. Serum cytokines where statistically significant alterations were observed between groups relative to ΔJ2R VACV treatment for LIX (B) and G-CSF (C). (D&E)Percentage of monocytes (D)and granulocytes (E) in spleens assessed by fsc-a and ssc-a characteristics. Statistical analysis was performed using one-way ANOVA where data was shown to be parametric, or Kruskal-Wallis testing when data was non-parametric with Dunnett's or Dunn's multiple comparisons test, respectively; *p<0.05, **p<0.01, ***p<0.001, ****p<0.0001. Data points represent individual mice with error bars denoting 95% CIs from the mean.

7.3 Discussion

Numerous oncolytic VACVs have been developed that harbour deletions of various viral genes[12], and many target genes have been suggested for removal from VACV to increase antitumor immunity, as was discussed in the previous chapter[12]. To our knowledge, however, there have been no systematic attempts at deciphering which gene deletions have an impact on a tumor bearing host, and what the relative contribution of gene removal has in the overall immune response against the virus in this context. In this chapter, we sought to decipher how removal of genes from the VACV genome could impact immune cells and systemic effects in the TME post-oncolytic virus treatment. We removed eight different genes from VACV and compared the effects of these deletions in head-to-head comparisons in immune-competent breast tumor models.

Removing individual genes from the VACV genome did indeed have the capacity to induce sustained changes to the TME that persist up to three weeks after the final administration of virus in the TuBo tumour model, and two weeks in the 4T1 tumour model. The presence of virus alone was capable of altering the overall immune cell composition in spleens and tumors. However, there did not appear to be drastic alterations between viruses where immune-modulating genes had been removed (with the exception of ΔF4LΔJ2R which showed decreased immune cells in the tumor overall). Rather, removing immune-modulating genes had more subtle effects on different cellular parameters, for instance, by improving the percentages of tumor antigen specific $CD8^+$ T cells, or upregulating PD-1 expression on $CD8^+$ T cells. In considering this information, rather than using immune-modulating gene deletions to cause drastic changes in the response to virotherapy, these deletions might be better suited for refining and fine-tuning immune responses to achieve a particular outcome. For instance, ΔB8RΔB18RΔJ2R increased tumor-specific $CD8^+$ T cell percentages and increased PD-1 expression, thus a combination of this particular gene-deleted virus with PD-1 checkpoint blockade may be particularly beneficial. In agreement with this notion, a B18R-deleted virus on its own demonstrates significant survival benefits when combined with anti-CTLA4[343], but perhaps anti-PD-1 may be more therapeutically beneficial in this context.

This echoes the idea that immunotherapy can be used to make 'cold tumours hot'[202]. As an example, for instance, in knowing that treatment with ΔB8RΔB18RΔJ2R increases PD-1 on the surface of CD8+ T cells, the tumours may now be more susceptible to checkpoint blockade with anti-PD-1 antibody, or that most virus treatment resulted in an increase of PMN-MDSCs within the tumour, MDSC inhibition is a rational combination target. It also suggests to us that although changes to the oncolytic VACV backbone by removal of immunomodulatory genes does indeed have the capacity to reprogram the tumour microenvironment, the continued use of therapeutic transgene or tumour antigen insertion will further benefit virotherapy.

We also observed that many viral-induced changes were similar in trend in both models tested, however the magnitude of the changes was more pronounced in our immunogenic TuBo tumour model compared to the non-

immunogenic 4T1 tumour model. An example is the general observation that virotherapy, independent of which virus mutant was used, increased CD8+ T cells in the tumour and decreased Tregs, but the changes were more drastic in TuBo tumours than 4T1 tumours. However, the most statistically significant improvements in survival were observed after treatment with our modified viruses in the 4T1 model even though these immunogenic alterations were more modest. This suggests the possibility that minor tweaks to the virus genome used to manipulate the TME even slightly may be more beneficial in non-immunogenic tumour models compared to tumours which are more susceptible to more drastic changes caused by treatment. Previous correlations have been found between oncolytic virus therapy and the immunogenicity of tumour models used in breast cancer models.

In instances where subtle improvements were observed in therapeutic efficacy but yet no significant or immediately apparent TME changes were observed relative to ΔJ2R treatment, as for instance was the case after treatment with ΔC6LΔJ2R, it is possible that changes were observed in other cell types that were not assayed such as natural killer (NK) cells, or B cells, or perhaps changes were not immune-cell mediated but possibly by other TME factors like vasculature changes or innate immune signalling. A recent study demonstrated that the efficacy of ΔN1LΔJ2R VACV treatment for treating flank lung tumour models was dependent on NK cells, suggesting this cell type should be explored further[344].

Although no viruses stood out as demonstrating a drastic survival benefit compared to the ΔJ2R virus deletion on its own, there were a few candidates that warrant further analysis based on improvements in median survival, complete response rates and immune stimulation. In particular, ΔB8RΔB18RΔJ2R was shown to increase anti-tumour CD8+ T cell percentages. It also demonstrated the highest median survival and 50% of mice showed long-term progression free survival with functional anti-tumour immunity. The Jennerex oncolytic VACV pipeline virus JX-795 candidate harbours a mutation in the B18R gene that may impart improved characteristics compared to a candidate where B18R is intact[162,350]. Other virus deletions also warrant additional attention. Although ΔC6LΔJ2R did not cause many drastic changes to the TME in our immunology studies, it appeared to cause the most drastic delay in tumour growth in the TuBo tumour model and demonstrated the most favorable Kaplan-Meir survival curve. In our 4T1 tumour model, this virus also had the least metastatic lesions on the lungs after 12 weeks of treatment. ΔC6L, along with ΔN1L also were the most beneficial viruses for use in the 4T1 tumour model and resulted in the most significant enhancement of survival.

Chapter 8: General discussion and future directions

8.1 General summary and key findings

The methods of enhancing the efficacy of oncolytic VACV for breast cancer treatment explored in this thesis provide a number of contributions to improve efficacy and present further opportunities for exploration.

With respect to viral manufacturing, we have shown that VACV can be grown to high levels and can be produced with sufficient purity for use in preclinical breast cancer models. This project was established due to issues encountered in initial pre-clinical studies where it was observed that the poor quality of virus preparations was contributing to toxicity in our mouse models of breast cancer. To circumvent these issues, we modified the virus preparation and purification procedure to improve the consistency of virus preparations. This was followed up by performing dose escalation experiments to ensure appropriate dosing was being delivered to our animal models by establishing the maximum tolerable dosing limits. The flow virometry protocol optimized to assess particle to PFU ratios using SYBRGold staining can also be used in other research purposes, such as determining defective virus particle production by VACV.

The primary objective of this dissertation was to improve the efficacy of VACV-mediated immunotherapy in breast cancer models. The first method tested to increase efficacy was by combining oncolytic ΔF4LΔJ2R therapy with IG-RT radiation. This combination, however, was unsuccessful and efficacy was actually reduced when combined with radiation therapy compared to radiation alone. This occurred despite increased CD8+ T cells in tumours. While PD-1 and PD-L1 were elevated in the TME, checkpoint inhibition with anti-PD1 therapy did not alter outcomes, suggesting antagonism was not due to immune exhaustion. These results are summarized in Figure 8.1. Although we could not determine the exact mechanism of antagonism, the contributions of these observations towards the understanding of immunotherapeutic drug interactions cannot be understated. It emphasizes the importance of thoroughly investigating drug combinations in preclinical models prior to introduction in a human setting.

The second strategy assessed for increasing the efficacy of virotherapy by deletion of immunomodulatory factors from the VACV genome yielded promising results. The results from this project suggested that deletion of VACV genes responsible for inhibiting interferon signalling in some capacity were ideal targets to mutate to improve efficacy and appeared to correlate with increased T-cell responses against cancer epitopes, as summarized in Figure 8.2. In particular, the ΔB8RΔB18RΔJ2R virus, in which we have removed genes that produce proteins that inhibit IFNs directly as decoy receptors, showed the most promise for improving oncolytic efficacy. It appeared that this pathway and gene deletion were superior compared to other deletions that did not inhibit innate detection/ interferon signalling. Our results suggest that a ΔB8RΔB18RΔJ2R backbone is a good candidate to build the next generation of oncolytic VACVs to further improve the efficacy of oncolytic VACV therapy for breast cancer.

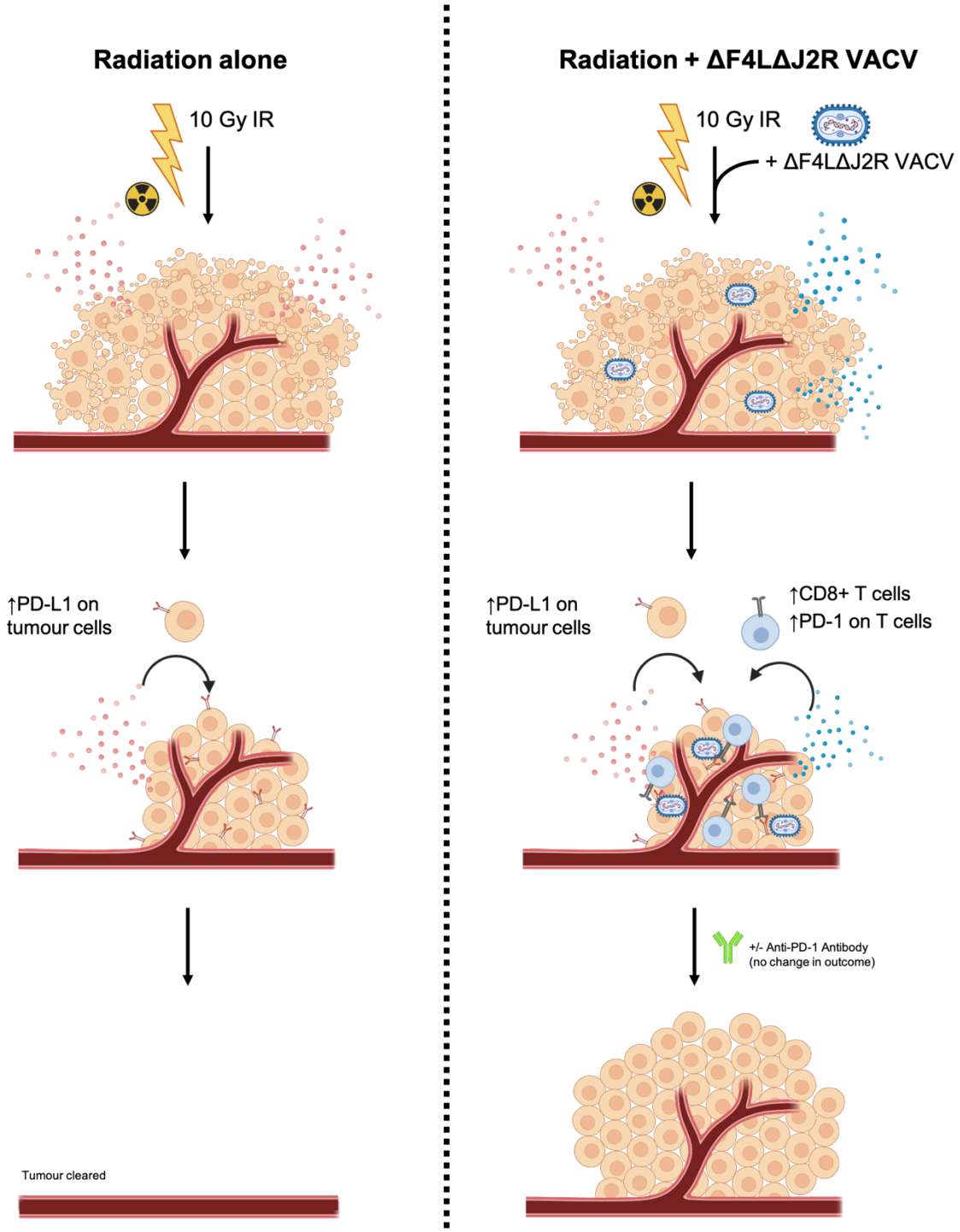

Figure 8.1. Summary of investigations into combining ΔF4LΔJ2R VACV with IG-RT in breast cancer models. Radiation treatment alone (left) and combining radiation and ΔF4LΔJ2R VACV (right). Both treatments reduced tumour size, which was accompanied by an increase in CD8+ T cells in the combination group, and an increase in PD-1 on these CD8+ T cells (middle right). Both groups increased PD-L1 expression on tumour cells. Despite this, checkpoint blockade failed to reverse the antagonistic response, and combination-treated tumours recurred.

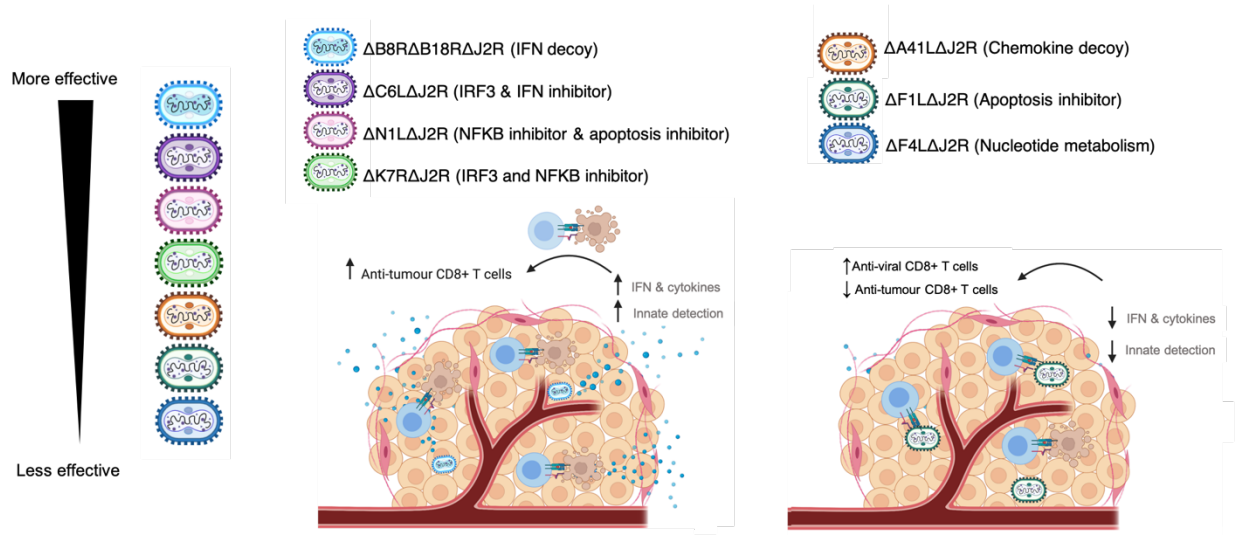

Figure 8.2. Summary of studies investigating the removal of immunomodulatory genes to improve VACV virotherapy. More effective VACVs corresponded with deletions of VACV proteins that impede IFN responses (left), whereas less effective viruses had IFN inhibitors intact (right). Grey text- hypothesized responses, black text- analyzed responses.

8.2 Experimental approach to testing oncolytic VACV therapy in breast cancer models

8.2.1 *In vitro* assays for virotherapy studies

Results from this study may help inform how future studies assess oncolytic potency in research. Traditionally, *in vitro* viral replicative characteristics have been used to assess the suitability of virus candidates for OV therapy. This is a common *in vitro* assessment that draws parallels between viral replication and therapeutic effectiveness. However, throughout these studies, we have demonstrated that this approach may not be particularly informative as a predicted measure of efficacy, as we noted no trends which suggested that virus replication impacted treatment outcomes. *In vitro*, ΔF4LΔJ2R and ΔB8RΔB18RΔJ2R yielded the lowest titers in TuBo cells *at* 72 hours post-infection. ΔF4LΔJ2R and ΔB8RΔB18RΔJ2R were also not detectable in TuBo tumours three weeks post-infection, while all other viruses were present at detectable levels. These two viruses yielded the highest percentage of VACV A52R-targeting CD8+ T cells, whereas only ΔB8RΔB18RΔJ2R had the highest percentage of tumour-targeting p66 HER2/*neu* tetramer+ CD8+ T cells. ΔB8RΔB18RΔJ2R also had the highest incidence of complete responses and caused the longed median survival time in the TuBo model. Contrarily, ΔK7RΔJ2R had no changes in virus replication *in vitro* or *in vivo*, did not alter the percentage of A52R-targetting CD8+ T cell percentages, yet did increase p66 HER2/*neu* anti-cancer CD8+ T cell percentages relative to ΔJ2R VACV. This demonstrates that viral replicative properties do not dictate anti-tumour immune responses. This observation is in agreement with previous oncolytic virus studies performed with herpes simplex virus, which suggest that *in vitro* replication viruses does not necessarily predict *in vivo* efficacy[319]. While markers of immunogenic cell death, such as HMGB-1 and ATP release are thought to be predictive *in vitro* indicators of immune responses[342], similar to our *in vitro* replication assays we observed no parallels between ATP & HMGB-1 release and immune stimulation. One caveat of our analysis is that to be classified as bona-fide ICD, calreticulin exposure at the cell surface is the third necessary marker, and we were unable to produce calreticulin exposure at the

cell surface with known ICD inducers mitoxantrone and doxorubicin[342], thus we were unable to determine if this critical third marker was present after VACV treatment.

The misleading results of *in vitro* studies was best exemplified in our combination therapy project. Results from our cell viability assays in assessing the combination of radiation with ΔF4LΔJ2R VACV were in direct contradiction to *in vivo* results and demonstrated a stark difference in predicted outcomes. While *in vitro* assays do have utility in assessing virus tropism /infectibility of cell types, replication and direct oncolysis, these assays are not a suitable replacement for *in vivo* studies, and our results underline the need to test therapies in both systems. These discrepancies between *in vitro* and *in vivo* results with our OV VACV candidates is perhaps not surprising given the complex and multi-mechanistic action of OVs and complexities of the TME. It was found that breast cancer three-dimensional cultures were more resistant to cell killing by HSV-1 than monolayer cultures due to the extracellular matrix impeding efficient spread[351]. Future studies could use three-dimensional spheroid cultures to better assess these physical constraints[144]. While direct tumour cell killing is indeed an important aspect of the mechanism of action, immune stimulation is becoming increasing recognized as a dominant driver of how well these viruses perform in pre-clinical models[319,320]. While oncolysis has been suggested to be a critical factor in the late phase of tumour regression[271], studies assessing inactivated Modified-vaccinia virus Ankara (MVA), which is a non-replicating VACV vector containing major genomic deletions, have shown that virus replication/tumour oncolysis is not necessary to achieve therapeutic benefits and in some instances might be more effective than live virus[295]. In assessing different *in vivo* tumour models infected with a TK-deleted oncolytic VACV, Hou *et al.*, observed that the efficacy of therapy in relation to early gene expression (and therefore virus replication) differed between tumour models[341]. In resistant tumour lines where virotherapy was shown to be less effective, early replication correlated with better responses. However, in susceptible cell lines where there were more significant improvements in treatment outcome, rapid and robust clearance of the virus was the common factor for the best responders to treatment[341]. Nevertheless, these complex interactions between different cells and molecules within the TME cannot be accurately recapitulated *in vitro*, and as such there is no true replacement for *in vivo* testing.

8.2.2 *In vivo* breast cancer models

Although orthotopic syngeneic murine mammary tumour models are more clinically relevant than *in vitro* assessments, they still have shortcomings when compared to human studies[352]. The tumour heterogeneity of breast cancer and the different molecular subtypes in humans are difficult to replicate in murine models[353,354]. In the current study we used the orthotopic syngeneic mouse models, TuBo and 4T1, which are useful for recapitulating non-metastatic HER/neu+ and TNBC, respectively[232,237]. Opting for orthotopic as opposed to subcutaneous ectopic injection is more representative of the human breast tumour microenvironment, representing the fatty tumour microenvironment, vasculature, cell infiltration and other native characteristics that are not apparent in ectopic tumours[354–356]. Nevertheless, it is important to recognize that the architecture of the human breast varies compared

to rodent mammary fat pads[357]. While using immortalized and passaged murine cell lines has the benefit of consistent tumour growth characteristics and ease of use, sequential passaging of cell lines gives rise to *in vitro* adaptations, but most importantly the implanted cells are homogenous in origin which does not represent the complex tumour heterogeneity observed in patients[353]. Alternatives to these systems include genetically engineered mouse models and humanized mouse models. While costly, genetically engineered models are able to mimic spontaneously arising tumours and are considered more scientifically representative of disease progression than passaged and implanted cell lines[353,354,358]. These models also eliminate the need to use Matrigel basement membrane, and limit the use of isoflurane and other anaesthetics during tumour establishment procedures which are additional factors to consider that may impact studies[359,360]. However, large numbers of mice must be bred to get consistent group sizes, and treatment schedules may be sporadic depending on the time of tumour development. Humanized mouse models are another option gaining traction, particularly in the immunotherapy community. In these studies, immune deficient mice are implanted with patient tumour samples, and the mouse immune system is reconstituted with human immune cells to better represent both human tumours and human immune cells[361,362]. While cost and complexity has limited widespread use of humanized mouse models, they represent another model to study these drugs and interactions for future studies that might better predict patient outcomes.

8.3 VACV and combination therapy

Previous studies have reported benefits to OV therapy when combined with radiation[166,167,266–268]. Our results demonstrating antagonism were unexpected, but interesting. These results present opportunities to uncover the mechanistic details between how therapies interact and is a unique demonstration of antagonism between two therapies. While our efforts focused on investigating the TiME to uncover insights behind the antagonism, we were unable to determine the cause. However, further studies can help narrow down what might be contributing to these effects. For instance, we do not know definitively that the immune system is involved. While studies in immunodeficient mice may help to provide further insights, we know from previous investigations in the laboratory of Dr. Mary Hitt that ΔF4LΔJ2R is curative as single-agent therapy at low doses in nude mice[144]. This presents a challenge since single agent therapy is curative, we do not have a window where antagonism might become apparent. To circumvent this challenge, depletion experiments could be performed. By using antibodies or drugs to deplete CD8, CD4, MDSC or other immune cells, we might be able to narrow down if a certain cell type is contributing to these negative effects. As we only assessed a limited array of immune cells and checkpoint molecules in these studies, it remains to be determined if the immune system does indeed play a role. NK cells, DCs, tumour-associated macrophages, among others could also be assayed. Using innovative research methodology such as single cell sequencing[363], or mass cytometry (CyTOF) testing[364] would enable a more comprehensive and intricate assessment of the immune system in these studies.

We also still do not know if the antagonism is limited to ΔF4LΔJ2R VACV. By trying different viral mutants, we might be able to see differences in study results. An obvious avenue to explore would be the replacement of ΔF4LΔJ2R VACV with ΔB8RΔB18RΔJ2R VACV in these combination therapy studies. This would allow us to determine if this feature is common to multiple VACVs in orthotopic murine tumour models. While other studies with VACV and radiation have not demonstrated antagonism, the differences in protocols, tumour models, radiation delivery, and virus modifications make comparisons between studies difficult. By keeping the tumour model consistent (orthotopic syngeneic mammary fat pad models), we could also test if other OVs contribute to similar outcomes. For instance, oncolytic reovirus could be trialled in an identical system to determine how widespread this antagonism might be with respect to different viruses.

While we assessed a combination of ionizing radiation with ΔF4LΔJ2R VACV, other therapeutic combinations could be tested in breast cancer models. Although we tested triple combination therapy by adding in immune checkpoint blockade with anti-PD-1 therapy to mice previously treated with both IG-RT and VACV, we could test VACV in combination with ICI only, without radiation. This would be anticipated to yield favourable results, as numerous studies have shown drastic therapeutic advancements by combining OVs with ICI. The success of this approach is in large part due to the ability of OVs to turn "cold" (non-inflamed) tumours "hot" by causing T cell recruitment and immune stimulation, giving the ICI a target within the direct TME to exert action on. Vaccinia has also been used in combination with CAR-T therapy [365], with other oncolytic viruses[366], and with cancer vaccines[367]. Chemotherapy is another obvious choice for combination therapy[368], however the systemic toxic effects of chemotherapies on normal cells is still a challenge. If a combination of approaches allows for dose reduction of chemotherapy to be used, this would be a valid treatment strategy and should be assessed further.

8.4 Designing the next generation of VACV oncolytics

8.4.1 Viral gene deletion

In a recent review, Guo *et al.* identified areas of research for improvement of oncolytic VACV virotherapy which included further modification of VACV viral vectors for improved immunogenicity, arming VACVs with genes and neoantigens, and use in combination with different therapies. With respect to deletion of immunomodulatory genes, Guo *et al.* identified a list of 20 candidate viral genes that represented "high priority" targets for removal to enhance viral vector immunogenicity[12]. Coincidentally, all target genes removed in our immunotherapy studies, F1L, N1L, K7R, C6L, A41L, B8R and B18R were included on this list, demonstrating the value of the contribution of these studies to the advancement of understanding VACV immunomodulation and viral oncolysis. Nevertheless, we only investigated 7 out of 20 candidate genes suggested, and therefore more opportunities remain for therapeutic enhancement. Furthermore, as new immunomodulatory functions of different VACV proteins continue to be uncovered, this presents additional opportunities to further modify the backbone of VACV to enhance antitumour effects. In 2019, it was discovered that the secreted M2 protein of VACV, in addition to its role as an NF-κB inhibitor[60], works to sabotage T

cell activation by binding to CD80 and CD86 to prevent T cell co-stimulation[61,369]. This was a unique discovery, given that most VACV proteins at this time have been demonstrated to act on innate immune pathways. This protein revealed that direct inhibitors of T cell activation exist within VACV, which had previously only been uncovered in other orthopoxviruses[370]. Furthermore, it was found that the M2 protein potentiates binding of CD80 to PD-L1[61]. With the mounting body of evidence demonstrating the importance of the CD80/CD28 signalling axis in T cell stimulation, and the inhibition of anti-tumour immune responses with CTLA-4, M2 represents a key immune-modulatory protein whose deletion might directly impact T cell responses to OV therapy.

In future studies it will be beneficial to assess if a combination of multiple deletions of these proposed gene-targets further enhances oncolytic efficacy. For instance, based on the current study we would propose a virus with multiple deletions of ΔB8R, ΔB18R, ΔC6L and ΔN1L. However, there are a few *caveats* with this strategy. One study investigating VACV as a vaccine vector found that ΔK7R, ΔN1L and ΔC6L gene deletions on their own increased immune responses against viral epitopes. However, when a triple-deleted mutant was created, immune responses were lessened, presumably due to enhanced viral clearance which hindered the host's ability to mount a sufficient immune response[164]. It will be interesting to determine if the same effect would be true in a tumour microenvironment. An appropriate balance must be found between immunogenic gene removal and enhanced viral clearance to maximize therapeutic efficacy. The second challenge when considering combining multiple deletions stems from a construction perspective. Creation of a virus with multiple gene targets categorically deleted would be challenging using the traditional targeted methods utilized in this study, as we are limited based on the number of combinations of selectable markers used to isolate our desired viruses and limited by the number of *lox*P sites a virus can contain without major genomic rearrangements. Although this strategy is challenging, it should be noted here that a previous study reported on the use of an oncolytic VACV with deletions in A48R, B18R, C11R and J2R demonstrating that such a virus is possible to selectively manufacture[160]. With the recent advent of new synthetic biology approaches the tools now exist to create 'designer' viruses with any variety of genetic changes desired, and do not have the same limitations as traditional cloning described above[291].

While we used a targeted strategy to remove immunomodulatory genes from VACV, other groups have used a technique known as directed evolution[10]. In this process, VACV is serially passaged in cancer cells to evolve the virus, resulting in large genomic deletions. This same process was used in the production of modified vaccinia virus Ankara (MVA), a highly attenuated VACV strain that no longer replicates in human cells due to serial passage in chicken embryonic fibroblasts. Similarly, directed evolution can be attained by co-infection of multiple VACV strains allowing for virus recombination to yield mixed chimeric viruses with genomic elements of all strains[10,150].

8.4.2 VACV-encoded transgenes

As previously discussed, the encoding of cytokines or other immune-stimulating factors by OVs is another strategy used in increase the effectiveness of therapy. As such, an avenue of exploration to consider for future projects is by encoding therapeutic molecules in the virus genome[162,275,371,372]. One *caveat* to encoding cytokines within the virus is the toxicity of high levels of systemic immunostimulatory molecules. For example, high levels of IL-2 or IL-12 have resulted in toxicity and adverse outcomes in clinical trials[373–376]. Creative ways to circumvent these systemic effects have been explored by tethering these molecules to the cell surface and restricting cytokine expression to the TME[376,377]. The addition of tumour antigens encoded within the virus genome also enhance the cancer vaccine properties of OVs, as has been investigated by the encoding of HER2 within with in a GM-CSF expressing VACV[155]. Other approaches include apoptosis inducing agents such as a TRAIL-armed TK deleted VACV[378], microRNAs[379], bi-specific T-cell engagers[159], enzymes that reduce suppressive cell types within the TME[380] and APC-activating ligands[381].

While deletion of immunogenic genes proved to be an effective method for increasing the potency of OV therapy, the addition of the other elements discussed (encoding therapeutic payloads, use in combination therapy) is the ideal way to produce a clinically useful oncolytic candidate. Research in the Evans laboratory has already started to build the next generation of oncolytic VACV using results obtained in these studies. Using the ΔB8RΔB18RΔB18R virus as a starting point, additional enhancements to the virus could be implemented by encoding novel molecules into the virus genome. With synthetic biology advances it will now be easier to rapidly create viruses with multiple gene deletions in addition to therapeutic gene insertion and the expression of antigenic targets[291]. The possibilities are essentially limitless for what can be encoded within the virus, as it can accommodate insertions of up to 25 kbp[130]. This flexibility permits VACV to be used as a therapeutic "toolbox" where elements can be deleted, modified, added and manipulated to create the desired effect within the TME.

8.5 VACV and breast cancer

The primary focus of this investigation was to increase the efficacy of oncolytic VACV for treating breast cancer models. While we were able to show that we could increase median survival in the TuBo orthotopic syngeneic breast cancer models using a modified ΔB8RΔB18RΔJ2R VACV to 192 days and 50% complete responses, the most successful therapy was IG-RT alone where median survival was >200 days with 73% complete responses. Other groups have reported varying levels of success using different VACV mutants to treat breast tumour models[269–279]. The breast tumour model systems in these studies vary from immune-competent to immune-deficient, in subcutaneous flank models as opposed to orthotopic mammary fat pad models, with some in mouse and canine models of breast cancer, and varying viral delivery methods of intravenous compared to intratumoural[269–279]. While these differences in study protocols make it difficult to draw comparisons between studies and to compare with our results, they do demonstrate the potential of VACV to treat breast cancer. Another important consideration is that in these studies the virus has been armed with additional factors to improve immunogenicity, again highlighting the utility of this approach. While

we did see improvements using unarmed VACV is seems that encoding additional factors is necessary for efficacious treatment of breast tumours, likely in addition to combining with other therapies.

Previous work in the laboratory has shown that VACV is effective in treating rat and mouse models of bladder cancer[119]. Preliminary work in Dr. Hitt's laboratory has also shown ΔF4LΔJ2R VACV holds promise for treatment of glioma, with promising preclinical results obtained when combined with radiation[382]. When one considers the TME of bladder, glioma and breast tumours, all are unique in both cellular parameters and tissue environment, and it is not surprising that differences are observed between VACV treatments. Based on these observations, breast cancer appears to be more resilient to treatment with our VACV mutants, and creative combinations of all strategies proposed to enhance efficacy are likely the route forward to render breast cancers more successfully treatable using this approach. It is becoming increasingly common to combine multiple of these strategies simultaneously, and the addition of checkpoint inhibitors is regularly included in most current OV studies. A VACV with deletions in TK and VGF, expressing IL-15 with a fusion protein was combined with anti-PD-1 therapy[383]. The same VACV backbone was also used to express CXCL11 and tested in combination with anti-PD-L1 therapy[312]. JX-594, which is a VACV deleted in TK and encodes GM-CSF showed success in treating breast cancer models when combined with both anti-CTLA-4 + Anti-PD-1 therapy[384]. An oncolytic TK-deleted VACV encoding the prostaglandin-inactivating enzyme hydroxy-prostaglandin dehydrogenase 15-(NAD) (HPGD), which reduces MDSCs in the TME due to depletion of prostaglandin E2, was tested in combination with checkpoint inhibitors[341]. While we showed in these studies that radiation was not a complementary combination with ΔF4LΔJ2R VACV, as previously suggested, using a ΔB8RΔ18RΔJ2R VACV backbone and encoding other transgenes might yield different results, particularly given the importance of IFN responses in RT therapy[261]. Surgical resection of breast tumours is first-line treatment in the clinic for breast cancer, and can be recapitulated in the 4T1 tumour model[237,277]. Surgical resection, VACV treatment with an improved virus backbone and encoded transgenes, along with checkpoint inhibition could be another avenue to explore. VACV is highly amenable to genetic manipulation, and the possibilities for encoding different molecules are endless. New creative VACVs clearly hold promise for treating breast cancer and other cancer subtypes and is an exciting field for future exploration.

8.6 Conclusions

OVs have demonstrated promising results for treating various tumour types. Although VACV has not been as successful in treating breast cancer when used as a single-agent therapy compared to other cancer models, progress is being made towards improving therapeutic responses. In this thesis, we establish improved production methods of pre-clinical grade VACV that improved safety in breast cancer models by increasing the consistency of virus preparations, establishing the maximum tolerable dosing limits in our models. To directly improve the efficacy of VACV therapy, we combined ΔF4LΔJ2R with IG-RT. Despite promising results *in vitro*, the combination was antagonistic *in vivo*. We were able to ascertain that, despite increased immune stimulation caused by the presence of VACV, immune

exhaustion and upregulation of PD-1 was not the culprit for antagonism. Further studies are needed to fully understand how VACV and IG-RT interact in murine models. Our second attempt at improving the efficacy of VACV therapy focused on the deletion of immunomodulatory genes from VACV. Through immune analysis we were able to uncover that deletion of VACV genes that inhibit IFN responses can improve response rates and anti-tumour immunity in breast cancer models. Future studies in the lab will continue to build upon these results by generating new VACV with enhanced therapeutic action and functionality by deleting additional immunomodulatory genes and encoding transgenes to even further improve response rates in breast cancers.

Literature Cited

1. Skinner, M.A., Buller, R.M., Damon, I.K., Lefkowitz, E.J., McFadden, G., McInnes, C.J., Mercer, A.A., Moyer, R.W. and Upton, C. Poxviridae - dsDNA Viruses - dsDNA Viruses (2011) - International Committee on Taxonomy of Viruses (ICTV). (2019). Available at: https://talk.ictvonline.org/ictv-reports/ictv_9th_report/dsdna-viruses-2011/w/dsdna_viruses/74/poxviridae. (Accessed: 14th October 2020)
2. World Health Organization. Global Commission for the Certification of Smallpox Eradication & World Health Organization. *The global eradication of smallpox : final report of the Global Commission for the Certification of Smallpox Eradication, Geneva, December 1979*. (1980).
3. Maurer, D. M., Harrington, B. C. & Lane, M. J. *Smallpox Vaccine: Contraindications, Administration, and Adverse Reactions - American Family Physician*. *American Family Physician* **68**, (2003).
4. Blancou, J. *et al.* Oral vaccination of the fox against rabies using a live recombinant vaccinia virus. *Nature* **322**, 373–375 (1986).
5. Brochier, B. *et al.* Large-scale eradication of rabies using recombinant vaccinia-rabies vaccine. *Nature* **354**, 520–522 (1991).
6. Maki, J. *et al.* Oral vaccination of wildlife using a vaccinia-rabies-glycoprotein recombinant virus vaccine (RABORAL V-RG®): A global review. *Veterinary Research* **48**, 57 (2017).
7. Rosatte, R. *et al.* Prevalence of tetracycline and rabies virus antibody in raccoons, skunks, and foxes following aerial distribution of V-RG baits to control raccoon rabies in Ontario, Canada. *J. Wildl. Dis.* **44**, 946–964 (2008).
8. Guo, Z. S. & Bartlett, D. L. Vaccinia as a vector for gene delivery. *Expert Opinion on Biological Therapy* **4**, 901–917 (2004).
9. Peplinski, G. R., Tsung, K. & Norton, J. A. Vaccinia virus for human gene therapy. *Surgical Oncology Clinics of North America* **7**, 575–588 (1998).
10. Pelin, A., Boulton, S., Tamming, L. A., Bell, J. C. & Singaravelu, R. Engineering vaccinia virus as an immunotherapeutic battleship to overcome tumor heterogeneity. *Expert Opin. Biol. Ther.* **20**, 1083–1097 (2020).
11. Torres-Domínguez, L. E. & McFadden, G. Poxvirus oncolytic virotherapy. *Expert Opin. Biol. Ther.* **19**, 561–573 (2019).
12. Guo, Z. S. *et al.* Vaccinia virus-mediated cancer immunotherapy: cancer vaccines and oncolytics. *J. Immunother. Cancer* **7**, 6 (2019).
13. Buist, J. B. *Vaccinia and variola : a study of their history*. (London : J. & A. Churchill, 1887).
14. Carter, G. C., Law, M., Hollinshead, M. & Smith, G. L. Entry of the vaccinia virus intracellular mature virion and its interactions with glycosaminoglycans. *J. Gen. Virol.* **86**, 1279–1290 (2005).
15. Law, M., Carter, G. G., Roberts, K. L., Hollinshead, M. & Smith, G. L. Ligand-induced and nonfusogenic dissolution of a viral membrane. *Proc. Natl. Acad. Sci. U. S. A.* **103**, 5989–5994 (2006).
16. Smith, G. L. Vaccinia Virus. in *Encyclopedia of Virology* 243–250 (Elsevier Ltd, 2008). doi:10.1016/B978-012374410-4.00525-2
17. Smith, G. L., Vanderplasschen, A. & Law, M. The formation and function of extracellular enveloped vaccinia virus. *Journal of General Virology* **83**, 2915–2931 (2002).
18. Smith, G. L. *et al.* Vaccinia virus immune evasion: mechanisms, virulence and immunogenicity. *J. Gen. Virol.* **94**, 2367–92 (2013).
19. Seet, B. T. *et al.* Poxviruses and immune evasion. *Annual Review of Immunology* **21**, 377–423 (2003).
20. Fagan-Garcia, K. & Barry, M. A Vaccinia Virus Deletion Mutant Reveals the Presence of Additional Inhibitors of NF- B. *J. Virol.* **85**, 883–894 (2011).
21. Bidgood, S. & Mercer, J. Cloak and Dagger: Alternative Immune Evasion and Modulation Strategies of Poxviruses. *Viruses* **7**, 4800–4825 (2015).
22. Nelson, C., Epperson, M., Singh, S., Elliott, J. & Fremont, D. Structural Conservation and Functional Diversity of the Poxvirus Immune Evasion (PIE) Domain Superfamily. *Viruses* **7**, 4873–4893 (2015).
23. Goebel, S. J. *et al.* The complete DNA sequence of vaccinia virus. *Virology* **179**, 247–266 (1990).
24. Charles A Janeway, J., Travers, P., Walport, M. & Shlomchik, M. J. The complement system and innate immunity. (2001).
25. Isaacs, S. N., Kotwal, G. J. & Moss, B. Vaccinia virus complement-control protein prevents antibody-

dependent complement-enhanced neutralization of infectivity and contributes to virulence. *Proc. Natl. Acad. Sci. U. S. A.* **89**, 628–632 (1992).
26. Girgis, N. M. *et al.* The Vaccinia Virus Complement Control Protein Modulates Adaptive Immune Responses during Infection. *J. Virol.* **85**, 2547–2556 (2011).
27. DeHaven, B. C. *et al.* Poxvirus Complement Control Proteins Are Expressed on the Cell Surface through an Intermolecular Disulfide Bridge with the Viral A56 Protein. *J. Virol.* **84**, 11245–11254 (2010).
28. Engelstad, M., Howard, S. T. & Smith, G. L. A constitutively expressed vaccinia gene encodes a 42-kDa glycoprotein related to complement control factors that forms part of the extracellular virus envelope. *Virology* **188**, 801–810 (1992).
29. Takahashi-Nishimaki, F., Funahashi, S. I., Miki, K., Hashizume, S. & Sugimoto, M. Regulation of plaque size and host range by a vaccinia virus gene related to complement system proteins. *Virology* **181**, 158–164 (1991).
30. Brandt, T. A. & Jacobs, B. L. Both Carboxy- and Amino-Terminal Domains of the Vaccinia Virus Interferon Resistance Gene, E3L, Are Required for Pathogenesis in a Mouse Model. *J. Virol.* **75**, 850–856 (2001).
31. Chang, H. W., Uribe, L. H. & Jacobs, B. L. Rescue of vaccinia virus lacking the E3L gene by mutants of E3L. *J. Virol.* **69**, (1995).
32. Rivas, C., Gil, J., Mělková, Z., Esteban, M. & Díaz-Guerra, M. Vaccinia virus E3L protein is an inhibitor of the interferon (IFN)- induced 2-5A synthetase enzyme. *Virology* **243**, 406–414 (1998).
33. García, M. A., Guerra, S., Gil, J., Jimenez, V. & Esteban, M. Anti-apoptotic and oncogenic properties of the dsRNA-binding protein of vaccinia virus, E3L. *Oncogene* **21**, 8379–8387 (2002).
34. Smith, E. J., Marié, I., Prakash, A., García-Sastre, A. & Levy, D. E. IRF3 and IRF7 Phosphorylation in Virus-infected Cells Does Not Require Double-stranded RNA-dependent Protein Kinase R or IκB Kinase but is Blocked by Vaccinia Virus E3L Protein. *J. Biol. Chem.* **276**, 8951–8957 (2001).
35. Myskiw, C., Arsenio, J., van Bruggen, R., Deschambault, Y. & Cao, J. Vaccinia Virus E3 Suppresses Expression of Diverse Cytokines through Inhibition of the PKR, NF-κB, and IRF3 Pathways. *J. Virol.* **83**, 6757–6768 (2009).
36. Bowie, A. *et al.* A46R and A52R from vaccinia virus are antagonists of host IL-1 and toll-like receptor signaling. *Proc. Natl. Acad. Sci. U. S. A.* **97**, 10162–10167 (2000).
37. Fedosyuk, S. *et al.* Vaccinia virus immunomodulator A46: A lipid and protein-binding scaffold for sequestering host TIR-domain proteins. *PLoS Pathog.* **12**, (2016).
38. Stack, J. *et al.* Vaccinia virus protein A46R targets multiple Toll-like-interleukin-1 receptor adaptors and contributes to virulence. *J. Exp. Med.* **201**, 1007–1018 (2005).
39. Perdiguero, B. *et al.* Deletion of the Vaccinia Virus Gene A46R, Encoding for an Inhibitor of TLR Signalling, Is an Effective Approach to Enhance the Immunogenicity in Mice of the HIV/AIDS Vaccine Candidate NYVAC-C. *PLoS One* **8**, e74831 (2013).
40. Eaglesham, J. B., Pan, Y., Kupper, T. S. & Kranzusch, P. J. Viral and metazoan poxins are cGAMP-specific nucleases that restrict cGAS–STING signalling. *Nature* **566**, 259–263 (2019).
41. de Motes, C. M. & Smith, G. L. Vaccinia virus protein A49 activates wnt signalling by targetting the E3 ligase β-TrCP. *Journal of General Virology* **98**, 3086–3092 (2017).
42. Mansur, D. S. *et al.* Poxvirus Targeting of E3 Ligase β-TrCP by Molecular Mimicry: A Mechanism to Inhibit NF-κB Activation and Promote Immune Evasion and Virulence. *PLoS Pathog.* **9**, (2013).
43. Neidel, S., Ren, H., Torres, A. A. & Smith, G. L. NF-κB activation is a turn on for vaccinia virus phosphoprotein A49 to turn off NF-κB activation. *Proc. Natl. Acad. Sci. U. S. A.* **116**, 5699–5704 (2019).
44. Pallett, M. A. *et al.* Vaccinia Virus BBK E3 Ligase Adaptor A55 Targets Importin-Dependent NF-κB Activation and Inhibits CD8 + T-Cell Memory . *J. Virol.* **93**, 51–70 (2019).
45. Di Pilato, M., Mejías-Pérez, E., Sorzano, C. O. S. & Esteban, M. Distinct Roles of Vaccinia Virus NF-κB Inhibitor Proteins A52, B15, and K7 in the Immune Response. *J. Virol.* **91**, (2017).
46. Harte, M. T. *et al.* The poxvirus protein A52R targets toll-like receptor signaling complexes to suppress host defense. *J. Exp. Med.* **197**, 343–351 (2003).
47. Chen, R. A.-J., Ryzhakov, G., Cooray, S., Randow, F. & Smith, G. L. Inhibition of IκB Kinase by Vaccinia Virus Virulence Factor B14. *PLoS Pathog.* **4**, e22 (2008).
48. Ember, S. W. J., Ren, H., Ferguson, B. J. & Smith, G. L. Vaccinia virus protein C4 inhibits NF-κB activation and promotes virus virulence. *J. Gen. Virol.* **93**, 2098–2108 (2012).
49. Deng, L. *et al.* Investigation of the immunological mechanisms underlying the attenuation of vaccinia virus lacking host-range factor C7. *J. Immunol.* **200**, (2018).

50. YANG, N., Shuman, S. & Deng, L. Vaccinia virus host-range factor C7 has dual inhibitory functions in type I IFN production and signaling. *J. Immunol.* **198**, (2017).
51. Meng, X. *et al.* Vaccinia Virus K1L and C7L Inhibit Antiviral Activities Induced by Type I Interferons. *J. Virol.* **83**, 10627–10636 (2009).
52. Bravo Cruz, A. G. & Shisler, J. L. Vaccinia virus K1 ankyrin repeat protein inhibits NF-κB activation by preventing RelA acetylation. *J. Gen. Virol.* **97**, 2691–2702 (2016).
53. Willis, K. L., Langland, J. O. & Shisler, J. L. Viral double-stranded RNAs from vaccinia virus early or intermediate gene transcripts possess PKR activating function, resulting in NF-κB activation, when the K1 protein is absent or mutated. *J. Biol. Chem.* **286**, 7765–7778 (2011).
54. Shisler, J. L. & Jin, X.-L. The Vaccinia Virus K1L Gene Product Inhibits Host NF-κB Activation by Preventing IκBα Degradation. *J. Virol.* **78**, 3553–3560 (2004).
55. Schröder, M., Baran, M. & Bowie, A. G. Viral targeting of DEAD box protein 3 reveals its role in TBK1/IKKepsilon-mediated IRF activation. *EMBO J.* **27**, 2147–57 (2008).
56. Teferi, W. M. *et al.* The vaccinia virus K7 protein promotes histone methylation associated with heterochromatin formation. *PLoS One* **12**, e0173056 (2017).
57. Schröder, M., Baran, M. & Bowie, A. G. Viral targeting of DEAD box protein 3 reveals its role in TBK1/IKKepsilon-mediated IRF activation. *EMBO J.* **27**, 2147–57 (2008).
58. Oda, S. ichiro, Schröder, M. & Khan, A. R. Structural Basis for Targeting of Human RNA Helicase DDX3 by Poxvirus Protein K7. *Structure* **17**, 1528–1537 (2009).
59. Benfield, C. T. O., Ren, H., Lucas, S. J., Bahsoun, B. & Smith, G. L. Vaccinia virus protein K7 is a virulence factor that alters the acute immune response to infection. *J. Gen. Virol.* **94**, 1647–57 (2013).
60. Gedey, R., Jin, X.-L., Hinthong, O. & Shisler, J. L. Poxviral Regulation of the Host NF-κB Response: the Vaccinia Virus M2L Protein Inhibits Induction of NF-κB Activation via an ERK2 Pathway in Virus-Infected Human Embryonic Kidney Cells. *J. Virol.* **80**, 8676–8685 (2006).
61. Kleinpeter, P. *et al.* By Binding CD80 and CD86, the Vaccinia Virus M2 Protein Blocks Their Interactions with both CD28 and CTLA4 and Potentiates CD80 Binding to PD-L1. *J. Virol.* **93**, 207–226 (2019).
62. DiPerna, G. *et al.* Poxvirus protein N1L targets the I-kappaB kinase complex, inhibits signaling to NF-kappaB by the tumor necrosis factor superfamily of receptors, and inhibits NF-kappaB and IRF3 signaling by toll-like receptors. *J. Biol. Chem.* **279**, 36570–8 (2004).
63. Maluquer de Motes, C. *et al.* Inhibition of apoptosis and NF-κB activation by vaccinia protein N1 occur via distinct binding surfaces and make different contributions to virulence. *PLoS Pathog.* **7**, e1002430 (2011).
64. Postigo, A. & Way, M. The Vaccinia Virus-Encoded Bcl-2 Homologues Do Not Act as Direct Bax Inhibitors. *J. Virol.* **86**, 203–213 (2012).
65. Ren, H. *et al.* Enhancement of CD8 + T-cell memory by removal of a vaccinia virus nuclear factor- κB inhibitor. *Immunology* **145**, 34–49 (2015).
66. Unterholzner, L. *et al.* Vaccinia virus protein C6 is a virulence factor that binds TBK-1 adaptor proteins and inhibits activation of IRF3 and IRF7. *PLoS Pathog.* **7**, e1002247 (2011).
67. Lu, Y. *et al.* Histone deacetylase 4 promotes type I interferon signaling, restricts DNA viruses, and is degraded via vaccinia virus protein C6. *Proc. Natl. Acad. Sci.* **116**, 201816399 (2019).
68. Sumner, R. P., Ren, H. & Smith, G. L. Deletion of immunomodulator C6 from vaccinia virus strain Western Reserve enhances virus immunogenicity and vaccine efficacy. *J. Gen. Virol.* **94**, 1121–6 (2013).
69. Gómez, C. E., Perdiguero, B., Sánchez-Corzo, C., Sorzano, C. O. S. & Esteban, M. Immune Modulation of NYVAC-Based HIV Vaccines by Combined Deletion of Viral Genes that Act on Several Signalling Pathways. *Viruses* **10**, (2017).
70. García-Arriaza, J. *et al.* A Candidate HIV/AIDS Vaccine (MVA-B) Lacking Vaccinia Virus Gene C6L Enhances Memory HIV-1-Specific T-Cell Responses. *PLoS One* **6**, e24244 (2011).
71. Peters, N. E. *et al.* A Mechanism for the Inhibition of DNA-PK-Mediated DNA Sensing by a Virus. *PLoS Pathog.* **9**, (2013).
72. Ferguson, B. J. *et al.* Vaccinia virus protein N2 is a nuclear IRF3 inhibitor that promotes virulence. *J. Gen. Virol.* **94**, 2070–2081 (2013).
73. Garcia-Arriaza, J., Gomez, C. E., Sorzano, C. O. S. & Esteban, M. Deletion of the Vaccinia Virus N2L Gene Encoding an Inhibitor of IRF3 Improves the Immunogenicity of Modified Vaccinia Virus Ankara Expressing HIV-1 Antigens. *J. Virol.* **88**, 3392–3410 (2014).

74. Najarro, P., Traktman, P. & Lewis, J. A. Vaccinia Virus Blocks Gamma Interferon Signal Transduction: Viral VH1 Phosphatase Reverses Stat1 Activation. *J. Virol.* **75**, 3185–3196 (2001).
75. Mann, B. A. *et al.* Vaccinia Virus Blocks Stat1-Dependent and Stat1-Independent Gene Expression Induced by Type I and Type II Interferons. *J. Interf. Cytokine Res.* **28**, 367–380 (2008).
76. Davies, M. V, Elroy-Stein, O., Jagus, R., Moss, B. & Kaufman, R. J. The vaccinia virus K3L gene product potentiates translation by inhibiting double-stranded-RNA-activated protein kinase and phosphorylation of the alpha subunit of eukaryotic initiation factor 2. *J. Virol.* **66**, 1943–1950 (1992).
77. Kawagishi-Kobayashi, M., Silverman, J. B., Ung, T. L. & Dever, T. E. Regulation of the protein kinase PKR by the vaccinia virus pseudosubstrate inhibitor K3L is dependent on residues conserved between the K3L protein and the PKR substrate eIF2alpha. *Mol. Cell. Biol.* **17**, 4146–4158 (1997).
78. Recombinant vaccinia virus K3L gene product prevents activation of double-stranded RNA-dependent, initiation factor 2 alpha-specific protein kinase. Available at: https://www.jbc.org/content/268/17/12837.short. (Accessed: 9th November 2020)
79. Liu, R. & Moss, B. Vaccinia Virus C9 Ankyrin Repeat/F-Box Protein Is a Newly Identified Antagonist of the Type I Interferon-Induced Antiviral State. *J. Virol.* **92**, (2018).
80. Meade, N. *et al.* Poxviruses Evade Cytosolic Sensing through Disruption of an mTORC1-mTORC2 Regulatory Circuit. *Cell* **174**, 1143-1157.e17 (2018).
81. Colamonici, O. R., Domanski, P., Sweitzer, S. M., Larner, A. & Buller, R. M. L. Vaccinia Virus B18R Gene Encodes a Type I Interferon-binding Protein That Blocks Interferon α Transmembrane Signaling. *J. Biol. Chem.* **270**, 15974–15978 (1995).
82. Symons, J. A., Alcamí, A. & Smith, G. L. Vaccinia virus encodes a soluble type I interferon receptor of novel structure and broad species soecificity. *Cell* **81**, 551–560 (1995).
83. Alcamí, A. & Smith, G. L. Vaccinia, cowpox, and camelpox viruses encode soluble gamma interferon receptors with novel broad species specificity. *J. Virol.* **69**, 4633–9 (1995).
84. Verardi, P. H., Jones, L. A., Aziz, F. H., Ahmad, S. & Yilma, T. D. Vaccinia Virus Vectors with an Inactivated Gamma Interferon Receptor Homolog Gene (B8R) Are Attenuated In Vivo without a Concomitant Reduction in Immunogenicity. *J. Virol.* **75**, 11–18 (2001).
85. Gómez, C. E. *et al.* Removal of vaccinia virus genes that block interferon type I and II pathways improves adaptive and memory responses of the HIV/AIDS vaccine candidate NYVAC-C in mice. *J. Virol.* **86**, 5026–38 (2012).
86. Spriggs, M. K. *et al.* Vaccinia and cowpox viruses encode a novel secreted interleukin-1-binding protein. *Cell* **71**, 145–152 (1992).
87. Alcami, A. & Smith, G. L. A soluble receptor for interleukin-1β encoded by vaccinia virus: A novel mechanism of virus modulation of the host response to infection. *Cell* **71**, 153–167 (1992).
88. Dai, K. *et al.* Pathogenicity and immunogenicity of recombinant Tiantan Vaccinia Virus with deleted C12L and A53R genes. *Vaccine* **26**, 5062–5071 (2008).
89. Ren, X. *et al.* Involvement of cellular death in TRAIL/DR5-dependent suppression induced by CD4+CD25+ regulatory T cells. *Cell Death Differ.* **14**, 2076–2084 (2007).
90. Saraiva, M. & Alcami, A. CrmE, a Novel Soluble Tumor Necrosis Factor Receptor Encoded by Poxviruses. *J. Virol.* **75**, 226–233 (2001).
91. Alcamí, A., Khanna, A., Paul, N. L. & Smith, G. L. Vaccinia virus strains Lister, USSR and Evans express soluble and cell-surface tumour necrosis factor receptors. *J. Gen. Virol.* **80**, 949–959 (1999).
92. Bahar, M. W. *et al.* Structure and Function of A41, a Vaccinia Virus Chemokine Binding Protein. *PLoS Pathog.* **4**, e5 (2008).
93. Clark, R. H., Kenyon, J. C., Bartlett, N. W., Tscharke, D. C. & Smith, G. L. Deletion of gene A41L enhances vaccinia virus immunogenicity and vaccine efficacy. *J. Gen. Virol.* **87**, 29–38 (2006).
94. Ng, A., Smith, G. L., Tscharke, D. C. & Reading, P. C. The vaccinia virus A41L protein is a soluble 30 kDa glycoprotein that affects virus virulence. *J. Gen. Virol.* **82**, 2095–2105 (2001).
95. Adams, E. *et al.* The vaccinia virus C12L protein inhibits mouse IL-18 and promotes virus virulence in the murine intranasal model. *J. Gen. Virol.* **83**, 2833–2844 (2002).
96. Symons, J. A. *et al.* The vaccinia virus C1 2L protein inhibits mouse IL-18 and promotes virus virulence in the murine intranasal model. *J. Gen. Virol.* **83**, 2833–2844 (2002).
97. Reading, P. C. & Smith, G. L. Vaccinia Virus Interleukin-18-Binding Protein Promotes Virulence by Reducing

Gamma Interferon Production and Natural Killer and T-Cell Activity. *J. Virol.* **77**, 9960–9968 (2003).
98. Gerlic, M. *et al.* Vaccinia virus F1L protein promotes virulence by inhibiting inflammasome activation. *Proc. Natl. Acad. Sci. U. S. A.* **110**, 7808–13 (2013).
99. Stewart, T. L., Wasilenko, S. T. & Barry, M. Vaccinia Virus F1L Protein Is a Tail-Anchored Protein That Functions at the Mitochondria To Inhibit Apoptosis. *J. Virol.* **79**, 1084–1098 (2005).
100. Ryerson, M. R., Richards, M. M., Kvansakul, M., Hawkins, C. J. & Shisler, J. L. Vaccinia Virus Encodes a Novel Inhibitor of Apoptosis That Associates with the Apoptosome. *J. Virol.* **91**, (2017).
101. Dobbelstein, M. & Shenk, T. Protection against apoptosis by the vaccinia virus SPI-2 (B13R) gene product. *J. Virol.* **70**, (1996).
102. Kettle, S. *et al.* Vaccinia virus serpin B13R(SPI-2) inhibits interleukin-1β-converting enzyme and protects virus-infected cells from TNF- and Fas-mediated apoptosis, but does not prevent IL-1β-induced fever. *J. Gen. Virol.* **78**, 677–685 (1997).
103. Qin, Y. *et al.* SPI-2/CrmA inhibits IFN-β induction by targeting TBK1/IKKε. *Sci. Rep.* **7**, (2017).
104. Rehm, K. E., Connor, R. F., Jones, G. J. B., Yimbu, K. & Roper, R. L. Vaccinia virus A35R inhibits MHC class II antigen presentation. *Virology* **397**, 176–186 (2010).
105. Rehm, K. E. & Roper, R. L. Deletion of the A35 gene from Modified Vaccinia Virus Ankara increases immunogenicity and isotype switching. *Vaccine* **29**, 3276–3283 (2011).
106. Walzer, T., Galibert, L. & De Smedt, T. Poxvirus semaphorin A39R inhibits phagocytosis by dendritic cells and neutrophils. *Eur. J. Immunol.* **35**, 391–398 (2005).
107. Liu, R., Olano, L. R., Mirzakhanyan, Y., Gershon, P. D. & Moss, B. Vaccinia Virus Ankyrin-Repeat/F-Box Protein Targets Interferon-Induced IFITs for Proteasomal Degradation. *Cell Rep.* **29**, 816-828.e6 (2019).
108. Froggatt, G. C., Smith, G. L. & Beard, P. M. Vaccinia virus gene F3L encodes an intracellular protein that affects the innate immune response. *J. Gen. Virol.* **88**, 1917–1921 (2007).
109. Dock, G. The influence of complicating diseases upon leukemia. *Am. J. Med. Sci.* **127**, 563 (1904).
110. Bierman, H. R. *et al.* Remissions in leukemia of childhood following acute infectious disease. Staphylococcus and streptococcus, varicella, and feline panleukopenias. *Cancer* **6**, 591–605 (1953).
111. Coffey, M. C., Strong, J. E., Forsyth, P. A. & Lee, P. W. K. Reovirus therapy of tumors with activated Ras pathway. *Science (80-.).* **282**, 1332–1334 (1998).
112. Strong, J. E., Tang, D. & Lee, P. W. K. Evidence That the Epidermal Growth Factor Receptor on Host Cells Confers Reovirus Infection Efficiency. *Virology* **197**, 405–411 (1993).
113. Norman, K. L. & Lee, P. W. K. Reovirus as a novel oncolytic agent. *Journal of Clinical Investigation* **105**, 1035–1038 (2000).
114. Garber, K. China approves world's first oncolytic virus therapy for cancer treatment. *J. Natl. Cancer Inst.* **98**, 298–300 (2006).
115. Pol, J., Kroemer, G. & Galluzzi, L. First oncolytic virus approved for melanoma immunotherapy. *Oncoimmunology* **5**, e1115641 (2016).
116. Research, Center for Drug Evaluation, F. Approved Drugs - Talimogene Laherparepvec. (2015).
117. Reichard, K. W. *et al.* Newcastle disease virus selectively kills human tumor cells. *J. Surg. Res.* **52**, 448–453 (1992).
118. Krishnamurthy, S., Takimoto, T., Scroggs, R. A. & Portner, A. Differentially Regulated Interferon Response Determines the Outcome of Newcastle Disease Virus Infection in Normal and Tumor Cell Lines. *J. Virol.* **80**, 5145–5155 (2006).
119. Potts, K. *et al.* Oncolytic vaccinia virus F4L (ribonucleotide reductase) mutants promote anti-tumor immunity with superior safety in bladder cancer models. *EMBO Mol. Med.* **May**; **9**, 638–654 (2017).
120. Kelly, E. & Russell, S. J. History of oncolytic viruses: Genesis to genetic engineering. *Molecular Therapy* **15**, 651–659 (2007).
121. Southam, C. & Epstein, A. *The Effect of Russian Encephalitis and Other Viruses on Mouse Leukemia**. (1953).
122. Svet-Moldavsky, G. J. & Hamburg, V. P. Quantitative relationships in viral oncolysis and the possibility of artificial heterogenization of tumours [32]. *Nature* **202**, 303–304 (1964).
123. Cassel, W. A. Multiplication of vaccinia virus in the Ehrlich ascites carcinoma. *Virology* **3**, 514–526 (1957).
124. Mackett, M., Smith, G. L. & Moss, B. General method for production and selection of infectious vaccinia virus recombinants expressing foreign genes. *J. Virol.* **49**, 857–864 (1984).
125. Southam, C. M. Division of Microbiology: Present status of oncolytic virus studies. *Trans. N. Y. Acad. Sci.* **22**,

657–673 (1960).
126. Kieser, Q., Noyce, R. S., Shenouda, M., James Lin, Y. C. & Evans, D. H. Cytoplasmic factories, virus assembly, and DNA replication kinetics collectively constrain the formation of poxvirus recombinants. *PLoS One* **15**, (2020).
127. Tolonen, N., Doglio, L., Schleich, S. & Krijnse Locker, J. Vaccinia virus DNA replication occurs in endoplasmic reticulum-enclosed cytoplasmic mini-nuclei. *Mol. Biol. Cell* **12**, 2031–2046 (2001).
128. Beaud, G. & Beaud, R. Preferential virosomal location of underphosphorylated H5R protein synthesized in vaccinia virus-infected cells. *J. Gen. Virol.* **78**, 3297–3302 (1997).
129. Morissette, G. & Flamand, L. Herpesviruses and Chromosomal Integration. *J. Virol.* **84**, 12100–12109 (2010).
130. Smith, G. L. & Moss, B. Infectious poxvirus vectors have capacity for at least 25 000 base pairs of foreign DNA. *Gene* **25**, 21–28 (1983).
131. Harrington, K. J. *et al.* A practical guide to the handling and administration of talimogene laherparepvec in Europe. *OncoTargets and Therapy* **10**, 3867–3880 (2017).
132. Jackson, E. B., Ley, A. C., Binn, L. N. & Smadel, J. E. Vaccination against Smallpox. *J. Immunol.* **77**, (1956).
133. Newman, F. K., Frey, S. E., Blevins, T. P., Yan, L. & Belshe, R. B. Stability of undiluted and diluted vaccinia-virus vaccine, Dryvax. *J. Infect. Dis.* **187**, 1319–1322 (2003).
134. Belongia, E. A. & Naleway, A. L. Smallpox vaccine: the good, the bad, and the ugly. *Clinical medicine & research* **1**, 87–92 (2003).
135. Cherry, J. D. *et al.* Primary percutaneous vaccination. *J. Infect. Dis.* **135**, 145–154 (1977).
136. Jacobs, B. L. *et al.* Vaccinia Virus Vaccines: Past, Present and Future. doi:10.1016/j.antiviral.2009.06.006
137. Couch, R. B. *et al.* Reducing the dose of smallpox vaccine reduces vaccine-associated morbidity without reducing vaccination success rates or immune responses. *J. Infect. Dis.* **195**, 826–832 (2007).
138. Downs-Canner, S. *et al.* Phase 1 Study of Intravenous Oncolytic Poxvirus (vvDD) in Patients with Advanced Solid Cancers. *Mol. Ther.* **24**, 1492–1501 (2016).
139. Zeh, H. J. *et al.* First-in-man study of western reserve strain oncolytic vaccinia virus: Safety, systemic spread, and antitumor activity. *Mol. Ther.* **23**, 202–214 (2015).
140. Park, S. H. *et al.* Phase 1b Trial of Biweekly Intravenous Pexa-Vec (JX-594), an Oncolytic and Immunotherapeutic Vaccinia Virus in Colorectal Cancer. *Mol. Ther.* **23**, 1532–1540 (2015).
141. Puhlmann, M. *et al. Vaccinia as a vector for tumor-directed gene therapy: Biodistribution of a thymidine kinase-deleted mutant*. (2000).
142. Buller, R. M. L., Smith, G. L., Cremer, K., Notkins, A. L. & Moss, B. Decreased virulence of recombinant vaccinia virus expression vectors is associated with a thymidine kinase-negative phenotype. *Nature* **317**, 813–815 (1985).
143. Cripe, T. P. *et al.* Phase 1 study of intratumoral Pexa-Vec (JX-594), an oncolytic and immunotherapeutic vaccinia virus, in pediatric cancer patients. *Mol. Ther.* **23**, 602–608 (2015).
144. Chaurasiya, S. *Virotherapy for Breast Cancer*.
145. Oweida, A. *et al.* Resistance to radiotherapy and PD-L1 blockade is mediated by TIM-3 upregulation and regulatory T-cell infiltration. *Clin. Cancer Res.* **24**, 5368–5380 (2018).
146. Buller, R. M., Chakrabarti, S., Cooper, J. A., Twardzik, D. R. & Moss, B. Deletion of the vaccinia virus growth factor gene reduces virus virulence. *J. Virol.* **62**, (1988).
147. King, C. S., Cooper, J. A., Moss, B. & Twardzik, D. R. Vaccinia virus growth factor stimulates tyrosine protein kinase activity of A431 cell epidermal growth factor receptors. *Mol. Cell. Biol.* **6**, 332–336 (1986).
148. McCart, J. A. *et al.* Systemic cancer therapy with a tumor-selective vaccinia virus mutant lacking thymidine kinase and vaccinia growth factor genes. *Cancer Res.* **61**, 8751–8757 (2001).
149. Gammon, D. B. *et al.* Vaccinia Virus–Encoded Ribonucleotide Reductase Subunits Are Differentially Required for Replication and Pathogenesis. *PLoS Pathog.* **6**, e1000984 (2010).
150. Ricordel, M. *et al.* Vaccinia Virus Shuffling: deVV5, a Novel Chimeric Poxvirus with Improved Oncolytic Potency. *Cancers (Basel).* **10**, 231 (2018).
151. Foloppe, J. *et al.* The Enhanced Tumor Specificity of TG6002, an Armed Oncolytic Vaccinia Virus Deleted in Two Genes Involved in Nucleotide Metabolism. *Mol. Ther. - Oncolytics* **14**, 1–14 (2019).
152. Rojas, J. J. & Thorne, S. H. Theranostic potential of oncolytic vaccinia virus. *Theranostics* **2**, 363–373 (2012).
153. Gnant, M., Puhlmann, M., Alexander, H. & Bartlett, D. Systemic administration of a recombinant vaccinia virus expressing the cytosine deaminase gene and subsequent treatment with 5-fluorocytosine leads to

tumor-specific gene expression and prolongation of survival in mice. *undefined* (1999).
154. McCart, J. A. *et al.* Complex interactions between the replicating oncolytic effect and the enzyme/prodrug effect of vaccinia-mediated tumor regression. *Gene Ther.* **7**, 1217–1223 (2000).
155. De Vries, C., Monken, C. & Lattime, E. The addition of recombinant vaccinia HER2/neu to oncolytic vaccinia-GMCSF given into the tumor microenvironment overcomes MDSC-mediated immune escape and systemic anergy. *Cancer Gene Ther.* **22**, 154–162 (2015).
156. Gulley, J. *et al.* Phase I study of a vaccine using recombinant vaccinia virus expressing PSA (rV-PSA) in patients with metastatic androgen-independent prostate cancer. *Prostate* **53**, 109–117 (2002).
157. Kleinpeter, P. *et al.* Vectorization in an oncolytic vaccinia virus of an antibody, a Fab and a scFv against programmed cell death -1 (PD-1) allows their intratumoral delivery and an improved tumor-growth inhibition. *Oncoimmunology* **5**, (2016).
158. Wang, G. *et al.* An engineered oncolytic virus expressing PD-L1 inhibitors activates tumor neoantigen-specific T cell responses. *Nat. Commun.* **11**, (2020).
159. Yu, F. *et al.* T-cell engager-armed oncolytic vaccinia virus significantly enhances antitumor therapy. *Mol. Ther.* **22**, 102–111 (2014).
160. Mejías-Pérez, E., Carreño-Fuentes, L. & Esteban, M. Development of a Safe and Effective Vaccinia Virus Oncolytic Vector WR-Δ4 with a Set of Gene Deletions on Several Viral Pathways. *Mol. Ther. - Oncolytics* **8**, 27–40 (2018).
161. Kelly, K. J. *et al.* Novel oncolytic agent GLV-1h68 is effective against malignant pleural mesothelioma. *Hum. Gene Ther.* **19**, 774–782 (2008).
162. Kirn, D. H., Wang, Y., Le Boeuf, F., Bell, J. & Thorne, S. H. Targeting of Interferon-Beta to Produce a Specific, Multi-Mechanistic Oncolytic Vaccinia Virus. *PLoS Med.* **4**, e353 (2007).
163. Di Pilato, M. *et al.* NFκB activation by modified vaccinia virus as a novel strategy to enhance neutrophil migration and HIV-specific T-cell responses. *Proc. Natl. Acad. Sci.* **112**, E1333–E1342 (2015).
164. Sumner, R. P., Ren, H., Ferguson, B. J. & Smith, G. L. Increased attenuation but decreased immunogenicity by deletion of multiple vaccinia virus immunomodulators. *Vaccine* **34**, 4827–34 (2016).
165. Acuna, S. A. *et al.* Oncolytic vaccinia virus as an adjuvant treatment to cytoreductive surgery for malignant peritoneal mesothelioma. *Ann. Surg. Oncol.* **21**, 2259–2266 (2014).
166. Gholami, S. *et al.* Vaccinia virus GLV-1h153 in combination with ^{131}I shows increased efficiency in treating triple-negative breast cancer. *FASEB J.* **28**, 676–682 (2014).
167. Mansfield, D. *et al.* Oncolytic Vaccinia virus and radiotherapy in head and neck cancer. *Oral Oncol.* **49**, 108–118 (2013).
168. Ottolino-Perry, K. *et al.* Oncolytic vaccinia virus synergizes with irinotecan in colorectal cancer. *Mol. Oncol.* **9**, 1539–1552 (2015).
169. Martin, N. T. & Bell, J. C. Oncolytic Virus Combination Therapy: Killing One Bird with Two Stones. *Molecular Therapy* **26**, 1414–1422 (2018).
170. Ottolino-Perry, K., Diallo, J. S., Lichty, B. D., Bell, J. C. & Andrea McCart, J. Intelligent design: Combination therapy with oncolytic viruses. *Molecular Therapy* **18**, 251–263 (2010).
171. Choi, A. H., O'Leary, M. P., Fong, Y. & Chen, N. G. From benchtop to bedside: A review of oncolytic virotherapy. *Biomedicines* **4**, (2016).
172. Angarita, F. A., Acuna, S. A., Ottolino-Perry, K., Zerhouni, S. & McCart, J. A. Mounting a strategic offense: Fighting tumor vasculature with oncolytic viruses. *Trends in Molecular Medicine* **19**, 378–392 (2013).
173. Breitbach, C. J. *et al.* Oncolytic vaccinia virus disrupts tumor-associated vasculature in humans. *Cancer Res.* **73**, 1265–1275 (2013).
174. Desilva, A. *et al.* Comparative functional evaluation of immunocompetent mouse breast cancer models established from PyMT-tumors using small animal PET with [(18)F]FDG and [(18)F]FLT. *Am. J. Nucl. Med. Mol. Imaging* **2**, 88–98 (2012).
175. Umer, B. A. *et al.* Deciphering the Immunomodulatory Capacity of Oncolytic Vaccinia Virus to Enhance the Immune Response to Breast Cancer. *Cancer Immunol. Res.* **8**, 618–631 (2020).
176. Mittal, D., Gubin, M. M., Schreiber, R. D. & Smyth, M. J. New insights into cancer immunoediting and its three component phases-elimination, equilibrium and escape. *Current Opinion in Immunology* **27**, 16–25 (2014).
177. Lei, X. *et al.* Immune cells within the tumor microenvironment: Biological functions and roles in cancer

immunotherapy. *Cancer Letters* **470**, 126–133 (2020).
178. Waldman, A. D., Fritz, J. M. & Lenardo, M. J. A guide to cancer immunotherapy: from T cell basic science to clinical practice. *Nature Reviews Immunology* **20**, 651–668 (2020).
179. Tsukumo, S. I. & Yasutomo, K. Regulation of CD8+ T cells and antitumor immunity by Notch signaling. *Frontiers in Immunology* **9**, 1 (2018).
180. Cibrián, D. & Sánchez-Madrid, F. CD69: from activation marker to metabolic gatekeeper. *European Journal of Immunology* **47**, 946–953 (2017).
181. Tanaka, A. & Sakaguchi, S. Regulatory T cells in cancer immunotherapy. *Cell Research* **27**, 109–118 (2017).
182. Sasidharan Nair, V. & Elkord, E. Immune checkpoint inhibitors in cancer therapy: a focus on T-regulatory cells. *Immunol. Cell Biol.* **96**, 21–33 (2018).
183. Garín, M. I. *et al.* Galectin-1: A key effector of regulation mediated by CD4 +CD25+ T cells. *Blood* **109**, 2058–2065 (2007).
184. Grossman, W. J. *et al.* Differential expression of granzymes A and B in human cytotoxic lymphocyte subsets and T regulatory cells. *Blood* **104**, 2840–2848 (2004).
185. Lebien, T. W. & Tedder, T. F. B lymphocytes: How they develop and function. *Blood* **112**, 1570–1580 (2008).
186. Souza-Fonseca-Guimaraes, F., Cursons, J. & Huntington, N. D. The Emergence of Natural Killer Cells as a Major Target in Cancer Immunotherapy. *Trends in Immunology* **40**, 142–158 (2019).
187. Veglia, F., Perego, M. & Gabrilovich, D. Myeloid-derived suppressor cells coming of age review-article. *Nature Immunology* **19**, 108–119 (2018).
188. Damuzzo, V. *et al.* Complexity and challenges in defining myeloid-derived suppressor cells. *Cytom. Part B Clin. Cytom.* **88**, 77–91 (2015).
189. Labani-Motlagh, A., Ashja-Mahdavi, M. & Loskog, A. The Tumor Microenvironment: A Milieu Hindering and Obstructing Antitumor Immune Responses. *Frontiers in Immunology* **11**, 940 (2020).
190. Toor, S. M., Sasidharan Nair, V., Decock, J. & Elkord, E. Immune checkpoints in the tumor microenvironment. *Seminars in Cancer Biology* **65**, 1–12 (2020).
191. Krummel, M. F. & Allison, J. P. CD28 and CTLA-4 have opposing effects on the response of T ceils to stimulation. *J. Exp. Med.* **182**, 459–465 (1995).
192. Walunas, T., Lenschow, D. & Bakker, C. CTLA-4 can function as a negative regulator of T cell activation. *Immunity* (1994).
193. Agata, Y. *et al.* Expression of the PD-1 antigen on the surface of stimulated mouse T and B lymphocytes. *Int. Immunol.* **8**, 765–772 (1996).
194. Muenst, S., Soysal, S. D., Tzankov, A. & Hoeller, S. The PD-1/PD-L1 pathway: biological background and clinical relevance of an emerging treatment target in immunotherapy. *Expert Opin. Ther. Targets* **19**, 201–211 (2015).
195. Freeman, G. J. *et al.* Engagement of the PD-1 immunoinhibitory receptor by a novel B7 family member leads to negative regulation of lymphocyte activation. *J. Exp. Med.* **192**, 1027–1034 (2000).
196. Dong, H. *et al.* Tumor-associated B7-H1 promotes T-cell apoptosis: A potential mechanism of immune evasion. *Nat. Med.* **8**, 793–800 (2002).
197. Wiemann, B. & Starnes, C. O. Coley's toxins, tumor necrosis factor and cancer research: A historical perspective. *Pharmacology and Therapeutics* **64**, 529–564 (1994).
198. McCune, J. S. Rapid Advances in Immunotherapy to Treat Cancer. *Clin. Pharmacol. Ther.* **103**, 540–544 (2018).
199. Leach, D. R., Krummel, M. F. & Allison, J. P. Enhancement of antitumor immunity by CTLA-4 blockade. *Science (80-.).* **271**, 1734–1736 (1996).
200. Topalian, S. L. *et al.* Safety, Activity, and Immune Correlates of Anti–PD-1 Antibody in Cancer. *N. Engl. J. Med.* **366**, 2443–2454 (2012).
201. Brahmer, J. R. *et al.* Safety and Activity of Anti–PD-L1 Antibody in Patients with Advanced Cancer. *N. Engl. J. Med.* **366**, 2455–2465 (2012).
202. Sharma, P. & Allison, J. P. Immune Checkpoint Targeting in Cancer Therapy: Toward Combination Strategies with Curative Potential. *Cell* **161**, 205–214 (2015).
203. Huehls, A. M., Coupet, T. A. & Sentman, C. L. Bispecific T-cell engagers for cancer immunotherapy. *Immunology and Cell Biology* **93**, 290–296 (2015).
204. Gauthier, L. *et al.* Multifunctional Natural Killer Cell Engagers Targeting NKp46 Trigger Protective Tumor

Immunity. *Cell* **177**, 1701-1713.e16 (2019).
205. Khair, D. O. *et al.* Combining immune checkpoint inhibitors: Established and emerging targets and strategies to improve outcomes in melanoma. *Frontiers in Immunology* **10**, 453 (2019).
206. Robert, C. *et al.* Ipilimumab plus Dacarbazine for Previously Untreated Metastatic Melanoma. *N. Engl. J. Med.* **364**, 2517–2526 (2011).
207. Hodi, F. S. *et al.* Improved Survival with Ipilimumab in Patients with Metastatic Melanoma. *N. Engl. J. Med.* **363**, 711–723 (2010).
208. Motzer, R. J. *et al.* Nivolumab versus Everolimus in Advanced Renal-Cell Carcinoma. *N. Engl. J. Med.* **373**, 1803–1813 (2015).
209. Powles, T. *et al.* MPDL3280A (anti-PD-L1) treatment leads to clinical activity in metastatic bladder cancer. *Nature* **515**, 558–562 (2014).
210. Cohen, E. E. W. *et al.* KEYNOTE-040: A phase III randomized trial of pembrolizumab (MK-3475) versus standard treatment in patients with recurrent or metastatic head and neck cancer. *J. Clin. Oncol.* **33**, TPS6084–TPS6084 (2015).
211. Hamanishi, J., Mandai, M., Ikeda, T. & Minami, M. Safety and Antitumor Activity of Anti-PD-1 Antibody, Nivolumab, in Patients With Platinum-Resistant Ovarian Cancer. *Artic. J. Clin. Oncol.* (2015). doi:10.1200/JCO.2015.62.3397
212. Whiteside, T. L., Demaria, S., Rodriguez-Ruiz, M. E., Zarour, H. M. & Melero, I. Emerging opportunities and challenges in cancer immunotherapy. *Clin. Cancer Res.* **22**, 1845–1855 (2016).
213. Garfall, A. L. *et al.* Chimeric Antigen Receptor T Cells against CD19 for Multiple Myeloma. *N. Engl. J. Med.* **373**, 1040–1047 (2015).
214. Maude, S. L. *et al.* Chimeric Antigen Receptor T Cells for Sustained Remissions in Leukemia. *N. Engl. J. Med.* **371**, 1507–1517 (2014).
215. Porter, D. L. *et al.* Chimeric antigen receptor T cells persist and induce sustained remissions in relapsed refractory chronic lymphocytic leukemia. *Sci. Transl. Med.* **7**, 303ra139-303ra139 (2015).
216. Hegde, P. S. & Chen, D. S. Top 10 Challenges in Cancer Immunotherapy. *Immunity* **52**, 17–35 (2020).
217. Haslam, A. & Prasad, V. Estimation of the Percentage of US Patients With Cancer Who Are Eligible for and Respond to Checkpoint Inhibitor Immunotherapy Drugs. *JAMA Netw. open* **2**, e192535 (2019).
218. Bassiony, M., Aluko, A. V. & Radosevich, J. A. Immunotherapy and Cancer. in *Precision Medicine in Oncology* 133–156 (Wiley, 2020). doi:10.1002/9781119432487.ch5
219. Breast Cancer - Canada.ca. Available at: https://www.canada.ca/en/public-health/services/chronic-diseases/cancer/breast-cancer.html. (Accessed: 26th October 2020)
220. Treatments for breast cancer - Canadian Cancer Society. Available at: https://www.cancer.ca/en/cancer-information/cancer-type/breast/treatment/?region=on. (Accessed: 18th November 2020)
221. Njeh, C. F., Saunders, M. W. & Langton, C. M. Accelerated partial breast irradiation using external beam conformal radiation therapy: A review. *Critical Reviews in Oncology/Hematology* **81**, 1–20 (2012).
222. Perou, C. M. *et al.* Molecular portraits of human breast tumours. *Nature* **406**, 747–752 (2000).
223. Basu, A. *et al.* Immunotherapy in breast cancer: Current status and future directions. in *Advances in Cancer Research* **143**, 295–349 (Academic Press Inc., 2019).
224. Sørlie, T. *et al.* Gene expression patterns of breast carcinomas distinguish tumor subclasses with clinical implications. *Proc. Natl. Acad. Sci. U. S. A.* **98**, 10869–10874 (2001).
225. Masood, S. Breast cancer subtypes: Morphologic and biologic characterization. *Women's Heal.* **12**, 103–119 (2016).
226. Dai, X. *et al.* Breast cancer intrinsic subtype classification, clinical use and future trends. *American Journal of Cancer Research* **5**, 2929–2943 (2015).
227. Goldhirsch, A. *et al.* Strategies for subtypes-dealing with the diversity of breast cancer: Highlights of the St Gallen international expert consensus on the primary therapy of early breast cancer 2011. *Ann. Oncol.* **22**, 1736–1747 (2011).
228. Russnes, H. G., Lingjærde, O. C., Børresen-Dale, A. L. & Caldas, C. Breast Cancer Molecular Stratification: From Intrinsic Subtypes to Integrative Clusters. *American Journal of Pathology* **187**, 2152–2162 (2017).
229. Yersal, O. & Barutca, S. Biological subtypes of breast cancer: Prognostic and therapeutic implications. *World Journal of Clinical Oncology* **5**, 412–424 (2014).
230. Slamon, D. J. *et al.* Use of Chemotherapy plus a Monoclonal Antibody against HER2 for Metastatic Breast

Cancer That Overexpresses HER2. *N. Engl. J. Med.* **344**, 783–792 (2001).
231. Carey, L. A. *et al.* Race, breast cancer subtypes, and survival in the Carolina Breast Cancer Study. *J. Am. Med. Assoc.* **295**, 2492–2502 (2006).
232. Rovero, S. *et al.* DNA vaccination against rat her-2/Neu p185 more effectively inhibits carcinogenesis than transplantable carcinomas in transgenic BALB/c mice. *J. Immunol.* **165**, 5133–42 (2000).
233. Ikuta, Y. *et al.* A HER2/NEU-derived peptide, a Kd-restricted murine tumor rejection antigen, induces HER2-specific HLA-A2402-restricted CD8+ cytotoxic T lymphocytes. *Int. J. Cancer* **87**, 553–558 (2000).
234. Sow, H. S. *et al.* Immunogenicity of rat-neu+ mouse mammary tumours determines the T cell-dependent therapeutic efficacy of anti-neu monoclonal antibody treatment. *Sci. Rep.* **10**, (2020).
235. Das Roy, L. *et al.* Breast cancer-associated metastasis is significantly increased in a model of autoimmune arthritis. *Breast Cancer Res.* **11**, R56 (2009).
236. Pulaski, B. A. & Ostrand-Rosenberg, S. Reduction of established spontaneous mammary carcinoma metastases following immunotherapy with major histocompatibility complex class II and B7.1 cell-based tumor vaccines. *Cancer Res.* **58**, 1486–93 (1998).
237. Pulaski, B. A. & Ostrand-Rosenberg, S. Mouse 4T1 Breast Tumor Model. in *Current Protocols in Immunology* **Chapter 20**, Unit 20.2 (John Wiley & Sons, Inc., 2001).
238. Coleman, R. E., Gregory, W., Marshall, H., Wilson, C. & Holen, I. The metastatic microenvironment of breast cancer: Clinical implications. *Breast* **22**, (2013).
239. Ali, H. R. *et al.* Association between CD8+ T-cell infiltration and breast cancer survival in 12 439 patients. *Ann. Oncol.* **25**, 1536–1543 (2014).
240. Wang, L. *et al.* Connecting blood and intratumoral Treg cell activity in predicting future relapse in breast cancer. *Nat. Immunol.* **20**, 1220–1230 (2019).
241. Salem, M. L. Estrogen, a double-edged sword: Modulation of TH1- and TH2-mediated inflammations by differential regulation of TH1/TH2 cytokine production. *Current Drug Targets: Inflammation and Allergy* **3**, 97–104 (2004).
242. Verma, C. *et al.* Natural killer (NK) cell profiles in blood and tumour in women with large and locally advanced breast cancer (LLABC) and their contribution to a pathological complete response (PCR) in the tumour following neoadjuvant chemotherapy (NAC): Differential restoration of blood profiles by NAC and surgery. *J. Transl. Med.* **13**, 1–21 (2015).
243. Garner, W. L., Minton, J. P., James, A. G. & Hoffmann, C. C. Human breast cancer and impaired NK cell function. *J. Surg. Oncol.* **24**, 64–66 (1983).
244. Shou, D. *et al.* Suppressive role of myeloid-derived suppressor cells (MDSCs) in the microenvironment of breast cancer and targeted immunotherapies. *Oncotarget* **7**, 64505–64511 (2016).
245. Youn, J.-I., Nagaraj, S., Collazo, M. & Gabrilovich, D. I. Subsets of myeloid-derived suppressor cells in tumor-bearing mice. *J. Immunol.* **181**, 5791–802 (2008).
246. Shang, B., Liu, Y., Jiang, S. J. & Liu, Y. Prognostic value of tumor-infiltrating FoxP3+ regulatory T cells in cancers: A systematic review and meta-analysis. *Sci. Rep.* **5**, 15179 (2015).
247. Bates, G. J. *et al.* Quantification of regulatory T cells enables the identification of high-risk breast cancer patients and those at risk of late relapse. *J. Clin. Oncol.* **24**, 5373–5380 (2006).
248. Liu, S. *et al.* Prognostic significance of FOXP3+ tumor-infiltrating lymphocytes in breast cancer depends on estrogen receptor and human epidermal growth factor receptor-2 expression status and concurrent cytotoxic T-cell infiltration. *Breast Cancer Res.* **16**, (2014).
249. Makhoul, I., Atiq, M., Alwbari, A. & Kieber-Emmons, T. Breast Cancer Immunotherapy: An Update. *Breast Cancer: Basic and Clinical Research* **12**, (2018).
250. Diaz-Montero, C. M. *et al.* Increased circulating myeloid-derived suppressor cells correlate with clinical cancer stage, metastatic tumor burden, and doxorubicin–cyclophosphamide chemotherapy. *Cancer Immunol. Immunother.* **58**, 49–59 (2009).
251. Diaz-Montero, C. M. *et al.* Increased circulating myeloid-derived suppressor cells correlate with clinical cancer stage, metastatic tumor burden, and doxorubicin-cyclophosphamide chemotherapy. *Cancer Immunol. Immunother.* **58**, 49–59 (2009).
252. Lawrence, M. S. *et al.* Mutational heterogeneity in cancer and the search for new cancer-associated genes. *Nature* **499**, 214–218 (2013).
253. Adams, S. *et al.* Current Landscape of Immunotherapy in Breast Cancer: A Review. *JAMA Oncol.* **5**, 1205–

1214 (2019).
254. Zhao, J. & Huang, J. Breast cancer immunology and immunotherapy: Targeting the programmed cell death protein-1/programmed cell death protein ligand-1. *Chinese Medical Journal* **133**, 853–862 (2020).
255. Luen, S., Virassamy, B., Savas, P., Salgado, R. & Loi, S. The genomic landscape of breast cancer and its interaction with host immunity. *Breast* **29**, 241–250 (2016).
256. Budczies, J. *et al.* Classical pathology and mutational load of breast cancer – integration of two worlds. *J. Pathol. Clin. Res.* **2**, 225–238 (2016).
257. Jaffray, D. A. & Gospodarowicz, M. K. Radiation Therapy for Cancer. in *Disease Control Priorities, Third Edition (Volume 3): Cancer* 239–247 (The World Bank, 2015). doi:10.1596/978-1-4648-0349-9_ch14
258. Lavelle, C. & Foray, N. Chromatin structure and radiation-induced DNA damage: From structural biology to radiobiology. *International Journal of Biochemistry and Cell Biology* **49**, 84–97 (2014).
259. Nguyen, H. Q. *et al.* Ionizing radiation-induced cellular senescence promotes tissue fibrosis after radiotherapy. A review. *Critical Reviews in Oncology/Hematology* **129**, 13–26 (2018).
260. Storozynsky, Q. & Hitt, M. M. The Impact of Radiation-Induced DNA Damage on cGAS-STING-Mediated Immune Responses to Cancer. *Int. J. Mol. Sci.* **21**, 8877 (2020).
261. Burnette, B. C. *et al.* The efficacy of radiotherapy relies upon induction of type I interferon-dependent innate and adaptive immunity. *Cancer Res.* **71**, 2488–2496 (2011).
262. Bhattacharyya, T., Purushothaman, K., Vadakke Puthiyottil, S. S., Bhattacharjee, A. & Muttah, G. Immunological interactions in radiotherapy-opening a new window of opportunity. *Annals of Translational Medicine* **4**, 51 (2016).
263. Hu, Z. I., McArthur, H. L. & Ho, A. Y. The Abscopal Effect of Radiation Therapy: What Is It and How Can We Use It in Breast Cancer? *Current Breast Cancer Reports* **9**, 45–51 (2017).
264. Emens, L. A. *et al.* Cancer immunotherapy: Opportunities and challenges in the rapidly evolving clinical landscape. *European Journal of Cancer* **81**, 116–129 (2017).
265. Formenti, S. C. & Demaria, S. Combining radiotherapy and cancer immunotherapy: a paradigm shift. *J. Natl. Cancer Inst.* **105**, 256–65 (2013).
266. Wilkinson, M. J. *et al.* Oncolytic vaccinia virus combined with radiotherapy induces apoptotic cell death in sarcoma cells by down-regulating the inhibitors of apoptosis. *Oncotarget* **7**, 81208–81222 (2016).
267. Buckel, L. *et al.* Combination of fractionated irradiation with anti-VEGF expressing vaccinia virus therapy enhances tumor control by simultaneous radiosensitization of tumor associated endothelium. *Int. J. Cancer* **133**, n/a-n/a (2013).
268. Stanziale, S. F. *et al.* Ionizing radiation potentiates the antitumor efficacy of oncolytic herpes simplex virus G207 by upregulating ribonucleotide reductase. *Surgery* **132**, 353–359 (2002).
269. Gentschev, I. *et al.* Use of an oncolytic vaccinia virus for the treatment of canine breast cancer in nude mice: Preclinical development of a therapeutic agent. *Cancer Gene Ther.* **16**, 320–328 (2009).
270. Wang, H., Chen, N. G., Minev, B. R. & Szalay, A. A. Oncolytic vaccinia virus GLV-1h68 strain shows enhanced replication in human breast cancer stem-like cells in comparison to breast cancer cells. *J. Transl. Med.* **10**, (2012).
271. Weibel, S. *et al.* Viral-mediated oncolysis is the most critical factor in the late-phase of the tumor regression process upon vaccinia virus infection. *BMC Cancer* **11**, 68 (2011).
272. Gholami, S. *et al.* A novel vaccinia virus with dual oncolytic and anti-angiogenic therapeutic effects against triple-negative breast cancer. *Breast Cancer Res. Treat.* **148**, 489–499 (2014).
273. Seubert, C. M. *et al.* Enhanced tumor therapy using vaccinia virus strain GLV-1h68 in combination with a β-galactosidase-activatable prodrug seco-analog of duocarmycin SA. *Cancer Gene Ther.* **18**, 42–52 (2011).
274. John, L. B. *et al.* Oncolytic virus and anti-4-1BB combination therapy elicits strong antitumor immunity against established cancer. *Cancer Res.* **72**, 1651–1660 (2012).
275. Deng, L. *et al.* Target therapy with vaccinia virus harboring IL-24 for human breast cancer. *J. Cancer* **11**, 1017–1026 (2020).
276. Adelfinger, M. *et al.* Preclinical Testing Oncolytic Vaccinia Virus Strain GLV-5b451 Expressing an Anti-VEGF Single-Chain Antibody for Canine Cancer Therapy. *Viruses* **7**, 4075–4092 (2015).
277. Gil, M., Seshadri, M., Komorowski, M. P., Abrams, S. I. & Kozbor, D. Targeting CXCL12/CXCR4 signaling with oncolytic virotherapy disrupts tumor vasculature and inhibits breast cancer metastases. *Proc. Natl. Acad. Sci. U. S. A.* **110**, E1291-300 (2013).

278. Gholami, S. *et al.* Vaccinia virus GLV-1h153 is a novel agent for detection and effective local control of positive surgical margins for breast cancer. *Breast Cancer Res.* **15**, (2013).
279. Zhang, Q. *et al.* Eradication of solid human breast tumors in nude mice with an intravenously injected light-emitting oncolytic vaccinia virus. *Cancer Res.* **67**, 10038–10046 (2007).
280. Search of: vaccinia | breast cancer | Phase 1 - List Results - ClinicalTrials.gov. Available at: https://clinicaltrials.gov/ct2/results?term=vaccinia&cond=breast+cancer&age_v=&gndr=&type=&rslt=&phase=0&Search=Apply. (Accessed: 18th November 2020)
281. Mohebtash, M. *et al.* A pilot study of MUC-1/CEA/TRICOM poxviral-based vaccine in patients with metastatic breast and ovarian cancer. *Clin. Cancer Res.* **17**, 7164–7173 (2011).
282. Gulley, J. L. *et al.* Pilot study of vaccination with recombinant CEA-MUC-1-tric0m pox viral-based vaccines in patients with metastatic carcinoma. *Clin. Cancer Res.* **14**, 3060–3069 (2008).
283. Study of TBio-6517, Given Intratumorally, Alone or in Combination With Pembrolizumab, in Solid Tumors - Full Text View - ClinicalTrials.gov. Available at: https://clinicaltrials.gov/ct2/show/NCT04301011?term=vaccinia&cond=breast+cancer&phase=0&draw=2&rank=6. (Accessed: 18th November 2020)
284. Rintoul, J. L. *et al.* A Selectable and Excisable Marker System for the Rapid Creation of Recombinant Poxviruses. *PLoS One* **6**, e24643 (2011).
285. Chou, T. C. Drug combination studies and their synergy quantification using the chou-talalay method. *Cancer Research* **70**, 440–446 (2010).
286. Chou, T. C. Theoretical basis, experimental design, and computerized simulation of synergism and antagonism in drug combination studies. *Pharmacological Reviews* **58**, 621–681 (2006).
287. Russell, S. J. & Peng, K. W. Viruses as anticancer drugs. *Trends in Pharmacological Sciences* **28**, 326–333 (2007).
288. Nagata, L. P., Irwin, C. R., Hu, W.-G. & Evans, D. H. Vaccinia-based vaccines to biothreat and emerging viruses Vaccinia-based vaccines to biothreat and emerging viruses. *Biotechnol. Genet. Eng. Rev.* **34**, 107–121 (2018).
289. Cotter, C. A., Earl, P. L., Wyatt, L. S. & Moss, B. Preparation of Cell Cultures and Vaccinia Virus Stocks. *Curr. Protoc. protein Sci.* **89**, 5.12.1-5.12.18 (2017).
290. Smallwood, S. E., Rahman, M. M., Smith, D. W. & McFadden, G. Myxoma virus: Propagation, purification, quantification, and storage. *Current Protocols in Microbiology* **Chapter 14**, (2010).
291. Noyce, R. S., Lederman, S. & Evans, D. H. Construction of an infectious horsepox virus vaccine from chemically synthesized DNA fragments. *PLoS One* **13**, e0188453 (2018).
292. Hughes, L. *et al.* A rapid Orthopoxvirus purification protocol suitable for high-containment laboratories. *J. Virol. Methods* **243**, 68–73 (2017).
293. Gstraunthaler, G., Lindl, T. & Van Der Valk, J. A plea to reduce or replace fetal bovine serum in cell culture media. *Cytotechnology* **65**, 791–793 (2013).
294. Dai, P. *et al.* Modified Vaccinia Virus Ankara Triggers Type I IFN Production in Murine Conventional Dendritic Cells via a cGAS/STING-Mediated Cytosolic DNA-Sensing Pathway. *PLOS Pathog.* **10**, e1003989 (1998).
295. Dai, P. *et al.* Intratumoral delivery of inactivated modified vaccinia virus Ankara (iMVA) induces systemic antitumor immunity via STING and Batf3-dependent dendritic cells. *Sci. Immunol.* **2**, (2017).
296. Katsafanas, G. C. & Moss, B. Colocalization of Transcription and Translation within Cytoplasmic Poxvirus Factories Coordinates Viral Expression and Subjugates Host Functions. *Cell Host Microbe* **2**, 221–228 (2007).
297. Tang, V. A. *et al.* Single-particle characterization of oncolytic vaccinia virus by flow virometry. *Vaccine* **34**, 5082–5089 (2016).
298. Chen, F., Lu, J. R., Binder, B. J., Liu, Y. C. & Hodson, R. E. Application of digital image analysis and flow cytometry to enumerate marine viruses stained with SYBR Gold. *Appl. Environ. Microbiol.* **67**, 539–545 (2001).
299. Overman, J. R. & Gordon Sharp, D. Ratios of vaccinia virus particles to virus infectious units. *J. Exp. Med.* **110**, 461–483 (1959).
300. Kim, S.-G., Ran, G. S., Kwon, H.-C. & Hwang, T.-H. Effect of NaCl on the Stability of Oncolytic Vaccinia Virus. *J. Life Sci.* **26**, 23–33 (2016).
301. Guo, Z. S. *et al.* Rapid Generation of Multiple Loci-Engineered Marker-free Poxvirus and Characterization of a Clinical-Grade Oncolytic Vaccinia Virus. *Mol. Ther. - Methods Clin. Dev.* **7**, 112–122 (2017).
302. Nicas, M., Hubbard, A. E., Jones, R. M. & Reingold, A. L. The Infectious Dose of Variola (Smallpox) Virus. *Appl.*

Biosaf. **9**, 118–127 (2004).
303. Fergusson, D. A. *et al.* Assessing the Completeness of Reporting in Preclinical Oncolytic Virus Therapy Studies. *Mol. Ther. - Oncolytics* **14**, 179–187 (2019).
304. Ungerechts, G. *et al.* Moving oncolytic viruses into the clinic: clinical-grade production, purification, and characterization of diverse oncolytic viruses. *Molecular Therapy - Methods and Clinical Development* **3**, 16018 (2016).
305. Esteva, F. J., Hubbard-Lucey, V. M., Tang, J. & Pusztai, L. Immunotherapy and targeted therapy combinations in metastatic breast cancer. *The Lancet Oncology* **20**, e175–e186 (2019).
306. Hennessy, M. L., Bommareddy, P. K., Boland, G. & Kaufman, H. L. Oncolytic Immunotherapy. *Surgical Oncology Clinics of North America* **28**, 419–430 (2019).
307. Mansfield, D. C. *et al.* Oncolytic vaccinia virus as a vector for therapeutic sodium iodide symporter gene therapy in prostate cancer. *Gene Ther.* **23**, 357–368 (2016).
308. Verhaegen, F., Granton, P. & Tryggestad, E. Small animal radiotherapy research platforms. *Physics in Medicine and Biology* **56**, R55 (2011).
309. Huovinen, M., Loikkanen, J., Myllynen, P. & Vähäkangas, K. H. Characterization of human breast cancer cell lines for the studies on p53 in chemical carcinogenesis. *Toxicol. Vitr.* **25**, 1007–1017 (2011).
310. Yerlikaya, A., Okur, E. & Ulukaya, E. The p53-independent induction of apoptosis in breast cancer cells in response to proteasome inhibitor bortezomib. *Tumor Biol.* **33**, 1385–1392 (2012).
311. Pierpaoli, E. *et al.* Effect of annatto-tocotrienols supplementation on the development of mammary tumors in HER-2/neu transgenic mice. *Carcinogenesis* **34**, 1352–1360 (2013).
312. Liu, Z., Ravindranathan, R., Kalinski, P., Guo, Z. S. & Bartlett, D. L. Rational combination of oncolytic vaccinia virus and PD-L1 blockade works synergistically to enhance therapeutic efficacy. *Nat. Commun.* **8**, 1–12 (2017).
313. Wang, Y. *et al.* Combining immunotherapy and radiotherapy for cancer treatment: Current challenges and future directions. *Frontiers in Pharmacology* **9**, 185 (2018).
314. Brooks, E. D. & Chang, J. Y. Time to abandon single-site irradiation for inducing abscopal effects. *Nature Reviews Clinical Oncology* **16**, 123–135 (2019).
315. Lamfers, M. L. M. *et al.* Potential of the Conditionally Replicative Adenovirus Ad5-Δ24RGD in the Treatment of Malignant Gliomas and Its Enhanced Effect with Radiotherapy. *Cancer Res.* **62**, (2002).
316. Lamfers, M. L. M. *et al.* Differential effects of combined Ad5-Δ24RGD and radiation therapy in in vitro versus in vivo models of malignant glioma. *Clin. Cancer Res.* **13**, 7451–7458 (2007).
317. Jorgensen, T. J. *et al.* Ionizing radiation does not alter the antitumor activity of herpes simplex virus vector G207 in subcutaneous tumor models of human and murine prostate cancer. *Neoplasia* **3**, 451–456 (2001).
318. Denis, M., Duruisseaux, M., Brevet, M. & Dumontet, C. How Can Immune Checkpoint Inhibitors Cause Hyperprogression in Solid Tumors? *Front. Immunol.* **11**, 492 (2020).
319. Sobol, P. T. *et al.* Adaptive Antiviral Immunity Is a Determinant of the Therapeutic Success of Oncolytic Virotherapy. *Mol. Ther.* **19**, 335–344 (2011).
320. Davola, M. E. & Mossman, K. L. Oncolytic viruses: how "lytic" must they be for therapeutic efficacy? *OncoImmunology* **8**, (2019).
321. Lichty, B. D., Breitbach, C. J., Stojdl, D. F. & Bell, J. C. Going viral with cancer immunotherapy. *Nat. Rev. Cancer* **14**, 559–567 (2014).
322. Demaria, S. *et al.* Ionizing radiation inhibition of distant untreated tumors (abscopal effect) is immune mediated. *Int. J. Radiat. Oncol. Biol. Phys.* **58**, 862–870 (2004).
323. Demaria, S., Bhardwaj, N., McBride, W. H. & Formenti, S. C. Combining radiotherapy and immunotherapy: A revived partnership. *Int. J. Radiat. Oncol. Biol. Phys.* **63**, 655–666 (2005).
324. Carvalho, H. de A. & Villar, R. C. Radiotherapy and immune response: the systemic effects of a local treatment. *Clinics (Sao Paulo, Brazil)* **73**, (2018).
325. Demaria, S. & Formenti, S. C. Sensors of ionizing radiation effects on the immunological microenvironment of cancer. *Int. J. Radiat. Biol.* **83**, 819–825 (2007).
326. Twyman-Saint Victor, C. *et al.* Radiation and dual checkpoint blockade activate non-redundant immune mechanisms in cancer. *Nature* **520**, 373–377 (2015).
327. Nava-Parada, P., Forni, G., Knutson, K. L., Pease, L. R. & Celis, E. Peptide vaccine given with a toll-like receptor agonist is effective for the treatment and prevention of spontaneous breast tumors. *Cancer Res.* **67**, 1326–

1334 (2007).
328. Russell, T. A. & Tscharke, D. C. Strikingly poor CD8+ T-cell immunogenicity of vaccinia virus strain MVA in BALB/c mice. *Immunol. Cell Biol.* **92**, 466–9 (2014).
329. Iwai, Y. *et al. Involvement of PD-L1 on tumor cells in the escape from host immune system and tumor immunotherapy by PD-L1 blockade*. *Proceedings of the National Academy of Sciences of the United States of America* **99**, (2002).
330. Aleksic, M. *et al.* Different affinity windows for virus and cancer-specific T-cell receptors: Implications for therapeutic strategies. *Eur. J. Immunol.* **42**, 3174–3179 (2012).
331. Azuma, T. *et al.* B7-H1 is a ubiquitous antiapoptotic receptor on cancer cells. *Blood* **111**, 3635–3643 (2008).
332. Demaria, S. & Formenti, S. C. Radiation as an immunological adjuvant: current evidence on dose and fractionation. *Front. Oncol.* **2**, 153 (2012).
333. Demaria, S. *et al.* Immune-mediated inhibition of metastases after treatment with local radiation and CTLA-4 blockade in a mouse model of breast cancer. *Clin. Cancer Res.* **11**, 728–734 (2005).
334. Chen, J. *et al.* Type i IFN protects cancer cells from CD8+ T cell-mediated cytotoxicity after radiation. *J. Clin. Invest.* **129**, 4224–4238 (2019).
335. Cornel, A. M., Mimpen, I. L. & Nierkens, S. MHC class I downregulation in cancer: Underlying mechanisms and potential targets for cancer immunotherapy. *Cancers* **12**, 1–33 (2020).
336. Garrido, F., Ruiz-Cabello, F. & Aptsiauri, N. Rejection versus escape: the tumor MHC dilemma. *Cancer Immunology, Immunotherapy* **66**, 259–271 (2017).
337. Mastrangelo, M. J. *et al.* Intratumoral recombinant GM-CSF-encoding virus as gene therapy in patients with cutaneous melanoma. *Cancer Gene Ther.* **6**, 409–422 (1999).
338. Quoix, E. *et al.* TG4010 immunotherapy and first-line chemotherapy for advanced non-small-cell lung cancer (TIME): results from the phase 2b part of a randomised, double-blind, placebo-controlled, phase 2b/3 trial. *Lancet Oncol.* **17**, 212–223 (2016).
339. Misinzo, G., Delputte, P. L. & Nauwynck, H. J. Inhibition of endosome-lysosome system acidification enhances porcine circovirus 2 infection of porcine epithelial cells. *J. Virol.* **82**, 1128–35 (2008).
340. Stuart, J. H., Sumner, R. P., Lu, Y., Snowden, J. S. & Smith, G. L. Vaccinia Virus Protein C6 Inhibits Type I IFN Signalling in the Nucleus and Binds to the Transactivation Domain of STAT2. *PLOS Pathog.* **12**, e1005955 (2016).
341. Hou, W., Sampath, P., Rojas, J. J. & Thorne, S. H. Oncolytic Virus-Mediated Targeting of PGE2 in the Tumor Alters the Immune Status and Sensitizes Established and Resistant Tumors to Immunotherapy. *Cancer Cell* **30**, 108–119 (2016).
342. Kepp, O. *et al.* Consensus guidelines for the detection of immunogenic cell death. *Oncoimmunology* **3**, e955691 (2014).
343. Rojas, J. J., Sampath, P., Hou, W. & Thorne, S. H. Defining Effective Combinations of Immune Checkpoint Blockade and Oncolytic Virotherapy. *Clin. Cancer Res.* **21**, 5543–5551 (2015).
344. Ahmed, J. *et al.* A new oncolytic v accinia virus augments antitumor immune responses to prevent tumor recurrence and metastasis after surgery. *J. Immunother. Cancer* **8**, 415 (2020).
345. Alspach, E., Lussier, D. M. & Schreiber, R. D. Interferon γ and Its Important Roles in Promoting and Inhibiting Spontaneous and Therapeutic Cancer Immunity. *Cold Spring Harb. Perspect. Biol.* **11**, a028480 (2019).
346. Medrano, R. F. V. *et al.* Immunomodulatory and antitumor effects of type I interferons and their application in cancer therapy. *Oncotarget* **8**, 71249–71284 (2017).
347. Parker, B. S., Rautela, J. & Hertzog, P. J. Antitumour actions of interferons: implications for cancer therapy. *Nat. Rev. Cancer* **16**, 131–144 (2016).
348. Pelin, A. *et al.* Deletion of Apoptosis Inhibitor F1L in Vaccinia Virus Increases Safety and Oncolysis for Cancer Therapy. *Mol. Ther. - Oncolytics* **14**, 246–252 (2019).
349. Donkor, M. K. *et al.* Mammary tumor heterogeneity in the expansion of myeloid-derived suppressor cells. *Int. Immunopharmacol.* **9**, 937–948 (2009).
350. Parato, K. A. *et al.* The oncolytic poxvirus JX-594 selectively replicates in and destroys cancer cells driven by genetic pathways commonly activated in cancers. *Mol. Ther.* **20**, 749–758 (2012).
351. Voros, A., Kormos, B., Valyi-Nagy, T. & Valyi-Nagy, K. Increased Resistance of Breast, Prostate, and Embryonic Carcinoma Cells against Herpes Simplex Virus in Three-Dimensional Cultures. *ISRN Oncol.* **2013**, 1–9 (2013).
352. Keller, B. A., Wedge, M. È., Surendran, A. & Ilkow, C. S. Generating Primary Models of Human Cancer to Aid

in the Development of Clinically Relevant Oncolytic Viruses. in *Methods in Molecular Biology* **2058**, 271–284 (Humana Press Inc., 2020).
353. Holen, I., Speirs, V., Morrissey, B. & Blyth, K. In vivo models in breast cancer research: Progress, challenges and future directions. *DMM Disease Models and Mechanisms* **10**, 359–371 (2017).
354. Sakamoto, K., Schmidt, J. W. & Wagner, K. U. Mouse models of breast cancer. *Methods Mol. Biol.* **1267**, 47–71 (2015).
355. Monsky, W. L. *et al.* Role of host microenvironment in angiogenesis and microvascular functions in human breast cancer xenografts: Mammary fat pad versus cranial tumors. *Clin. Cancer Res.* **8**, 1008–1013 (2002).
356. Oliver, A. J. *et al.* Tissue-specific tumor microenvironments influence responses to immunotherapies. *Clin. Transl. Immunol.* **8**, (2019).
357. Dontu, G. & Ince, T. A. Of Mice and Women: A Comparative Tissue Biology Perspective of Breast Stem Cells and Differentiation. *Journal of Mammary Gland Biology and Neoplasia* **20**, 51–62 (2015).
358. Stewart, T. A., Pattengale, P. K. & Leder, P. Spontaneous mammary adenocarcinomas in transgenic mice that carry and express MTV/myc fusion genes. *Cell* **38**, 627–637 (1984).
359. Aisenbrey, E. A. & Murphy, W. L. Synthetic alternatives to Matrigel. *Nature Reviews Materials* **5**, 539–551 (2020).
360. Meier, A. *et al.* Isoflurane impacts murine melanoma growth in a sex-specific, immune-dependent manner: A brief report. *Anesth. Analg.* **126**, 1910–1913 (2018).
361. Rosato, R. R. *et al.* Evaluation of anti-PD-1-based therapy against triple-negative breast cancer patient-derived xenograft tumors engrafted in humanized mouse models. *Breast Cancer Res.* **20**, 108 (2018).
362. Tian, H., Lyu, Y., Yang, Y. G. & Hu, Z. Humanized Rodent Models for Cancer Research. *Frontiers in Oncology* **10**, 1696 (2020).
363. Vegh, P. & Haniffa, M. The impact of single-cell RNA sequencing on understanding the functional organization of the immune system. *Brief. Funct. Genomics* **17**, 265–272 (2018).
364. Sahaf, B., Rahman, A., Maecker, H. T. & Bendall, S. C. High-Parameter Immune Profiling with CyTOF. in *Methods in Molecular Biology* **2055**, 351–368 (Humana Press Inc., 2020).
365. Aalipour, A. *et al.* Viral Delivery of CAR Targets to Solid Tumors Enables Effective Cell Therapy. *Mol. Ther. - Oncolytics* **17**, 232–240 (2020).
366. Le Boeuf, F. *et al.* Synergistic interaction between oncolytic viruses augments tumor killing. *Mol. Ther.* **18**, 888–95 (2010).
367. Li, J. *et al.* Chemokine expression from oncolytic vaccinia virus enhances vaccine therapies of cancer. *Mol. Ther.* **19**, 650–657 (2011).
368. Lun, X. Q. *et al.* Efficacy of systemically administered oncolytic vaccinia virotherapy for malignant gliomas is enhanced by combination therapy with rapamycin or cyclophosphamide. *Clin. Cancer Res.* **15**, 2777–2788 (2009).
369. Wang, X. *et al.* Cowpox virus encodes a protein that binds B7.1 and B7.2 and subverts T cell costimulation. *Proc. Natl. Acad. Sci. U. S. A.* **116**, 21113–21119 (2019).
370. Alzhanova, D. *et al.* T Cell Inactivation by Poxviral B22 Family Proteins Increases Viral Virulence. *PLoS Pathog.* **10**, e1004123 (2014).
371. Pearl, T. M., Markert, J. M., Cassady, K. A. & Ghonime, M. G. Oncolytic Virus-Based Cytokine Expression to Improve Immune Activity in Brain and Solid Tumors. *Molecular Therapy - Oncolytics* **13**, 14–21 (2019).
372. Meko, J. B., Yim, J. H., Tsung, K. & Norton2, J. A. *High Cytokine Production and Effective Antitumor Activity of a Recombinant Vaccinia Virus Encoding Murine Interleukin 12'*. *CANCER RESEARCH* **55**, (1995).
373. Cohen, J. Clinical Trials: IL-12 Deaths: Explanation and a Puzzle. *Science (80-.).* **270**, 908a – 908 (1995).
374. Atkins, M. B. *et al. Phase I Evaluation of Intravenous Recombinant Human Interleukin 12 in Patients with Advanced Malignancies1*. *Clinical Cancer Research* **3**, (1997).
375. Leonard, J. P. *et al.* Effects of single-dose interleukin-12 exposure on interleukin-12 associated toxicity and interferon-γ production. *Blood* **90**, 2541–2548 (1997).
376. Liu, Z. *et al.* Modifying the cancer-immune set point using vaccinia virus expressing re-designed interleukin-2. *Nat. Commun.* **9**, 4682 (2018).
377. Ge, Y. *et al.* Oncolytic vaccinia virus delivering tethered IL-12 enhances antitumor effects with improved safety. *J. Immunother. Cancer* **8**, 710 (2020).
378. Hu, J., Wang, H., Gu, J., Liu, X. & Zhou, X. Trail armed oncolytic poxvirus suppresses lung cancer cell by

inducing apoptosis. *Acta Biochim. Biophys. Sin. (Shanghai).* **50**, 1018–1027 (2018).
379. Lei, W. *et al.* Combined expression of miR-34a and Smac mediated by oncolytic vaccinia virus synergistically promote anti-tumor effects in Multiple Myeloma. *Sci. Rep.* **6**, 1–11 (2016).
380. Hou, W., Sampath, P., Rojas, J. J. & Thorne, S. H. Oncolytic Virus-Mediated Targeting of PGE2 in the Tumor Alters the Immune Status and Sensitizes Established and Resistant Tumors to Immunotherapy. *Cancer Cell* **30**, 108–119 (2016).
381. Pelin, A. *et al.* Abstract PR19: Utilizing novel oncolytic vaccinia virus for selective expression of immunotherapeutic payloads in metastatic tumors. *Cancer Immunol. Res.* **8**, PR19–PR19 (2020).
382. Fung, R. Combination Radiation Therapy and Oncolytic Vaccinia Virus Therapy in Preclinical Models of Glioma. (University of Alberta, 2017).
383. Kowalsky, S. J. *et al.* Superagonist IL-15-Armed Oncolytic Virus Elicits Potent Antitumor Immunity and Therapy That Are Enhanced with PD-1 Blockade. *Mol. Ther.* **26**, 2476–2486 (2018).
384. Chon, H. J. *et al.* Tumor microenvironment remodeling by intratumoral oncolytic vaccinia virus enhances the efficacy of immune-checkpoint blockade. *Clin. Cancer Res.* **25**, 1612–1623 (2019).